Small molecules abet neuronal Cytoskeleton integrity and attenuate pathological Tau aggregation and Glycation

by

Shweta Kishor Sonawane
10BB14J26024

A thesis submitted to the
Academy of Scientific & Innovative Research
for the award of the degree of
DOCTOR OF PHILOSOPHY
in
SCIENCE

Under the supervision of
Dr. Subashchandrabose Chinnathambi

CSIR- National Chemical Laboratory, Pune

Academy of Scientific and Innovative Research
AcSIR Headquarters, CSIR-HRDC campus
Sector 19, Kamla Nehru Nagar,
Ghaziabad, U.P. –201 002, India

December - 2020

Certificate

This is to certify that the work incorporated in this Ph.D. thesis entitled, "*Small molecules abet neuronal Cytoskeleton integrity and attenuate pathological Tau aggregation and Glycation*", submitted by *Shweta Kishor Sonawane* to the Academy of Scientific and Innovative Research (AcSIR) in fulfillment of the requirements for the award of the Degree of *Doctor of Philosophy in Sciences*, embodies original research work carried-out by the student. We, further certify that this work has not been submitted to any other University or Institution in part or full for the award of any degree or diploma. Research material(s) obtained from other source(s) and used in this research work has/have been duly acknowledged in the thesis. Image(s), illustration(s), figure(s), table(s) etc., used in the thesis from other source(s), have also been duly cited and acknowledged.

Shweta 12/12/20

(Signature of Student)

Name with date

Shweta Kishor Sonawane

12 DEC 2020

(Signature of Supervisor)

Name with date

Dr. Subashchandrabose Chinnathambi

STATEMENTS OF ACADEMIC INTEGRITY

I Shweta Kishor Sonawane, a Ph.D. student of the Academy of Scientific and Innovative Research (AcSIR) with Registration No. 10BB14J26024 hereby undertake that, the thesis entitled "Small molecules abet neuronal Cytoskeleton integrity and attenuate pathological Tau aggregation and Glycation" has been prepared by me and that the document reports original work carried out by me and is free of any plagiarism in compliance with the UGC Regulations on *"Promotion of Academic Integrity and Prevention of Plagiarism in Higher Educational Institutions (2018)"* and the CSIR Guidelines for *"Ethics in Research and in Governance (2020)"*.

Signature of the Student
Date : 8/12/20
Place : Pune

It is hereby certified that the work done by the student, under my/our supervision, is plagiarism-free in accordance with the UGC Regulations on *"Promotion of Academic Integrity and Prevention of Plagiarism in Higher Educational Institutions (2018)"* and the CSIR Guidelines for *"Ethics in Research and in Governance (2020)"*.

Signature of the Supervisor
Name : Dr. Subashchandrabose Chinnathambi
Date : 08/12/20
Place : Pune

This Thesis is dedicated to two people who mean a world to me!!!!
My tenacious Mother and my highly supportive Father
Mamma, Papa this is for you
Thank you for everything…….

Acknowledgements

The path of my PhD. was fraught with innumerable challenges and it would have been impossible to traverse this path without the kind help of many people whom I met along this journey. The journey along with its people have transformed me into a more confident and capable individual. For this I would really like to thank my mentor, Dr. Subashchandrabose Chinnathambi and parents for constant support and encouragement and for having faith in me.

I am highly obliged to my research guide Dr. Subashchandrabose Chinnathambi for granting the opportunity to work with him and for his immense patience with me and my research work. I would like to thank him for his relentless support and providing with a well-equipped laboratory creating a healthy and competitive environment to work in. I thank him for igniting scientific thinking in me and believing and supporting my ideas. He has provided his valuable and critical comments, which has aided in improving the quality of work and obtaining some very interesting results.

I would like to extend my gratitude to my Doctoral Advisory Committee members, Dr. Moneesha Fernandes, Dr. Dhanasekaran Shanmugam and Dr. Mahesh Kulkarni for constantly monitoring my research progress and providing essential suggestions to improve the work.

I am grateful to Director, CSIR-National Chemical Laboratory for the opportunity to do my doctoral work and Chair, Biochemical Sciences for providing divisional facilities like animal cell culture lab. I would like to thank Department of Biotechnology (DBT) for my fellowship and DST and CSIR for providing the financial aid to our laboratory. I am thankful to Academy of Scientific and Innovative Research (AcSIR) for the academic proceedings for PhD.

I sincerely thank all the labs and members of the Biochemical Sciences Division for their help in using their lab facilities. I am thankful to Dr. Dhanasekaran and his lab members Dr. Anurag, Dr. Meenakshi, Dr. Rahul, Dr. Rupali, Parag, Sindhuri, Tejashri and Ajinkya. I would like to thank Dr. Sureshkumar Ramasamy and his lab members Dr. Manu, Dr. Deepak, Dr. Ameya, Dr. Yashpal, Dr. Vijay, Dr. Deepanjan and Debjyoti for their immense help during our initial lab set up. I thank Dr. Kiran Kulkarni lab, Dr. Anand, Zenia, Sneha, Debopriya and Aishwarya. I am thankful to Dr. Mahesh Kulakrni and his lab members Dr. Sneha, Dr. Kedar, Dr. Jagdeesh, Dr. Reema, Yugendra, Shakuntala, Prachi, Rajeshwari, Shabda, Arvind, Meera and Babasaheb. I am immensely thankful to Dr. Thulasiram and his lab members Dr. Avinash, Dr. Kritika, Dr. Aarti, Shrikant and Sharvani for giving a complete access to the Molecular Biology Lab (MBL) facilities which has helped a lot to initiate our lab work.

I would sincerely like to thank the people who made this journey feasible and interesting, my lab mates. Thank you Nalini, Abhishek anna, Tushar, Rashmi, Smita, Hari, Lisni and Tanuja without you guys I possibly wouldn't have made it this far. I thank my lab mates for always being there and encouraging me during my rough times. I would like to thank my trainees, Ananya, Kunal, Urvi and Abhibroto for their contributions in my studies. I would like to thank all my room mates Leena chechi, Smita Patil, Nalini and Monika Mathur for all the good times and memories. I would like to thank my best friends Kiran, Megalakshmi and Ishita for always being there whenever I needed them. All of these people have made my journey really memorable.

I would like to thank my collaborators Dr. Absar Ahmed for the nanoparticles work. I am thankful to Dr. Sureshkumar Ramasamy, Debjyoti and Hari for the *in silico* studies on Baicalein and EGCG. I thank Dr. Mahesh Kulkarni, Dr. Shantakumari and Yugendra for helping me with MALDI-TOF experiments. I am thankful to Abhishek and Nalini for their contributions to the Baicalein, Polyamines and EGCG work.

I would extend my gratitude to Central NMR facility at NCL, Dr. Uday Kiran Marelli and Abha, Organic Chemistry Division for their collaborative NMR experiments on small molecules. I am thankful to Central Electron Microscopy facility and Mr. Gholap from Centre for Material Characterization for the access to the T20 electron microscope. I thank Pankaj and Venkatesh for their immense help in scanning the TEM samples. I thank Dr. Moneesha Fernandes, Organic Chemistry Division, for giving me access to her Circular Dichroism facility.

I am highly obliged to my parents Mr. Kishor Sonawane and Mrs. Madhuri Sonawane and I thank them for always standing strong with me, supporting and having faith in all my decisions. They have been the strongest pillars of my life. I would like to thank all my family members especially Avantika Naik, Santhosh Naik, Sakshi and Shrushti and my grandparents for supporting me in my endeavors.

List of Abbreviations

Aβ	**Amyloid β**
AD	**Alzheimer's disease**
AG	**Aminoguanidine**
AGEs	**Advanced glycation end products**
AIS	**Axon initial segment**
ALS	**Amyotrophic lateral sclerosis**
ANS	**8-Anilinonaphthalene-1-sulfonic acid**
APP	**Amyloid precursor protein**
BBB	**Blood-brain barrier**
BDNF	**Brain-derived neurotrophic factor**
CBD	**Corticobasal degeneration**
CD	**Circular Dichroism**
CHIP	**C-terminus of the Hsc70-interacting protein**
Dyrk1A	**Tyrosine-phosphorylated and regulated kinase 1A**
EB1	**End-binding protein 1**
EGCG	**Epigallocatechin gallate**
EGF	**Epidermal growth factor**
FTDP-17	**Frontotemporal Dementia with Parkinsonism Linked to Chromosome-17**
HSA	**Human serum albumin**
HD	**Huntington's disease**
IDPs	**Intrinsically disordered proteins**
ITC	**Isothermal titration calorimetry**
LDH	**Lactate dehydrogenase**
MAPK	**Mitogen-activated protein kinase**
MAPT	**Microtubule-associated protein Tau**
MG	**Methyl glyoxal**
MMP	**Mitochondrial membrane potential**
MSTD	**Multiple system Tauopathy with presenile dementia**
MTOC	**Microtubule organizing centre**
MTT	**3-(4,5-dimethylthiazol-2-yl)-2,5-diphenyltetrazolium bromide**
NDs	**Neurodegenerative diseases**
NFTs	**Neurofibrillary tangles**
NGF	**Nerve growth factor**
ODC	**Ornithine decarboxylase**
PCC	**Pearson's co-relation co-efficient**

PCH	**Pericentrometric heterochromatin**
PD	**Parkinson's disease**
PDGF	**Platelet-derived growth factor**
PHFs	**Paired helical filaments**
Pin1	**Peptidyl-prolyl cis/trans isomerase**
PKA	**cAMP-dependent protein kinase**
PRD	**Proline rich domain**
PSP	**Progressive supranuclear palsy**
PTMs	**Post-translational modifications**
RAGE	**Receptor for advanced glycation end products**
ROS	**Reactive oxygen species**
SAM	**Decarboxylated S-adenosylmethionine**
SEC	**Size-exclusion chromatography**
SIM	**Structured illumination microscopy**
TAIs	**Tau aggregation inhibitors**
TEM	**Transmission electron microscopy**
ThS	**Thioflavin S**
ThT	**Thioflavin T**
TNIs	**Tau Nuclear Indentations**

List of Tables

List of figures

Contents

Chapter 1

Introduction

1.1 Neurodegenerative diseases

Neurodegenerative diseases (NDs) involve loss of brain function in part or whole depending on the region affected, stage and progression of the pathology[1]. In general, neurodegenerative diseases are slow progressing and become aggressive with age with few exceptions of early onsets due to genetic mutations. Neurodegeneration is generally manifested in the form of two clinical symptoms. These include diseases with cognitive clinical symptoms or motor symptoms. The symptoms are accounted for, by the loss of set of neurons responsible for cognition or motor abilities. The major causes for the neurodegeneration are enlisted as genetic mutations or sporadic proteinopathies. The genes involved in neurodegeneration are microtubule-associated protein Tau (MAPT), FUS, TDP-43, progranulin, presenilin *etc*. Proteinopathies involve added pathogenic gain of function to the cellular proteins due to variety of factors like mutations, environmental stress, abnormal processing and post-translational modifications (PTMs). Neurodegenerative diseases involving such proteinopathies include Alzheimer's disease (AD), Parkinson's disease (PD), Huntington's disease (HD), and Amyotrophic lateral sclerosis (ALS) *etc*. These diseases involve misfolding, aggregation and accumulation of proteins in the neurons increasing the load on the clearance machinery and finally leading to neuronal death. These patho-proteins do not remain restricted to a single brain region but rather spread across the synaptically connected regions spreading the pathology[2,3]. Additionally, other cellular systems including ubiquitin-proteasomal system, oxidative stress, mitochondrial dysfunction, disturbed bioenergetics, and neuroinflammatory pathways also play a key role in pathogenesis of the disease. The proteins involved in the NDs are amyloid-β and Tau in AD, α-synuclein in PD, Huntingtin in PD and SOD1 in ALS.

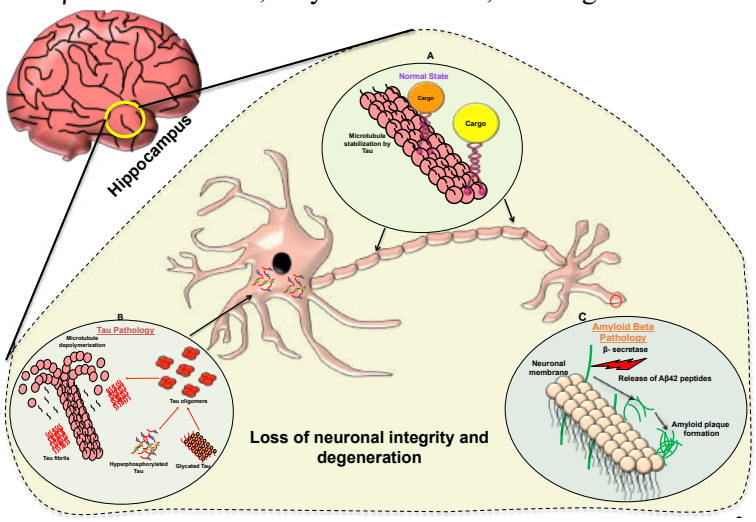

Figure 1.1. Physiological and pathological role of Tau. The hippocampus region of the brain is responsible for memory formation and storage and is composed of neurons. Neuronal structure is essential for its functions and microtubules and its associated proteins like Tau play a pivotal role in this aspect. A) The physiological role of Tau protein is to stabilize the axonal microtubules and aid in normal vesicular transport and neuronal functioning. B) In diseased state, Tau is subjected several insults and modifications, which leads to decreased affinity for the microtubules and their destabilization. Microtubule destabilization disrupts the vesicular transport and neuronal functioning. The modified Tau dissociates from microtubules and self-interact to form Tau oligomers, which act as seeds for paired helical filament formation. C) Aβ pathology in AD is characterized by faulty processing of membrane bound Amyloid Precursor Protein (APP) by α and β pathways. The processing of APP by α- secretases is non-amyloidogenic. But cleavage of APP by β-secretases followed by γ-secretases releases Aβ-42 peptides. These sticky peptides are amyloidogenic, which aggregate and accumulate to form extracellular plaques, which disturb the synaptic transmission and lead to neuronal dysfunction finally leading to neuronal death. The figure is reproduced from Sonawane *et al.,* JoMN, 2018.

1.2 Alzheimer's disease

Alzheimer's disease is the most common type of dementia accounting for 60-80 % of the total dementia cases. AD is characterized by progressive memory deficits, behavioral alterations, poor judgement and motor deficits in the very late stages of the disease[4]. Anatomically, the region of the brain that is affected

in AD is hippocampus, which is located under the cerebral cortex. The hippocampus is the seat of memory storage and formation. It is divided into following regions CA1, CA2, CA3, CA4, dentate gyrus, subiculum and entorhinal area[5]. In AD, the hippocampal areas get affected in stage specific manner with the disease progression[6]. Two types of pathologies affect the hippocampus in AD, the extra neuronal amyloid beta plaques and intra neuronal Tau tangles (Fig. 1.1).

In neuronal cells, the amyloid precursor protein (APP) is encoded as a 695 amino acids containing single trans membrane protein. This protein is cleaved sequentially by α, β and γ secretases in normal physiological conditions[7]. The mutations in the APP gene cluster especially near the cleavage sites and lead to abnormal processing of the APP giving rise to increased formation of Aβ-42 peptide[8]. This Aβ-42 peptide is prone to aggregation and deposits on the external neuronal membrane affecting its function and neuronal synapses[9]. The other important pathological event leading to AD is formation and deposition of Tau tangles. Tau is a microtubule-associated protein aiding in microtubule dynamics and cargo transport. Under stress conditions or due to excessive post-translational modifications like phosphorylation, glycation, truncation *etc.,* Tau dissociates from microtubules and self-associates to form oligomers and subsequently Tau paired helical filaments (PHFs). This causes microtubule destabilization and disruption of neuronal architecture leading to degeneration of neurons[10].

1.3 Tau protein

Tau was discovered in 1975 as a heat-stable fundamental factor for microtubule assembly[11,12]. Subsequently, the purification procedures and the physico-chemical properties of Tau were discovered[13]. The phosphorylated status of Tau by various kinases and its significance in microtubule assembly was reported in the following studies but its pathogenic impact in neurodegeneration was realized by the studies done by Grundke-Iqbal and group in 1986. They reported hyperphosphorylated Tau to be the major component of the neurofibrillary tangles found in AD[14]. Tau is a 441 amino acid containing protein found in the axons of the neuronal cells. Human Tau has 6 isoforms based on the alternative splicing of the Tau gene, which is located on the q arm of chromosome number 17[15]. The longest isoform of human Tau40 is 441 amino acids long and is broadly divided into two domains, the N-terminal projection domain and the C-terminal microtubule-binding domain. The N-terminal has two inserts, which are recently reported to impact the global conformation of Tau and its complex with tubulin[16]. The C-terminal of Tau consists of 4 imperfect repeats (R1 to R4) of ~30 amino acids each. These play a crucial role in physiological as well as pathological role of Tau. Based on the presence of repeat 2, Tau isoforms are divided into 3R and 4R isoforms. The 3R isoforms predominate in fetal brain and resist aggregation[17]. The repeats interact with microtubules and aid in their dynamic instability. Tau binds the tubulin dimers at the interface of α and β tubulin heterodimers *via* the conserved residues that are also essential for the pathogenic misfolding of Tau[18]. In addition to the repeats, the upstream and the downstream flanking regions augment the binding of Tau to the acidic exterior of the microtubules famously called as the Jaws model for the Tau-tubulin interaction[19]. The repeats involved in the mechanistic function of Tau also acts as a core for its pathogenic aggregation. Tau aggregation proceeds *via* various stages beginning with nucleation, which requires Tau dimerization, as dimers acts potential elementary unit for nucleation. A nucleus composed of 8-14 monomers is sufficient for Tau PHFs formation[20]. The *in vitro* Tau polymerization is induced by either polyanions like heparin and RNA or fatty acids such as arachidonic acid. In the neurons, Tau aggregates due to various reasons especially due to hyperphosphorylation. Tau belongs to the class of intrinsically disordered proteins (IDPs) with no rigid secondary structure. It is a highly flexible protein but adopts transient secondary structure on binding with its interacting partners like microtubules and nucleic acids. Tau is reported to adopt transient α-helical structures on interaction with microtubules as well as on phosphorylation[21,22]. In solution, Tau adopts a hairpin/paperclip conformation wherein the C-terminal folds upon the repeats as well as N-terminal forming a paperclip structure. The N-terminal stays away from the repeat region[23].

The aggregation of Tau is accompanied by formation of β-sheet rich structure in the PHFs as opposed to random coil conformation of the native protein[24]. Thus, a natively unstructured protein Tau, forms orderly parallel or anti-parallel arrays on self-association leading to loss of mechanistic function and gaining toxic transition leading to disease pathology[25].

1.4 Role of Tau in AD and other Tauopathies

The neurofibrillary tangles of Tau are one of the major reasons for pathological manifestations of AD. Several causal events for this pathology have been reported with hyperphosphorylation being the most acclaimed. Hyperphosphorylation is known to induce and precede Tau aggregation[26,27]. Phosphorylation is thought to cause a conformational change in Tau such that the action of PP2a phosphatases is hampered and the aberrant Tau assembly is enhanced[28]. The cytotoxic effect of Tau aggregation results due to excess Tau levels as the hyperphosphorylated Tau sequesters normal Tau and affects the Tau-mediated microtubule stabilization. The loss of microtubule dynamics along with accumulation of Tau aggregates lead to cytotoxity and neuronal death in AD. The pathological features of Tau like increased levels, abnormal phosphorylation and aggregate formation is common to many Tauopathies including Pick's disease, Down's syndrome, corticobasal degeneration, Frontotemporal Dementia with Parkinsonism Linked to Chromosome-17 (FTDP-17), Progressive supranuclear palsy (PSP) *etc.* Frontotemporal dementia displays behavioural changes, aphasia, disinhibition, impulsivity *etc.* The brain morphology changes associated with FTDP-17 is atrophy of the frontotemporal lobes with asymmetric degeneration[29]. The role of Tau in FTDP-17 pathology was confirmed after the mutations in the Tau gene locus 17q21-22 were reported[30]. These mutations are autosomal dominant and include both intronic and exonic mutations. The intronic mutations affect the alternative splicing of the exon 10 and results in increased 4R Tau isoforms. This mutation lies at the 5' splice site of exon 10 and mechanistically affects a stem loop structure in the RNA, which is involved in regulating the splicing of exon 10 [31]. The increased 4R Tau isoforms are related to Tau aggregation as the studies with sarkosyl insoluble Tau extracted from the deposits in familial multiple system Tauopathy with presenile dementia (MSTD) showed dominance of 4R Tau[32,33]. Additionally the tip of balance between the 3R and 4R Tau isoforms alters the aggregation pattern, filament length, which have been implicated in the pathogenesis.

The missense Tau mutations occur in the exons of Tau and alter the splicing as well as total Tau levels. The missense mutations of Tau altering its functionality include P30lL, R406W, G272V, and V337M among others. The missense mutations occur in the functional microtubule-binding domain of Tau, which either alters its microtubule interactions or enhances aggregation or both[34,35]. The mutations enhancing Tau assembly include G303V, G272V, P301L, S352L and S320F[36]. The microtubule assembly in presence of FTDP-17 mutant Tau shows discreet patterns. Mutant Tau P301L, G303V and S320F decline the pace of microtubule assembly whereas V337M and E342V escalate the tubulin assembly. The FTDP-17 mutations are common in AD pathogenesis as well an account for 2-5 % of cases and leads to early onset[37,38]. The FTDP-17 mutations have been reported to modulate the phosphorylation and glycation pattern of Tau (Fig. 1.2). The FRET sensor studies reveal the impact of FTDP-17 mutants of Tau conformation and microtubule interactions.

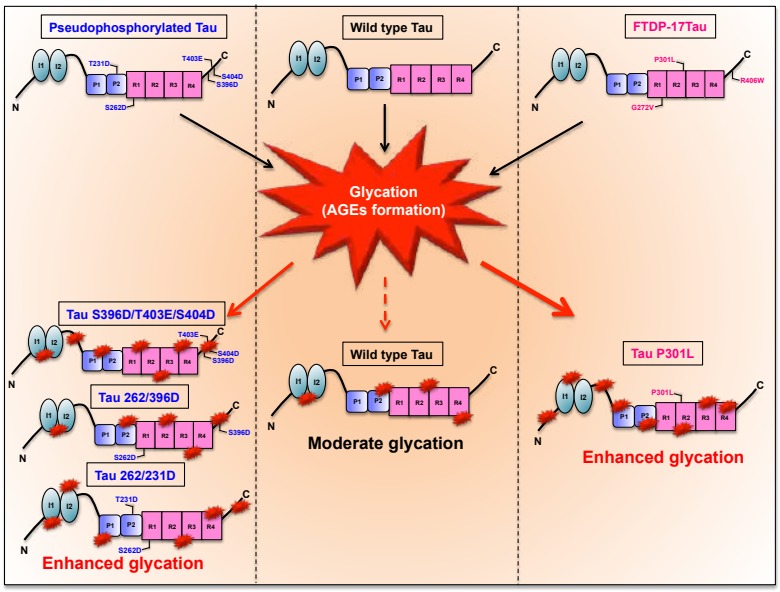

Figure 1.2. MG-induced glycation of Pseudophosphorylated and FTDP-17 mutants. The wild type Tau consisting of 441 amino acids is composed of two major functional domains namely the N-terminal projection domain and C-terminal microtubule-binding domain. The projection domain consists of 2 inserts and the microtubule region comprises of proline-rich region and 4 imperfect repeats. These repeats play a major role in microtubule binding and their stabilization. The reaction of wild type Tau with methylglyoxal leads to moderate glycation whereas the glycation of pseudophosphorylated double (262/396D, 262/231D) and triple mutants (S396D/T403E/S404D) leads to enhanced glycation as compared to wild type Tau. On the other hand, the dementia mutant P301L showed increased glycation propensity as compared to wild type Tau.

The wild type Tau when bound to microtubules takes up hairpin conformation with decreased distance between N and C-terminal with increased FRET signal. On the other hand, the presence of P301L mutation extends the conformation of Tau even when bound to microtubules as witnessed by decreased FRET signals[39]. Thus, the FTDP-17 mutants modulates the self-assembly and microtubule-binding affinity of Tau by altering the phosphorylation pattern and protein conformation.

1.5 Tau PTMs and their impact on Tau physiology and pathology

Post-translational modifications are generally enzymatic covalent modifications of the amino acid side chains or the terminals of the nascent peptide, which are essential in its folding or functional activation. Tau is also subject to varied PTMs, which either enhance its aggregation and hamper its physiological functions or prevent its aggregation. Tau becomes more prone to modification given its flexibility and lack of rigid secondary structures exposing the amino acids to PTMs.

1.5.1 Phosphorylation

The most extensive modification of Tau is phosphorylation. Tau is a phosphoprotein with 2 phosphates per Tau molecule found in the normal adult brain[40]. Tau has 85 potential sites, which can be phosphorylated which include 80 serines+threonines and 5 tyrosines. The tip of balance in the kinase or phosphatases activities in AD leads to hyperphosphorylation of Tau. In AD, Tau phosphorylation increases abnormally to 8 or more phosphates per molecule of Tau[40]. The hyperphosphorylated Tau self-associates to form the paired helical filaments and curtails its microtubule-binding affinity. The toxicity of phosphorylated Tau does not depend on extent or single residue phosphorylation but is influenced by combination of phosphorylated residues that cause toxicity *in vivo*. Phosphorylation of Tau is detected by various epitope-specific antibodies such as AT8* (S202/T205), AT100 (S212/T214), AT180 (T231), AT270 (T181), PHF-1 (S396/S404), PHF-6 (T231), which also serve as the diagnostic markers for AD[41,42]. Tau is phosphorylated by proline and non-proline-directed kinases. Proline-directed kinases essentially phosphorylate the serine/threonine residues followed by a proline residue.

These are termed as SP/TP motifs and Tau has 14 such motifs[43]. The proline-directed kinases that phosphorylate Tau include CDK5, GSK-3β, cdc2, MAPK and JNK. The other motifs, which, are highly phosphorylated in Tau, include KXGS sites in the repeat regions of Tau. Each repeat has one KXGS motif, which is phosphorylated by non-proline directed kinases like MARK and AMPK family of kinases. Phosphorylation of Tau at specific residues is known to disrupt its microtubule interaction and hamper the microtubule assembly. For example, the phosphorylation at S262 by MARK kinase in repeat 1 abolishes Tau's microtubule binding affinity in AD brain[44]. In addition to the microtubule-binding repeats, the flanking as well as the far-off regions also play a role in Tau's activity of microtubule polymerization as well as self-assembly[45]. The tyrosine-phosphorylated and regulated kinase 1A (Dyrk1A) mediated phosphorylation of the proline-rich domain of Tau have mild effect on Tau's activity and self-assembly[26,46]. The phosphorylation at S396 and S404 by GSK-3β enhanced both the microtubule assembly as well as self-assembly of Tau. The phosphorylation of Tau over a longer span covering the proline-rich region till the C-terminal tail by cAMP-dependent protein kinase (PKA) inhibited 70% of Tau's activity disrupting the microtubules[46]. In addition to the action of individual kinases, interplay of two or more kinases also leads to enhanced Tau phosphorylation. One such example is the GSK-3β, which readily phosphorylates the pre-phosphorylated or primed substrates. The priming of Tau by PKA enhances the GSK-3β-mediated Tau hyperphosphorylation and memory impairments in adult rats[47]. While most of the kinases lead to Tau hyperphosphorylation and impair microtubule binding, the peptidyl-prolyl *cis/trans* isomerase Pin1 enhances Tau-microtubule interaction. The levels of Tau with phospho-threonine 231 increase with AD progression and decrease the ability to bind microtubules. Pin 1 binds to pT231 Tau and causes a conformation change by *cis/trans* isomerization such that the microtubule-Tau interaction is re-established[48]. It also leads to dephosphorylation of Tau by making the phosphorylated residues accessible to PP2a phosphatase[49]. The exact mechanism by which hyperphosphorylation leads to Tau aggregation is still unclear but the *in silico* molecular dynamics and simulations have revealed the exposure and attraction of Tau repeats on hyperphosphorylation and increased forces of repulsion between N- and C-terminals depending on the phosphorylated sites[50].

Other Tau PTMs

Though phosphorylation plays a key role in Tau pathology, several other PTMs either accelerate or prevent it. The non-enzymatic glycation of Tau has been reported to stabilize the PHFs in the AD brain. The sites of glycation have been mapped to be present in the functional domain in majority thus lowering the microtubule affinity.

1.5.2 Ubiquitination

Ubiquitination is the modification involving addition of a chain of ubiquitin molecules to the lysine residues of the target protein marking it for the ubiquitin-proteasome system-mediated proteolytic degradation. The PHFs purified from the AD brains were found to be ubiquitinated at the lysines in R1 and R4[51]. The role of ubiquitination on Tau biology is still debatable. The C-terminus of the Hsc70-interacting protein (CHIP), an E3 ligase, ubiquitinates Tau, inducing its proteasomal degradation[52]. This may occur in physiological as well as pathological conditions irrespective of Tau hyperphosphorylation[53]. Nevertheless, it has been reported that hyperphosphorylation is a requirement for the recognition of Tau by CHIP-Hsc70 complex with an E2 ligase[54]. The molecular chaperone Hsp70 interacts with Tau and is known to suppress the activity of CHIP thus, having opposing effect on Tau ubiquitination. The levels of CHIP and Hsp70 were found to increase in AD[55]. The overexpression of CHIP in the cell based system demonstrated accumulation of aggregated Tau[52]. By contrast, the mouse model system devoid of CHIP demonstrated presence of insoluble aggregated Tau[55].

Thus, the intricate molecular events of Hsp70-CHIP complex might play a major role in Tau ubiquitination in physiology and pathology.

1.5.3 Acetylation

Acetylation modifies the N-terminal of majority of human proteins and plays a key role in epigenetic modulation by acetylating the histone proteins. It is an enzymatic modification involving the addition of acetyl group from acetyl-CoA to the lysines of target protein by acetyltransferases. The *in vitro* acetylation adds an overall of 6 acetyl groups per Tau molecule[56]. The major putative sites of Tau acetylation reside in the microtubule-binding domain with few lysines in the proline-rich domain. The highly acetylated lysines include K163, K240, K280, K281, K294 and K369[57]. Of the 23 apparent acetylation sites, the ones, which regulate Tau function, include K174, K274, K280, and K281. Acetylated K280 Tau is detected in NFTs and is absent in control brains. Additionally, acetylation at this site plays a role in Tau fibrillization and reduces microtubule affinity[58]. The *Drosophila* model of acetylation-mimic mutant Tau K280Q demonstrated increased phosphorylation at epitopes S62 and T212/S214 pointing out the toxic effect of Tau acetylation[59]. Acetylation of K274 and K281 hampered the cytoskeletal architecture in the axon initial segment (AIS) in the acetylation mimicking mutant (K274/281Q) mice and primary neurons by destabilizing the microtubules. The disruption of microtubule network barrier in AIS leads to Tau missorting to somatodendritic compartment[60]. The acetylation of K174 in the proline-rich region leads to reduction in Tau clearance, elevated levels of Tau and induce memory and behavioural deficits[61]. Taken together, Tau acetylation can enhance the pathology by two mechanisms. Firstly, since the sites of Tau ubiquitination and acetylation are same, acetylation would prevent Tau ubiquitination stalling its degradation *via* UPS leading to Tau accumulation. This would cause formation and build-up of Tau aggregates, which would be difficult to clear. The second mechanism involves disruption of Tau's function of microtubule binding due to charge neutralization of Tau, which impairs its ability to bind the negative charges on microtubules.

1.5.4 Methylation

Methylation of Tau has been discovered relatively recently. Methylation modifies lysine and arginine residues. Although, Tau from AD brains is methylated at 7 residues, methylated Tau is also found in normal brains[62]. The methylated residues are K180, K267, K290, R126, R155 and R349[63]. Similar to acetylation, methylation sites also overlap with the sites of ubiquitination and prevent Tau degradation. Additionally S262 is found to be often phosphorylated in presence of methylated K267[62]. Since, methylation is found to play a role in protein-protein interactions, it has been postulated that methylation might enhance the self-assembly of Tau leading to its aggregation.

1.5.5 Truncation

In addition to all above PTMs, Tau also undergoes truncation as one of its modification, which is thought to be an early event in the Tau pathology in AD. Tau is a substrate for various proteases like caspases, calpain, thrombin *etc.* and the aberrant proteolysis is known to occur with aging[64-66]. Moreover, the activity of caspases is reported to be enhanced in AD brains. Caspases cleave Tau at several residues, especially capsase-3, which proteolytically cleaves Tau at aspartic acid-421 (D421) causing C-terminal truncation[67,68]. D421 truncated Tau is enriched in the AD brain extracts[69]. The D421 Tau enhances the Tau aggregation as compared to the full-length Tau *in vitro*. The presence of D421 truncated Tau is preferentially observed in the early stages of AD[69]. It has been postulated that the C-terminal truncation induces the conformational changes in the Tau molecule with truncated N-terminal such that it increases the interaction between PRD and RD contributing to stabilization of the Tau filaments[70]. Another C-terminal truncation is reported at Glutamate-391 (E391) and presence of this truncated Tau was in accordance with the progress of dementia by Braak staging. The *in vitro*

biochemical analysis showed enhanced assembly rate as compared to full-length Tau on induction with arachidonic acid[71]. In addition to C-terminal truncation, Tau also undergoes N-terminal truncation at Q26 generating a 20-22 KDa fragment, which accumulates at the synaptic terminals. This fragment causes altered mitochondrial trafficking hampering the neuronal transmission[72]. Thus, the Tau truncation is an early event in AD pathology and is also known to induce other abnormal PTMs such as glycation and ubiquitination, which enhance and stabilize the Tau inclusion in the later stages.

1.5.6 Glycation

The non-enzymatic post-translational modifications involve covalent reaction of the amino acid side chains causing their functional and structural modulations. Carbamylation, carbonylation, homocysteinylation, nitrosylation, and glycation, *etc.* are few examples of the non-enzymatic PTMs, which are profoundly associated with disease pathologies[73]. Glycation of proteins modify the ε-amino group of the lysine chains by reaction with sugar or their reactive intermediates. Glycation proceeds through 3 major phases with each consisting of multiple reactions (Fig. 1.3A). The initiation phase involves early events of reactions of free amino group of the amino acids with reducing sugars to form a Schiff's base, which is relatively unstable. The Schiff's base undergoes bond rearrangement reactions to form more stable Amadori products[74]. The process of rearrangement requires the auto-oxidation reactions, which yield the intermediates such as glyoxal, methyl glyoxal and 3-deoxyglucosone. These are termed as reactive dicarbonyls and act as propagators of the glycation reaction as they independently cause the glycation of proteins. This phase is known as propagation and involves rapid glycation of proteins, as the propagators are 200-50,000 fold more reactive than glucose. Though, physiologically, concentration of these dicarbonyls is 10,000-50,000 lower than glucose, the enhanced potency makes them crucial players of glycation progression. In the late phase of glycation reaction, advanced glycation end products (AGEs) are formed through series of oxidations, dehydration, crosslinking and replacement reactions. AGEs-modified proteins undergo crosslinking, functional impairments due to structural misfolding and accelerated aggregation. The pathogenicity of AGEs is executed by various signalling events on interaction with the receptor for advanced glycation end products (RAGE). Binding of AGEs with RAGE activates the transcription factor NF-κB, which increases the expression of genes responsible for inducing oxidative stress and inflammation[75]. This results in increased levels of pro-inflammatory cytokines, DNA damage and apoptosis causing disease complications like diabetes, cataracts, atherosclerosis and neurodegenerative diseases including AD. The role of glycation in AD was brought into being in the early nineties, when the immunolabelling revealed presence of advanced maillard end products like pentoside and pyralline in the NFTs and senile plaques of AD brain tissue[76]. The AD brains contained 3-4 fold higher AGEs adducts as compared to healthy brains[77]. This modification was accounted for the longer half-life and insolubility of the proteins present in the lesions. The studies for Tau glycation in the PHFs demonstrated similar results wherein Tau glycation was prominent in AD brains and absent in non-demented brains[78]. The further biochemical analysis of glycated Tau in the PHFs confirmed the preferential glycation of lysines present in the repeat region of Tau[79]. The assessment of *in vitro* glycated Tau disclosed 13 putative sites[80] for glycation 6 of which are present in the microtubule-binding domain (Fig. 1.3B). The functional consequence of Tau glycation is its reduced affinity for the microtubules as well as induction of oxidative stress in the neuronal cells[81]. The biochemical and biophysical analyses of *in vitro* Tau glycation suggests that glycation is able to shift the kinetic equilibrium towards polymerization of Tau but it cannot enhance Tau fibrillization[82]. Glycation is proposed to modulate phosphorylation of Tau and enhance the aggregation of full-length Tau as compared to other Tau isoforms[83].

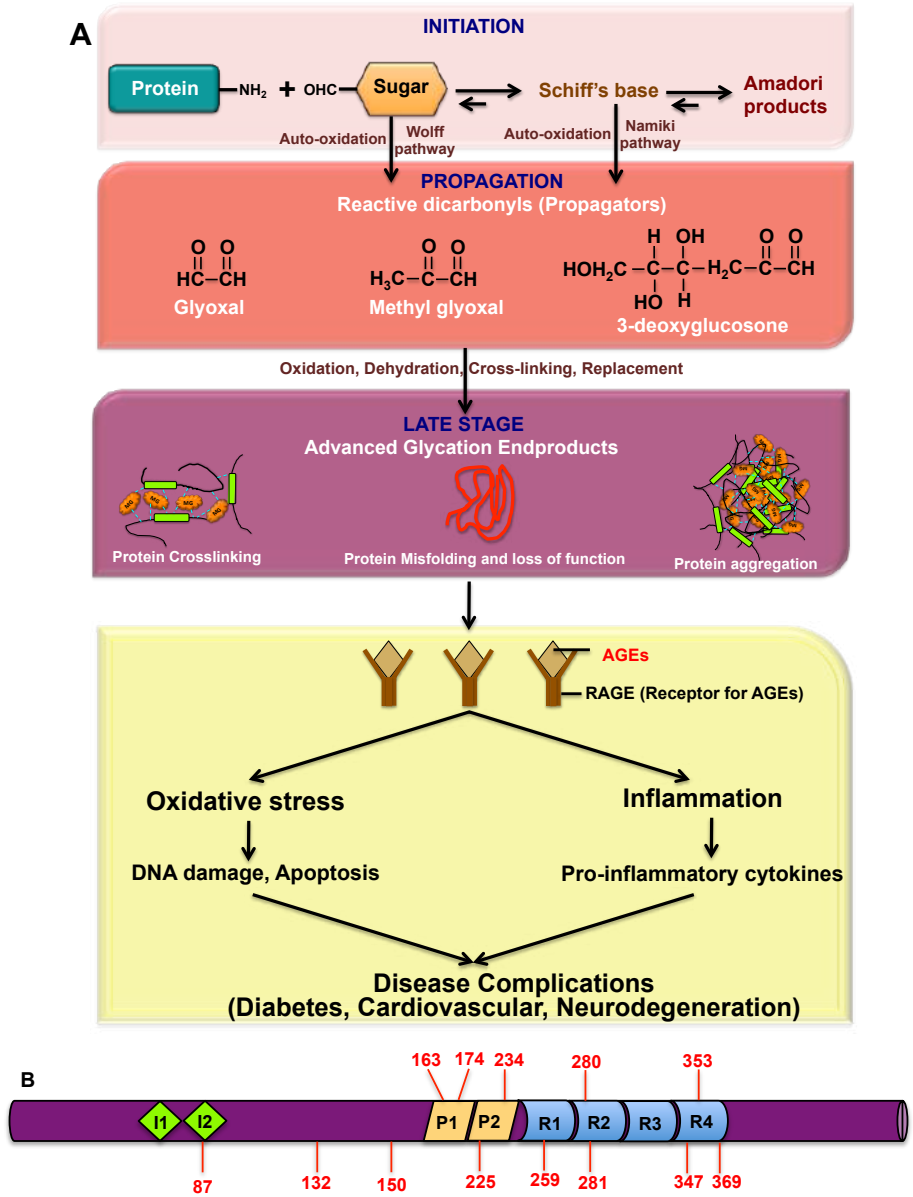

Figure 1.3. Stages of general protein glycation and glycation sites in Tau protein. A) The non-enzymatic reaction of protein and sugar termed, as glycation comprises of three major phases. The initiation phase includes the reaction of amino group of amino acid side chain with sugar leading to formation of Schiff's base and Amadori products. These reactions are reversible under physiological conditions. In the next propagation phase of reaction, the auto-oxidation of sugar and the products formed leads to the formation of reactive dicarbonyls such as glyoxal, methyl glyoxal and 3-deoxyglucosone. These propagators are highly reactive and react rapidly with the proteins in a series of reactions forming products, which cannot be reversed. The interaction of propagators with the proteins leads to excessive protein crosslinking, which constitutes the advanced phase of glycation. The excessive cross-linking leads to protein misfolding, disrupting its structure and function. Furthermore, glycation leads to protein aggregation and accumulation leading to cellular stress. The advanced glycation end products (AGEs) formed as a result of protein glycation interact with their receptor aka RAGE (Receptor for Advanced glycation end products) to induce oxidative stress and inflammation. Oxidative stress leads to cell death *via* DNA damage whereas the inflammation leads to increased pro-inflammatory cytokines. Together this results in various disease complications-like diabetes, cardiovascular disorders, neurodegenerative diseases *etc.* B) Tau protein undergoes glycation at the 13 sites. Most of the glycation sites reside in the proline-rich and repeat region of Tau, which is involved in physiological function of Tau of microtubule binding.

The glycation and formation of advanced glycation end products activate cascades of cellular signalling which adds up to the AD pathology (Fig. 1.4). The activation of RAGE by AGEs triggers NF-κB mediated increased expression of genes responsible for ROS generation, APP and pro-inflammatory

cytokines. ROS further activates various cascades including activation of cell death pathway. The levels of p53 and caspase-3 are increased with decreased bcl-2/bax ratio forcing the cell towards apoptosis and neuronal death[84]. The ROS-mediated pathway also increases the expression and processing of APP and generates Aβ[85,86]. The Aβ plaques deposition curtails synaptic transmission and accelerates AD pathology. On the other hand, ROS activates series of kinases like JNK, GSK-3β, ERK ½ and certain Ca^{+2} activated kinases like CAMK2B and AMPK. All these kinases hyperphosphorylate Tau leading to tangles formation[87]. JNK is also responsible for increasing activation of caspase-3, which truncates Tau, and this truncated Tau is more prone to aggregation. Furthermore, RAGE signalling is also implicated in cellular migration *via* the activation of Rac-2 and CD42 GTPases. The increased production of pro-inflammatory cytokines also activates cell migration[88]. Also the increase in inflammation causes cell death leading to neurodegeneration. Thus, glycation plays a significant role in the pathogenesis of AD.

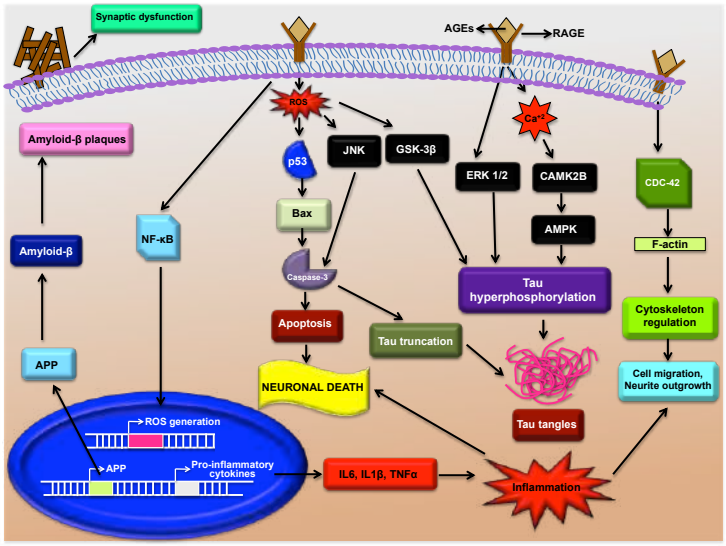

Figure 1.4. Downstream cascades of glycation in AD. The interaction of AGEs with its receptor RAGE activates various cascades affecting the neuronal cells in AD. RAGE activation leads to ROS formation *via* activation of NF-κB and transcription of ROS related genes. The ROS activate apoptosis pathway *via* activation of caspase-3. ROS generation also activates series of kinases such as JNK and GSK-3β. RAGE signalling also activates kinases such as ERK1/2, CAMK2B and AMPK *via* increased calcium influx. All these kinases (black boxes) lead to Tau hyperphosphorylation resulting in Tau tangles formation. The activation of caspase-3 leads to Tau truncation and this truncated Tau is more prone to aggregation, which enhances AD pathology. The RAGE-mediated activation of NF-κB leads to transcriptional activation of many genes including amyloid precursor protein (APP) and pro-inflammatory cytokines. The increased expression of APP leads to amyloid plaques formation, which, accumulate on the neuronal membrane leading to synaptic dysfunction in AD. The increase in levels of cytokines like IL-6, IL-1β, TNF-α accelerates the process of inflammation leading to neuronal death. The inflammation and RAGE signalling activates rho GTPase CDC42, which regulates actin cytoskeleton and enhance cell migration.

1.5.7 Dual modification of Tau (Pseudophosphorylation and glycation)

Post-translational modifications are one of the major causes of Tau pathology in AD. Abnormal phosphorylation is a decisive factor in Tau pathology. The study of site-specific phosphorylation faces certain obstacles in the *in vitro* kinase assay, as the sites to be modified cannot be controlled. In order to achieve this, the serine and threonine amino acids are replaced by aspartic acid or glutamic acid. Since, phosphorylation imparts a negative charge, these negatively charged residues mimic the charge-based modification and the proteins bearing such replacements are termed as pseudophosphorylation mutants[89,90]. Such Tau pseudophosphorylation mutants have been employed in various studies. The domain specific pseudophosphorylation has revealed discrete effects on Tau assembly with C-terminal having an enhancing effect and N-terminal having an inhibitory effect[46]. As mentioned above there are some unique phospho-epitopes associated with Tau pathology in AD. One of these is epitope recognized by antibody AT8 *i.e.* Tau phosphorylated at S202 and T205. The functional relevance of AT8 epitope

was determined utilizing the phospho-mimicking mutant with glutamic acid replacement. It was revealed that this Tau shows enhanced self-assembly but does not affect the microtubule binding. Moreover, the filament assembly is sensitive to Tau concentration[91]. Another Tau phospho-mimicking mutant T212E increases the aggregation propensity of Tau and generates degradation resistant filaments. The mutant Tau shows increased nucleation rate for filament assembly[92]. The study of combinatorial phosphorylation at T231, S262, S396 and S404 for the microtubule assembly shows loss of function for each of the single phospho-mimicking mutant. Surprisingly, the double mutants showed the contrary effect on the microtubule assembly. The double mutants showed enhanced assembly of microtubules, thus, making a point that effect of phosphorylation does not directly correlate with the total number of residues phosphorylated but the combination of phosphorylated residues decides the fate of protein.[93] The Tau-microtubule interactions are perturbed by the conformational changes of phospho-mimicking mutants 262, 293, 324 and 356 and S262 phosphorylation severely affects Tau-tubulin interactions[94]. Although, phosphorylation has been reported to promote Tau aggregation, the studies with repeat domain of Tau with specific pseudophosphorylation mutations at pS356, pS356/pS262 and pS356/pS262/pS258 inhibited the Tau aggregation with increase in the number of pseudophosphorylated sites as opposed to expected increased aggregation propensity[95]. Thus, the co-occurrence of various phosphorylated residues may have very different effects. Additionally, other PTMs are thought to enhance the pathology of hyperphosphorylated Tau that includes glycation. The studies for dual modification of Tau have revealed that MG-induced glycation of S396D/T403E/S404D and double mutants 262/396D, 262/231D showed enhanced aggregation as compared to single mutants[96] (Fig. 2) These studies shed some light on the effect of multiple PTMs on Tau pathology in AD.

1.6 Trans cellular (Prion-like) spreading of Tau

The notion of Tau pathology spread in the form of oligomers and filaments to different parts of the brain was proved in early nineties by Braak and Braak wherein a characteristic distribution of NFTs in the brain of AD patients marks the six stages of disease evaluation[6]. The exact mechanism of the spread of Tau pathology was still unclear. The spread of pathology requires the seeds not only to transfer transcellularly among the neurons but also induce the aggregation of soluble Tau in the target cells. The initial studies involved in deciphering the trans cellular as well as seeding effect of Tau aggregates revealed that cultured cells preferentially uptake aggregates over monomers and acts as seed for fibrillization of the intracellular Tau[97]. Moreover, the brain lysate of aggregate prone P301S Tau transgenic mice prompts fibrillization of wild type Tau in the target transgenic mice[98]. The uptake of Tau aggregates is facilitated by the cell surface heparan sulphate proteoglycans *via* macropinocytosis[99]. It has been also suggested that the transfer of Tau aggregates takes place through nanotubes between the cells[100]. But the need of tunneling nanotubes for Tau transfer is refuted by the results showing Tau can be transferred between the cells *via* medium and increased synaptic activity enhances Tau release[101,102]. The *in vitro* recombinant Tau filaments are more resistant to the action of proteinase K and guanidine hydrochloride as compared to filaments obtained from transgenic mice or AD brains and shows lower seeding potency[103]. This is in concordance with the prion propagation theory, wherein the conformation of the seed plays a decisive role in the characteristic aggregation. The seeding and recruitment concept has been proved for Tau spreading wherein minute quantities of seeds efficiently sequester the intracellular soluble Tau and cause microtubule destabilization. The AD-derived Tau oligomers injected in mice showed spread through the regions like carpous callousum, cortex and hypothalamus[104]. Moreover, the spread of Tau pathology is seen to occur among the connected brain regions rather than the proximity. But the necessity of synaptic contacts for the spread was elucidated by using artificial neuronal circuits *in vitro.* This study demonstrated that the physical presence of synaptic contacts along with the cell adhesion molecules enhance the spread of Tau pathology[105]. Many

studies have shown that uptake of Tau takes place *via* bulk endocytosis from the extracellular milieu[106]. The critical size of misfolded Tau species to be taken up is not less than 3 monomeric Tau units[107]. Once inside the target cells, the endocytosed Tau is suggested to solubilize the enclosing membrane and release in to the cell and seed the aggregation of endogenous soluble Tau[108,109]. Additionally, Tau aggregates are also reported to be taken up *via* the clathrin coated endosomes in brain slices as well as the cultured neurons[110].

An important characteristic of propagation is formation of specific conformers or strains. Some idea regarding this was obtained when the Tau filament morphology varied with the type or nature of mutation. Further studies evidenced that the propagation of Tau aggregates is conformer specific wherein introduction of brain lysates of CBD or AD into the transgenic mice affected only the oligodendrocytes and neurons respectively[111]. This might be attributed to specific conformational variations in donor seeds, which confers the ability to induce Tau aggregate formation only the specific target cell type. The formation and clonal propagation of Tau in the form of distinct strains have been reported in HEK cell lines. These conformers faithfully propagated through 3 generations of transgenic mice while maintaining the strain pathology as well as properties[102]. Based on these studies that confirm the prion-like spread of Tau pathology, we hypothesize that PTMs, which play a major role in the pathological transition of Tau would enhance the seeding and spread of pathological Tau[112]. As already discussed, glycation affects the protein structure and function leading to aberrant protein aggregation. Both the modifications *i.e.* phosphorylation and glycation increases overall negative charge of the protein, which might play a role in its prion-like behavior. According to our hypothetical model of propagation of post-translationally-modified Tau, one pathway would include binding of AGE-modified Tau to its receptor RAGE and scavenger receptors (Fig. 1.5).

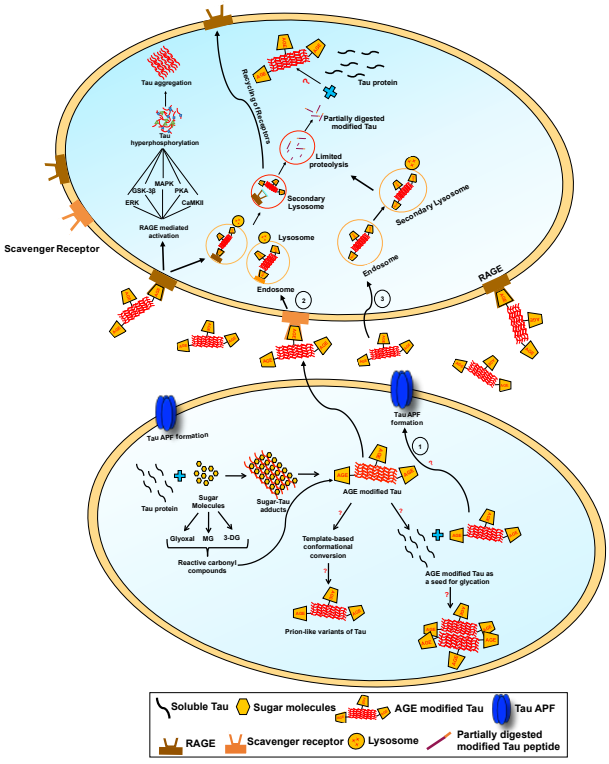

Figure 1.5. Hypothetical trans-cellular spreading of glycated Tau. Tau glycation by sugar molecules as well as its reactive intermediates like glyoxal, methylglyoxal (MG) and 3-deoxyglucosan (3-DG) leads to its cross-linking leading to AGE modified Tau formation. This AGE modified Tau might act as a seed for glycation, converting normal Tau into modified Tau. It can also form prion-like variants of Tau protein by template-based conformational conversion. The AGE modified Tau

(glycated Tau) might show its propagation by various modes. 1. Modified Tau might form membrane structures called annular protofibrils (APF) and propagate itself *via* such membrane pores. 2. The modified Tau can enter the neighboring cells *via* receptor-mediated endocytosis through RAGEs. The AGE modified Tau and RAGE dissociate after fusing with the lysosome. RAGE is recycled back to the membrane whereas the modified Tau is partially digested due to limited proteolysis of protease resistant glycated Tau. These partially digested Tau peptides may act as more potent glycation seeds to glycate the normal Tau thus forming a vicious circle. The activation of RAGE signaling would trigger various kinases (involved in Tau hyperphosphorylation) as shown in the figure and lead to Tau aggregation resulting in further enhancement in Tau pathology. 3. Glycated Tau can also be taken up by bulk endocytosis and propagated in a similar way as shown in the figure. The figure is reproduced from Sonawane *et al.,* JoMN, 2018.

The majority of these belong to the immunoglobulin superfamily class of receptors. The AGEs are internalized by clathrin-dependent or independent mechanisms in the early endosomes where the AGE-RAGE complex is dissolved. The AGE-modified Tau would undergo processing by the endosomal proteases. The protease-resistant glycated Tau may undergo only partial degradation to release the modified peptides, which may act as seed to sequester and modify the endogenous soluble Tau. These partially digested peptides may also be released into the extracellular space, which may affect the neighboring neuron. RAGE activation also leads to triggering of inflammatory pathways which ends in cell death and release of cell contents in the surrounding that may lead to increased exposure of other cells to the modified or partially digested modified Tau. Moreover, since the PTMs alter the surface charge and hydrophobicity of the proteins, modified Tau may form annular rings in the neuronal membranes in a similar way as Aβ. The role of phosphorylation or glycation or both on propagation properties needs to be explored in depth as it may have important consequences on the spread of Tau pathology.

1.7 Tau and neuronal cytoskeleton

Neurons are specialized cells, which carry out the most complicated functions of brain. Like other cell types, neuronal cytoskeleton consists of networks of actin, tubulin and intermediate filaments but these elements form the complex and intricate structures of the neurons, which make them different from other body cell types. Neurons are polarized cells with asymmetric structure. A typical neuron consists of a dominant extension called as the axon and several small dendrites. The coordinated assemblies of these cytoskeletal elements leads to formation of intricate structures like growth cones, filopodia, lamellopodia, synapses *etc*, which assist in neuronal functions. These specialized structures aid in migration, development, plasticity and thus account for the major functions of the neurons. Both the actin and the tubulin cytoskeleton play crucial roles in neuronal functioning. The dynamicity of actin-spectrin cytoskeleton maintains the axon diameter[113]. Axon diameter impacts the transmission of nerve impulses and is subject to variation due to neuronal types, contractility of neuron and active state of neuron. Actin also plays a role in memory and learning as it maintains dendritic spine density[114]. The short half-life accompanied with rapid dynamics helps maintain the morphology and stability of the dendritic spines. Microtubules maintain the gross morphology of neuron to maintain its polarity. It stabilizes the axonal structure, which can be as long as 1 meter. Microtubules also play a major role in neuron development and differentiation, migration and axon guidance.

Microtubule-associated protein as it is called Tau, plays a significant role in assembly and stabilization of the neuronal cytoskeleton. The well-coordinated activities of tubulin and actin cytoskeleton regulate many cellular functions. Tau plays an active role in the coordinated assembly of actin and tubulin networks. Tau not only binds actin and tubulin but also aids their co-assembly without compromising on the growth properties for both the cytoskeletal filaments (Fig. 1.6). The domain-wise mutation analysis suggested that N-terminal is dispensable for the coupled growth and 2 of the 4 repeats are essential for Tau-mediated bridging of the actin and tubulin filaments with one repeat binding to each polymer[115]. To gain a deeper insight into the co-binding mechanisms, NMR studies were employed in

conjunction with electron microscopy and co-sedimentation assays[116]. F-actin consists of a cysteine residue adjacent to its hydrophobic pocket, which is solvent exposed. This hydrophobic pocket acts as binding site for Tau between subdomains 1 and 3 of actin. Tau binds actin *via* conserved mechanisms of other actin binding proteins like cofilin 1 and toxofilin through short stretches of helices separated by flexible linkers in the C-terminal region. Tau contains 7 actin-binding helices and each helix can bind a single actin filament suggesting that single Tau molecule can link 7 actin filaments at a time. Moreover, the two helices lying between 254-290 residues are also essential for the bundling and assembly of actin. Tau interacts with microtubules at tubulin dimer interface with 6 binding stretches of Tau. When Tau is exposed to both F-actin and microtubules there is a competition for 3 binding sites but the remaining 3 binding sites preferentially bind to F-actin. Thus, such interactions with shared and exclusive binding sites of Tau for F-actin and microtubules suggest a multivalent dynamic model of Tau-mediated cross-linking of actin and tubulin cytoskeleton.

Abnormalities in the cytoskeleton of pyramidal neuron were detected in adult human brains in early nineties by mere silver gallyas staining and immunostaining with AT8 antibody. These changes worsened with the Braak stages of AD diagnosis[117]. Several studies thereafter have been focused on the abnormality of actin and tubulin cytoskeleton. Neurodegeneration involves abnormal bundling of actin rods and their accumulation in the neuronal cells, which have multiple implications[118]. Under physiological conditions, cofilin senses the local G-actin concentration and severs the slow growing ends of actin filaments creating barbed ends and increase in actin monomers for new filament formation at required position. Thus, it maintains actin dynamics by polymerizing and depolymerizing the F-actin depending on the regional F-actin concentration. For example, when the concentration of cofilin/actin is at saturation, cofilin leads to F-actin saturation in a twisted form. This enhances bundling and confers stability to F-actin. On the other hand, the non-saturating ratio of cofilin/actin enhances cofilin-mediated severing of F-actin, generating barbed ends, which are involved in F-actin re-organization[119]. Thus, cofilin maintains actin dynamicity at physiological conditions. This process differs mechanistically from abnormal F-actin bundling observed in diseased conditions. For example, in the oxidative environment disuphide bridging occurs between cofilin and ADP-actin forming cofilin-actin rods, which are resistant to depolymerization[120,121].The presence of actin-rich inclusions termed as Hirano bodies have been observed in AD[122]. As already discussed, wild type Tau aids in co-polymerization of F-actin and tubulin but in *Drosophila* AD models especially with the FTDP-17 mutant Tau excess abnormal actin bundling is observed. Moreover, this effect is mediated by hyperphosphorylated Tau and the mutations trigger this aberrant phosphorylation at PHF1 and AT180 sites. The excess stabilization of actin cytoskeleton modulates the downstream pathways-like autophagy and UPR in these models. On the other hand, FTDP-17 mutations and Tau hyperphosphorylation disassemble the tubulin cytoskeleton and trigger Tau aggregation[123]. Additionally, excess activation of cofilin makes it preferentially bind to microtubules and disrupt their assembly by competing with Tau for microtubule binding.

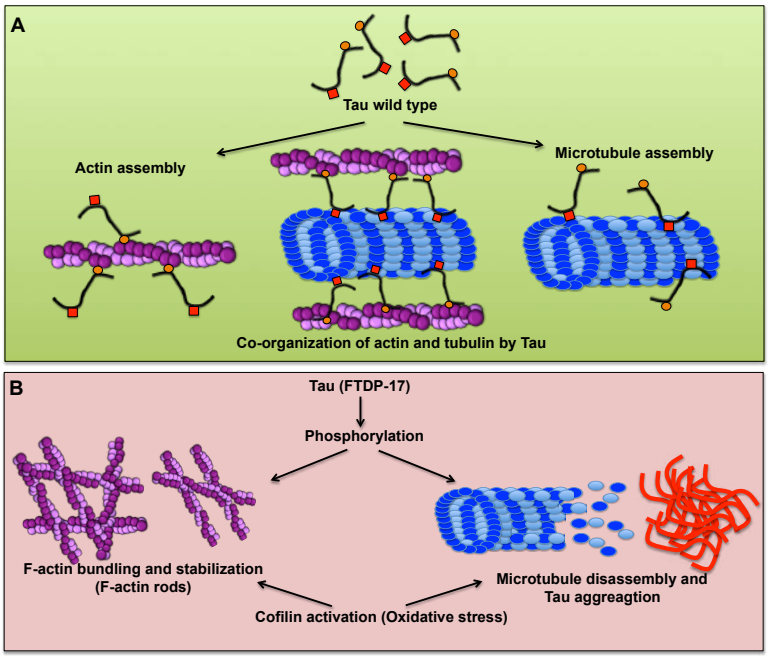

Figure 1.6. Tau-mediated co-assembly of actin and tubulin cytoskeleton A) Tau protein interacts with actin and tubulin to aid in their co-organization. Tau contains several sites of interaction for both F-actin and microtubules. The sites responsible for F-actin binding consist of short segments in the repeat region having helical structure whereas tubulin-binding residues form hairpin structure. B) On the other hand, the FTDP-17 mutations in Tau enhance its phosphorylation. The phosphorylated Tau leads to excess stabilization of actin cytoskeleton leading to F-actin bundling. The phosphorylated Tau loses its affinity for microtubules and detaches from them. This leads to microtubule disassembly and aggregation of dissociated Tau.

Tau also plays a role in specialized neuronal structures such as neurite extensions, growth cone, synapses, axon initial segment, *etc* (Fig. 1.7). Growth cones are the locomotive ends of the axons with regenerating neurites. Axon guidance requires a controlled cross talk between actin and tubulin cytoskeleton at the growth cone[124]. The growth cone migrates with the help of actin-rich structures called lamellopodia and filopodia[125]. It has been recently discovered that Tau is located at the interface of actin and tubulin filaments in filopodia. The depletion of Tau leads to disruption of microtubule bundling and penetration in the filopodia curtailing the interaction between actin and tubulin filaments. This disorients the growth cone directionality and reduces outgrowths[126]. Thus, Tau plays a pivotal role in microtubule bundling at the growth cone periphery and its interaction with actin filaments. Though the function of Tau is almost always associated with microtubules, Tau also functions independently of microtubule- binding. Tau induces neurite outgrowth on stimulation with growth factors like nerve growth factor (NGF), epidermal growth factor (EGF), platelet-derived growth factor (PDGF) and brain-derived neurotrophic factor (BDNF)[127,128]. The growth factor stimulation induces Tau to activate kinases such as mitogen-activated protein kinase (MAPK) and Src kinase. MAPK further activates transcription factor AP-1, which is involved in various cellular processes such as proliferation, differentiation *etc.* The activation of MAPK by Tau requires Tau phosphorylation at T231, which occurs in response to NGF stimulation. Similar Tau-induced morphological plasticity was observed in rat hippocampal neurons on stimulation with BDNF. Tau is known to interact with the SH3 domain of Src. PDGF-stimulation induces Tau to prime Src protein tyrosine kinases, which lead to actin rearrangements and neuritic outgrowths[129]. In the Tau depleted state, growth factor stimulation does not lead to neurite growth. This highlights the role of Tau in neurite growth and plasticity independent of microtubule-binding.

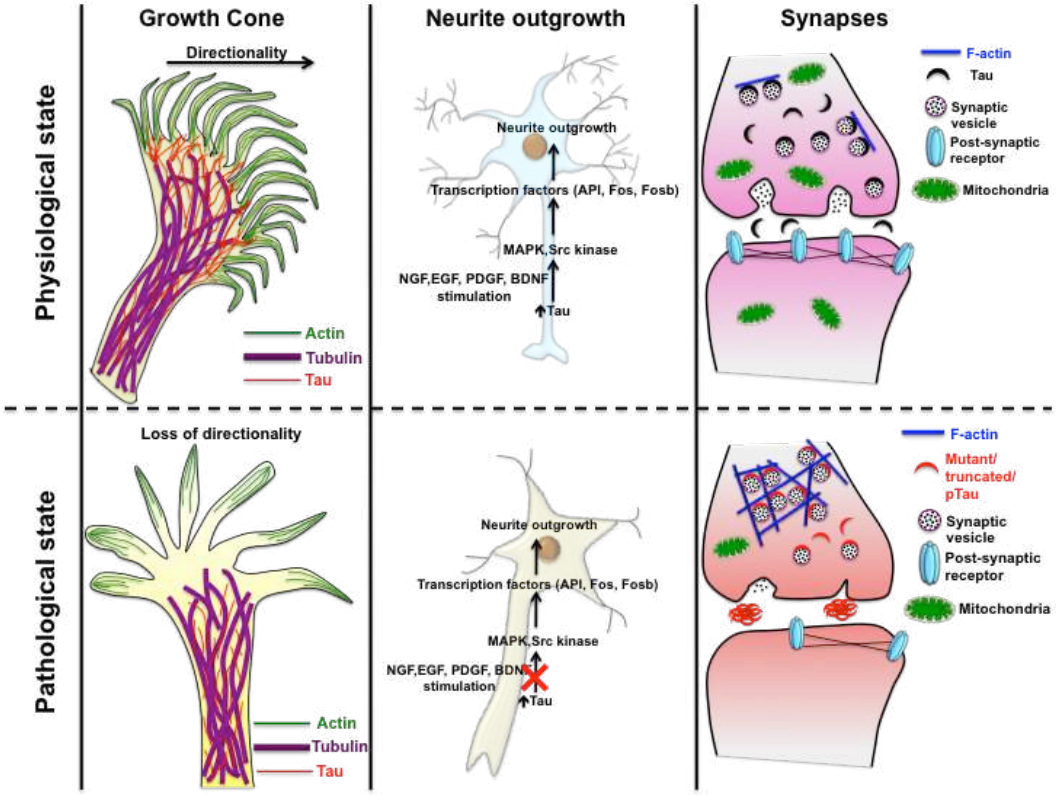

Figure 1.7. Tau and specialized neuronal structures. Growth cones are the locomotive ends of the axons with regenerating neurites. The motility of growth cones is achieved by dynamic actin-rich structures and microtubule cytoskeleton. The interactions between actin and microtubules are mediated by Tau. Tau links the actin filaments and microtubules at the interface in the progressing filopodia structures and aid the directionality of the growth cone. In pathological conditions of decreased Tau levels, the ability of microtubules to penetrate the transition region is hampered resulting in growth cone motility defects and loss of directionality. The intracellular concentration of Tau also plays a key role in enhancing neurite outgrowths. On stimulation with growth factors-like NGF, EGF, PDGF and BDNF, Tau stimulates neuritic extensions *via* activation of kinases such as MAPK and Src, which in turn activate transcription factors involved in neurite extension process. In case of deregulation of Tau levels, the stimulation by growth factors does not activate the downstream signaling and curtails neurite outgrowth. At synapses, Tau regulates the transport and trafficking of mitochondria required for neurotransmitter release. In the extracellular space Tau stimulate mAchR. It also plays a role in maintaining the synaptic density of the receptors. Pre-synaptic Tau interacts with the synaptic vesicles and help in their mobilization. In presence of Tau mutations, phosphorylation or truncation, Tau leads to F-actin bundling and hampers the mobilization of synaptic vesicles and their release.

Synaptic loss and dysfunction is one of the major consequences of AD pathology. Tau has a function in regulating the synapses. Tau at synapses co-ordinate multiple activities. It maintains the pool of mitochondria in the presynaptic terminal in order to energize the neurotransmitter release from vesicles[130-132]. At post-synaptic terminal, Tau traffics mitochondria to the dendritic spines *via* microtubule network. When released in the extracellular space Tau stimulates acetylcholine receptors or gets internalized into the post synaptic terminal[133,134]. Here, Tau plays a role in targeting glutamatergic receptors to the spines and maintains the synaptic density *via* interaction with scaffolding protein PSD95 and Fyn kinase[135-137]. Tau interacts with the presynaptic vesicles *via* its N-terminal and regulates actin-mediated release of vesicles. In the diseased conditions, wherein Tau is hyperphosphorylated or mutated, it abruptly polymerizes actin through its PRD and repeat domain such that the synaptic vesicles are crosslinked to each other[118,138]. This impedes the mobilization of vesicles and their release thus curtailing neurotransmission. Thus, Tau acts as central axis in maintaining neuronal cytoskeleton and the related structures.

1.8 Role of small molecules in ameliorating Tau pathology

The factors leading to Tau pathology and the following consequences make it a very vital target to ameliorate the disease. The pathological transition of Tau proceeds through oligomers, protofibrils, PHFs and NFTs. Though the toxicity of oligomers is more pronounced, the following assemblies also increase the aggregate burden of the cellular clearance machineries. Accordingly, the therapeutics are designed to target these species in order to delay the progression as a complete cure is still under study. Currently, methylene blue and its derivatives are gaining attention due to their potential in inhibiting Tau aggregation *via* cysteine oxidation[139,140]. Moreover, methylene blue could not show memory restoring effect in the transgenic mouse models[141]. The kinase inhibitors and phosphatase activators too did not show promising results due to compromised specificity and efficiency. Epithilone D, an antifungal agent was found to stabilize microtubules and it also recovered cognition defects mouse models[142]. A surplus amount of natural molecules are coming up with potential to alleviate Tau pathology. Oleocanthal from olive oil prevents Tau assembly by covalent modification of Tau[143]. Cinnamaldehyde and proanthocyanidin trimer from cinnamon extract inhibited Tau filament formation without affecting tubulin assembly[144]. Curcumin, isolated from turmeric rhizome *Curcuma longa L.* binds Tau in the microtubule-binding domain and inhibits its oligomerization. Curcumin prevents β-sheet formation in Tau and is also able to dissolve oligomers and filaments[145]. The fungal secondary metabolites azaphilones are more potent in dissolving preformed Tau filaments without affecting microtubule assembly[146]. Recently, the derivatives from neem plant *Azadirachta indica* showed protective effect on various AD pathologies. The intermediate (nimbin) and final (salannin) limnoids showed dual potency in inhibiting Tau aggregation as well as disintegrating the Tau filaments[147]. The basic limnoids gedunin, epoxyazadiradione, azadirone and azadiradione showed multi-target potency. These compounds inhibited aggregation and disassembly of Tau as well as activated the chaperone pathway. Basic limnoids activated heat shock factor (HSF1), a transcription regulator of stress-responsive genes in HEK293T cells. HSF1 activation led to its accumulation in nucleus and increased expression of chaperone Hsp70[148]. Hsp70 is involved in many protein folding processes including refolding of misfolded proteins. Thus, limnoids show promising results for future Tau therapeutics. Another important ayurvedic herb brahmi (*Bacopa monnieri*) has been implicated in neuroprotection and suggested to be an efficient candidate for Tau pathology[149]. Interestingly, in addition to plant compounds and fungal metabolites, a neurohormone melatonin also plays a role in AD[150]. Melatonin, secreted from pineal gland and other non-pineal sites maintain circadian rhythms in organisms. In case of Tau, melatonin inhibits aggregation of Tau but more efficiently dissolves the Tau fibrils[151]. Melatonin prevented membrane roughness induced by Tau aggregates thus, maintaining the membrane morphology[152]. Another class of molecules playing large role in cellular processes, polyamines, have been studied in protein misfolding diseases-like AD and PD. Mammals synthesize two polyamines, spermine and spermidine from precursor putrescine. The levels of polyamines are found to decline with age[153]. Polyamines have been studied for their effect on Aβ and α-synuclein aggregation and have been reported to enhance the aggregation of these proteins[154,155]. The effect of polyamines on Tau is under investigation. The molecules of synthetic origin are also finding their way as Tau therapies. Aminothienopyridazine compounds have been screened *via* high-throughput screening and found to be potent Tau inhibitors[156]. Anthraquinones, another class of compounds inhibited PHF assembly and dissolved PHF with equal potency. The compounds showed potency in preventing Tau aggregation in the neuroblastoma cells[157]. Metals are generally related to Tau toxicity but new studies with cobalt metal complexes yielded contrasting results. The cobalt-based metal complexes not only prevented *in vitro* Tau aggregation but also prevented the toxicity in neuroblastoma cells[158]. Another unique approach to AD therapy is employment of photodynamic treatment. The photo-excitation of two dyes toluidine blue and rose bengal has been reported to successfully prevent Tau aggregation *in vitro*[159]. Moreover, they reduced ROS levels in neuronal cells and restored memory in a *Drosophila* model of AD[160]. This current work focuses on polyphenolic molecules namely Baicalein and EGCG on Tau pathology in AD.

Baicalein is known to have several disease alleviating roles in cancer, inflammation, and cardiovascular disorders. Baicalein has shown dual effect on α-synuclein aggregation and disassembly[161]. It prevented Aβ-mediated pathology in the transgenic mouse model[162]. EGCG, an active component of green tea is implicated in a repertoire of disorders[163]. EGCG also plays preventive role in protein misfolding. It inhibits aggregation of transthyretin and islet amyloid polypeptide involved in peripheral neuropathy and type-2 diabetes respectively[164]. It also prevented aggregation of prion protein and Aβ involved in Scrapie and AD respectively[165,166]. AD manifests due to dysfunction of various cellular processes (Fig. 1.8). The Aβ forms senile plaques as well as induces glutamate excitotoxicity due to excess release of glutamte[167]. The excess neuron firing leads to neuronal death[168]. Baicalein protects the effects of excitotoxicity in primary rat cortical neurons probably by acting as antagonist of AMPA and NMDA receptors[169]. Both the polyphenols are found to suppress the formation of plaques from the sticky Aβ peptide. AD involves various cellular stresses, which generates excessive reactive oxygen species. The ROS mediates abnormal post-translational modifications of Tau such as glycation and hyperphosphorylation ultimately leading to Tau aggregation. EGCG is a well-known antioxidant and protects against the deleterious effects of the ROS[170]. EGCG prevents Tau hyperphosphorylation as well as aids in clearance of the hyperphosphorylated Tau from primary neurons[171,172]. The cellular stress causes mitochondrial dysfunction resulting in disturbed mitochondrial membrane potential (MMP), decreased ATP and increased ROS levels[173,174].

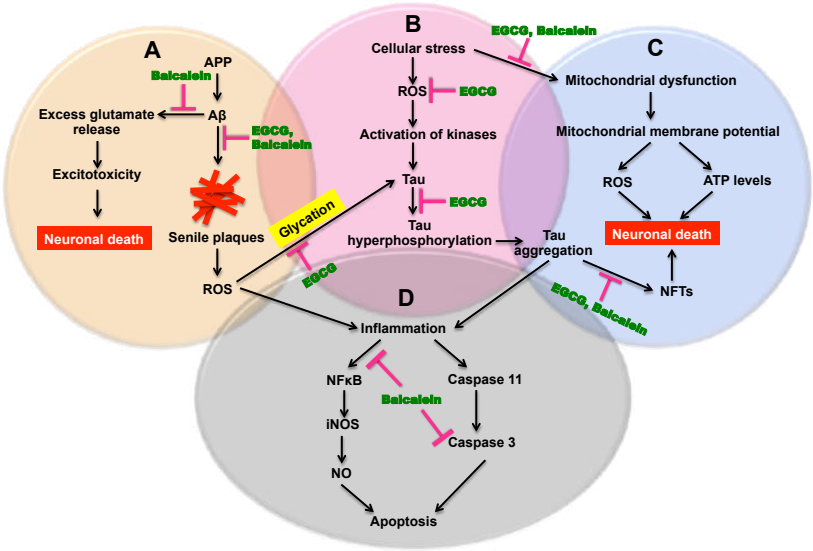

Figure 1.8. Polyphenols cascades in AD (Baicalein and EGCG). A) The amyloid beta cascade in AD leads to formation of senile plaques and their deposition generating ROS. The excess Aβ leads to excitoxicity and neuronal death *via* increased release of glutamate neurotransmitter. Baicalein prevents the Aβ-mediated release of glutamate and EGCG and Baicalein prevent the formation of the senile plaques. B) The cellular stress generates ROS, which activate series of kinases that cause Tau hyperphosphorylation leading to its aggregation. ROS is also responsible for Tau glycation, which enhances its aggregation. EGCG acts at multiple levels to prevent ROS damage, Tau glycation and Tau hyperphosphorylation. C) The cellular stress leads to mitochondrial dysfunction deregulating the mitochondrial membrane potential, ATP levels and ROS generation causing neuronal death. The polyphenols, Baicalein and EGCG prevent the mitochondrial dysfunction thus, preventing cell death. D) The ROS and Tau aggregation increases inflammation, giving rise to activation of NF-κB leading to nitric oxide production and activation of caspases-like caspase 11 and caspase 3. The nitric oxide and the caspases together lead to apoptosis of neuronal cells. Baicalein inhibits this inflammation-mediated neuronal death and prevents neurodegeneration.

Mitochondrial dysfunction triggers abrupt apoptosis leading to neuronal death. Both the polyphenols act at multiple steps in this cascade and prevent cells from degeneration[175]. An important consequence of ROS and accumulation of Tau aggregates is induction of inflammatory response, which activates apoptosis *via* various pathways including excess production of nitric oxide in response to activated

nitric oxide synthase[176]. Inflammation activates the cascade of caspases triggering apoptosis. Baicalein inhibits NO production by inhibiting NF-κB activation[177,178]. Thus, to deal with AD pathogenesis, molecules with potency against multiple targets are of utmost importance.

Materials and Methods

1.0 Materials

1.1 List of chemicals and cell growth media

Sr. No	Chemical/Reagent/Media	Company/Suppliers
1.	3-(4, 5-dimethylthiazol-2-yl)-2, 5-diphenyltetrazolium bromide (MTT reagent)	Sigma
2.	4′,6-diamidino-2-phenylindole (DAPI reagent)	ThemoFisher Scientific
3.	8-Anilinonaphthalene-1-sulfonic acid (ANS dye)	Sigma
4.	Acrylamide	Invitrogen
5.	Advanced DMEM F12	Invitrogen
6.	Agarose	Invitrogen
7.	Ammonium acetate	MP Biomedicals
8.	Ammonium persulphate (APS)	MP Biomedicals
9.	Ampicillin	MP Biomedicals
10.	Baicalein	Sigma
11.	BES	Sigma
12.	Bicinchoninic acid	Sigma
13.	Bis-acrylamide	Invitrogen
14.	Bovine Serum Albumin (BSA std)	Sigma
15.	Bradford Reagent	Bio-Rad
16.	Bromophenol blue	MP Biomedicals
17.	Calcium chloride dihydrate	Sigma
18.	Clarity™ Western ECL Substrate	Bio-Rad
19.	Coomassie brilliant blue R-250	MP Biomedicals
20.	Copper sulfate (II)	Sigma
21.	Dimethyl sulfoxide (DMSO)	Life Tech /MP biomedicals
22.	Dithiothretol	Calbiochem
23.	Dulbecco's Modified Eagle Medium (DMEM)	Invitrogen
24.	EnzChek™ Caspase-3 Assay Kit	Thermo Scientific
25.	Epigallocatechin-3-gallate (EGCG)	Sigma
26.	Ethanol	MP Biomedicals
27.	Ethylene glycol tetraacetate (EGTA)	MP Biomedicals
28.	Fetal Bovine Serum	Thermo Fisher
29.	Formaldehyde	MP Biomedicals
30.	Gel Loading Dye (6X) (For DNA)	New England Biolabs
31.	Glacial acetic acid	MP Biomedicals
32.	Glycerol	MP Biomedicals
33.	Glycine	Invitrogen
34.	Guanidinium HCl	Invitrogen
35.	Heparin (MW~17500 Da)	MP Biomedicals
36.	Horse serum	Invitrogen
37.	Imidazole	MP Biomedicals
38.	IPTG	MP Biomedicals
39.	Isopropanol	MP Biomedicals
40.	Lactate dehydrogenase release assay kit	Thermo Scientific
41.	L-glutamine	Invitrogen
42.	LB Broth	Invitrogen/HiMedia
43.	LB Agar	Invitrogen
44.	Magnesium chloride hexahydrate	MP Biomedicals
45.	Magnesium sulfate heptahydrate	MP Biomedicals
46.	MES hydrate	Sigma
47.	Methanol	MP Biomedicals

48.	Methyl glyoxal (MG)	Sigma
49.	Nucleospin Plasmid DNA isolation kit	Machery Nagel
50.	Paraformaldehyde	Invitrogen
51.	Penicillin-Streptomycin	Invitrogen
52.	Polysorbate 20	MP Biomedicals
53.	Polyvinylidene fluoride membrane	Merck Milipore
54.	Potassium acetate	MP Biomedicals
55.	Potassium chloride	MP Biomedicals
56.	Potassium phosphate dibasic trihydrate	MP Biomedicals
57.	Potassium phosphate dibasic trihydrate	MP Biomedicals
58.	Potassium phosphate monobasic anhydrous	MP Biomedicals
59.	Protease inhibitor Cocktail	Roche
60.	Precision Plus ProteinTM Dual Color Standards	Bio-Rad
61.	RIPA buffer	Thermo Scientific
62.	Sinapinic acid	Sigma
63.	Sodium acetate trihydrate	MP Biomedicals
64.	Sodium azide	MP Biomedicals
65.	Sodium bicarbonate	MP Biomedicals
66.	Sodium carbonate anhydrous	MP Biomedicals
67.	Sodium chloride	MP Biomedicals
68.	Sodium dodecyl sulfate	Sigma
69.	Sodium hydroxide	MP Biomedicals
70.	Sodium MOPS	MP Biomedicals
71.	Sodium phosphate dibasic anhydrous	MP Biomedicals
72.	Sodium phosphate monobasic mono hydrate	Sigma
73.	Sodium thiosulfate pentahydrate	MP Biomedicals
74.	Spermidine	Sigma
75.	Spermine	Sigma
76.	SYBR Safe	Invitrogen
77.	Tetrafluoroacetic acid	Sigma
78.	Tetramethylethylenediamine	Invitrogen
79.	Thioflavin S	Sigma
80.	Thioflavin T	Sigma
81.	Terrific broth	Invitrogen
82.	Tris base	Biorad
83.	Tris HCl	Invitrogen
84.	Triton X 100	Sigma
85.	Trypan blue	Invitrogen
86.	Trypsin-EDTA	Invitrogen

1.2 List of antibodies

Sr. No	**Antibodies**	**Company/Suppliers**
1.	Anti-AGE (Advanced Glycated End-products) Antibody goat polyclonal (AB9890)	Merck Milipore
2.	Alpha-Tubulin (ab176560)	Abcam
3.	Beta-actin loading control (MA515739)	ThermoFisher Scientific
4.	Donkey anti goat IgG Hand L (HRP) (ab6885)	Abcam
5.	EB1Monoclonal Antibody (KT51)	ThermoFisher Scientific
5.	Goat anti-mouse - alexa fluor 555 (A28180)	ThermoFisher Scientific
6.	Goat anti-mouse IgG HRP (32430)	ThermoFisher Scientific
7.	Goat anti-rabbit - alexa fluor 488 (A-11008)	ThermoFisher Scientific

8.	Goat anti-rabbit IgG HRP (31460)	ThermoFisher Scientific
9.	Pan Tau (K9JA) (A0024)	Dako
10.	Phospho-Tau (Thr212, Ser214) (MN1060)	ThermoFisher Scientific
11.	Rabbit anti-Goat IgG - Alexa Fluor 594 (A27016)	ThermoFisher Scientific

1.3 Laboratory Instruments and Equipment

Sr. No	**Instrument/Equipment**	**Suppliers**
1.	AKTA Pure FPLC system	GE Healthcare
2.	AKTA Start FPLC system	GE Healthcare
3.	Amersham Imager 600	GE Healthcare
4.	Amersham Semi Dry blotting apparatus	GE Healthcare
5.	Analytical weighing balances	Mettler Toledo
6.	Autoclave	Spire
7.	Avance III HD 700 MHz NMR spectrometer equipped with TXI probe	Bruker
8.	Avanti JXN26 High speed Centrifuge	Beckman Coulter
9.	BioSafety cabinet/Clean bench	Thermo Fisher Scientific
10.	CO2 incubator	Thermo Fisher Scientific
11.	Dry bath	Genei
12.	Elyra 7 with Lattice SIM microscope	Zeiss
13.	Far-UV CD spectrometer J-815	Jasco
14.	Forma 900 series -80°C	Thermo Scientific
15.	Gel rocker	Benchmark
16.	Heratherm Hot Air Oven	Thermo Scientific
17.	Heraeus Incubator	Thermo Scientific
18.	High Speed Centrifuge 5804R	Eppendorf
19.	Homogenizer	Constant Systems Ltd.
20.	Laminar Air Flow	Microfilt
21.	Magnetic Stirrer	Genei
22.	Microcentrifuge 5418 R	Eppendorf
23.	MicroCal PEAQ-ITC	Malvern
24.	MiliQ Unit Direct 16	Millipore
25.	Microplate reader Infinite 200 PRO	Tecan
26.	Miniprotean Tetra vertical electrophoresis system	Biorad
27.	MiniVE Vertical electrophoresis System	Amersham
28.	MiniVE Horizontal agarose electrophoresis System	Amersham
29.	MiniSpin Plus Table top centrifuge	Eppendorf
30.	Molecular Imager Gel Doc™ XR+	BioRad
31.	Optima XPN10 Ultracentrifuge	Beckman Coulter
32.	pH meter Five Easyplus	Mettler Toledo
33.	Shaker Incubator (H1010-MR)	Benchmark Scientific
34.	Shaker Incubator Multitron Standard	Infors HT
35.	SimpliNano (Nanodrop)	GE Healthcare
36.	T20 Transmission Electron Microscope	Tecnai
37.	UV-Visible spectrophotometer V-530	Jasco
38.	Vacuum Pump	Millipore
39.	Vortexer mixer	Genei
40.	Water bath	Genei
41.	Zeiss Axio observer 7 microscope with Apotome 2.0	Zeiss

1.4 Software's

Sr. No	Software	Developer
1.	ImageJ /Fiji	NIH
2.	Image Lab	BioRad
3.	ImageQuant TL	GE
4.	Magellan™ Data analysis software	Tecan
5.	MicroCal PEAQ-ITC analysis software	Malvern
6.	Sigma Plot 10.0	Systat softwares
7.	Spectra Manager™	Jasco
8.	Topspin 3.2	Bruker
9.	Zeiss Imaging Software	Zeiss
10.	Zeiss Image processing Software	Zeiss

1.5 Bacterial strains

DH5 α, BL21*, pLysE

1.6 Mammalian cell lines

Neuro2a (CCL-131)-ATCC

2.0 Methods

2.1 Preparation of competent cells (Chemical method)

In order to be replicated and expressed, the plasmid DNA (containing the gene for protein of interest) needs to be transformed into the bacterial host cells. But plasmid DNA cannot enter the host cell by itself and requires assistance to traverse the bacterial membranes. Thus, the host cells are made competent to take up the plasmid DNA by modulating their cell wall *via* chemical and physical methods. Competent cells have a higher affinity for binding and uptake of DNA. The chemical method of making the cells competent involves use of divalent cations such as Ca^{+2}, which reduces the repulsion between like charged bacterial membranes and the plasmid DNA. It helps the adsorption of DNA on the bacterial membrane and facilitates its uptake.

Buffers

1. Transformation buffer I (freshly made) pH 5.8

100 mM KCl
300 mM $K^{+}CH_3COO^{-}$
10 mM $CaCl_2$
15% Glycerol
50 mM $MnCl_2.4H_2O$

2. Transformation buffer II pH 7.0

10 mM KCl
10 mM NaMOPS
75 mM $CaCl_2.H_2O$
15% Glycerol

Protocol

1. The Luria agar (LA) plate with the culture of the required cells (DH5 α, BL21*, pLysE) was streaked and incubated at 37°C overnight to obtain isolated colonies.
2. The single isolated colony was carefully picked up and inoculated into 5 mL of Luria broth (LB) and allowed to grow at 37°C in an shaker incubator overnight.

3. Next day, the overnight grown culture was re-inoculated into 250 mL of fresh LB (1:100 dilution) and incubated at 37°C at 200 rpm. The O.D at 600 nm was monitored till it reached 0.5 approximately.
4. The culture was cooled on ice for 15 minutes and centrifuged in sterile, pre-chilled centrifuge bottles at 4°C for 10 minutes at 4500 rpm.
5. The supernatant media was discarded and the pellet was gently resuspended in 30 mL of cold transformation buffer I. The suspension was incubated on ice for 60-90 minutes.
6. The cells were pelleted at 4°C for 5 minutes at 4500 rpm. The supernatant was discarded and the cells were resuspended in 2 mL cold transformation buffer II.
7. The competent cells were aliquoted as 50-100 µL and stored at -80 °C.

2.2 Transformation of the competent cells with plasmid DNA

The competent cells have an altered cell wall, which helps the adsorption of the DNA on the cell wall. In order to facilitate the entry of this DNA two methods are employed; the native heat-shock method and electroporation. The brief heat shock to the competent cells incubated with the plasmid DNA transiently makes the bacterial cell wall permeable to the DNA and allows the uptake of DNA in the cytosol. The electroporation method involves exposure of competent cells to a brief pulse of high-voltage electric field, which induces temporary pores in the cell membranes and helps the uptake of DNA.

SOC media

2% Tryptone
0.5% Yeast extract
10 mM NaCl
2.5 mM KCl
10 mM $MgCl_2$
20 mM Glucose
10 mM $MgSO_4$

Protocol

1. A vial of competent cells from the -80°C storage was placed on ice for 20 minutes.
2. The plasmid DNA carrying the gene of interest was added to the competent cells and incubated for 30-40 minutes on ice.
3. A brief heat shock was given to the cells for 90 seconds at 42 °C and cells were re-incubated on ice for 5 minutes.
4. The SOC media was added to the cells (750-1000 µL) and the cells were incubated in a shaker incubator at 37 °C for 1 hour.
5. The cell suspension was plated on the LA plate containing specific antibiotic for the plasmid and incubated overnight at 37 °C.
6. The transformed cells were visualized as the single pinpoint colonies on the antibiotic containing agar plate, which could be used for the further scale-up cultures.

2.3 Plasmid isolation and purification

The most common and efficient strain of *E.coli* employed to increase the copy number of plasmids is DH5α. This strain has 3 mutations; recA, which inhibits its recombinase activating preventing homologous recombination, endA1, inhibits the endonucleases thus preventing the degradation of the transformed plasmid DNA and lacZM15, which aids in blue-white screening. The isolation and purification of the plasmid from the transformed cells involves three basic steps; growth of bacterial culture, bacterial lysis and purification of plasmid. The growth of bacterial culture involves inoculation of a single isolated transformed colony from the agar plate into the LB, which is grown overnight. The lysis of the cells can be carried out by various methods using detergents, heat, organic solvents and alkali. The lysis method to be employed depends on the plasmid size, *E.coli* strain and the subsequent technique utilized for the plasmid purification. For a smaller plasmid size of <15kb severe methods like alkaline lysis could be utilized as the chances of plasmid shearing are minimum. We utilized alkaline lysis miniprep method for the purification of plasmid by the kit method (Machery Nagel). These

methods lyse the bacterial cells by lysis buffer containing SDS and NaOH. In addition to disrupting the cell wall and cell membrane, this method disrupts the base pairing of the DNA and shearing of the chromosomal DNA of the host cells. The plasmid DNA is spared from the shearing due to its closed circular nature. Further, the renaturing conditions allow the complete reformation of the super helical plasmid DNA molecules. The sheared chromosomal host DNA and the other cell debris are precipitated and separated by centrifugation. The plasmid DNA is subjected to the ethanolic precipitation and bound to the silica columns which is eluted either in buffer or ultrapure MilliQ water.

Protocol

1. An isolated colony of the transformed DH5α cells was inoculated in the 5 mL of LB media containing appropriated antibiotic. The culture was incubated at 37°C in a shaker incubator for overnight growth.
2. The cells were pelleted down by brief centrifugation at room temperature and resuspended in 250 µL Buffer A1. The tube was thoroughly vortexed to avoid the clumps of the cells.
3. The Buffer A2 was thoroughly mixed to dissolve any precipitated SDS before adding to the reaction tube. 250 µL of Buffer A2 was added to the tubes and mixed gently by inverting the tube several times. The gentle mixing ensures that the genomic DNA is not sheared. The mixture was let to stand till the lysate was clear.
4. Next, 300 µL Buffer A3 was added and the contents were mixed until the sample turned from blue to colorless completely.
5. The lysate was clarified by centrifugation at 11000*g* for 5 minutes at room temperature and the supernatant was separated.
6. The NucloSpin columns were placed in the collection tubes and the clarified supernatant was added to the column. The collection tube with column was centrifuged for 1 minute at 11000*g*. The flow through was discarded and the column was washed with Buffer AW.
7. Buffer A4 (supplemented with ethanol) was added to the washed column and centrifuged for a minute at 11000*g*. The flow through was discarded and the column was placed in a fresh collection tube.
8. The plasmid DNA was eluted in 50-µL warm TE buffer by centrifuged at 11000*g* for 1 minute. The plasmid concentration was measured by nanodrop and the quality was analyzed by agarose gel electrophoresis.

2.4 Agarose gel electrophoresis

The nucleic acids are resolved based on their size, charge and the conformation on the agarose gel under the electric field. The level of resolution is determined by the pore size of the agarose gel, which is obtained by various percentages of the gel. In addition to resolving the nucleic acids agarose gel electrophoresis also helps determine the molecular weights of the nucleic acids with respect to a specific DNA/RNA ladder. The supercoiled plasmid DNA migrate more as compared to the linear DNA molecules. Thus, it also helps to determine the quality of the DNA molecule under study.

Reagents

1. 50X TAE Buffer

Sr. No.	Reagent	Molarity (in 50X)	Amount/Volume for 100 mL buffer
1.	Tris	2M	24.2 g
2.	Acetic acid	1M	5.7 mL
3.	EDTA	50 mM	10 mL from 0.5 M stock

2. 1 % agarose gel

0.5 g of agarose was weighed and dissolved in 1X TAE buffer by heating the solution. After complete dissolution SYBR safe dye was added to the solution and the gel was poured onto the casting tray with appropriate comb for sample wells.

Protocol

1. The casting tray with solidified agarose gel was placed in the buffer tank and 1X TAE was added to the buffer tank.
2. The plasmid samples were diluted in 6X gel loading dye and added to the wells of the agarose gel. The DNA molecular weight ladder was also added in one of the wells.
3. The electrophoresis was carried out by applying the current till the dye front migrated around 80% of the gel length.
4. The agarose gel was placed in UV light in a gel imager for visualization of the plasmid DNA.

2.5 Protein expression

2.5.1 Mini-induction method

The expression of Tau proteins was carried out in the *E.coli* expression strain BL21* or pLyseE. BL21* has a DE3 lysogen which expresses T7 RNA polymerase under the *lac*UV5 promoter. This enables the BL21* to express high amount of proteins which are encoded by genes under T7 promoters. Moreover, the mutation in the RNAse E gene of the strain aids in enhanced stability of mRNA transcripts, which results in high protein yields. The degradation of the heterologous protein is prevented due to absence of *lon* and *OmpT* (outer membrane) proteases. pLyseE expression strain has a T7 RNA polymerase gene on the host chromosome under the *lac*UV5 promoter which gives enhanced expression of protein of interest on IPTG induction. Additionally pLyseE strain has T7 lysozyme encoded on the plasmid, which reduces basal expression of protein of expression by the T7 RNA polymerase. The expression of protein of interest is carried out by IPTG, which is an analog of lactose called allolactose. Allolactose cannot be metabolized by the cells and thus helps to have a constant expression of the protein as opposed to lactose, which is readily metabolized by the cells.

Protocol for mini-induction of Tau proteins

1. The plasmids encoding Tau proteins (wild type and mutants) were transformed into the *E.coli* expression strains BL21* and pLyseE (hTau40 231/262D) respectively and a single isolated colony was inoculated in 10 mL of the LB media containing amplicillin (100 µg/ml).
2. The tubes were incubated at 37 °C shaker incubator until the O.D at 600 nm reached around 0.6. 2 mL of the uninduced culture was collected and IPTG at a final concentration of 0.5 mM was added to the remaining culture.
3. The induction was carried out for 4 hours at 37 °C in a shaker incubator after which 2 mL of the culture was taken into a centrifuge tube. Both the uninduced (UI) and induced (I) cultures were pelleted down and lysed in MES buffer with rigorous vortexing.
4. The crude lysates for UI and I were mixed with lammelli buffer and heated at 90°C for 10 minutes. The samples were separated onto 10% SDS-PAGE to check for the induction.
5. The colonies with high levels of expression were selected and glycerol stocks were made accordingly for further use.
6. The stocks were stored at -80 °C till further use.

2.5.2 Scale-up Tau protein preparation

Tau is a natively unfolded protein with an overall positive charge. The purification of the recombinant Tau is thus based on heating the cell lysate to separate out the other structured proteins. Further, the charged-based purification is carried out by cation exchange chromatography, which binds the positively charged Tau that is further eluted by salt ionic gradient.

Reagents

1. Cell lysis buffer pH 6.8	**2. Dialysis buffer pH 6.8**
50 mM MES	20 mM MES
1 mM EGTA	50 mM NaCl
2 mM $MgCl_2$	1 mM EGTA
5 mM DTT	1 mM $MgCl_2$
1 mM PMSF	2 mM DTT
Protease inhibitor cocktail	0.1 mM PMSF

Ion Exchange Chromatography buffers

Sepharose Buffer A pH 6.8	Sepharose Buffer B pH 6.8
20 mM MES	20 mM MES
50 mM NaCl	1 M NaCl
1 mM EGTA	1 mM EGTA
1 mM $MgCl_2$	1 mM $MgCl_2$
2 mM DTT	2 mM DTT
0.1mM PMSF	0.1 mM PMSF

Size-Exclusion Chromatography (SEC) buffer
10 X Phosphate buffered saline stock (1000 mL) pH 7.4

Molarity	Quantity
1.37M NaCl	80 g
27 mM KCL	2 g
100 mM Na_2HPO_4	14.2 g
18 mM KH_2PO_4	2 g

Size-Exclusion Chromatography buffer
1X Phosphate buffered Saline pH 7.4 2 mM DTT

Protocol

1. The primary inoculum for the transformed *E.coli* expression strains was obtained by inoculating the glycerol stock into the 100 mL OF LB media containing ampicillin (100 µL/mL) and incubating at 37 °C in a shaker incubator overnight. The secondary culture (6L) was inoculated from the primary inoculum (1:100) and incubated at °C in a shaker incubator till O.D reached around 0.6.
2. The culture was induced with 0.5 mM IPTG and incubated for 4 hours at 37 °C in a shaker incubator. After the induction period, the cells were harvested by centrifugation at 4500 rpm for 10 minutes at 4 °C.
3. The cell pellet was resuspended in the lysis buffer and vortexed to disrupt all the clumps of the cells and to obtain a homogenous suspension. The cell lysis was carried out under high pressure (15000 psi) in a microfluidic cell disruptor device.
4. The cell lysate was collected and supplemented with 0.5 M NaCl and 5 mM DTT. This lysate was heated at 90 °C for 20 minutes and cooled down before centrifugation. The heating step allows the denaturation and precipitate of the structured proteins and aids their separation from natively disordered Tau protein.
5. The cooled lysate was further centrifuged at 40,000 rpm in an ultracentrifuge for 50 minutes at 4°C. The supernatant containing the Tau protein was carefully separated and subjected to dialysis overnight with a single buffer change. Next, the dialyzed sample was subjected to ultracentrifugation to ensure removal of particulate or precipitated matter if any.
6. For ion exchange chromatography the Sepharose fast flow manually packed 24 mL column was equilibrated with the Sepharose buffer A pH 6.8. The centrifuged lysate was filtered prior to loading on the column.
7. After, the binding column was washed thoroughly with Sepharose buffer A pH 6.8 to remove any non-specific weakly bound proteins. Tau protein was eluted with a linear gradient of Sepharose buffer B pH 6.8 with 1M NaCl. The fractions under the peak were pooled and concentrated and preceded for the size-exclusion chromatography.
8. The SEC was carried out in Hi-Load Superdex 75 pg (16/600) column in SEC buffer. The fractions obtained were concentrated and the protein concentration was estimated by

Bicinchoninic Acid (BCA) assay. The concentrated protein was aliquoted and snap frozen and stored in -80 °C.

2.5.3 ^{15}N Labelling and purification of repeat Tau

The repeat Tau protein lacks the N-terminal projection domain and the C-terminal tail. It consists of only 4 functional repeats of Tau protein, which is utilized in various studies. For NMR studies, the repeat Tau was employed which was labelled with heavy isotope of nitrogen ^{15}N to obtain an NMR signal. The method of purification was followed in a similar way as for unlabeled recombinant Tau mentioned in ***2.4.2***. our lab reference need to be included!

Reagents

1) 5X M9 salts (autoclaved) pH 7.2

Salt	**Quantity (100mL)**
KH_2PO_4	1.5g
Na_2HPO_4	3g
NaCl	0.25g
NH_4Cl (^{15}N labelled)	0.5g

2) 1X M9 salts unlabeled (autoclaved) pH 7.2 1000 mL

Salt	**Quantity (1000mL)**
KH_2PO_4	3g
Na_2HPO_4	5g
NaCl	0.5g

3) 1M $MgSO_4$ (autoclaved)

4) 1M $CaCl_2$ (autoclaved)

5) 20% Glucose (filter sterilized)

6) 5 mg/mL Thiamine hydrochloride (filter sterilized)

5) Minimal Growth Media (1.5 L)

5X M9 Salts	300 mL
D- Glucose	30 mL
Thiamine hydrochoride	9 mL
1M $MgSO_4$	3 mL
1M $CaCl_2$	150 µL

Protocol

1. The E.coli expression strain was grown in LB with suitable antibiotic (1L X 6 flasks) at 37 °C till the O.D reaches 5.5 to 6 at 600 nm.
2. The cells were pelleted down at 5000*g* for 30 mins. The pellet was washed with unlabeled 1X M9 salts (without carbon and nitrogen source).
3. The pellet was resuspended in minimal media + antibiotic (1.5 L minimal media for 6L pellet in LB). The culture was incubated in minimal media at 37 °C for one hour for recovery of growth and clearance of unlabeled metabolites.
4. The induction was carried out with IPTG (0.5mM for Tau) and incubated at 37 °C for 4 -5 hours.
5. The cells were harvested and preceded for the protein preparation.

2.6 Methods for estimation of the protein concentration

The estimation of protein concentration is an essential step before proceeding for any further biophysical and biochemical analysis. The different types of methods available include Biuret method, UV absorption, BCA assay, Bradford assay and Lowry assay. All these methods differ in the sensitivity of protein detection but work on the common basis of the presence of aromatic amino acids in the protein. We utilized BCA assay for the estimation of recombinant Tau proteins and Bradford assay for the estimation of the protein content in the mammalian cell lysates.

2.6.1 Bicinchoninic Acid (BCA) assay

It is a highly sensitive method for protein estimation and detects proteins at a lower concentration of 1 µg. This method works on the principle of binding of copper ions to the Nitrogens in the protein which further form complex with Bicinchoninic acid which gives purple color, the intensity of which depends on the concentration of protein. The method is especially useful for estimation of Tau protein as it lacks the tryptophan residues, which is an essential requirement for other protein estimation methods.

Reagents

1. 1 mg/mL BSA protein standard (Sigma)
2. Bicinchoninic acid solution (Sigma)
3. CuSO4 solution (Sigma)
4. Ultrapure MilliQ water

Protocol

1. The BSA standards are prepared in duplicates in ultrapure MilliQ water as given in the table.
2. Tau protein is diluted in ultrapure MilliQ water (1:50, 1:100 and 1:200) in duplicates
3. The BCA: $CuSO_4$ (50:1) reagent is calculated and prepared freshly 200 µL per sample.
4. 25 µL of standards and protein dilutions are thoroughly mixed with 200 µL of the BCA reagent and added to 96 well plate. The plate is incubated at 37 °C for 1 hour.
5. The absorption is measured at 562 nm in a plate reader and the concentration is obtained from the BSA standard graph in MS Excel spreadsheet.

Sr.No.	BSA (µg/mL)	BSA (µL)	Water (µL)
1	0	0	25
2	5	1.5	23.5
3	10	2.5	22.5
4	15	3.75	21.25
5	20	5	20
6	25	6.25	18.75

2.6.2 Bradford's assay for protein estimation

Bradford's assay is a sensitive dye-binding method that works on the principle of binding of Coomassie brilliant blue G-250 dye to the negatively charged carboxyl groups of protein molecules which leads to deprotonation of the dye and formation of the blue color.

Reagents

1. 1 mg/mL BSA protein standard (Sigma)
2. Bradford's reagent (Sigma)
3. Ultrapure MilliQ water

Protocol

1. The BSA standards are prepared in duplicates in ultrapure MilliQ water as given in the table.
2. The mammalian cell lysates are diluted 1:10 in ultrapure MilliQ water in duplicates.
3. The Bradford reagent was diluted 1:4 in water and filtered prior to use. 10 µL of the standards and lysate dilutions were mixed with 200 µL of the reagent and added to the 96 well plate.
4. The plate was incubated in dark for 5 minutes at room temperature and the resding was taken in a plate reader at 595 nm. The concentration was determined from the standard BSA graph in MS Excel spreadsheet.

Sr.No.	BSA (µg/mL)	BSA (µL)	Water (µL)
1	0	0	10
2	5	0.5	9.5
3	10	1	9
4	15	1.5	8.5
5	20	2	8.0
6	25	2.5	7.5

2.6 Tau aggregation and glycation assays

2.6.1 Tau aggregation assay

Reagents

Component	Stock concentration
BES buffer pH 7.4	20 mM
NaCl	1M
Sodium azide	0.5%
DTT	100 mM
Heparin	1 mM

Protocol

1. The Tau protein aliquot was taken from the -80 °C storage and thawed. The protein was subjected to ultracentrifugation at 60,000 rpm for one hour at 4°C. This was to ensure that the starting material of the assay is pure monomer and do not contain any preformed aggregates.
2. The *in vitro* assembly of 20 µM full-length and repeat Tau was induced by 5 µM heparin at 1:4 ratio of heparin to Tau in 20 mM BES buffer, pH 7.4. The assembly buffer was supplemented with 25 mM NaCl, 0.01% sodium azide, 1 mM DTT and protease inhibitor cocktail.
3. The components were mixed and used for further assays including fluorescence assays, SDS-PAGE analysis, CD, TEM, SEC.
4. The reaction mixture was incubated at 37 °C after each time point measurement.

2.6.1 Tau aggregation inhibition assay

The inhibition of Tau aggregation is one of the most important therapeutic strategies in overcoming Tau pathology. We screened few small molecules belonging to natural origin against Tau aggregation. These molecules were screened independently one at a time in a reaction mixture. Our lab references!

Reagents

Component	Stock concentration
BES buffer pH 7.4	20 mM
NaCl	1M
Sodium azide	0.5%
DTT	100 mM
Heparin	1 mM
Baicalein	1 mM
EGCG	5 mM
Spermine	10 mM
Spermidine	42.68 mM

Protocol

1. The Tau protein aliquot was taken from the -80 °C storage and thawed. The protein was subjected to ultracentrifugation at 60,000 rpm for one hour at 4°C. This was to ensure that the starting material of the assay is pure monomer and does not contain any preformed aggregates.

2. The *in vitro* assembly of 20 µM full-length and repeat Tau was induced by 5 µM heparin at 1:4 ratio of heparin to Tau in 20 mM BES buffer, pH 7.4. The assembly buffer was supplemented with 25 mM NaCl, 0.01% sodium azide, 1 mM DTT and protease inhibitor cocktail.
3. The control tube was set as above and the inhibition in presence of each compound was studied by adding varying concentrations of respective compounds.
4. The components were mixed and used for further assays including fluorescence assays, SDS-PAGE analysis, CD, TEM, SEC.
5. The reaction mixture was incubated at 37 °C after each time point measurement.

2.6.2 Tau Disaggregation assay

Reagents

Component	Stock concentration
BES buffer pH 7.4	20 mM
NaCl	1M
Sodium azide	0.5%
DTT	100 mM
Heparin	1 mM
Baicalein	1 mM
EGCG	5 mM

Protocol

1. The Tau protein aliquot was taken from the -80 °C storage and thawed. The protein was subjected to ultracentrifugation at 60,000 rpm for one hour at 4°C.
2. Tau aggregates were set up at the concentration of 100 µM with 25 µM heparin. All the other components were maintained same as aggregation assay set up.
3. The aggregates were allowed to form at 37 °C for 5-8 days. The quality of aggregates was analyzed by SDS-PAGE and transmission electron microscopy.
4. The disaggregation assay was set up by diluting the aggregates to 20 µM in BES buffer and addition of different concentrations of the compounds.
5. The disaggregation was monitored by fluorescence assays, SDS-PAGE, CD and TEM analysis.

2.6.3 Tau glycation assay

Glycation of Tau was carried out to study the propensity of FTDP-17 mutants and the pseudophosphorylated mutants to undergo methyl glyoxal-induced aggregation and advanced glycation end products (AGEs) formation. Methyl glyoxal is a reactive intermediate of glucose metabolism, which causes abnormal protein glycation leading to cross-linking, aggregation and accumulation.

Reagents

Component	Stock concentration
BES buffer pH 7.4	20 mM
NaCl	1M
Sodium azide	0.5%
DTT	100 mM
Methyl glyoxal	1 mM

Protocol

1. The wild type and Tau mutants were centrifuged at 60,000 rpm for one hour at 4°C in a tabletop ultracentrifuge.
2. 20 µM wild type Tau and mutants were incubated in BES buffer pH 7.4 with 2.5 mM methyl glyoxal as a glycating agent. The assay mixture was supplemented with 25 mM NaCl, 0.01% sodium azide, 1 mM DTT and protease inhibitor cocktail.

3. The extrinsic fluorophores were added to the reaction mixtures to a concentration of 2.5 µM for thioflavin S and thioflavin T and 400 µM for ANS respectively. The mixtures were made in opaque tubes to avoid fluorescence bleaching.
4. The reactions were incubated at 37 °C incubator and the aggregation was monitored at the 24 hours' time interval.

2.7 Fluorescence based assays

The Tau aggregation, aggregation inhibition, disaggregation and glycation were monitored by fluorophores like Thioflavin S, Thioflavin T, ANS and AGEs-specific fluorescence. The aggregation inhibition and disaggregation was monitored by classical method of fluorescence monitoring of ThS and ANS. On the other hand the glycation-induced aggregation was monitored by incubating the fluorophores in the glycation reactions as explained below.

2.7.1 Thioflavin S assay

Thioflavin S preferentially binds to the β-sheet conformation acquired during the protein aggregation process and emits fluorescence upon binding. It is used to determine the progress of aggregation of proteins in a time-dependent manner.

Reagents

Component	Concentration
Thioflavin S	200 µM
Ammonium acetate pH 7.0	50 mM

Protocol

Classical method:

1. For measurement of ThS fluorescence ThS was diluted to 8 µM in 50 mM ammonium acetate solution and aliquoted as 45 µL in the tubes.
2. 5 µL from the 20 µM Tau reaction mixtures was added to these tubes making the final measuring concentration of Tau as 2 µM. Thus Tau: ThS is maintained as 1:4.
3. The mixture was mixed thoroughly and added to the 384 black well plates in triplicates for each reaction mixture.
4. The plate was incubated at room temperature for 10 minutes and the fluorescence reading was taken in Tecan Infinite 200 Pro plate reader.
5. The excitation/emission was adjusted to 440/521 nm and the background fluorescence was subtracted from the readings.

Glycation-induced aggregation:

1. Since the reaction mixtures already contained the ThS fluorophore, Tau was diluted to 5 µM in ammonium acetate buffer and added to the 384 black well plate.
2. The excitation/emission was given as 440/521 nm in the Tecan plate reader and the readings were obtained. The background fluorescence was subtracted before plotting the kinetics.

2.7.2 Thioflavin T assay

Thioflavin T can bind to aggregates as well as monomers of proteins giving enhanced fluorescence. We used ThT only for studying the MG-induced aggregation in Tau and its mutants.

Protocol

1. The Tau reaction mixtures containing ThT fluorophore were diluted in ammonium acetate buffer to a final concentration of 5 µM of Tau.
2. The samples were added to 384 well plate and reading was taken in a Tecan plate reader. The ThT was excited at 435 nm and the emission was collected at 485 nm. The buffer background was subtracted from the readings.

2.7.3 8-anilino 1-naphthasulfonic acid (ANS) fluorescence Assay

During the aggregation, Tau forms various intermediate species, which involves exposure of the hydrophobic patches in the proteins. ANS dye binds to these exposed hydrophobic patches and emits fluorescence. It is used widely to study protein hydrophobicity changes occurring during protein unfolding and misfolding.

Reagents

Component	Concentration
ANS	10 mM
Ammonium acetate pH 7.0	50 mM

Protocol

Classical method:

1. The measuring concentration of Tau :ANS was maintained at 1:20. Accordingly ANS was diluted to 40 µM in ammonium acetate buffer and aliquoted as 45 µL in tubes.
2. 5 µL from the Tau reaction mixtures was added to the 40 µM ANS and mixed thoroughly. The mixture was added to 384 black well plate and incubated in dark for 20 minutes at room temperature.
3. The reading was taken in Tecan plate reader wherein the excitation/emission wavelength for ANS was set as 390 nm and 475 nm respectively. The buffer readings were subtracted before plotting the assay kinetics.

Glycation-induced aggregation:

1. The reaction mixtures already containing the ANS fluorophore, Tau was diluted to 5 µM in ammonium acetate buffer and added to the 384 black well plate.
2. The excitation/emission was given as 390/475 nm in the Tecan plate reader and the readings were obtained. The background fluorescence was subtracted before plotting the kinetics.

2.7.4 Measurement of AGEs-specific fluorescence

The advanced glycation end products have a property of autofluorescence, which helps to identify relative glycation of proteins. We employed AGEs autofluorescence to study relative glycation propensity of Tau mutants with respect to Tau wildtype.

Protocol

1. The reaction mixture was set as mentioned above ***(Section 2.6.3)*** except the addition of the extrinsic fluorophores.
2. For measurement of AGEs-specific fluorescence, the 50 µL of 20 µM reaction mixture was aliquoted in 384 black-well plate and reading was acquired at excitation/emission 370 nm/430 nm in TECAN Infinite series 200 Pro plate reader.
3. Buffer background was subtracted from the obtained readings.

2.8 SDS-PAGE analysis

SDS-PAGE is typically utilized to separate protein based on their molecular weights and eliminates the influence of protein charge and conformation. This is achieved by the detergent sodium dodecyl sulphate, which denatures the proteins by binding to the backbone and linearizes the proteins by imparting a negative charge. The polyacrylamide gel imparts a sieving effect depending on the percentage and the pore size of the gel. Thus, the proteins migrate through the polyacrylamide gel from negative to positive electrode under the applied electric field. The gel is composed of two parts; stacking and resolving gel, which vary in their pH and the percentage. The stacking gel has a lower pH of 6.8, which helps the stacking of protein molecules between glycine and chloride ions due to differential ion mobility. The gel loading dye has bromophenol blue, which tracks the migration of the proteins and migrates faster on the gel. The resolving gel has a pH of 8.8, which declines the rate of glycine migration and subjects the separation based on the molecular weight. After the migration of 80-90% is achieved the proteins are visualized on the gel by staining with staining solution containing CBB R-250.

Reagents

1. SDS Gel running buffer

Component	Molarity
Tris base	25 mM
Glycine	192 mM
SDS	0.1%

2. Lammelli buffer/6X loading dye

Component	Molarity
Tris-Cl pH 6.8	300 mM
SDS	12%
Bromophenol blue	0.6%
Glycerol	60%
DTT	600 mM

3. 40% Acrylamide solution
4. 1.5 M Tris buffer pH 8.8
5. 1 M Tis buffer pH 6.8
6. 10 % SDS
7. Ammonium persulphate (APS)
8. TEMED

Protocol

1. The required percentage of the resolving gel is made as per the table.
2. The samples are diluted in the 6X loading dye and loaded onto the wells
3. A voltage of around 90-100 V is applied in a vertical electrophoresis unit in presence of gel running buffer.
4. The gel is run till the tracking dye reaches 90% of the gel and the gel is removed. This can further be utilized either for transfer in western blotting experiment or stained in order to visualize the protein bands.

2.8.1 Gel staining

After the completion of electrophoresis the gel is stained in order to visualize the proteins. The most common method of staining is by Coomassie dye, which in acidic conditions binds to hydrophobic protein residues and turns to bright blue colour. The method is compatible with separated proteins having further applications like mass spectrometry analysis as the stain can completely be removed since no chemical modification of protein takes place.

Reagents

1. Staining solution (1000 mL)

Component	Quantity
CBB R-250	1 g
Methanol	450 mL
Glacial acetic acid	90 mL

Make up the volume to 1000 mL and filter the stain before use.

2. Intensive destaining solution (1000 mL)

Component	Quantity
Methanol	500 mL
Acetic acid	100 mL

Make up the volume to 1000 mL.

3. Normal destaining solution (1000 mL)

Component	Quantity
Methanol	50 mL
Acetic acid	75 mL

Make up the volume to 1000 mL.

Protocol

1. After the electrophoresis, wash the SDS-PAGE gel gently once with water and place in the staining solution for 20 minutes on a rocker.
2. Decant the stain and add intensive staining solution and keep on rocker for 20 minutes
3. Remove the intensive destaining solution and place the gel in normal destaining solution. Keep changing the normal destaining solution till the gel is properly destained.
4. Remove from normal destaining solution and place in water.

2.9 Western blotting

Western blotting analysis helps to confirm the presence or the levels of specific protein or its modification by utilizing the antibodies. In general western blotting can be used to study the specific modification of the recombinant protein or the levels of intracellular proteins. The proteins on the SDS-PAGE are transferred onto the PVDF membrane and mapped by specific primary antibodies, which are further detected by secondary antibodies tagged with an enzyme or fluorescent molecule.

Reagents

1. SDS Gel running buffer

Component	**Molarity**
Tris base	25 mM
Glycine	192 mM
SDS	0.1%

2. Transfer buffer (freshly prepared)

Component	**Molarity**
Tris base	25 mM
Glycine	192 mM
Methanol	20%

3. 1X PBST

Component	**Quantity**
PBS pH 7.4	1X
Tween 20	0.1%

4. Blocking buffer

5% skimmed milk in PBST

5. Ponceau S stain (200 mL)

Component	**Quantity**
Ponceau S	0.4 g
Glacial acetic acid	2 mL

6. Stripping buffer pH 2.8

Component	**Molarity**
Glycine	0.2 M
NaCl	0.5 M

7. Neutralizing solution pH 8.5

Component	**Molarity**
Tris-HCl	1 M

Protocol

1. Semi-dry blot transfer (Amersham biosciences)
2. The gel was run as per SDS-PAGE.
3. The transfer membranes were cut in the 8 cm X 7 cm dimensions (for Bio-rad gel)
4. The transfer buffer was prepared and stored at 4 °C.
5. The filter papers (same size as membrane and gels) were soaked in the transfer buffer in a tray.
6. After the electrophoresis the gel was soaked in transfer buffer. The membrane was activated in 100%methanol (only for PVDF membranes) and equilibrated in transfer buffer.
7. 2 stacks of soaked filter papers were placed on the dry blot platform followed by the membrane. The air bubbles were removed.
8. The gel was placed on the membrane without air bubbles. The gel once placed on the membrane should not be moved.
9. Another stack of soaked filter paper was placed on the gel and the transfer buffer was added over the sandwich made.
10. The lid of the apparatus was closed and the current was set to 200 mA for 2 hours.
11. The blot was stained with Ponceau stain to make sure the transfer of proteins was done.
12. The blot was destained and put in blocking buffer for 1 hour at room temperature (RT).
13. The blot was incubated in primary antibody for 1 hour overnight.
14. The membrane was washed with PBST 3 X 10 mins to remove unbound antibody.
15. The blot was incubated with HRP conjugated secondary antibody.
16. The membrane was washed with PBST 3 X 10 mins to remove unbound antibody.
17. The blot was developed using ECL reagent.

2.10 Circular Dichroism (CD) Spectroscopy

CD Spectroscopy is a type of light absorption spectroscopy and works on the basis on the difference between absorption of left and right circularly polarized by a molecule. It is highly sensitive secondary structure of proteins. The aligned arrays of amides of polypeptide backbones have a shift or split in their optical transitions, which results in the characteristic CD spectra. The CD analysis was carried out for soluble and aggregated Tau as well as for reaction mixtures of Tau aggregation inhibition by small molecules.

Reagents

1. 50 mM phosphate buffer pH 6.8

Protocol

1. The Jasco J-815 CD spectrometer was purged with nitrogen gas to create an inert environment.
2. The spectra for 50 mM phosphate buffer was acquired and subtracted as a baseline from the further spectra containing Tau.
3. The Tau soluble, and aggregation reaction mixture was diluted to 1-3 μM for full-length and repeat Tau respectively in the phosphate buffer.
4. The spectra were recorded in a quartz cuvette with 1 mm pathlength at 1 nm bandwidth and 100 nm/min scan speed. The spectra were recorded in the range of 190-250 nm with average of 5 acquisitions. All the measurements were carried out at 25 °C.
5. The CD spectra were plotted in Sigma plot 10.0.

2.11 Transmission electron microscopy (TEM)

Transmission electron microscope has a very high resolution of 10 Å and employs a high-energy electron beam to pass through the sample and the transmitted electrons are used to obtain the image. The biological samples like proteins needs contrast enhancing agents such as uranyl acetate for better visualization of the image. We used TEM to study the morphology of Tau aggregates in presence and absence of inhibitors screened by negatively staining them with uranyl acetate.

Reagents

1. 2% Uranyl acetate

Protocol

1. The Tau samples were diluted to a concentration of 2 μM in ultrapure MilliQ water and applied onto 400 mesh carbon coated copper grids (TED Pella) for 1 minute.
2. The excess protein solution was gently blotted and grids were given 2 quick washes of MilliQ water
3. The grids were stained in 2% uranyl acetate for 5 minutes and dried completely before scanning
4. The dried grids were scanned on TECNAI T20 electron microscope at 200 KV.

2.12 Size exclusion chromatography for aggregation inhibition of full-length Tau by EGCG and polyamines.

Tau aggregation progresses through formation of various higher molecular weight species, which can have heterogenous physical and biological properties. These higher order species can be separated by size exclusion chromatography and further analyzed for their discreet properties. In order to study the effect of small molecules on the properties of Tau species with respect to control untreated Tau species.

Reagents

1. Tau assembly buffer and small molecules

Component	Stock concentration
BES buffer pH 7.4	20 mM
NaCl	1M
Sodium azide	0.5%
DTT	100 mM
Heparin	1 mM
EGCG	5 mM
Spermine	10 mM
Spermidine	42.68 mM

2. Size exclusion chromatography buffer

1X Phosphate buffered Saline pH 7.4

Protocol

1. The SEC column Superdex 200 increase was equilibrated with the SEC buffer. 20 μM of full-length Tau was incubated in assembly buffer in absence and presence of EGCG (100 μM), Spermine (100 μM) and Spermidine (200 μM) respectively.
2. These reaction mixtures were subjected to SEC at 0, 3 and 24 hours for EGCG and 0, 24 and 48 for polyamines Spermine and Spermidine.
3. The retention volumes of the higher order species of control and treated Tau were noted and the elution fractions were further used for cell viability studies in neuro2a cells
4. In case of polyamines, the fractions containing higher order species were also mapped for hydrophobicity by ANS fluorescence assay.

2.14 Tau-small molecules interaction studies

2.14.1 Isothermal Titration Calorimetry

Isothermal Titration Calorimetry (ITC) is a sensitive technique to study the interaction between two proteins, two ligands or protein and a ligand. It is largely employed to study enzyme kinetics. ITC detects the heat changes in the system, which accompanies the interaction between two molecules. This heat change is utilized to deduce various binding parameters like dissociation constant (K_d), binding stoichiometry (n), entropy (ΔS) and enthalpy changes (ΔH) etc. We utilized ITC to study the interaction between full-length Tau and EGCG in Malvern PEAQ ITC instrument.

Reagents

Component	Molarity
Sodium phosphate buffer pH 7.4	50 mM
Tau	20 μM

EGCG	500 µM

Protocol

1. Tau protein was rebuffered in the sodium phosphate buffer pH 7.4 and the ligand EGCG was also diluted in sodium phosphate buffer for minimizing the buffer interferences and mismatch in the titration.
2. 20 µM Tau was titrated against 500 µM EGCG in sodium phosphate buffer pH 7.4 at 25 °C.
3. The titration consisted of 25 injections of 1.5 µL each for 3 seconds with an interval of 180 seconds between two consecutive injections. In order to stabilize the reaction cell an initial injection of 0.4 µL was given.
4. The data was analyzed and interpreted using PEAQ-ITC software using one set of sites model.
5. The final baseline corrected data and heat plot were plotted using Sigma plot 10.2. The values of ΔG, ΔH and TΔS were used to calculate the binding constant for the interaction.

2.14.2 Nuclear Magnetic Resonance Spectroscopy

The interaction of proteins with ligand molecules have a great impact in biological systems and these interactions assist in the drug development. NMR is a powerful tool deducing the interactions of proteins and ligands especially for the residue-specific interaction. The simplest NMR interaction studies involve chemical-shift titration studies that maps the chemical shifts of proteins in response to ligand interaction. We studied the interaction of repeat Tau with EGCG and polyamines by ^{1}H-^{15}N HSQC NMR chemical shift experiment.

Reagents

Component	Concentration
Phosphate buffer pH 6.8	50 mM
DTT	1 mM
D_2O	10%
^{15}N labelled repeat Tau	200 µM

Protocol

1. 200 µM solution of ^{15}N labelled repeat Tau protein was prepared in 10:90 D_2O: H_2O aqueous medium of 50 mM phosphate buffer also containing 1 mM DTT.
2. For EGCG interaction studies, the repeat Tau was titrated with the EGCG:Tau ratios of 0, 0.5, 2.5, 5 and 10. For polyamines, the titrations were carried out at the ratios 0, 1, 2, 4, 8, 16 (Polyamines:Tau).
3. All NMR experiments were acquired at 278 K on Bruker Advance III HD 700 MHz spectrometer equipped with a TXI probe.
4. ^{1}H-^{15}N HSQC experiments have been acquired using 512 increments and 2k complex points in the indirect and direct dimension, respectively, and 16 scans per increment.
5. The data was processed by Bruker topspin software and analyzed using Sparky.

2.14.3 In Silico interaction studies

Molecular modelling. To procure templates for homology model building, a similarity search using Basic Local Alignment Search Tool (BLAST) algorithm was performed against the Protein Data Bank (PDB), to identify high-resolution crystal structures of homologous proteins. The sequence identity cut off was set to ≥ 30% (E-value cut off = 1). Homology modeling of Tau K18 was then carried out using Modeller 9.16 by taking structures homologous to the target proteins as templates, in order to study their structural features, binding mode and affinity with the substrates.

Model validation and refinement. The initial models obtained, were evaluated for the stereochemical quality of the protein backbone and side chains using PROCHECK and RAMPAGE. ERRAT server checked the environments of the atoms in the protein model. Errors in the model structures were also checked with ProSA server. After model validation, initial models were refined using imperf

minimization of protein preparation wizard and Impact 5.8 minimization. These energy minimized final models were further used for the binding studies with their substrates.

Ligand–protein preparation and docking studies. The ligand molecule considered in the present study was downloaded from ZINC compound database in the mol2 format. The protein and ligands were prepared first before proceeding with the docking studies. The water molecules and other heteroatom groups were removed from the protein structures using protein preparation utility of Maestro. Hydrogens were added subsequently to carry out restrained minimization of the models. The minimization was done using impref utility of Maestro in which the heavy atoms were restrained such that the strains generated upon protonation could be relieved. The root mean square deviation (RMSD) of the atomic displacement for terminating the minimization was set as 0.3. Similarly, ligands were refined with the help of LigPrep 2.5 to define their charged state and enumerate their stereoisomers. The processed receptors and ligands were further used for the docking studies using Glide 5.848. Sitemap analysis was performed on the prepared receptor molecule, to identify the probable binding sites for our ligands of interest, since no prior information was available regarding the same. Next, grids were generated by selecting any of the Sitemap points obtained above. Pls revise! Flexible ligand docking was carried out using the standard precision option. A total of 6 poses with the respective ligand and different sites were generated and scored on the basis of their docking score, glide score and E-model values. The hydrogen bond interactions between the protein and ligands were visualized using PyMOL.

Molecular dynamics simulations. The docked complex with the lowest Glide score and Glide E-model values were used to perform molecular dynamics simulation using the GROningen MAchine for Chemical Simulations V4.5.4 (GROMACS) with the CHARMM36 force field. The docked complex was placed in the center of a dodecahedron box solvated in water. The ligand topology files and the other force field parameter files pertaining to the ligand were created using the official CHARMM General Force Field server CGenFF. The SPC216 water model was used and the distance between the solute and the box was set to 10. The dimensions of the initial simulation cell were kept at approximately 90 Å~ 90 Å~ 90. for the simulation and the initial energy minimization of the system was carried out by steepest descent minimization for 50,000 steps, till a tolerance of 10 kJ/mol was attained, to make sure that the high energy interactions and steric clashes in the system could be avoided during simulation. A suitable number of Cl^- ions were added to balance the total negative charges on the docked structures to make the whole system neutral using the genion program of GROMACS and the system was again subjected to energy minimization by steepest descent minimization retaining the same parameters. The system was stabilized at 300 K temperature and pressure of 1 bar using the Vrescale, a modified Berendsen thermostat, temperature coupling and Parrinello-Rahman pressure coupling methods. The Partial Mesh Ewald (PME) algorithm was employed for computing electrostatic and van der Waals interactions. A cut off distance of 9 and 14. was set for Coulomb and van der Waals interactions, respectively. The LINCS algorithm was used to apply rotational constraint to all the bonds. No positional constraints were applied on the system. Periodic boundary conditions were applied in all three directions. The complex in the medium was equilibrated for 100 ps in NPT and NVT ensembles. Finally, 20 ns molecular dynamics simulation was carried out for the protein–ligand complex and all trajectories were stored every 2 ps for further analysis. The trajectories were visualized using Visual Molecular Dynamics program (VMD) 58. The energies and RMSD of the complex in each trajectory were monitored with respect to simulation time. The intermolecular interactions between the target and substrate were assessed to check the stability of the complexes. The Rg (Radius of gyration) was also monitored for the protein and ligand backbones to check their stability in the active site pocket as well as their overall compactness.

2.15 **Cell biology studies**

2.15.1 Cell growth and maintenance

For the entire cell-based studies neuro2a (N2a) cells were used. Neuro2a cells were purchased from ATCC. It is mouse neuroblastoma cell line and is being widely used for neuronal studies.

Reagents

1. Cell growth media

Advanced DMEM
L-glutamine
Penstrep antibiotic cocktail
Fetal Bovine Serum (USA origin)
Trypsin-EDTA
1X PBS

Protocol

Cell growth:

1. The cells were maintained in Advanced DMEM supplemented with 10% FBS, penstrep and glutamine.
2. The cells were incubated at 37 °C in a CO_2 incubator with 95% humidity.
3. The cells were passaged after reaching 80% confluency in the culture dish.

Cell passage:

1. After reaching 80% confluency, cells were passaged by removing the growth media and washing with 1X PBS.
2. 1X trypsin EDTA was added to the culture dish and incubated at 37 °C for 5-10 minutes.
3. The trypsin-EDTA helps detachment of the cells from the culture dish. The reaction of trypsin was stopped by adding the growth media containing 10% FBS.
4. The suspension was collected in a centrifuge tube and centrifuged at 800 rpm for 5 minutes to pellet down the cells.
5. The supernatant was discarded and the cell pellet was resuspended in fresh growth media. The cells were added to a fresh culture dish with a split ration of 1:3.
6. The culture dishes were incubated at 37 °C in a CO_2 incubator with 95% humidity.

2.15.2 Cell viability assays

Cell viability is an important tool to study the biocompatibility of the candidate therapeutic molecules. There are various classes of cell viability assays like dye exclusion (trypan blue), colorimetric (MTT and LDH), fluorometric and luminometric assay. Based on the applications a particular type of assay can be employed to study. We used MTT and LDH assay to study the toxicity of various small molecules in neuro2a cells. We also studied the toxicity of Tau treated with molecules in an aggregation inhibition reaction as compared to untreated aggregated Tau.

2.15.2.1 3-(4, 5-dimethylthiazol-2-yl)-2, 5-diphenyltetrazolium bromide (MTT) Assay

MTT assay is a widely used colorimetric assay for cell toxicity studies. It determines the mitochondrial function of cells by measuring the mitochondrial enzymes. MTT is a tetrazolium salt, which is reduced to purple formazan crystals by NADP. These crystals are solubilized in an organic solvent and the intensity of colour developed is measured at 500-600 nm.

Protocol

1. Neuro2a cells were seeded at a density of 10,000 cells in a 96 well plate and grown in the growth media at 37 °C CO_2 incubator.
2. Next day, these cells were treated with varying concentrations of compounds and compound treated Tau species and incubated for 24 hours at 37 °C CO_2 incubator.
3. Post-treatment cells were treated with 0.5 mg/mL of MTT (3-(4,5-dimethylthiazol-2-yl)-2,5 diphenyltetrazolium bromide) and incubated for 4 h.
4. The formed formazone crystals were dissolved in 100 µL of DMSO. This leads to the formation of purple coloured complex whose absorbance was measured at 590 nm in TECAN Infinite Series Pro 200 spectrofluorometer.

2.15.2.2 Lactate dehydrogenase (LDH) assay

LDH enzyme is physiologically present in the cell cytoplasm. The membrane leak caused due to various toxic molecules leads to release of this enzyme extracellularly. LDH assay measures this leaked LDH enzyme by its activity in two steps. In the first step, LDH catalyzes the conversion of lactate to pyruvate and thus NAD is reduced to $NADH/H^+$. In a second step, catalyst (diaphorase) transfers H/H^+ from $NADH/H^+$ to the tetrazolium salt 2-(4-iodophenyl)-3-(4-nitrophenyl)-5-phenyltetrazolium chloride (INT), which is reduced to red formazan. We utilized LDH assay to determine the effect of polyamine-treated Tau on cell membrane integrity.

Protocol

1. Cells were seeded at the density of $1X\ 10^4$ cells/well in growth media supplemented with 10% FBS and penstrep for 24 hours.
2. Tau treated with polyamines at various concentrations for 72 hours was added to cells in serum-starved media for 24 hours.
3. LDH release assay was carried out according to manufacturer's protocol (Pierce, Thermo Scientific).

2.15.2.3 Caspase 3/7 activity assay

Caspase-3 is an effector caspase in the apoptosis pathway and plays a pivotal role in progression of cell towards apoptosis. Additionally in AD, it is known to cause aberrant cleavage of Tau, which leads to its pathogenic aggregation. We studied the effect of polyamines on the Caspase 3/7 activity in neuro2a cells.

Protocol

1. Caspase 3/7 activity in polyamine treated cells was determined by EnzChek™ Caspase-3 Assay Kit (Molecular Probes).
2. $1X10^5$ neuro2a cells were plated in 12 well plate and treated with polyamines for 12 hours.
3. Caspase 3/7 activity assay was carried out according to the given protocol. Cells were lysed using the lysis buffer provided in the kit for 30 minutes on ice.
4. The supernatant was collected after centrifugation and incubated with the substrate provided (DEVD-Rhodamine 110) for different time intervals.
5. The fluorescence was measured at 496 nm and 520 nm excitation and emission wavelength respectively in TECAN Infinite® 200 PRO plate reader.

2.15.2.4 Apoptosis assay by flow cytometry

Cellular apoptosis is governed by various factors and polyamines are involved in the cellular apoptosis pathways. Apoptosis of terminally differentiated cells like neurons can prove fatal and lead to neurodegenerative diseases. We studied the effect of polyamines in inducing apoptosis in neuronal cells.

Protocol

1. Neuro2a cells were plated at the density of $1X10^5$ in a 12 well culture plate. Cells were treated with various concentrations of spermine and spermidine for 12 hours and harvested for the analysis of apoptosis.
2. Apoptosis assay was carried out using the kit (FITC Annexin V/Dead Cell Apoptosis Kit Molecular Probes) using manufacturer's protocol. In brief, cells were washed in cold 1X PBS and resuspended in 100 µL 1X Annexin binding buffer with 5 µL of FITC annexin V and 1 µL of propidium iodide (100 µg/mL) for 15 minutes at room temperature.
3. Apoptosis analysis was carried out in BD Accuri C6 flow cytometer. 10,000 cells were counted for each sample.
4. The controls were set up as follows i. Unstained cells, ii. FITC Annexin V alone (no PI), iii. PI alone (no FITC Annexin V). Unstained cells were measured to remove dead cells and debris.
5. Viable cells with high forward scatter (FSC) and low side scatter (SSC) were selected and gating was done accordingly.
6. Apoptotic rate was determined by applying 4 quadrants for i. lower left (LL) Annexin V^-/PI^- (non-apoptoic cells), ii. Lower right (LR) Annexin V^+/PI^- (early apoptoic cells), iii. Upper right (UR) Annexin V^+/PI^+ (late apoptotic cells), iv. Upper left (UL) Annexin V^-/PI^- (necrtotic cells). The rate of apoptosis was determined as (LR+UR).

2.15.2.5 Immunofluorescence

Immunofluorescence is a powerful tool for visualizing the interplay of intracellular molecules and architecture. It employs mapping of specific proteins with primary antibodies and visualization by fluorescently tagged secondary antibodies. In addition to visualization, immunofluorescence can also aid in getting the colocalization of two or more proteins. We employed immunofluorescence to study the levels, localization and colocalization of various intracellular proteins in EGCG-mediated glycation inhibition.

Protocol

1. Neuro2a cells were maintained in Advanced DMEM supplemented with 10% FBS and antibiotics penicillin streptomycin.
2. For immunofluorescence studies $5X10^4$ cells were seeded on glass coverslip in a 12 well culture plate for 24 hours.
3. Four experimental groups were maintained as cell control, EGCG (100 µM) treated, MG (1 mM) treated and MG+EGCG treated. Treatment was carried out for 24 hours after which, the cells were fixed with ice-cold methanol.
4. Cell permeabilization was carried with 0.2% TritonX 100. After 3 PBS washes cells were blocked in 5% horse serum for 1 hour at 37°C. Cells were incubated with primary antibodies at 4 °C overnight. Further, cells were washed with 1X PBS and incubated with respective antibodies anti-mouse secondary antibody conjugated with Alexa flour-488, Goat anti-Rabbit IgG (H+L) Cross-Adsorbed Secondary Antibody with Alexa Fluor 555 (A-21428) followed by 300 nM DAPI.
5. The coverslips were mounted in 80% glycerol and sealed and were observed under 63X oil immersion lens in Axio Observer 7.0 Apotome 2.0 (Zeiss) microscope using ZEN pro software.

Aims of the Study

Alzheimer's disease is a protein misfolding disorder culminating in excessive brain atrophy and dementia. Amyloid-β and Tau are two important proteins which lead to AD pathology due to misfolding, aggregation an accumulation in brain. Aβ aggregates deposit extracellularly on the neurons and hamper synaptic transmission and Tau forms intracellular neurofibrillary tangles leading to cytoskeleton destabilization leading to neuronal death. The aggregation of Tau is attributed to various factors, of which we focused our studies on the Tau mutations and post-translational modifications and screening of small molecules to inhibit the PTMs and aggregation. Tau mutations known as FTDP-17 mutations alter Tau functions and trigger its aggregation. The PTMs like phosphorylation and glycation are also implicated in the pathological transition of Tau to aggregation. Based on this background we designed the following aims for our studies:

I. The effect of glycation on the aggregation propensity of mutant Tau and dual modification (pseudophosphorylation and glycation) of Tau.

II. The effect of green tea polyphenol EGCG on glycation inhibition and neuronal cytoskeletal integrity

III. Role of polyphenols Baicalein and EGCG on aggregation of full-length Tau

IV. Role of polyphenols in inhibiting Tau aggregation and modulation of neuronal apoptosis.

Chapter 2

Effect of glycation on predisposed Tau mutants and aggregation propensity by dual modification (phosphorylation and glycation) of Tau

2.1 The FTDP-17 mutations of Tau and the polyol pathway

The predisposition of an individual due to genetic Tau mutations termed as FTDP-17 mutations puts them at increased risk of early onset of Alzheimer's disease due to compromised functions of Tau[37]. Tau maintains the integrity of axonal microtubules and secures neuronal function. The mutations affect the binding affinity to microtubules as well as induces Tau self-assembly[34,35]. In addition to this, the surplus of abrupt modifications worsens the Tau pathology, as these modifications stabilize Tau aggregates and might help in spreading of the pathologic Tau seeds. We studied the effect of methyl glyoxal-induced glycation on the 3 missense FTDP-17 mutants G272V, P301L and R406W present in R1, R2 and in the C-terminal respectively (Fig. 2.1A). Glycation of Tau hampers its function and is suggested to stabilize the PHFs. In the normal physiological concentration, glucose is channelled *via* hexokinase pathway. The surge of glucose levels due to diabetic complications saturate the hexokinase pathway and hence the flux is diverted to alternative pathways like polyol pathway or Maillard reaction (Fig. 2.1B). As already introduced, Maillard reaction forms Schiff's base followed by conversion to Amadori products leading to the formation of advanced glycation end products (AGEs). The polyol pathway metabolizes sugars into alcohol by aldose reductase enzyme[179]. Accordingly, glucose is converted to sorbitol which is further converted to fructose. Fructose being more reactive, it is converted to reactive dicarbonyls including methyl glyoxal (MG) (Fig. 2.1C), which trigger the formation of AGEs.

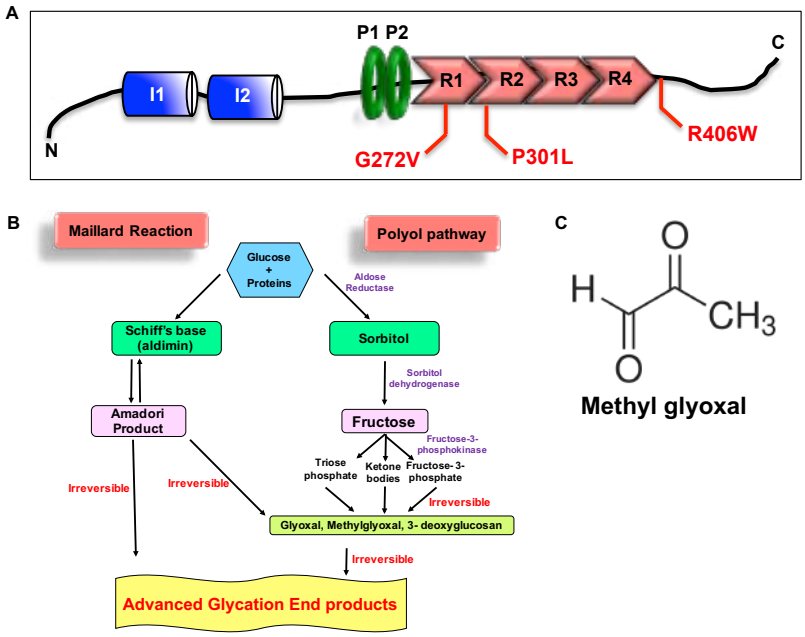

Figure 2.1. Tau FTDP-17 mutants and polyol pathway of AGEs formation. A) Tau protein organization having two inserts (blue blocks) at the N-terminal. Polyproline-rich region denoted by green rings and 4 imperfect repeats (red arrows) involved in microtubule-binding and also involved in Tau aggregation. The Tau missense mutations are denoted in red, G272V, P301 L, and R406W, which are involved in Tau dysfunction. B) The polyol pathway showing the formation of reactive metabolites like glyoxal and methyl glyoxal (MG) that are precursors of advanced glycation end products. C) Structure of MG, a reactive aldehyde accumulating in aging brain. The figure is reproduced from Sonawane *et al*., Journal of Alzheimer's Disease, 2020.

2.2 Effect of MG-induced aggregation on FTDP-17 mutant Tau

Elevated levels of methyl glyoxal in AD affects many events like signal transduction, redox balance and energetics of cells[180]. More importantly, MG induces cross-linking and aggregation of Tau protein. Since, the FTDP-17 mutations are known to enhance Tau assembly, we monitored effect of MG on the aggregation of Tau dementia mutants. The aggregation was assayed by 3 fluorescence-based probes thioflavin S (ThS), thioflavin T (ThT) and 8-Anilinonaphthalene-1-sulfonic acid (ANS). ThS and ThT

are derived by methylation of dehydrothiotoluidine in presence of sulphonic acid and hydrochloric acid respectively making them structurally different. Although, both the fluorophores bind to β-sheets, ThS preferentially binds to mature fibrils over monomers. The ThS aggregation kinetics of Tau and its dementia mutants displayed increased ThS fluorescence for the 2 mutants G272V and P301L as compared to wild type Tau suggesting enhanced aggregation (Fig. 2.2A). On the other hand, the mutant R406W had decreased ThS intensity than wild type Tau. The ThT kinetics confirmed these results with same pattern of aggregation of wild type and mutant Tau (Fig. 2.2B). Tau aggregation proceeds through variety of intermediate species formation, which involves increased exposure of hydrophobic patches in proteins. ANS dye binds the hydrophobic regions of proteins and fluoresces[6]. Though, the aggregation pattern differed between wild type and mutants, the hydrophobicity pattern remained similar (Fig. 2.2C). The relative analyses of the endpoint fluorescence for all 3 extrinsic fluorescence revealed enhanced MG-induced aggregation in G272V and P301L mutants as compared to wild type (Fig. 2.2D). The missense mutations of Tau differentially modulated the aggregation kinetics.

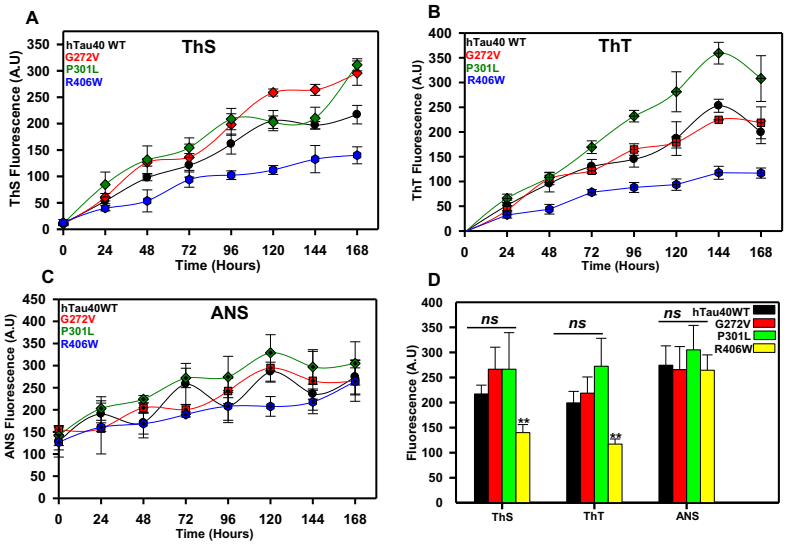

Figure 2.2 MG-induced aggregation of Tau and FTDP-17 mutants. A) ThS fluorescence analysis for MG-induced aggregation showing enhanced aggregation of mutants G272V and P301L as compared to control. B) ThT fluorescence assay shows similar observation as ThS analysis wherein the mutants show enhanced aggregation propensity as compared to control. C) The hydrophobicity transitions probed by ANS fluorescence reveal no distinct change in wild-type Tau versus mutants. D) The comparative analysis of all fluorophores show that R406W shows suppressed aggregation in presence of MG as compared to wild-type whereas G272V and P301 L follow the wild-type Tau with increased aggregation by MG ($p < 0.01$). The figure is reproduced from Sonawane *et al*., Journal of Alzheimer's Disease, 2020.

2.3 The in vitro propensity of Tau dementia mutants to form MG-induced AGEs

The advanced glycation end products formed due to protein modification by sugars or reactive dicarbonyls have a characteristic yellow-brown autofluorescence. This property is utilized as a non-invasive method to detect the skin fluorescence and determine the extent of diabetic complications[181]. AGEs fluoresce with the emission range of 420-600 nm on excitation at 300-420 nm. We checked the effect of MG on formation of Tau AGEs. The hypothesis was the mutations would affect the modification either to enhance or supress the AGEs formation (Fig. 2.3A). The AGEs-specific fluorescence gradually increased for Tau and its dementia mutants with P301L showing increased intensity as compared to wild type Tau (Fig. 2.3B). Other two mutants, G272Vand R406W showed reduced intensity for AGEs fluorescence. This pattern was followed throughout the kinetics till 168 hours. The comparative analysis at the end of kinetics revealed that the mutant P301L showed enhanced AGEs formation as compared to other Tau proteins (Fig. 2.3C). We report the effect of glycation on aggregation propensity of FTDP-17 mutants for the first time but reports are available for hyperphosphorylation of these mutants. The mutant P301L was shown to have enhanced aggregation

and MG-induced AGEs formation in our study. P301L Tau was also shown to have enhanced phosphorylation and NFTs deposition in the transgenic model of diabetes mellitus[182]. On the other hand, the mutant R406W displayed reduced MG-induced aggregation and glycation as compared to wild-type[183]. This mutant is also found to resist the phosphorylation and aggregation in various model system. Thus, the modification of FTDP-17 mutants depends largely on the inherent properties it imparts to the protein.

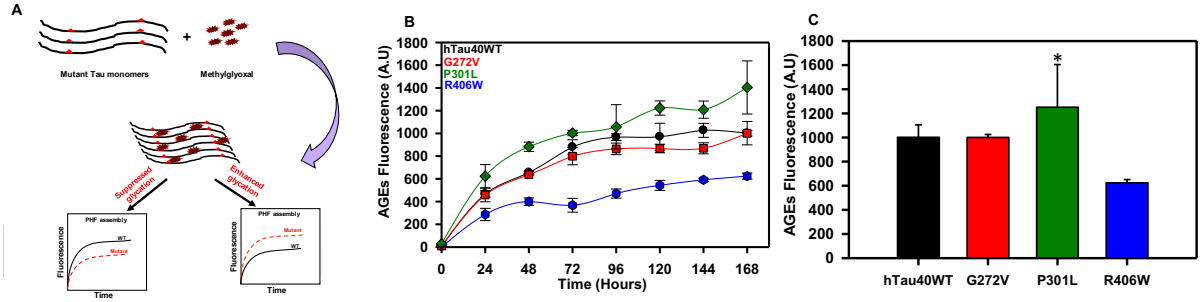

Figure 2.3. Advanced glycation end products formation propensity of Tau and its mutants. A) Hypothetical model to predict the effect of glycation on AGEs formation. The mutants can either demonstrate an increased or decreased propensity for AGEs formation as compared to wild type Tau that is quantitated by AGEs-specific fluorescence. B) The AGEs-specific fluorescence reveals increase in intensity with time for Tau and its mutants. P301L mutant shows highest AGEs formation as compared to control. C) The comparison of last time point fluorescence intensity reveals that the mutant P301L shows more propensities for glycation as compared to wild-type Tau ($p < 0.05$). The figure is reproduced from Sonawane *et al*., Journal of Alzheimer's Disease, 2020.

2.4 Morphology of MG-induced Tau aggregates

Protein cross-linking is the major manifestation of protein glycation which makes it protease resistant and difficult to degrade. This results in build-up of these protein aggregates hampering cellular functioning. The MG-treated Tau and its mutants were analysed on SDS-PAGE at regular intervals. The starting point proteins had a single monomer band without any higher order species confirming absence of any preformed higher order species in the reaction mixture. The soluble protein was modified by MG with progressing time and was visible as a smear of protein throughout the lane (Fig. 2.4A).

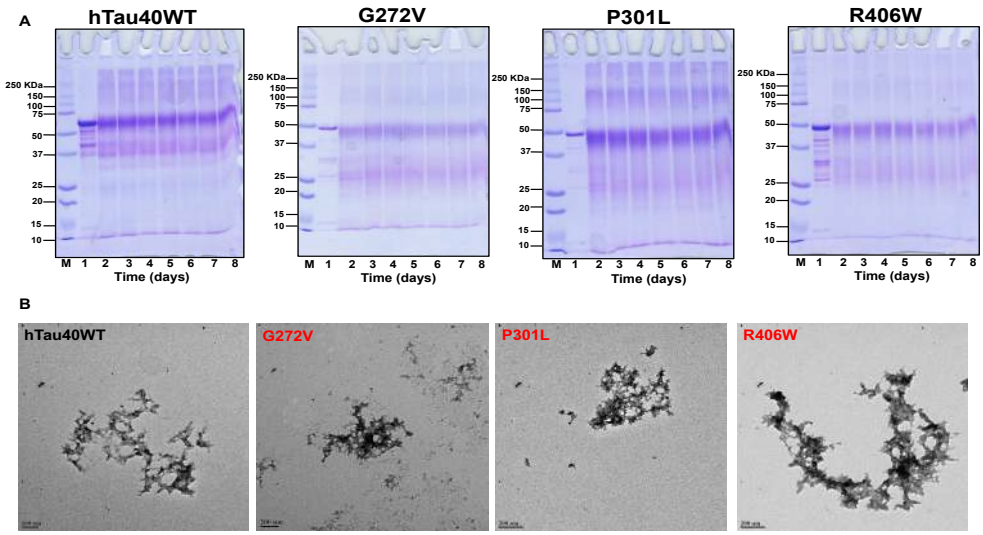

Figure 2.4. SDS-PAGE and morphological evaluation of glycated Tau proteins. A) SDS-PAGE evaluation of glycated Tau shows formation of SDS-resistant glycated proteins, which aggregate and can be visualized as a trail on the separating gel at higher molecular weight than the soluble protein. B) Electron micrographs of the glycated Tau and its mutants reveal formation of amorphous aggregates. The figure is reproduced from Sonawane *et al*., Journal of Alzheimer's Disease, 2020.

The cross-linking might have given a trail of proteins rather than specific bands. Moreover, the glycated protein were SDS-resistant and extent of glycation differed among wild type Tau and its mutants. The results were in concordance with aggregation studies with P301L showing enhanced glycation and other two mutants showing reduced glycation as compared to control. Further, these glycated proteins were visualized by transmission electron microscopy. The morphology of glycated proteins varied from the heparin-induced aggregates (Fig. 2.4B). Glycation formed amorphous aggregates as opposed to fibrillar aggregates formed in presence of other inducers.

2.5 Global conformation of native and glycated Tau

Protein molecular assemblies are associated with intermolecular interactions and conformational changes and are influenced by each other. The process of aggregation involves a common mechanism of increase in β-sheet conformation in proteins involved in different diseases. The amino acid mutations increase the flexibility of the protein causing destabilization, which favour the partially folded conformations having greater propensity for aggregation[184]. Glycation has been reported to decrease the inherent α-helical structure of proteins-like human serum albumin (HSA) and hemoglobin (Hb) and increase the β-sheet content[185]. The glycation of HSA by methyl glyoxal induced structural transitions and alteration by reducing the α-helical content of the protein[186]. Tau is an intrinsically disordered protein with complete random coil conformation. On aggregation the full-length Tau adopts partial β-sheet conformation whereas the repeat domain of Tau (K18WT) adopts complete β-sheet conformation. We studied the conformations of the native and glycated full-length Tau wild type and mutants by CD spectroscopy. The native conformation of Tau and its mutants showed a spectra for random coil conformation with maximum ellipticity at 198 nm (Fig. 2.5A). The MG-induced glycation did not show any change in the global conformation of Tau and its mutants (Fig. 2.5B). Thus, glycation does not alter the conformation of Tau and its FTDP-17 mutants.

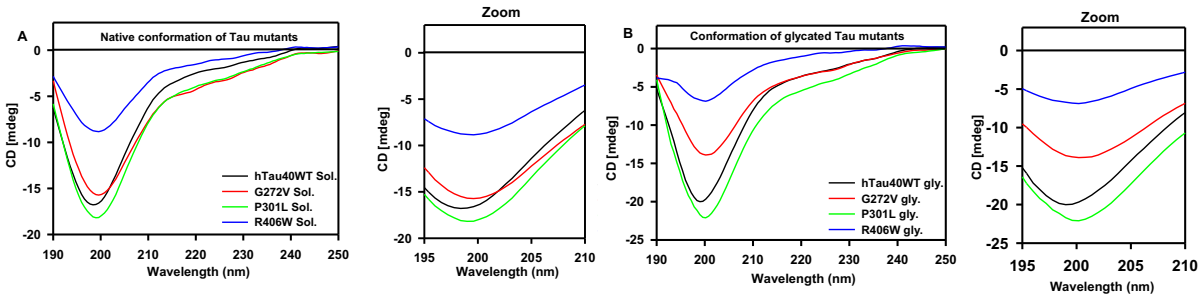

Figure 2.5. Effect of glycation on global conformation of Tau proteins. A) The native conformation of Tau and its FTDP-17 mutants show random coil conformation and maximum ellipticity at 198 nm. B) Glycation does not alter the global conformation of Tau and its mutants. Glycated proteins show native conformation with maximum ellipticity at 198 nm. The figure is reproduced from Sonawane *et al*., Journal of Alzheimer's Disease, 2020.

2.6 Pseudophosphorylation of Tau

Tau is a phosphoprotein requiring a balance of phosphorylation and dephosphorylation for its physiological functioning. In AD, an imbalance of this process results in abnormal phosphorylation of Tau, which increases the overall negative charge of the protein. Low net charge of the protein is reported to be one of the important parameters for protein aggregation[187]. The effect of hyperphosphorylation on Tau function and self-assembly is studied by utilizing the charge mimicking pseudophosphorylation mutants. The negative charge of phosphate group is added to the protein by replacing the specific sites of phosphorylation, serine and threonine by negatively charged amino acids aspartic acid or glutamic acid. This approach has helped to study the effect of site-specific phosphorylation on Tau aggregation and microtubule assembly rather than *in vitro* Tau phosphorylation by kinases which uncontrollably phosphorylate several sites. We employed similar approach to study the effect of dual modification,

glycation and phosphorylation on Tau. The phospho-mimicking Tau sites T231D, S262D, S396D and S404D were studied as double mutants (Fig. 2.6A). The combinations were, (262/404D, 262/396D and 231/262). Methyl glyoxal was used to glycate the phospho-mimicking mutants. The glycation reaction causes intra-molecular and inter-molecular cross-linking which favors the self-assembly of protein forming aggregates. Pseudophosphorylation is also found to enhance the Tau aggregation. The question we posed was whether pseudophosphorylation can enhance MG-induced cross-linking of Tau (Fig. 2.6B).

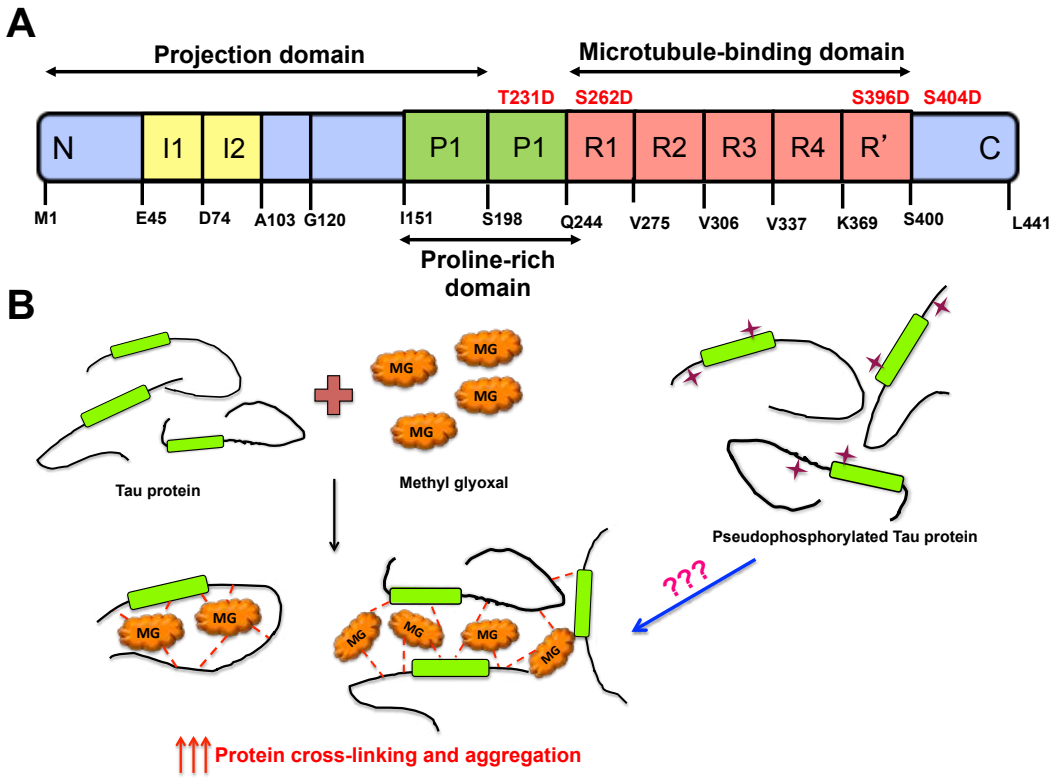

Figure 2.6. Tau pseudophosphorylated mutants. A) Tau protein is composed of two insert regions toward the N-terminal followed by a poly-proline stretch. The C-terminal region harbors a repeat region consisting of 4 imperfect repeats contributing to microtubule binding. The pseudophosphorylation sites studied are mentioned in red. B) The hypothesis model depicting glycation of pseudophosphorylated mutants by methyl glyoxal. Methyl glyoxal leads to intra-molecular as well as intermolecular protein cross-linking by modifying the amine side-chains. The phospho-mutants might interfere this cross-linking to either enhance or reduce the MG-induced aggregation. The figure is reproduced Sonawane *et al*., from ACS Omega (under revision), 2020.

2.7 Dual modification of Tau

The levels of reactive dicarbonyls have been found to increase in diabetic complications[179]. Especially, methyl glyoxal levels are found to increase in AD. Moreover, glycation plays an important role by inducing oxidative stress in AD. The effect of phosphorylation and glycation was studied on Tau aggregation. The aggregation was recorded for 168 hours using extrinsic fluorophore ThT. The kinetics steadily increased over the time suggesting progression of aggregation (Fig. 2.7A). The end time point fluorescence graph suggested that the aggregation propensity did not differ between Tau and the pseudophosphorylated mutants (Fig. 2.7B). However, the mutants and the wild type Tau did not follow a similar pattern of assembly. In the initial 36 hours, the kinetics increased gradually and equally for wild type and the phospho-mutants 262/396D and 231/262. Post 36 hours the kinetics for the phospho-mutant 262/396D drew apart from that of wild type with increased intensity suggesting increased aggregation. On the other hand, the phospho-mutant 262/404D showed only a minimal increase in intensity throughout the kinetics thus, confirming reduced rate of MG-induced aggregation as compared

to wild-type Tau. A previous study with a similar objective of studying dual modification of Tau have reported analogous results. The pseudophosphorylated Tau double mutants did not show significant differences in the MG-induced aggregation with respect to wild type[96]. This effect can be attributed to residue-specific phospho-mutants with varied aggregation propensity. The residue S262 plays an important role on Tau aggregation. The phosphorylation at S262 residue suppresses the Tau aggregation with overall increase in the phosphorylated sites on Tau[94]. The 3 double mutants employed in our studies have a common pS262, which might be responsible for suppressing MG-induced aggregation. Thus, site-specific pseudophosphorylation affects MG-induced Tau assembly.

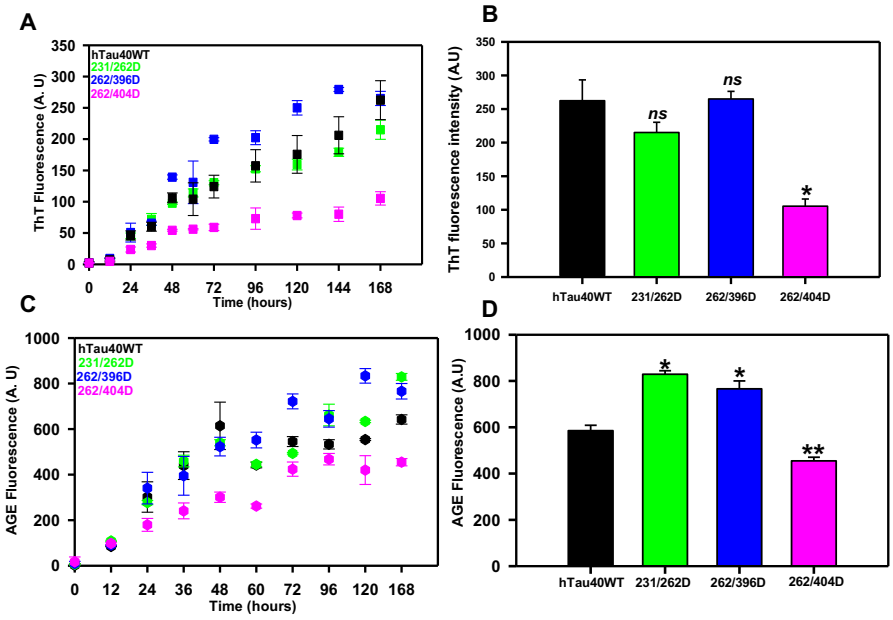

Figure 2.7. Dual modification of Tau. A) The ThT fluorescence assay for MG-induced Tau aggregation showed enhanced aggregation of mutant 262/396D and decreased aggregation in 396/404D as compared to wild-type Tau. B) The end time point fluorescence intensity of MG-induced aggregation does show lower aggregation propensity of the phospho-Tau mutant 262/396D. ($p < 0.05$). C) The AGEs fluorescence kinetics did not differ for the proteins until a later time point. D) The 168 hours analysis of AGEs fluorescence revealed increased AGEs fluorescence in 231/262D and 262/396D. ($p < 0.05$). The values are mean ± std. deviation. The statistical analysis was carried out by Student's unpaired T- test with respect to hTau40 wild type. *** $p \leq 0.001$, ** $p \leq 0.01$, * $p \leq 0.05$. *ns:* non-significant p value. The figure is reproduced from Sonawane *et al*., ACS Omega (under revision), 2020.

The extent of glycation by sugars or reactive dicarbonyls are determined by several quantitative methods including antibody-based techniques and AGEs autofluorescence[23]. Autofluorescence of AGEs is due to the specific compounds formed due to side chain modifications of amino acids. These compounds differ with the glycating agent. For example, modification of HSA by glucose forms argpyrimidine and pentoside with excitation maxima between 325 nm and 335 nm and emission maxima at 395 nm. MG-modified N-α-acetylarginine forms fluorescent compound N-α-acetyl-N-δ-(5-methyl-4-imidazolon-2-yl) ornithine with excitation/emission 320/398 nm. The AGE-modified lens proteins have excitation/emission of 360/430[188] nm. We used this approach in our study to decipher the extent of MG-mediated modification of Tau. As for aggregation results, same observation was made with respect to AGEs-specific fluorescence wherein the pattern for phospho-mutants and wild type remained same for first 36 hours of incubation (Fig. 2.7C). The AGEs fluorescence for wild type Tau became stagnant at 60 hours whereas the mutants 231/262D and 262/396D continued to show gradual increase in fluorescence. This suggests increased AGEs formation in 231/262D and 262/396D mutants as compared to wild type Tau. The mutant 262/404D showed reduced AGEs levels as compared to wild type. The comparative analyses revealed enhanced glycation in 231/262D and 262/396D with respect to wild type Tau (Fig. 2.7D).

2.8 Effect of dual modification on Tau conformation

Glycation imparts various characteristics to proteins such as resistance to proteases and detergents making them insoluble and aggregation prone. The doubly modified Tau proteins were subjected to SDS-PAGE analysis at various time points. The MG-induced glycation formed SDS-resistant Tau aggregates in all the proteins with 262/404D having least intensity among others (Fig. 2.8A). Phospho-mimicking mutants are reported to form SDS-resistant higher order Tau aggregates upon glycation. After confirming the presence of higher order aggregates, we studied the conformation of these modified proteins by CD spectroscopy. The unmodified Tau and its phospho-mimicking mutants demonstrated a random coil spectra with absorption maxima at 198 nm (Fig. 2.8B). Moreover, dual modification did not tend to alter the native conformation of Tau and its mutants (Fig. 2.8C). Pseudophosphorylation of Tau is known not to cause any significant changes to global conformation of protein. Similarly, glycation did not affect the global conformation of wild type Tau as well as phospho-mutants. Thus, the dual modification might be involved in local conformational changes which leads to enhanced modification in some mutants as compared to wild type. The visualization of modified Tau proteins demonstrated presence of amorphous aggregates (Fig. 2.8D). Such type of aggregates have been reported to be formed by the glycation of pseudophosphorylated Tau by reactive dicarbonyls like glyoxal, methyl glyoxal and acrolein.

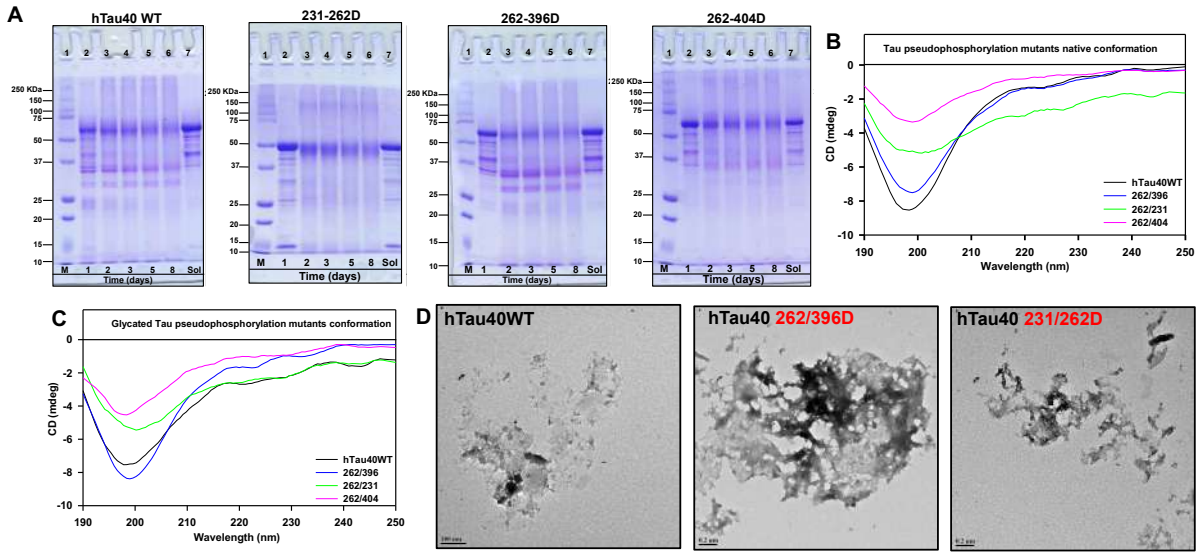

Figure 2.8. Conformational analyses of glycation and phosphorylation on Tau. A) The SDS-PAGE analysis of MG-treated Tau showed presence of higher order cross-linked proteins at various time points. The mutants 262/396D and 231/396D show presence of cross-linked products even at lower molecular weights. B) The CD spectra of Tau and its phospho-mutants showed a native conformation of random coil. The mutations did not alter the global conformation of Tau. C) The conformation of Tau and the phospho-mutants was not altered by MG-induced glycation. D) Electron micrographs of modified Tau. The glycated Tau showed presence of amorphous aggregates under electron microscope. The values are mean ± std. deviation. The statistical analysis was carried out by Student's unpaired T- test with respect to hTau40 wild type. *** p≤0.001, **p≤0.01, *p≤0.05. *ns:* non-significant p value. The figure is reproduced from Sonawane *et al*., ACS Omega (under revision), 2020.

Thus, the study on the effect of glycation Tau bearing predisposition to pathological transition suggests that glycation can act as an enhancing factor to trigger self-assembly and stabilize the aggregates by imparting resistance to detergents *via* excessive cross-linking.

Chapter 3

Role of EGCG in Tau glycation inhibition and maintaining neuronal cytoskeleton integrity

Advanced glycation end products are formed *via* series of chemical reactions initiated by modification of free amino groups by reducing sugars. The factors influencing AGEs formation are concentration of sugars and their reactive intermediates, extent of oxidative stress and protein turnover rate[189]. The early steps of glycation leads to the formation of reactive dicarbonyls like glyoxal, methylglyoxal (MG) which further lead to oxoaldehydes-derived AGEs formation. MG is reported to be one of the most highly reactive dicarbonyls that rapidly modifies side chains of amino acids forming AGEs. In addition to modification of lysine and arginine side chains, MG can also modify thiol groups in cysteines forming carboxyethylcysteine[190]. The derivatives of MG-modified amino acids in proteins are used as diagnostic markers for the progression of diabetic complications[191]. Protein modification by MG has substantial effect on protein functions as it inactivates cellular enzymes and impacts cellular pathways and signalling. Increased levels of AGEs have also been related to neurodegeneration especially in AD brains increasing oxidative stress and leading to neuronal pathology. Thus, investigation into synthesis and discovery of potent glycation inhibitors can acts as novel therapeutic approach to prevent the disease complications. Accordingly, various AGEs inhibitors belonging to synthetic and natural origin have been developed, which either act by inhibiting the formation or breaking the cross links. Very few of the synthetic AGEs inhibitors act at the early stage of AGEs formation that is at the initiation step wherein sugars attach to the free amino groups in the proteins. The compounds such as aspirin, diclofenac, pioglitazone, metformin and pentoxifylline exert their effect to prevent glycation at an early stage[192]. Most of the synthetic inhibitors like aminoguanidine (AG), pyridoxamine, buformin, quinine, carnosine, pyrraline *etc.* act at the late stages of glycation reaction wherein these act to scavenge the reactive carbonyls and free radicals. AG has potency to interact with β-dicarbonyls formed in the glycation reactions which helps in prevention of overt AGEs formation. Although, the synthetic compounds show excellent potency in preventing glycation, their application as a therapeutic is limited due to the side effects. For example, the clinical trials for AG were discontinued due to severe side effects such as anaemia, gastro-intestinal disturbance and flu-like symptoms. On the other hand, the natural compounds act as potent and relatively safe options for glycation inhibitors. Most natural inhibitors show dual properties of anti-glycation and anti-oxidant. A lot of flavonoids are found to be inhibitors of glycations including green tea polyphenols, epigallocatechin gallate (EGCG), epigallocatechin (EGC) and theaflavin-3,3′-digallate (TF3). These green tea polyphenols are found to scavenge the reactive dicarbonyls like glyoxal and methyl glyoxal and form primary adducts[193]. As already mentioned, one of the factor responsible for AGEs formation is concentration of proteins, the extent of glycation would increase with increased concentration and low turnover rate of proteins. Cytoskeletal proteins like actin and tubulin make up a substantial amount of intracellular proteins. Moreover, these proteins play a crucial role in neuronal cells in maintaining their morphology as well as functioning. The experimental model of diabetes showed glycation of actin and tubulin and reduced expression of tubulin isoform important for nerve growth and regeneration. Thus, it becomes important to prevent glycation in brain to ensure proper functioning of neurons.

3.1 Inhibition of Tau glycation by EGCG

Along with accumulation of AGEs, glycation is found to be present in PHFs of the demented patients' brains. Tau glycation preferentially occurs at its microtubule-binding region and weakens its affinity for microtubules (Fig. 3.1A). Moreover, glycation is suggested to stabilize the Tau PHFs and thus, enhance the toxic accumulation of these aggregates. EGCG, a green tea polyphenol (Fig. 3.1B), is reported to prevent glycation and glycation-induced ROS toxicity. We investigated the role of EGCG in inhibiting Tau glycation. Methyl glyoxal which is one of the reactive dicarbonyls was used as a glycating agent. Aminoguanidine, a synthetic glycation inhibitor known for its potency to interact with dicarbonyls and inhibit glycation was used as a positive control. Tau aggregation was monitored by

ThS fluorescence which showed steady increase in intensity in control and AG-treated Tau. The fluorescence intensity showed a decreasing pattern for EGCG treated Tau in a concentration- dependent manner suggesting reduced aggregation (Fig. 3.1C). The end time point fluorescence analysis revealed 60% inhibition of aggregation by 500 µM EGCG (Fig. 3.1D) whereas AG did not show significant reduction in MG-induced Tau aggregation. Further, the extent of glycation by MG was recorded by AGEs-specific fluorescence. The AGEs-specific fluorescence increased steadily for untreated control Tau indicating increased formation of AGEs with time. The intensity of fluorescence decreased with increased dosage of EGCG (Fig. 3.1E). At 144 hours, 500 µM EGCG displayed 72% inhibition of MG-induced Tau glycation as opposed to 42% inhibition by 1mM AG (Fig. 3.1F). Thus, EGCG demonstrated better potency in inhibiting *in vitro* Tau aggregation as compared to the positive control AG.

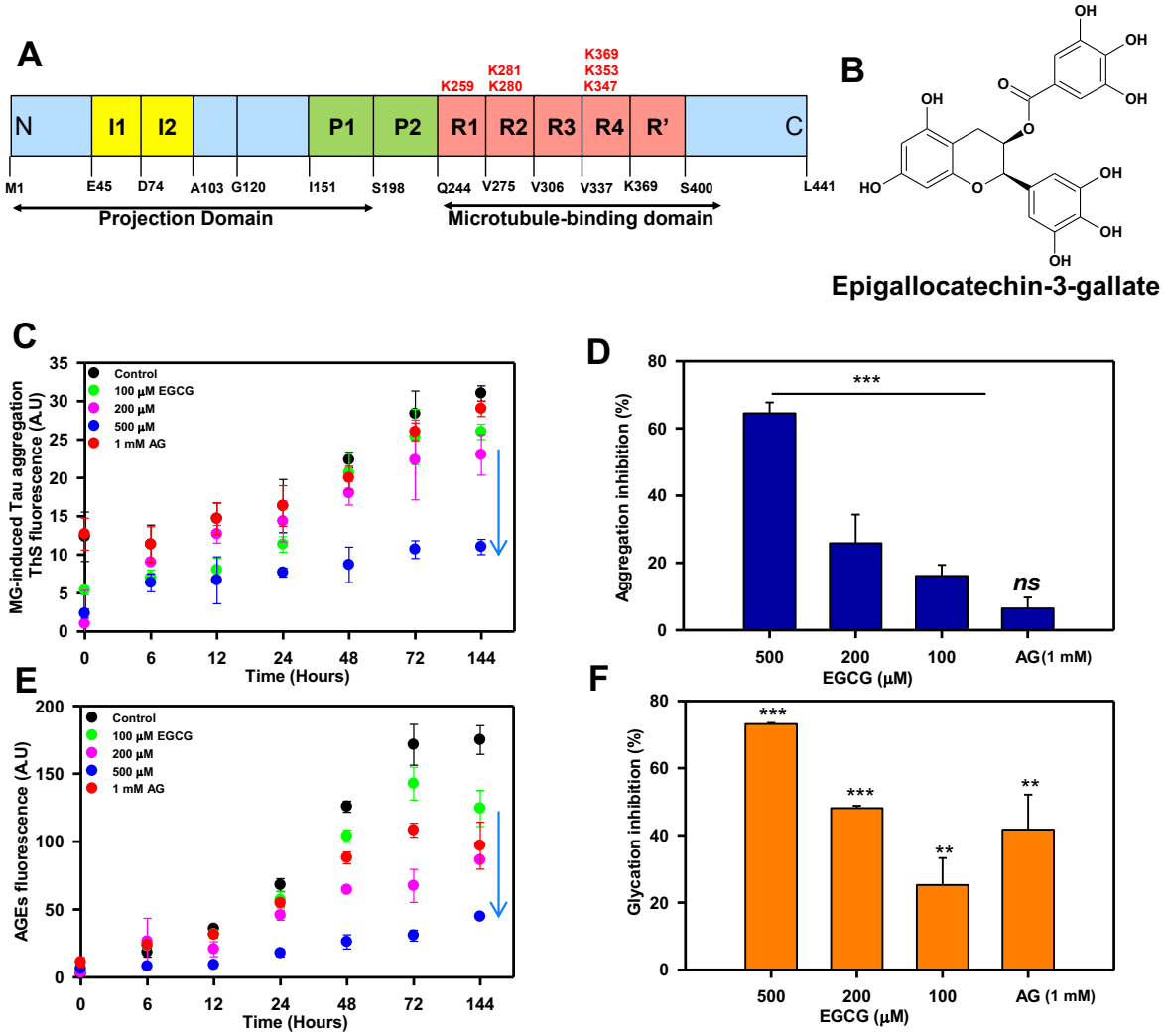

Figure 3.1. EGCG inhibits Tau glycation. A) Full-length Tau domain organization highlighting the glycation sites. B) Structure of EGCG. C) The ThS analysis of MG-induced Tau aggregation revealed that in absence of EGCG there is increase in ThS fluorescence suggesting aggregation. Increase in concentration of EGCG showed decrease in ThS intensity with lowest at 500 µM of EGCG. The positive control for glycation inhibition, aminoguanidine (AG) showed constant ThS fluorescence. D). The percent inhibition shows EGCG inhibits MG-induced Tau glycation but AG (1mM) does not rescue this aggregation. E) The AGEs auto fluorescence revealed that in presence of EGCG there is less AGEs formation as compared to untreated control. F) EGCG inhibits glycation more efficiently than the positive control AG (1mM) (The values are mean ± std. deviation of two independent experiments. The statistical analysis was carried out by Student's unpaired T- test with respect to untreated control. *** p≤0.001, **p≤0.01, *p≤0.05. *ns:* non-significant p value). This figure is adopted from Sonawane *et al.,* Oncotarget (under revision), 2020.

3.2 Characterization of Tau glycation inhibition by EGCG

Glycation is known to cause protein cross-linking and aggregation. The fluorescence assays revealed decreased MG-induced Tau aggregation and extent of AGEs formation in presence of EGCG, hence further characterization was done for the glycation reactions on SDS-PAGE and western blotting. The time-dependent SDS-PAGE displayed presence of monomer in all reaction mixtures at 0 hour of the assay (Fig. 3.2A). The protein glycation and cross linking increased with incubation time (24 hrs) and was observed as a trail of higher order Tau species on the SDS-PAGE (Fig. 3.2A). Moreover, the cross-linked higher order Tau species decreased in EGCG treated samples in a concentration dependent manner at 144 hrs (Fig. 3.2A). The intensity quantification revealed decreased intensity in 500 µM EGCG treated reaction mixture in time-dependent manner (Fig. 3.2B). However, the positive control AG did not show decrease in glycated Tau on SDS-PAGE (Fig. 3.2A, B).

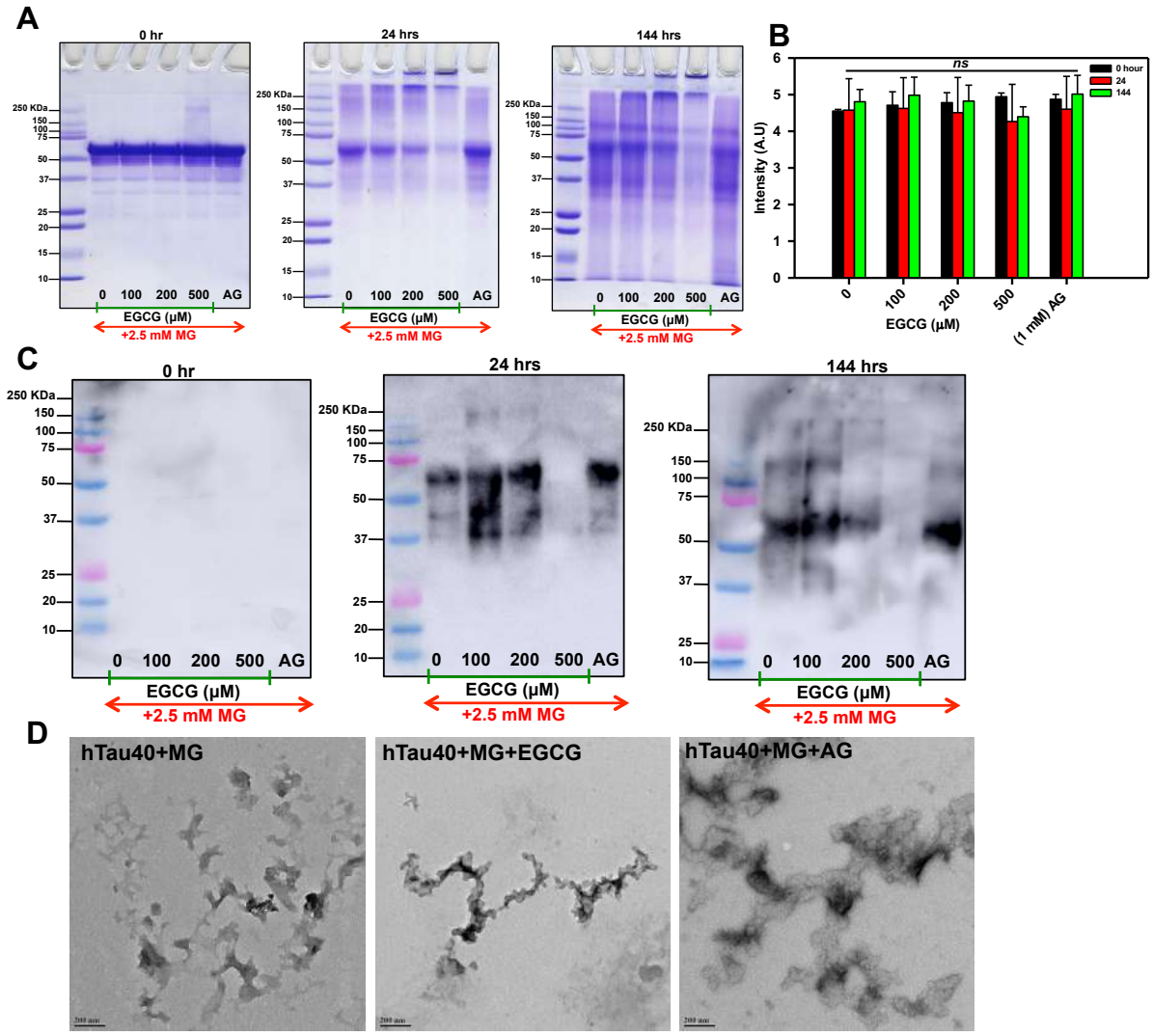

Figure 3.2. Inhibition of SDS-resistant Tau glycation. A) The SDS-PAGE analysis showed the formation of glycated Tau as smear above the soluble protein band. In presence of EGCG the higher order glycated Tau decreased with increasing concentration and time. B) Quantification of SDS-PAGE shows decrease in intensity in 500 µM EGCG in time dependent manner. C) Immunoblots with AGEs-specific antibody confirm EGCG inhibits Tau glycation in concentration and time dependent manner more efficiently than known glycation inhibitor aminoguanidine. D) The TEM images show presence of amorphous aggregates of glycated Tau and the morphology is not altered by EGCG treatment. This figure is adopted from Sonawane *et al.,* Oncotarget (under revision), 2020.

To confirm glycation and AGEs formation and their inhibition by EGCG, we immunoblotted the reaction mixtures at various time intervals with AGEs-specific antibody. The 0 hour reaction mixtures showed complete absence of AGEs formation. Further time intervals showed increased Tau-AGEs in

control reaction sample. The extent of AGEs decreased with increased concentration of EGCG (Fig. 3.2C). The immunoblotting results confirmed the observations from fluorescence assays and SDS-PAGE highlighting potency of EGCG in inhibiting MG-induced Tau glycation. Next, we assessed the morphological characteristics of EGCG-treated glycated Tau. The transmission electron microscopy displayed amorphous aggregates of Tau-induced by MG (Fig. 3.2D). The morphology remained same for EGCG treatment as well thus emphasizing EGCG inhibited glycation of Tau by MG without altering its qualitative characteristics.

3.3 Inhibition of intraneuronal MG-induced AGEs by EGCG

MG is reported to induce apoptosis in *in vitro* cultured hippocampal neurons as well as increase the oxidative stress in neuronal cells. The levels of intracellular AGEs and RAGE are also increased by exposure of neuro2a cells to MG. We investigated whether EGCG could modulate the induction of intracellular AGEs by MG (Fig. 3.3A). As expected MG treatment-induced increased AGEs formation as compared to control and EGCG treated cells. Moreover, the levels of AGEs were considerably lowered when the cells were treated with MG in presence of EGCG (Fig. 3.3B, C). Thus, EGCG showed inhibition of AGEs formation in the neuroblastoma cells by MG. This observation was further supported by the immunofluorescence studies. The AGEs fluorescence was increased on MG exposure as compared to untreated and EGCG-treated cells. The increase in AGEs by MG was rescued in presence of EGCG (Fig. 3.3D). The fluorescence intensity analysis displayed significant elevation in the levels of AGEs in MG exposed cells, which were lowered by EGCG in presence of MG (Fig. 3.3E). The orthogonal sections revealed a uniform AGEs formation in all the groups (Fig. 3.4A). Another observation reports role of MG in increasing intracellular Tau hyperphosphorylation. Thus, we studied the effect of EGCG on phospho-Tau AT 100 epitope.

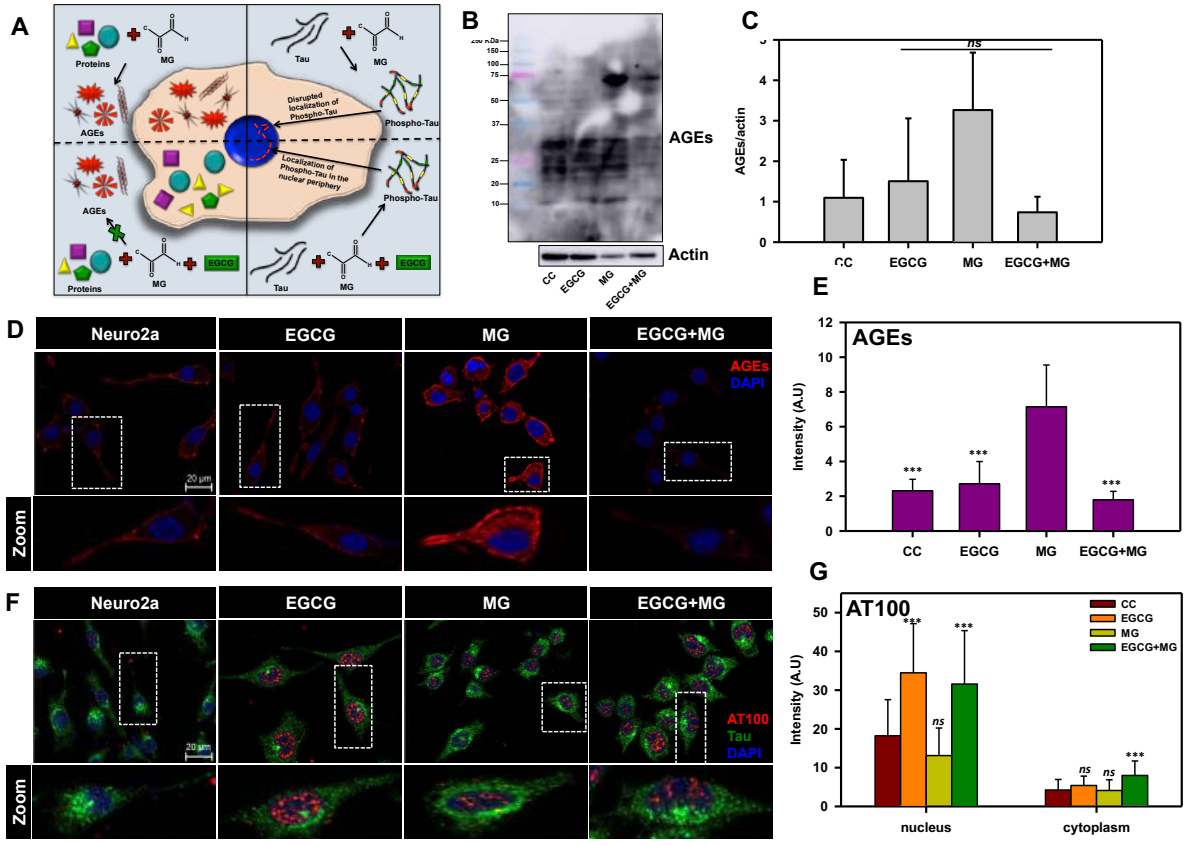

Figure 3.3. EGCG inhibits MG-induced AGEs formation in neuronal cells. A) A hypothetical model proposing effect of EGCG on MG-induced AGEs formation and Tau phosphorylation. Left panel depicts the effect of MG in inducing AGEs formation, which is abolished in presence of EGCG; the right panel shows the MG-induced Tau phosphorylation and its

modulation by EGCG. B) Western blotting of neuronal cells treated with MG for AGEs shows increased AGEs formation in presence of MG as compared to untreated and EGCG treated. The level of glycation by MG is observed to decrease in presence of EGCG. C) Quantification of AGEs formation normalized to actin levels show increased AGEs in MG treated cells as compared to other treatment groups. D) Untreated and EGCG treated cells show basal level of AGEs. MG-induced cells show increased intensity for AGEs. EGCG show decrease in AGEs induced by MG. The pseudocolors represent respective antibody staining; Red: AGEs, Blue: DAPI. E) Quantification for AGEs fluorescence confirms increased glycation in MG treated cells and rescue in MG treated cells supplemented with EGCG. F) AT100 Tau phospho-epitope is present in negligible levels in control cells and distributed uniformly. EGCG treatment shows a distinct nuclear localization of AT100 Tau around the periphery, which is disrupted in presence of MG. EGCG along with MG shows to restore this AT100 distribution in the nucleus. The pseudocolors represent respective antibody staining; Red: phospho-Tau AT100, Green: Total Tau, Blue: DAPI.G) Tau phosphorylated at AT100 epitope shows enhanced nuclear localization in EGCG treated cells as compared to other groups. (The values are mean ± std. deviation of two independent experiments. The statistical analysis was carried out by Student's unpaired T- test with respect to MG treatment group. *** p≤0.001, **p≤0.01, *p≤0.05. *ns:* non-significant p value). This figure is adopted from Sonawane *et al.,* Oncotarget (under revision), 2020.

This is one of the AD-associated epitopes with Tau phosphorylated at S212/T214. The fluorescence imaging revealed a distinct pattern of AT 100 distribution rather than total levels of phospho-Tau. The untreated control showed uniform distribution of AT 100 throughout the cells. But EGCG treatment displayed localization of AT 100 phospho-Tau at the nuclear periphery (Fig. 3.3F). The orthogonal projections aided in clear visualization of this unique localization. (Fig. 3.4B). The MG treatment showed disturbed arrangement of AT 100 Tau but treatment of MG in presence of EGCG restored the nuclear peripheral localization of phospho-Tau. We further carried out quantitative analysis to decipher the distribution of AT 100 phospho-Tau in nucleus and cytoplasm in accordance with the treatment groups. The groups with EGCG treatment showed enhanced nuclear localization of AT 100 Tau as compared to control and MG treated groups (Fig. 3.3G).

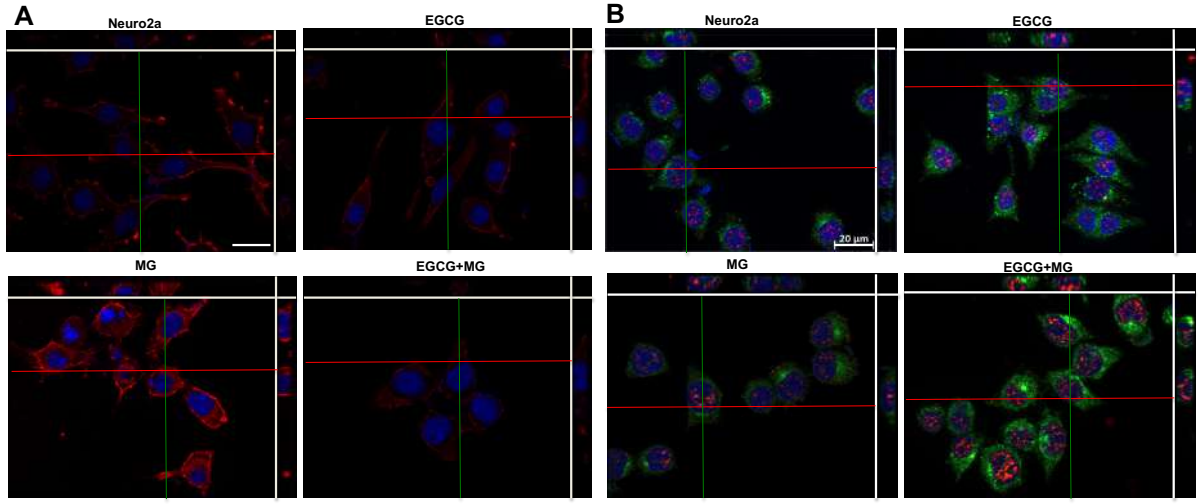

Figure 3.4. Orthogonal section image analysis of MG-induced AGEs and Tau phosphorylation. A) Orthogonal projectional analysis shows basal level of AGEs in untreated and EGCG treated cells. MG treatment induces global glycation in the cells resulting in enhanced AGEs formation in the cells. EGCG is found to inhibit this effect of MG and reduce the global AGEs formation in the cells. The pseudocolors represent respective antibody staining; Red: AGEs, Blue: DAPI. B) AT100 phospho-Tau is present at basal levels in control cells and distributed throughout the cytoplasm and nucleus. EGCG treatment is found to change the localization of phospho-Tau in the nucleus at the periphery in a ring like manner. MG treatment disrupts this arrangement in as seen in the orthogonal projections whereas MG and EGCG together maintain the AT100 phospho-Tau in the nucleus. The pseudocolors represent respective antibody staining; Red: phospho-Tau AT100, Green: Total Tau, Blue: DAPI. Scale bar: 20 µm. This figure is adopted from Sonawane *et al.,* Oncotarget (under revision), 2020.

3.4 EGCG promotes formation of neuronal extensions

Neuronal extensions or neurites are highly dynamic structures at the end of growth cones. Neuronal extensions form the foundation of neuronal wiring and transmission of electric impulses. The peripheral

domain of growth cone is rich in F-actin and comprises of filopodia and lamellopodia structures[194]. Axon is the dominant neurite of the neuron and is a key element in maintaining neuronal polarity. The axonal mechanics is being maintained in part by the actin rings and spectrin plays an essential role in maintaining structural integrity of axons[195]. The immunofluorescence studies for intracellular AGEs formation by MG revealed an interesting observation wherein the MG treatment completely disturbed the neuronal morphology with the gross loss of neuritic extensions. Thus, we investigated the status of actin cytoskeleton in these treatment groups. In order to better understand the spatial distribution of actin-rich neurites, we captured 3D stacks of the cells probed for actin and obtained a cumulative image for each treatment group. The control group displayed a uniformly distributed actin cytoskeleton in the neuroblastoma cells. The exposure of cells to EGCG formed enhanced neuritic extensions as compared to control. On the contrary, MG treatment disrupted the actin cytoskeleton in the neuronal cells and curtailed the neuritic extension formation. A considerable population of cells were rounded off with very short or no neuritic extensions. The exposure of cells together with MG and EGCG revived and enhanced the neuritic extensions thus attenuating the actin disrupting effect of MG (Fig. 3.5A). The analyses of neuritic lengths revealed significant differences between the MG treatment and other groups. MG treatment severely affected the neuritic formations, which was successfully rescued by EGCG and was enhanced as compared to control (Fig. 3.5B).

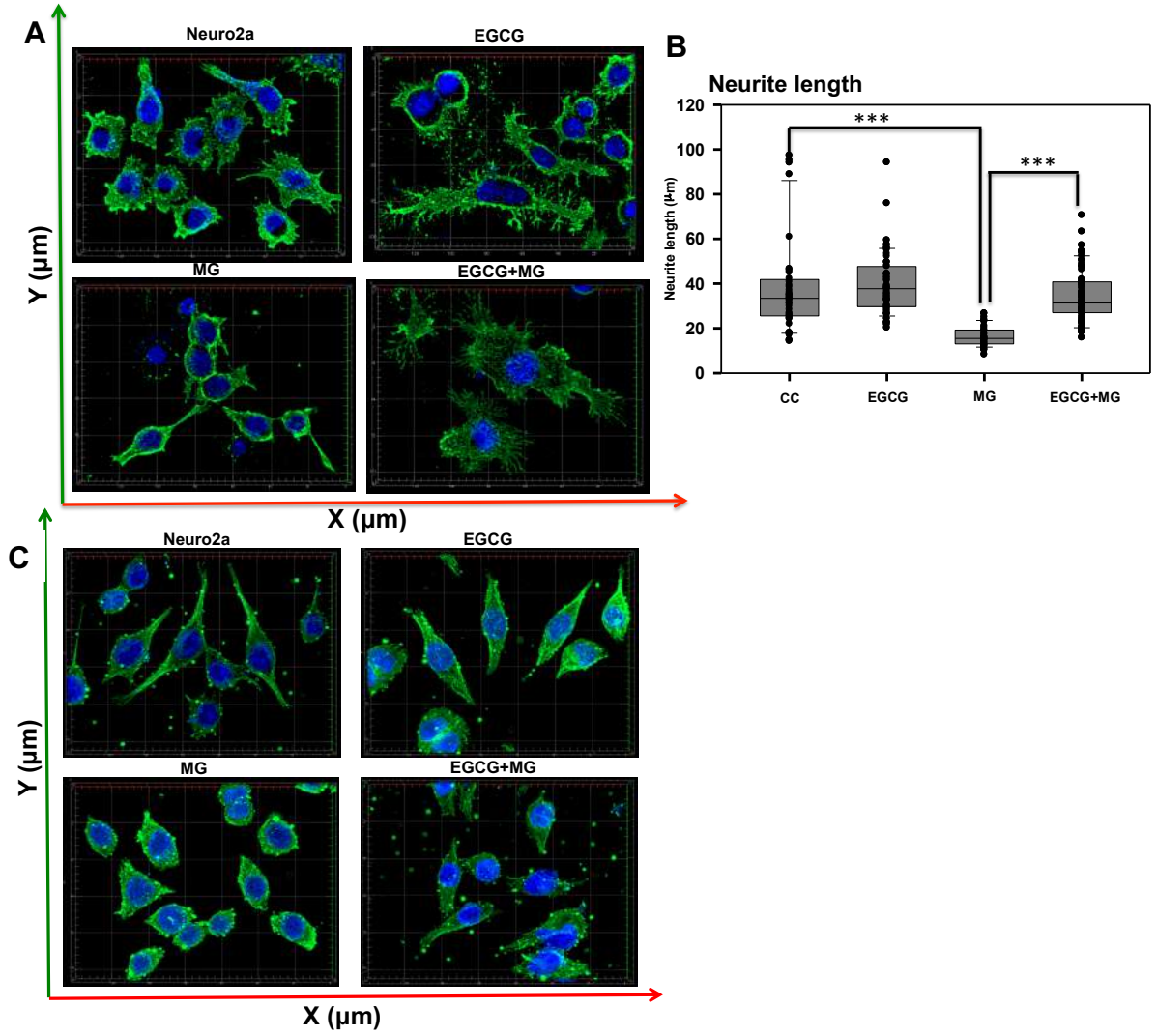

Figure 3.5. Effect of EGCG on actin and tubulin cytoskeleton remodeling. A) 3D analysis of actin cytoskeleton shows neuritic extensions, which are maintained in control cells and enhanced in EGCG treated cells. MG disrupts the neuritic extensions severely whereas EGCG restores the actin-rich neuritic extensions. The pseudocolors represent respective antibody

Green: Actin, Blue: DAPI. B) MG treatment drastically reduced the neuritic extensions in cells as compared to control. EGCG treatment rescued the MG affected neurites and maintained the neuronal cell morphology. C) Tubulin cytoskeleton was maintained in control and EGCG treated cells with intact MTOC. MG treated cells did not show severe disruption of microtubules but it lead to loss of MTOC integrity. EGCG re-established the integrity of microtubules and MTOC. The statistical analysis was carried out by Student's unpaired T- test with respect to MG treatment group. *** p≤0.001, **p≤0.01, *p≤0.05. *ns:* non-significant p value). The pseudocolors represent respective antibody staining; Green: Tubulin, Blue: DAPI. This figure is adopted from Sonawane *et al.,* Oncotarget (under revision), 2020.

In association with actin, tubulin cytoskeleton also plays an important role in maintaining neuronal structure and function. Microtubules are polarized filaments of tubulin dimers with polymerization occurring at plus ends directed towards the axonal terminal. The polarity of microtubules also aids in maintaining the neuronal polarity. Since, MG was found to disrupt the actin cytoskeleton in the neuronal cells, we mapped the tubulin cytoskeleton to check its status on MG treatment. As anticipated, MG treatment affected the tubulin architecture in the neuronal cells leading to loss of cell morphology. EGCG averted this MG-induced disruption of tubulin cytoskeleton keeping the morphology undefiled (Fig. 3.5C). Thus, EGCG not only prevented MG-induced disruption of actin and tubulin architecture but enhanced the neuronal structural elements.

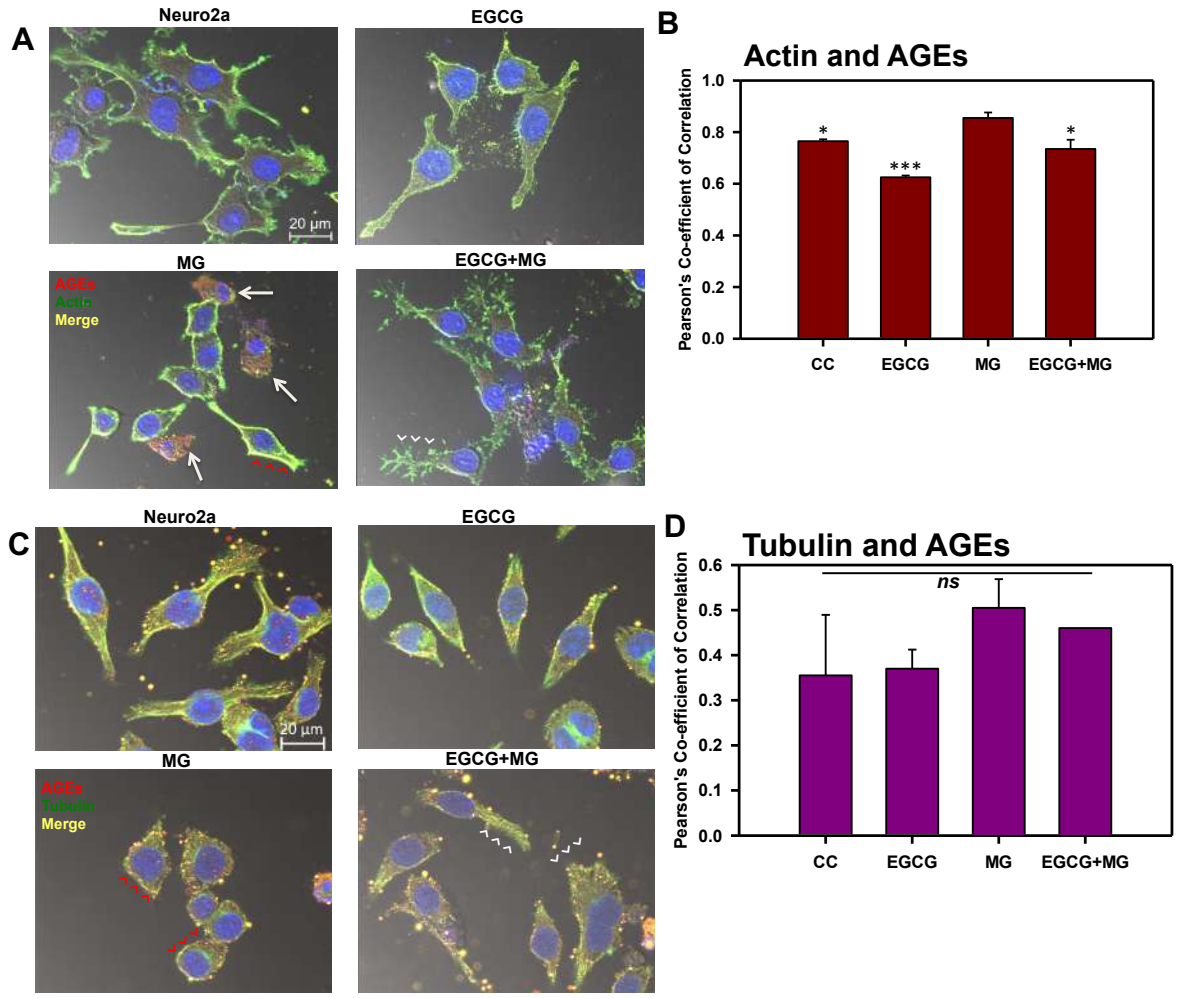

Figure 3.6. EGCG-mediated rescue of neuronal cytoskeleton glycation. A) The actin cytoskeleton is severely glycated in presence of MG which is visualized as yellow fluorescence (red arrowheads). The cells with completely disrupted actin cytoskeleton show high levels of AGEs cytoskeleton (white arrows). Alternatively, EGCG together with MG showed decreased actin glycation (white arrowheads) and restoration of the extensions. B) The Pearson's co-efficient of correlation for co-localization analysis to study the actin glycation by MG showed a higher value as compared to untreated control and EGCG. EGCG was found to decrease the PCC in presence of MG suggesting less colocalization and inhibition of MG-induced

glycation. C) The control and EGCG treated cells showed intact tubulin cytoskeleton with basal levels of AGEs. MG-induced the glycation of tubulin cytoskeleton and lead to its disruption (red arrowheads). On complementation with EGCG, the glycation was inhibited (white arrowheads) and the intact morphology of cells was preserved. D) The PCC for tubulin and AGEs co-localization did not show significant changes among the groups. (The values are mean ± std. deviation. The statistical analysis was carried out by Student's unpaired T-test with respect to MG treatment group. *** p≤0.001, **p≤0.01, *p≤0.05. *ns:* non-significant p value). The pseudocolors represent respective antibody staining; Red: AGEs, Green: Tubulin, Blue: DAPI. This figure is adopted from Sonawane *et al.,* Oncotarget (under revision), 2020.

3.5 EGCG protects MG-induced glycation of actin and tubulin

As discussed, the extent of glycation of a specific protein in the cells depends on the concentration and turnover rate of the protein. Actin and tubulin being the cytoskeletal proteins contribute to a large pool of intracellular proteins. The earlier observations demonstrated the effect of MG in disrupting the actin and tubulin cytoskeleton and their restoration by EGCG. Further, we studied the glycation of actin and tubulin by MG and effect of EGCG on the MG-induced glycation. The glycation was studied by immunofluorescence and colocalization analysis of AGEs and the respective actin or tubulin proteins. The AGEs were stained with red fluorescence and actin/tubulin with green. The extent of glycation was detected by merged yellow fluorescence. The control and EGCG treated cells displayed dominantly green fluorescence of actin/tubulin cytoskeleton with intact morphology and neurites (Fig. 3.6A, C). MG treatment lead to excessive glycation of both the cytoskeletal proteins observed as yellow fluorescence (Fig. 3.6A, C). Additionally, the dead cells in MG treatment showed abundant build-up of AGEs (Fig. 3.6A). The MG-induced glycation of actin and tubulin was inhibited in presence of EGCG (Fig. 3.6A, C white arrow heads) and the neuronal structure and morphology was also revived. The degree of glycation was deciphered by the co-localization analysis for the two epitopes that is AGEs+actin and AGEs+tubulin fluorescence by *coloc2* plugin in Fiji on the background subtracted images. The Pearson's co-relation co-efficient (PCC) for the colocalization of AGEs+actin fluorescence (glycation of actin) increased in MG exposure as compared to control or EGCG treated group. This suggests excessive MG-induced glycation of actin. On the other hand, the value for PCC for MG +EGCG treatment was reduced as compared to MG treatment, suggesting decreased colocalization thus, revealing decrease in the extent of glycation (Fig. 3.6B). Thus, EGCG was found to prevent actin glycation thereby restoring the neurites. In case of tubulin, the MG treated cell showed increased PCC as compared to other groups, though the difference was not significant (Fig. 3.6D).

3.6 EGCG maintains distribution of neuronal cytoskeletal proteins

The neuronal morphology and polarization is maintained by the two core components of cytoskeletal elements, microtubules and actin. Both the polymers are polarized in nature with plus and minus ends. The spatial distribution of these polarized fibres aid in various neuronal morphological modulations like protrusion of membranes for migration or enhancement of neuronal extensions and their branching. Actin is more abundant in the contractile and protrusive tips of growth cones. β-actin is enriched more in cellular cortex region. Microtubules, on the hand, are present more in the interior. Microtubules are formed from the microtubule organizing centre (MTOC) by polymerization of the α and β-tubulin at the plus ends, which point to the cell periphery which is axon terminals in neurons[196]. The mammalian dendrites have a mixed orientation of microtubules. The orientation and interconnections among the actin and microtubules are crucial for neuronal functions and modulation of these could alter the neuronal health leading to neurodegeneration. The probing of neuronal cells for actin and tubulin together revealed abundant cortical actin and intact network of microtubules in the interior of cells in control and EGCG treated cells (Fig. 3.7A, B). These cells displayed an intact MTOC with radial arrays of microtubules emerging from MTOC. Exposure of cells to MG hampered the cell morphology with extensive loss of neurites (Fig. 3.7A). A closer observation at the peripheral regions of cells revealed excessive disruption of actin cytoskeleton by MG (Fig. 3.7C). Interestingly, EGCG protected the

cytoskeleton from MG-mediated disruption of both actin and tubulin cytoskeleton maintaining their integrity and neuronal morphology (Fig. 3.7A, B, C). In order to gain better insight into the spatial distribution of actin and microtubules, 3D imaging was done from the Z-stacks obtained for each treatment group (Fig. 3.7D). The enlargement of the peripheral sections revealed predominance of actin in the terminal neurites and neuronal extensions whereas microtubules maintained their network in the interior regions of the cells. The cell cytoskeleton was found to be severely disorganized on MG treatment which was rescued in presence of EGCG.

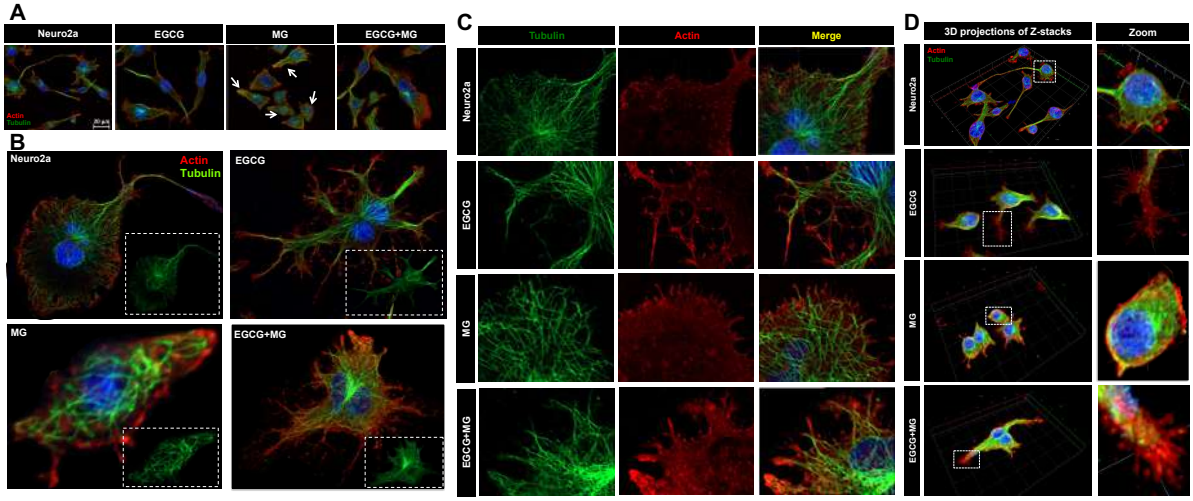

Figure 3.7. Distribution of cytoskeletal elements. A) Complete cell image showing multiple cells in various treatment groups. Untreated and EGCG treated cells maintain the cytoskeleton structure. MG treated all the cells show loss of cytoskeleton integrity and distribution whereas EGCG treated cells show maintained cytoskeleton distribution and restored integrity. B) Single cell image of the same treatment groups with detailed distribution of cytoskeleton. C) The actin and tubulin cytoskeleton are differentially distributed with actin enriched in small neuritic extensions followed by tubulin fibres. This distribution was found to be hampered on MG treatment with excess loss of actin extensions and loss of MTOC integrity. This was unhampered in EGCG treatment along with MG. D) The 3D analysis of the distribution of cytoskeletal elements shows clear cortical actin as opposed to tubulin in the cytoskeleton. The control and EGCG treated cells shows presence of minute actin extensions protruding out which might be involved in their motility towards other neurons in the vicinity. MG treated cells show loss of these minute extensions. EGCG together with MG showed restoration of these minute actin extensions. The pseudocolors represent respective antibody staining; Red: Actin, Green: Tubulin, Blue: DAPI. This figure is adopted from Sonawane *et al.,* Oncotarget (under revision), 2020.

Though, the wide field microscopy imaging revealed modulation of cytoskeletal elements by MG and EGCG, the minute details about the cytoskeleton organization was achieved by applying one of the super-resolution microscopy technique, structured illumination microscopy (SIM). The super-resolution microscopy techniques have surpassed the diffraction limits and raised the resolution towards nanometres scale thus allowing visualizing the minute details in viable cells which was previously not possible. SR-SIM utilizes illumination pattern with periodic interferences such that the periodicity lies close to the diffraction limit. SR-SIM improves the lateral and axial resolution in comparison to wide field microscope. The advantages of SR-SIM include no special sample preparation requirements and no special fluorophore requirements. Thus, we scanned our samples on ELYRA7, lattice SIM for fine and detailed visualization of cytoskeletal distribution pattern. The SIM images re-iterated the results with more clarity of the images (Fig. 3.8A). The region of interest (ROI) was selected for each image and details were observed wherein MG was found to have severe effect on actin cytoskeleton as compared to the tubulin network. EGCG was found to completely block the MG-induced disruption of actin and microtubules as visualized from the ROI. The cumulative images of Z-stacks gave improved spatial resolution showing intact MTOC in control and EGCG treated cells and complete loss of MTOC in MG-treated cells. Moreover, these cells also displayed stunted neuritic extensions with altered

morphology (Fig. 3.8B). Alternatively, MG+EGCG treated-cells showed presence of MTOC and enhanced neuritic extensions confirming the role of EGCG in inhibiting the toxic action of MG.

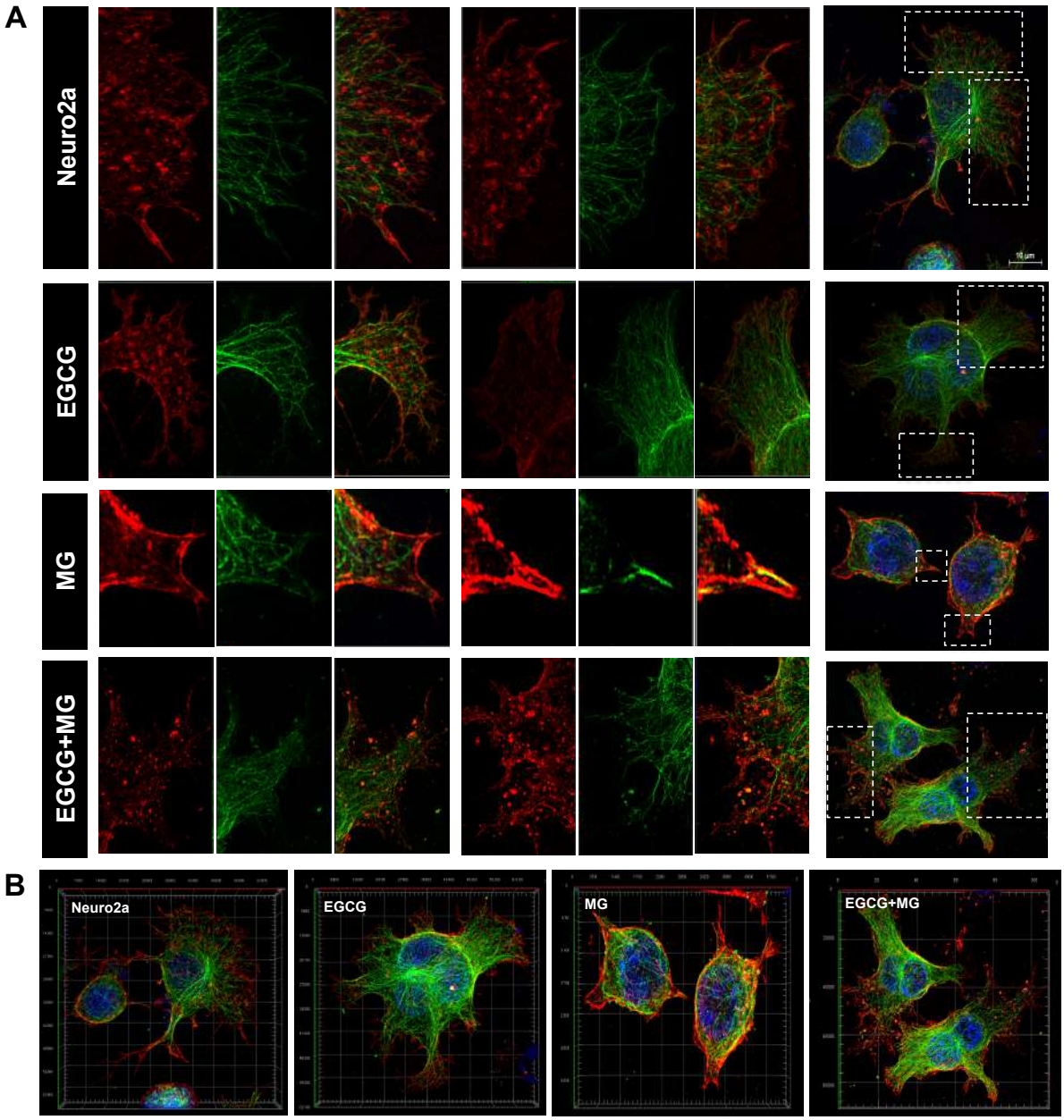

Figure 3.8. Super-resolution microscopy images for detailed analysis of cytoskeleton. The detailed analysis of distribution of actin and tubulin cytoskeleton was carried out by structured illumination microscopy. A) The SIM images distinct distribution of actin and tubulin cytoskeleton in control and EGCG treated cells. MG disrupted actin cytoskeleton severely but EGCG prevented this disruption and maintained the cytoskeleton integrity including MTOC. B) The cumulative image for the Z-stacks reveals spatial distribution of actin and tubulin cytoskeleton. The pseudocolors represent respective antibody staining; Red: Actin, Green: Tubulin, Blue: DAPI. This figure is adopted from Sonawane *et al.,* Oncotarget (under revision), 2020.

3.7 EGCG maintains neuronal morphology by enhancing microtubule-EB1 interaction

The end-binding proteins are microtubule interacting proteins, which associate with the plus ends of microtubules and help in their treadmilling. End-binding protein 1 (EB1) belongs to a class of +TIPS (microtubule plus end binding proteins) which aid in polymerization of microtubules at the plus ends. We investigated the localization of EB1 protein in our treatment groups *via* immunofluorescence studies. The cells were stained for tubulin and EB1 and showed concentration of EB1 towards the microtubule ends in control and EGCG treated cells (Fig. 3.9A). The single cell image analysis revealed

distribution of EB1 throughout the cells with less abundance in MG-treated cells (Fig. 3.9B). The exposure of cells together with MG and EGCG showed abundance of EB1 at the microtubules ends suggesting rescue of microtubule-EB1 interactions by EGCG (Fig. 3.9B). Though we tried to gain a deeper insight into the EB1 localization by 3D imaging in widefield fluorescence microscope we could not get better resolution to confirm our observation (Fig. 3.9C).

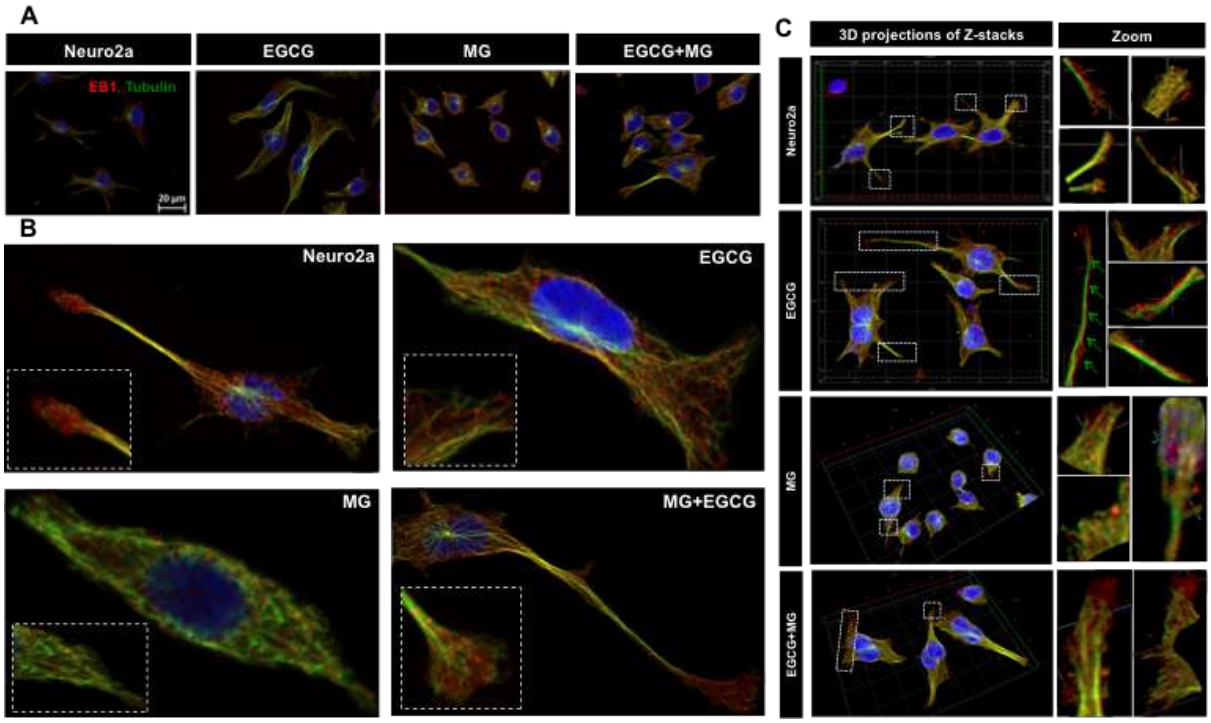

Figure 3.9. Microtubule stabilization by EB1 maintained by EGCG. A) Cell images showing distribution of EB1 with microtubules in different treatment groups. B) Single cell images showing EB1 maintains the growing end of microtubules helping in its tread milling, which is important for cellular functions. EB1 is bound to microtubules (inset) at the ends of the extension but this is not observed in case of MG treatment. MG treatment shows irregular distribution of EB1, which is maintained and resumed by EGCG. The inset enlarged images show the localization of EB1 at the growing ends of microtubules but disrupted by MG. C) 3D images of Z-stacks show distinct distribution of EB1 protein at the ends of the microtubules (zoom). MG treatment disrupts the microtubules and hence the localization of EB1. EGCG maintains the microtubule EB1 localization in presence of MG thus stabilizing the microtubules. The pseudocolors represent respective antibody staining; Red: EB1, Green: Tubulin, Blue: DAPI. This figure is adopted from Sonawane *et al.,* Oncotarget (under revision), 2020.

Thus, we acquired the 3D stacks in SR-SIM and analysed the neuronal cells for microtubule-EB1 localization. The microtubule-EB localization was observed in abundance in all the groups except MG treated group (Fig. 3.10). A clear rescue of EB1 localization was observed in MG+EGCG treatment group. The colocalization of microtubules and EB1 at the tips of neurons was observed as yellow fluorescence. Thus SR-SIM images displayed role of EGCG in maintaining the integrity of microtubules *via* EB1.

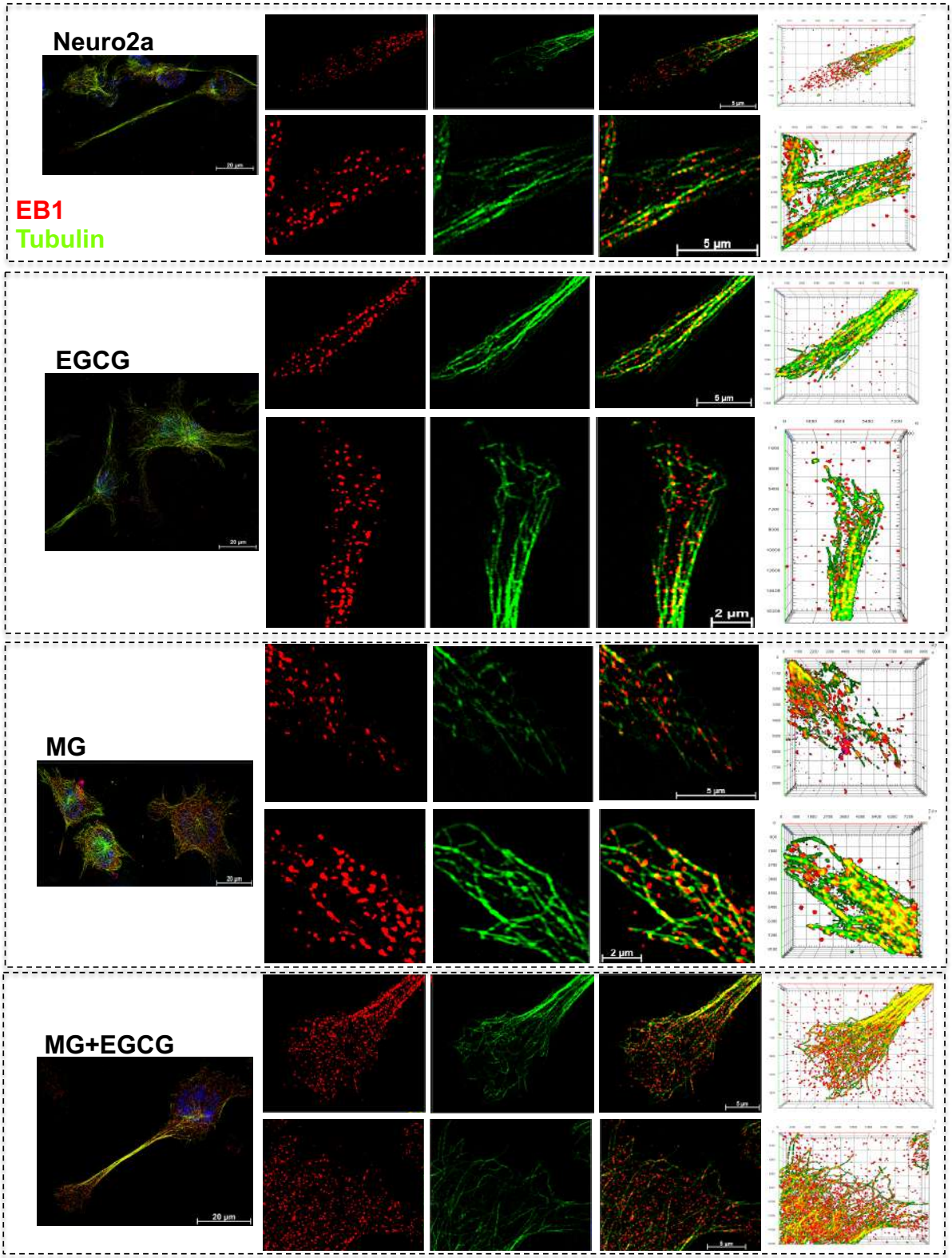

Figure 3.10. Super-resolved images for EB1-mediated microtubule stabilization. The SIM images reveal clear localization of EB1 at the ends of microtubules in the control and EGCG treated cells. The EB1 localization was severely hampered and less abundant in MG treated cells. This effect of MG is inhibited in presence of EGCG. The rescued colocalization is visualized as yellow fluorescence. The pseudocolors represent respective antibody staining; Red: EB1, Green: Tubulin, Blue: DAPI. This figure is adopted from Sonawane *et al.,* Oncotarget (under revision), 2020.

Thus, EGCG is not only a potent glycation inhibitor but acts an enhancer of neuronal extensions regulator of maintaining neuronal cytoskeleton integrity.

Chapter 4
Effect of polyphenols on Tau aggregation

Polyphenols are non-essential nutrients found abundantly in fruits and vegetables and are known to have beneficial effects in varied diseases like cancer, cardiovascular disorders and neurodegenerative diseases. The phenolic rings, hydroxylation patterns and the conjugation of double bonds are important for their mechanism of action in various pathological features of disease. For example, the iron chelating activity of polyphenols require presence of at least one catechol group in the molecule to make it a potent quencher of divalent metal ions and ROS[197]. Another important property of polyphenols is to inhibit self-assembly of amyloidogenic proteins such as Aβ, Tau and α-synuclein involved in neurodegenerative diseases. The aromatic interactions and phenol rings are postulated to reduce the cross-β-sheet structure involved in self-assembly[198]. Most polyphenols are known to interfere the aggregation by hydrophobic and π-stacking interactions[199]. Moreover, Epigallocatechin-3-gallate (EGCG) has been reported to form covalent bond to inhibit aggregation[200]. Tau on the other hand is known to interact with several molecules at various domains, which act on Tau aggregation (Fig. 4. 1A). Here, we studied effect of two distinct polyphenols Baicalein and EGCG on Tau pathology and their modes of interaction with Tau.

4.1 Baicalein and Tau pathology

Baicalein is isolated from the roots of a Chinese herb *Scutellaria baicalensis Georgi* and has shown beneficial effects in various pathologies including neurodegenerative diseases (Fig. 4.1B). Baicalein prevents aggregation of α-synuclein protein involved in Parkinson's disease pathology and supresses inflammation in the *nigro-striatal* dopaminergic system[201,202]. Baicalein attenuates ROS generation and mitochondrial dysfunction caused by prion protein in cell cultures. In AD, Baicalein is reported to recover Aβ-mediated memory impairments and prevent Tau hyperphosphorylation by supressing GSK-3β activity[203]. Since, the systemic effects of Baicalein in ameliorating neurodegenerative diseases is known, we focused our study on the molecular interaction of Tau with Baicalein and its effect on *in vitro* heparin-induced Tau aggregation.

4.1.1 In silico analysis of Tau-Baicalein interaction

The interaction studies by molecular docking and simulation were carried out by modelling repeat Tau region containing the two hexapeptide motifs ^{275}VQIINK^{281} and ^{306}VQIVYK^{311} at the initiation of R2 and R3 respectively (Fig. 4.1C). The full-length Tau has disordered regions at both N- and C-terminals which makes it difficult to model it. The repeat Tau model generated displayed 98% of residues in the allowed region of Ramachandran plot. The model was refined and set to restrained minimization by merging the non-hydrogen atoms to an RMSD of 0.3 in OPLS 2005 force field. Further, the model was subjected to energy minimizations and was used for docking and simulation. The Tau-Baicalein docking yielded a best pose having glide score of -5.06 and E-model value of -44.365. The O1 atom of Baicalein was found to interact with NH_2 group of Asn 265 and NH group of imidazole ring of His 268 respectively. The hydroxyl groups of Baicalein involving O3 and O4 atoms showed interaction with the carboxyl O^- of Glu 338 *via* hydrogen bonds (Fig. 4.1D) The interaction distance was observed to be 2.7 Å, 2.0 Å and 1.8 Å respectively. The interaction distance of Baicalein and NH_2 group of Asn 265 of Tau was found to be 2.3 Å. Tyr 310 belonging to hexapeptide motif ^{306}VQIVYK^{311} and Val 313 formed hydrophobic interactions with Baicalein. The interaction of His 299 *via* water bridges was found to be crucial since it is postulated to be involved in Baicalein-mediated Tau disaggregation. The stability of Baicalein-Tau complex was analyzed by simulation for 15 ns. The RMSD graph with time (nanoseconds) on X-axis and RMSD of Cα of protein and ligand in Å on left and right Y-axis, respectively were plotted (Fig. 4.1E). The RMSD of Cα was overall stable with minor reposition of Baicalein at the ^{306}VQIVYK^{311} hexapeptide motif. The Cα RMSD of 10 Å between initial and final simulation suggested conformational change upon binding. During the course of the simulation, a few

residues namely Asn 296, Ile 297, His 299, Gln 307, Tyr 310, Lys 311, Val 313 and Leu 315 out of which three residues belong to the hexapeptide region mentioned above, were found to form an increasingly high number of interactions with Baicalein, indicating that these may be crucial residues to stabilize the complex (Fig. 4.1F).

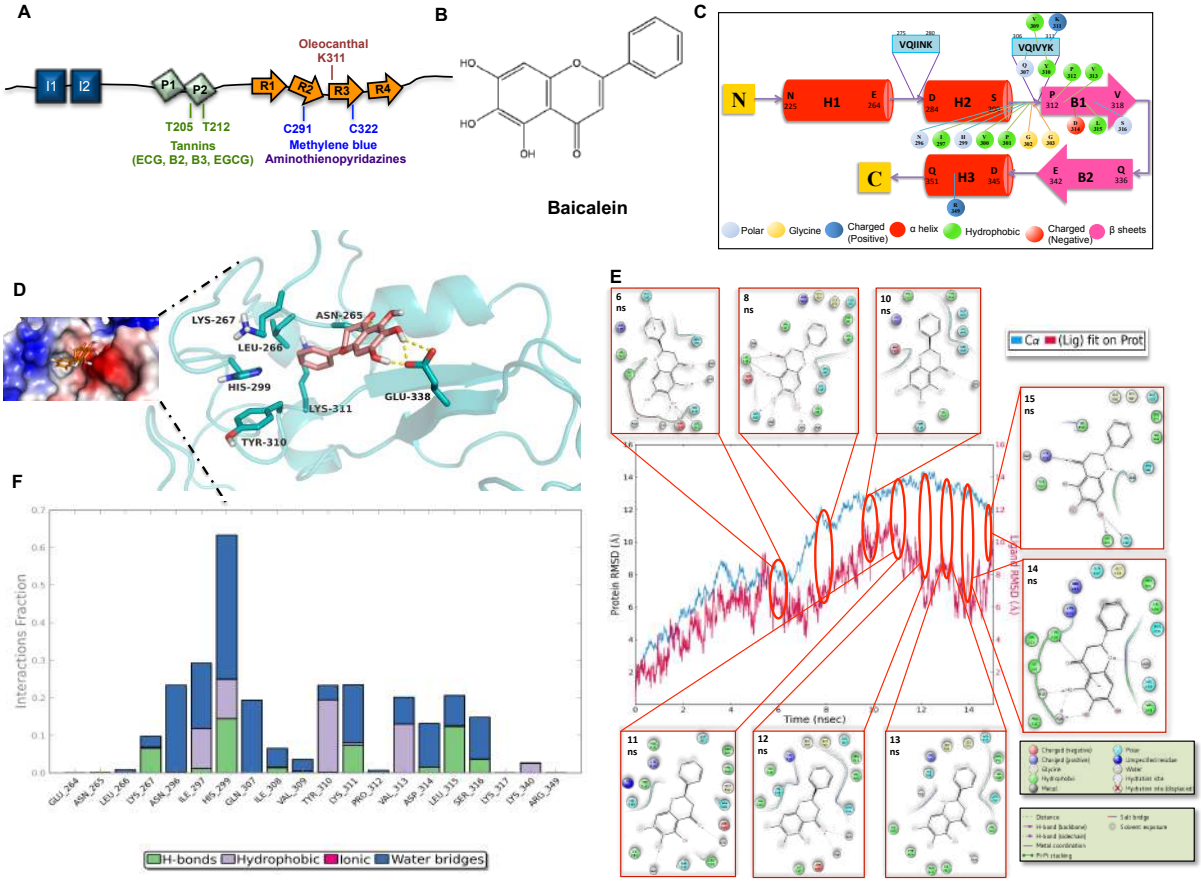

Figure 4.1. The interaction of Tau with Baicalein. A) Tau protein domain organization with the known binding sites for the small molecule inhibitors of Tau aggregation. B) Chemical structure of the flavonoid Baicalein. C) A schematic diagram of the repeat Tau model secondary structure depicting three predicted α helices (H1, H2, and H3) and two predicted β sheets (B1, B2) with two distinct and characteristic hexa-peptide regions 275VQIINK280 and 306VQIVYK311. The predicted ligand interacting residues, color coded according to their type of interaction is also shown. D) A detailed snapshot of the ligand-binding pocket of Baicalein in our proposed model of repeat Tau including the interacting residues as indicated and the corresponding surface represented in terms of electrostatic potential. E) The above plot shows the RMSD evolution of the protein, Tau (left Y-axis) and a comparative view of the RMSD evolution of the ligand, Baicalein (right Y-axis) through the similar time-scale, which indicates how stable the Baicalein is with respect to the binding pocket in Tau. The interactions are shown in detail, for different nanoseconds for comparative relevance. The diagram indicates a dynamic pocket of interaction of Tau, which is to be expected since Tau is a highly flexible soluble protein. F) A bar diagram depicting the extent of interaction over the course of 15 ns simulation using the same docked structure which indicates that the residues mentioned are majorly involved in the binding and probable biochemistry of the ligand binding to Tau. The protein ligand interactions or contacts are categorized into four types: Hydrogen Bonds, Hydrophobic, Ionic and Water Bridges. This figure is reproduced from Sonawane *et al*., ABB, 2019.

4.1.2 Baicalein inhibits Tau aggregation by inducing oligomer formation and stabilization

Tau aggregation inhibitors (TAIs) are screened in a classical way utilizing the approach of cell free assays by inducing Tau aggregation by heparin. The primary screening of TAIs utilizes fluorescence-based assays such as ThS/ThT, which monitor the aggregation of Tau protein in solution. We employed a time-based ThS fluorescence assay to determine the effect of Baicalein on aggregation of full-length and repeat Tau. 20 μM Tau proteins were treated with 0, 5, 10, 25, 50, 100 and 500 μM of Baicalein in a reaction buffer containing heparin. For the full-length Tau assembly the rate of fibrillization was

monitored every 5 hours for the first 24 hours of the incubation period (Fig. 4.2A). Though, for the first 24 hours significant differences were not observed in ThS fluorescence for most concentrations of Baicalein, the effect of higher concentrations (100 and 500 µM) of Baicalein were clearly observed. These concentrations displayed an increased fluorescence till 5-10 hours after which the intensity began to drop (Fig 4.2B), this suggested inhibition of heparin-induced Tau aggregation in presence of Baicalein. The lower concentrations of Baicalein showed aggregation inhibition but at the later time points (Fig. 4.2A). On the contrary, the untreated wild type Tau showed steady increase in fluorescence suggesting progress and saturation of aggregation. Thus, ThS kinetics revealed Tau aggregation inhibition by Baicalein in a concentration-dependent manner. The percent inhibition calculated at the end time point (168 hours) demonstrated significant inhibition of Tau aggregation at all the concentrations of Baicalein with highest concentration of 500 µM having 85% inhibition (Fig 4.2C). The IC_{50} for Tau inhibition by Baicalein was observed to be 27.6 µM (Fig. 4.2D). The transition of Tau from soluble protein to fibrillar aggregates follows through formation of intermediate species, which show increase in their hydrophobicity due to exposure of hydrophobic patches in the proteins. Such changes in hydrophobicity are mapped by ANS which is a fluorescent dye having specificity for exposed hydrophobic patches. The study of Tau hydrophobicity in presence of Baicalein by ANS showed a similar pattern of an initial increase followed by decrease in fluorescence intensity (Fig. 4.2E, F). The 500 µM of Baicalein was found to induce more hydrophobicity as compared to other concentrations (Fig. 4.2G). The increase in hydrophobicity suggested induction of Tau oligomers by Baicalein.

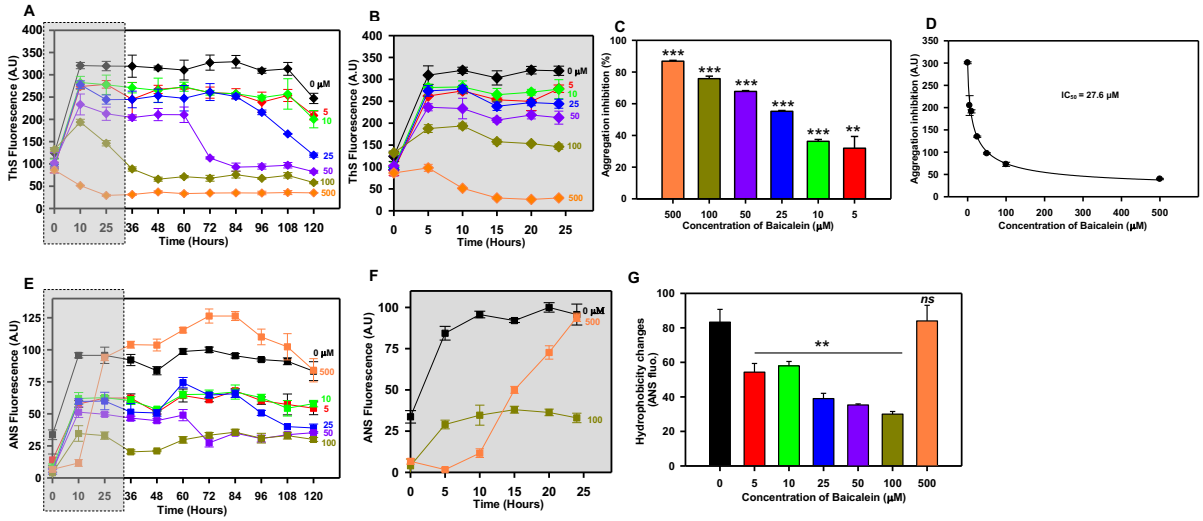

Figure 4.2. Tau aggregation inhibition by Baicalein. A) ThS fluorescence for aggregation kinetics of full-length Tau in presence of varying concentrations of Baicalein. The ThS fluorescence decreased with increase in dose of Baicalein showing concentration dependent inhibition of Tau aggregation. B) ThS fluorescence for Baicalein treated samples at the initial time point revealed that the higher concentrations had immediate effect on inhibiting Tau aggregation within first 24 hours. C) The ThS percent inhibition of Tau aggregation at different concentrations of Baicalein. The highest concentration of Baicalein 500 µM showed around 85% inhibition followed by 75% by 100 µM of Baicalein. D) The IC_{50} value for full-length Tau aggregation inhibition, which was found to be 27.69 µM of Baicalein. E) ANS fluorescence for aggregation kinetics of full-length Tau in presence of varying concentrations of Baicalein. F) The highest concentration (500 µM) of Baicalein induced Tau oligomerization within 15 hours of incubation as evidenced by sharp rise in ANS fluorescence. G) The hydrophobicity changes at the end of 120 hours revealed that 500 µM of Baicalein showed increased hydrophobicity which is characteristic property of oligomers. This figure is reproduced from Sonawane *et al.*, CCAS (under revision), 2020.

Repeat domain of Tau consisting of 4 repeats is more prone to aggregation as compared to full-length Tau and readily forms oligomers. Repeat Tau aggregates rapidly and attains saturation within couple of hours. Hence, we checked the efficacy of Baicalein in inhibiting assembly of repeat at the same

concentrations as full-length Tau. Since the heparin induction rapidly aggregates repeat Tau, the fluorescence kinetics were monitored every hour for first 6 hours of the incubation. The untreated repeat Tau aggregated within 2 hours and attained saturation by 3-4 hours of incubation (Fig. 4.3A). The Baicalein treated samples showed gradual decrease in ThS fluorescence in a concentration-dependent manner as time advanced suggesting inhibition of Tau aggregation. The inhibition of repeat Tau by Baicalein occurs at earlier time points as compared to full-length Tau (Fig. 4.2A, 4.3A). Moreover, the inhibition for repeat Tau is significant at higher concentrations from 50-500 µM as compared to full-length Tau (Fig. 4.2C, 4.3B). The IC_{50} value for inhibition of repeat Tau aggregation was also a little higher *i.e.* 35.8 µM when compared to full-length Tau (Fig. 4.3C). This might be attributed to rapid rate of repeat Tau aggregation as compared to full-length Tau. The trend of ThS kinetics of surge and fall suggested oligomer formation induced by Baicalein. To confirm this, ANS assay was carried out to reveal the status of hydrophobicity of Baicalein-treated Tau. As opposed to ThS fluorescence, ANS fluorescence followed exactly opposite pattern of initial decrease followed by increase in fluorescence (Fig. 4.3D), which was more prominent at higher concentrations of 100 and 200 µM (Fig. 4.3E). The ANS fluorescence increased at 24 hours for 100 and 200 µM Baicalein, which coincided with the time point of drop of ThS fluorescence indicating enhanced oligomer formation but inhibition of complete fibrillization.

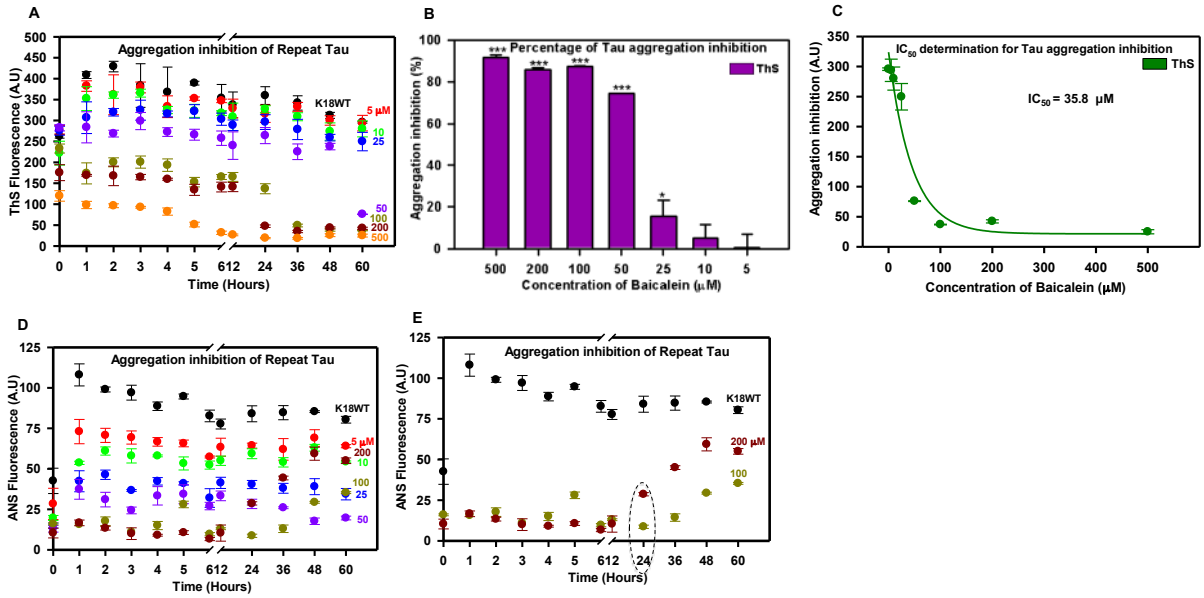

Figure 4.3. Repeat Tau aggregation inhibition by Baicalein. A) The ThS fluorescence show a concentration dependent decrease in intensity suggesting inhibition of repeat Tau aggregation by increasing dose of Baicalein. B) The percent inhibition for repeat Tau for Baicalein. C) The IC50 value for repeat Tau aggregation inhibition was found to be 35.8 µM of Baicalein. D) The ANS analysis of Baicalein treated Tau from 5-200 µM shows initial decrease in the fluorescence followed by increase at the later time points suggesting increase in Tau hydrophobicity. E) The ANS fluorescence for the higher concentrations of Baicalein showing initial decrease and further rapid increase in fluorescence at 24 h (dotted circle). This figure is reproduced from Sonawane *et al*., ABB, 2019.

4.1.3 Characterization of Baicalein-induced Tau oligomers

The fluorescence assays especially ANS kinetics indicated probable role of Baicalein in inducing oligomers of both full-length and repeat Tau. In order to characterize these oligomers we performed SDS-PAGE for the reaction mixtures at different time points. The 0 hour reaction mixtures showed presence of only Tau monomers. The progression of time lead to the formation of higher order Tau species. The intensities of these species on SDS-PAGE increased with increase in concentration of Baicalein. The 100 µM Baicalein displayed presence of intense oligomers at 48 hours of incubation (Fig. 4.4A). The trend of fluorescence kinetics also started varying at this particular time point

suggesting Tau oligomers formation with the prolonged incubation. The population of Tau oligomers started to decrease in Baicalein treated samples (Fig. 4.4A) as compared to untreated control (Fig. 4.4A). The intensity quantification revealed decrease in intensity of Baicalein treated Tau with time (Fig. 4.4B). The presence of Baicalein-induced oligomers was confirmed by immunoblotting the reaction mixtures of 0, 100 and 200 µM Baicalein with antibody against total Tau (K9JA). At 0 hour, 200 µM Baicalein treated Tau showed presence of minute amount of oligomers, which increased at 24 hours of incubation as compared to untreated control (Fig. 4.4C). Moreover, the oligomer population decreased in treated samples with increase in incubation. Thus, immunoblotting confirmed the ANS and SDS-PAGE analysis supporting Baicalein-mediated Tau oligomerization of full-length Tau. Similarly, the Baicalein-induced repeat Tau oligomers were also analyzed by SDS-PAGE. The repeat Tau oligomerization was visualized at 6 hours in 500 µM Baicalein-treated sample in the form of dimers and tetramers (Fig. 4.4D). At 24 hours, 200 µM treated Tau showed formation of dimers and tetramers but the oligomers from 500 µM treated Tau were no more visible. This time point matched with the fall in ThS fluorescence and rise in ANS fluorescence confirming the oligomer formation on Baicalein treatment. Moreover, at the end time point only tetramers were visible in 50-500 µM Baicalein showing its potency in inducing and sequestering Tau in oligomeric state without allowing fibril formation (Fig. 4.4D, E).

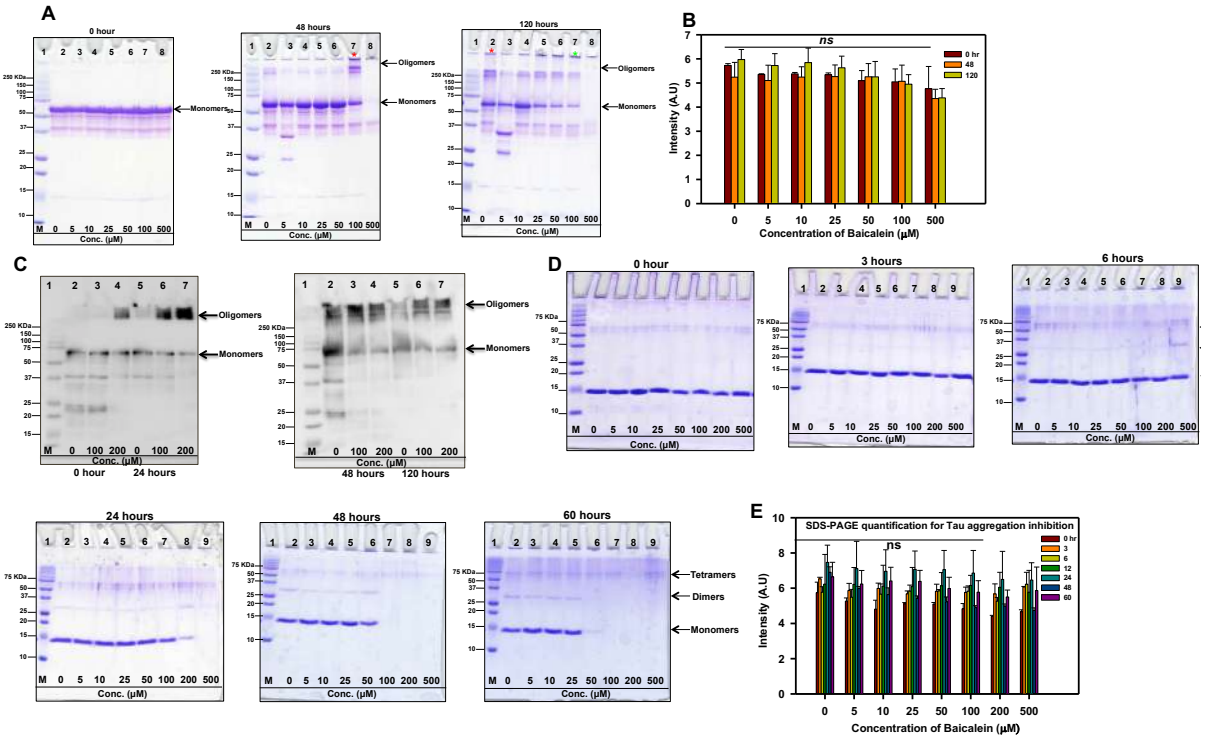

Figure 4.4. SDS-resistant Tau oligomers-induced by Baicalein. A) SDS-PAGE analysis of Tau oligomers. The zero time point did not show presence of any aggregates in control as well as treated samples. At the end of 48 hours higher order aggregates (red asterisk) were observed in the 100 µM Baicalein treated sample as compared to control. The 120 hours incubated sample showed a decrease in aggregates (green asterisk) in treated samples as compared to control. B) The SDS-PAGE quantification for different time points indicate the initial increase followed by the decrease in the aggregates at higher concentrations of Baicalein shows significant decrease in 500 µM Baicalein at 48 and 120 hours. C) The formation of Tau oligomers-induced by Baicalein in presence of heparin confirmed by immunoblot analysis showed higher order oligomers in Baicalein treated samples (lane 6, 7) as opposed to control (lane 2) at 24 hours. After 48 hours of incubation the oligomers population was seen to increase (lane 3, 4) but at 120 hours the decrease in the oligomer load was observed (lane 7). D) The SDS-PAGE analysis at zero time point control as well as treated samples does not show presence of any higher order aggregates. The higher order oligomers were observed after 6 hours of incubation. At 24 hours, the 500 µM of Baicalein (lane 9) showed the presence of dimer as well as tetramer. At 48 and 60 hours, the oligomers were seen in all treated samples with differential intensity. E) Quantification for the SDS-PAGE at different time points and different Baicalein concentrations

shows decrease in the aggregates at higher concentrations of Baicalein. This figure is reproduced from Sonawane *et al*., ABB, 2019 and Sonawane *et al*., CCAS (under revision), 2020.

Next, the Baicalein-induced Tau oligomers were characterized for their conformation changes by CD spectroscopy. The native conformation of Tau is composed of loops with maximum ellipticity at 198 nm as evidenced by 0 hour treated and untreated full-length Tau (Fig. 4.5A). On aggregation full-length Tau adopts a partial β-sheet structure with slight shift of maximum ellipticity towards 200-208 nm. At 120 hours of incubation Baicalein treated Tau showed partial β-sheet conformation (Fig. 4.5B). On the other hand, repeat Tau shows complete transition to β-sheet conformation on aggregation. The repeat Tau treated with Baicalein showed a complete β-sheet conformation as compared to soluble Tau (Fig. 4.5C). Thus, the conformational characterization along with the above results suggest induction and stabilization of Baicalein induced Tau oligomers. Further we analyzed the morphology of Baicalein treated Tau by transmission electron microscope. The untreated full-length Tau displayed long fibrillar aggregates. Treatment of Baicalein showed presence of small filaments at 48 and 120 hours with absence of long fibrillar aggregates (Fig. 4.5D). Similarly, untreated repeat Tau showed filamentous aggregates at 60 hours of incubation but Baicalein treated Tau had only small fragments of Tau (Fig. 4.5E). Taken together, these results suggest inhibition of Tau aggregation by Baicalein by inducing and arresting the oligomers preventing their further fibrillization.

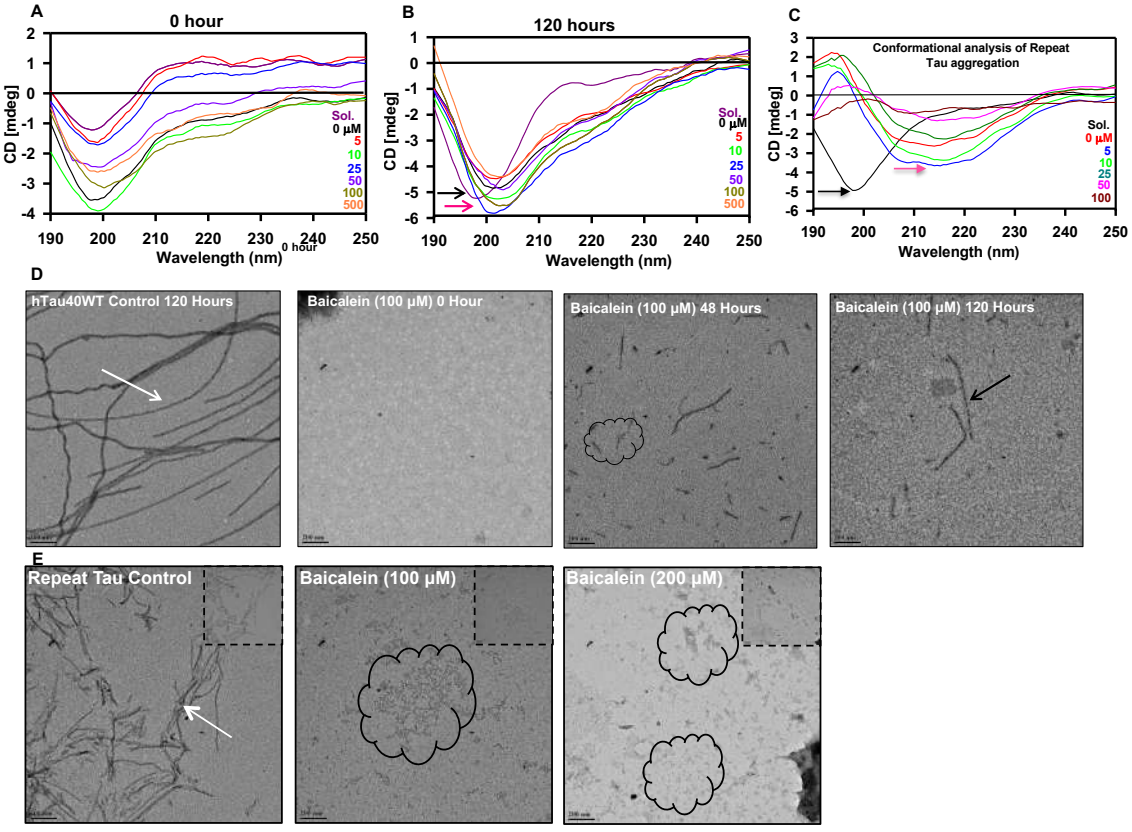

Figure 4.5. Tau aggregation inhibition studied by CD spectroscopy. A) The conformational analysis of Baicalein treated and control samples showed the typical spectra of a random coil structure. The Sol. represents soluble protein without heparin. B) At the end of 120 hours the pattern of spectrum remained same with respect to soluble (black arrow) and treated samples (pink arrow) showed a partial β-sheet conformation. C) The CD analysis of the repeat Tau aggregation shows a shift in the spectra (pink arrow) in control as well as treated samples as compared to soluble protein (black arrow) indicating a shift towards β-sheet structure. The Sol. represents soluble protein. The control untreated sample shows the presence of long filaments (white arrows) at day 5. D) The treatment with 100 μM Baicalein at the initial time points showed presence of intermediately long filaments (white arrow) and small broken filaments. As the time advanced, Baicalein was shown to inhibit Tau aggregation as only broken pieces (highlighted by black border and black arrow) of Tau filaments were visualized in the electron micrographs. E) The electron micrographs show the presence of filamentous aggregates (white arrow) in control as

opposed to amorphous aggregates (encircled black) in the Baicalein treated samples. This figure is reproduced from Sonawane *et al*., ABB, 2019 and Sonawane *et al*., CCAS (under revision), 2020.

4.1.4 Effect of Baicalein on soluble Tau

The biophysical and biochemical characterization of Baicalein-mediated Tau inhibition revealed a potential role of Baicalein in Tau oligomerization in heparin-induced Tau assembly. Next, we studied whether Baicalein can influence Tau aggregation in absence of heparin. The experimental reactions were set accordingly by maintaining heparin-induced Tau aggregation as a positive control and only Tau in absence of heparin as a negative control. Two test reactions were set up with Tau and Baicalein 25 and 100 µM in absence of heparin. The fluorescence assays were employed to study the progression of the aggregation. The reactions with absence of heparin did not increase the aggregation as evident by lack of change in fluorescence intensities (Fig. 4.6 A-D). The positive controls for both full-length and repeat Tau showed gradual increase in ThS and ANS intensities with time of incubation indicating Tau aggregation. Additionally, the positive controls also showed presence of higher order Tau species in SDS-PAGE analysis with increase in time of incubation commencing at 24 hours (Fig. 4.6 E-G).

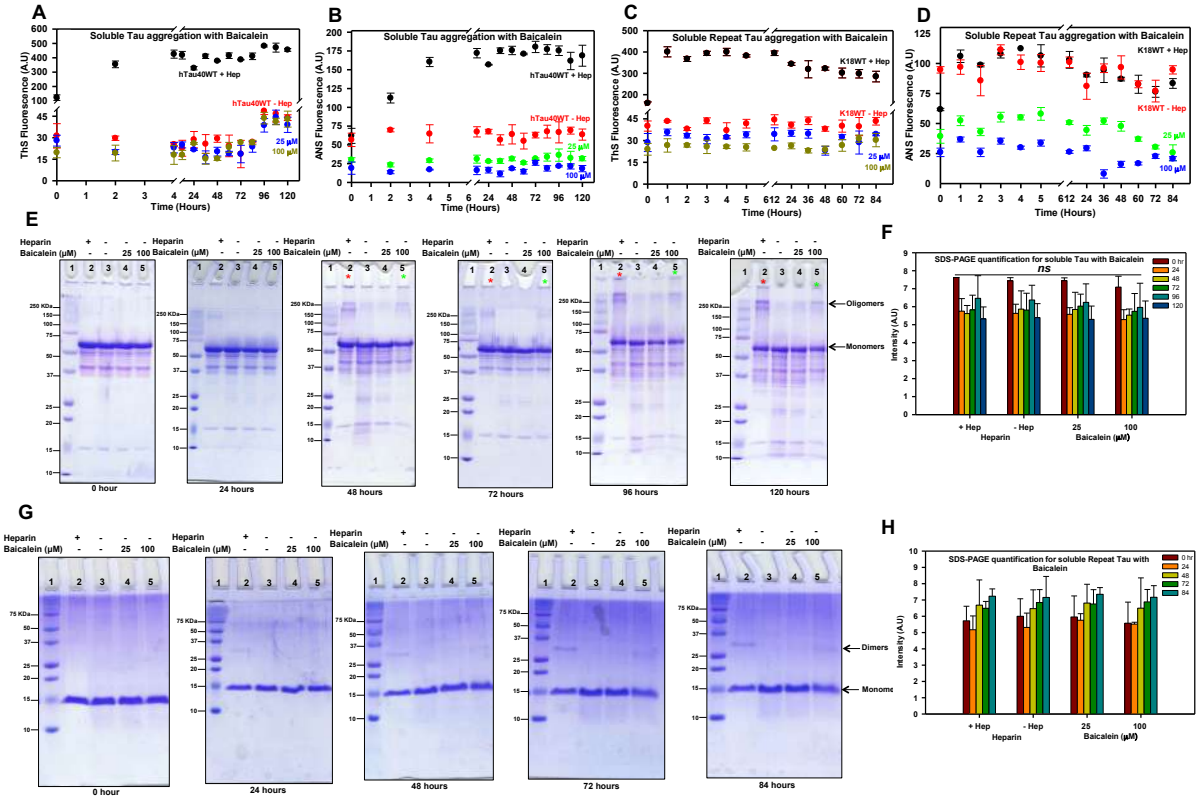

Figure 4.6. Effect of Baicalein on Tau aggregation without inducer A) The aggregation of Tau was monitored by ThS fluorescence. The positive control (heparin) showed an increase in intensity with respect to time as opposed to heparin negative control. The Baicalein treated soluble protein did not show any increase in fluorescence as compared to positive control. B) The hydrophobicity imparted by Baicalein alone without heparin was monitored by ANS fluorescence. The intensity did not increase significantly as compared to the positive control. C) ThS fluorescence show increase in intensity in the heparin treated positive control whereas no increase in fluorescence was observed in the negative control as well as Baicalein treated samples for repeat Tau. D) Baicalein did not increase the hydrophobicity of repeat Tau as revealed by ANS fluorescence. E) The SDS-PAGE analysis revealed a time-dependent increase in higher molecular aggregates in the positive control from 24 hours of incubation (lane 2). No higher molecular weight aggregates were observed in negative control as well as sample treated with 25 µM of Baicalein (lanes 3, 4 respectively) but faint bands of higher order oligomers were observed in 100 µM treated sample from 72 hours onwards (lane 5), suggesting formation of oligomers. F) Quantification for SDS-PAGE for soluble Tau with Baicalein. G) SDS-PAGE analysis for repeat Tau shows the presence of dimer and tetramers in the positive control from 24 hours onwards (lane 2). A faint band of dimer and a tetramer is observed in 100 µM Baicalein treated sample from 48 hours onwards but has a lesser intensity as compared to positive control. H) Quantification for SDS-PAGE for soluble repeat Tau

with Baicalein. This figure is reproduced from Sonawane *et al*., ABB, 2019 and Sonawane *et al*., CCAS (under revision), 2020.

Tau treated with higher concentration of Baicalein 100 µM, displayed presence of a faint higher order band at 120 hours and 84 hours for full-length and repeat Tau respectively. This indicated Baicalein-induced Tau oligomers in absence of heparin at a much slower pace.

Further the conformational characterization was carried out for these oligomers, which revealed absence of β-sheet conformation in samples without heparin (Fig. 4.7A,C). The positive controls for both proteins on the other hand, showed partial β-sheet conformation. The conformational analyses suggested that Baicalein does not cause change in conformation of full-length and repeat Tau. Further, the TEM analysis revealed absence of Tau fibrils (Fig. 4.7B, D) thus, confirming that Baicalein alone does not cause Tau conformational change and induces oligomerization at a much slower pace.

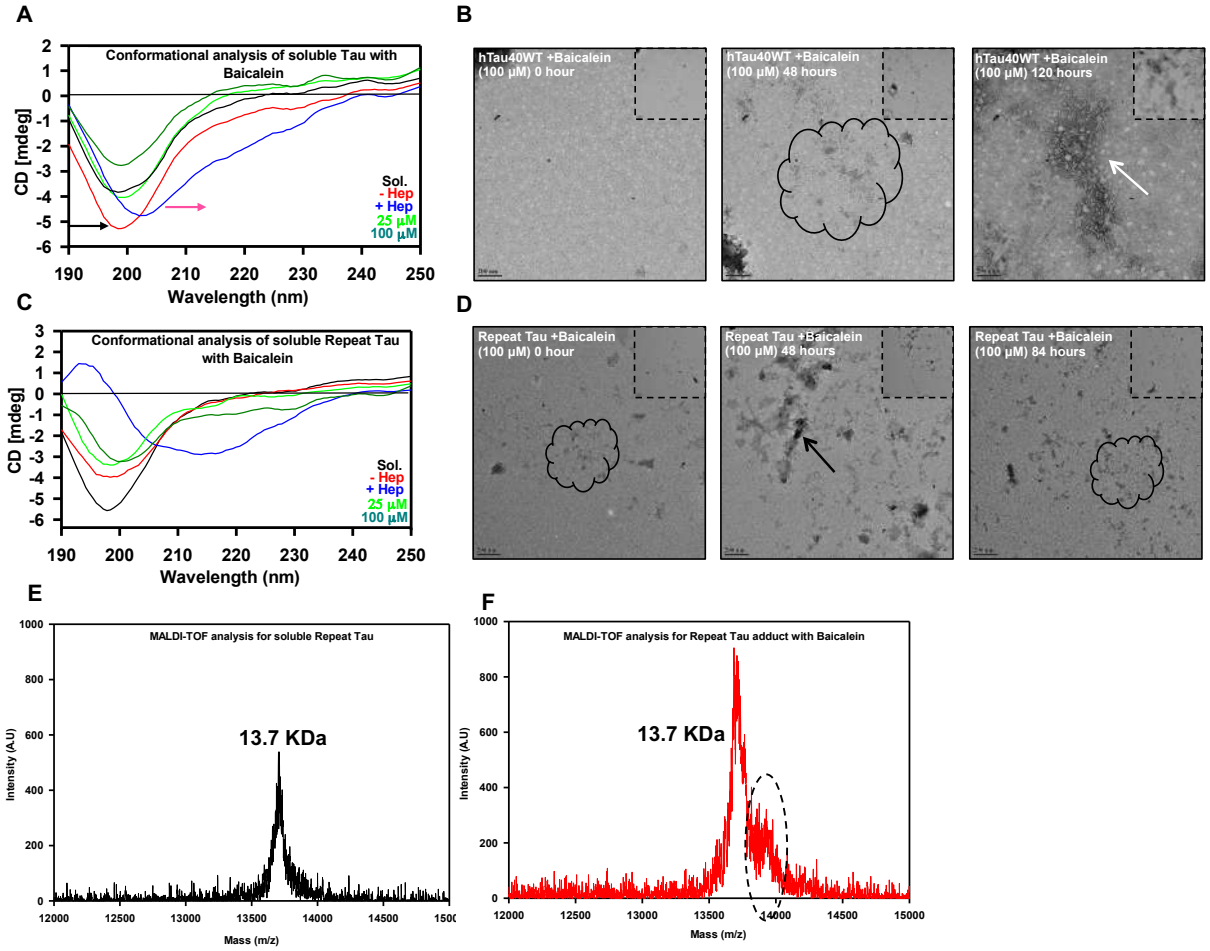

Figure 4.7. Conformational analysis of soluble Tau with Baicalein. A) The CD analysis showed normal spectra for negative control and Baicalein treated soluble Tau but a slight shift in the positive control (aggregated) Tau. B) The electron micrographs at different time points reveal presence of amorphous aggregates at the initial time points and clumps of oligomers at the end point. C) The CD spectra show shift towards beta sheet whereas the Baicalein treated samples shows the spectra of a typically random coiled protein. D) Amorphous aggregates of repeat Tau formed at different time points in presence of Baicalein as observed by electron microscopy. E) The MALDI-TOF analysis of soluble repeat Tau showing 13.7 KDa molecular weight. F) The Baicalein modified Tau showing an adjacent peak of 13.9 KDa in addition to 13.7 KDa peak suggesting covalent modification of repeat Tau by Baicalein. This figure is reproduced from Sonawane *et al*., ABB, 2019 and Sonawane *et al*., CCAS (under revision), 2020.

4.1.5 Baicalein covalently modifies Tau to induce oligomerization

The potency of Baicalein in inhibiting Tau aggregation by induction and sequestering oligomers was evident from various experimental results, but the mechanism of its action was still unknown. Hence,

MALDI-TOF analysis was carried out to check the effect of Baicalein on Tau modification. Repeat Tau was incubated with a series of concentrations of Baicalein for 1 and 12 hours respectively. After one hour of incubation untreated repeat Tau showed a single peak corresponding to 13.7 KDa (theoretical molecular weight of repeat Tau) (Fig. 4.7E). The sample with Tau:Baicalein 1:4 stoichiometry showed an additional peak on the higher side of soluble Tau peak after 1 hour of incubation (Fig. 4.7F). This additional peak suggested covalent modification of Tau by Baicalein. All the 12 hours Baicalein incubated samples showed an additional peak suggesting covalent modification. Thus, Baicalein induced Tau oligomerization by modifying the Tau protein.

4.1.6 Dissolution of mature fibrils of full-length Tau by Baicalein

The toxicity of Tau oligomers is more pronounced as compared to the PHFs, but excess accumulation of PHFs especially at the synaptic compartments is detrimental to the neurons[204]. Thus, in addition to inhibition of Tau aggregation, dissolution of PHFs is also an important requirement for a molecule to be potent against Tau pathology. Hence, we studied whether Baicalein can dissolve preformed Tau filaments. The mature fibrils of full-length Tau were prepared and incubated with Baicalein (0-500 µM) in the reaction buffer. The status of aggregates was monitored by ThS fluorescence. The untreated Tau filaments showed a steady fluorescence throughout the kinetics but the Baicalein treatment led to decrease in fluorescence with respect to concentration suggesting disaggregation of Tau filaments (Fig. 4.8A). Baicalein showed enhanced potency in Tau disaggregation with highest concentration of 500 µM giving 90% disaggregation (Fig. 4.8B). The DC_{50} analysis gave a value of 24.6 µM (Fig. 4.8C).

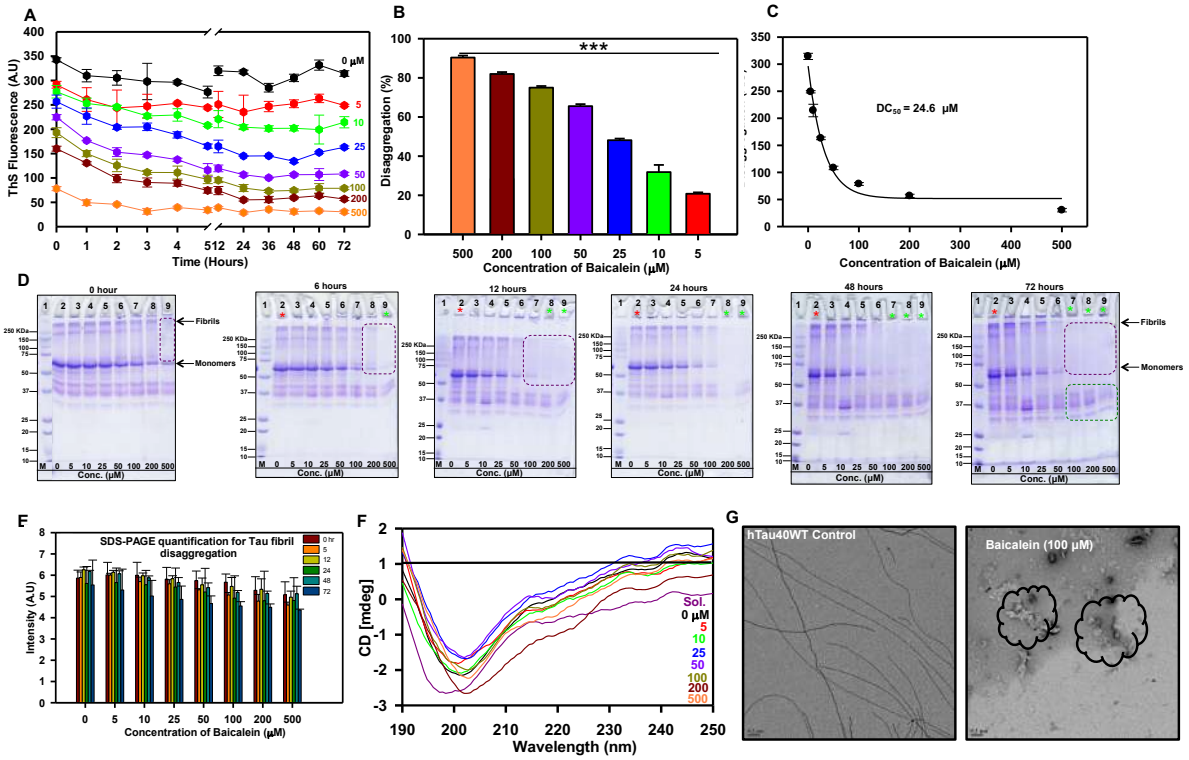

Figure 4.8. **Dissolution of Tau aggregates by Baicalein.** A) The effect of Baicalein on the dissolution of mature Tau aggregates was studied using ThS fluorescence, which showed a decrease after 5 hours of incubation in a concentration-dependent manner. B) The percent disaggregation plot shows a maximum of 85% disaggregation by 500 µM of Baicalein treatment. C) The plot shows the DC_{50} value for Tau disaggregation as 24.6 µM. D) Figure shows the time-dependent SDS-PAGE analysis of Tau aggregates dissolution. After 72 hours, the higher concentrations of Baicalein showed a maximum decrease in the aggregates (lane 7, 8, 9 green asterisk) as compared to control (lane 2 red asterisk). E) The SDS-PAGE quantification for different time points indicate the initial increase followed by the decrease in the aggregates at the higher concentrations of Baicalein. F) The CD analysis of disaggregated Tau by Baicalein shows the presence of mixed structures. The Sol. represents soluble protein. G) Transmission electron micrographs showed the untreated mature fibrils (white arrow)

versus disaggregated amorphous (encircled black), Baicalein treated fibrils of full-length Tau. This figure is reproduced from Sonawane *et al*., CCAS (under revision), 2020.

Next the samples were analyzed by SDS-PAGE for disaggregation at various intervals. Interestingly, Baicalein was found to disaggregate Tau immediately after addition (Fig. 4.8D, 0 hour, 500 μM). With an increase in time the Baicalein treated samples showed dissolution of Tau fibrils (Fig. 8D) whereas the untreated samples showed intact fibrils over the incubation period (Fig. 4.8D). The intensity quantification revealed concentration dependant decrease suggesting Baicalein-mediated disaggregation (Fig. 4.8E). The CD analyses detected presence of mixed population of Tau aggregates (Fig. 4.8F). The microscopic analysis displayed presence of long filamentous aggregates in untreated control and amorphous aggregates in Baicalein-treated samples (Fig 4.8E). This suggests potency of Baicalein in dissolving aggregates in addition to aggregation inhibition.

4.1.7 Effect of Baicalein and Baicalein-treated Tau on neuronal cells

Tau oligomers have been reported to have a toxic role in synaptic dysfunction as well as membrane leakage. Hence, it was necessary to determine the toxicity of Baicalein-induced oligomers in neuronal cells. Initially, Baicalein was screened for its toxicity in neuronal cells at a range of 5 nM to 25 μM and was found to be non-toxic (Fig. 4.9A). To study the toxicity of Baicalein-induced oligomers cells were exposed for 24 hours to Tau: Baicalein reaction mixtures (1:0.25, 1:0.5, 1:1, 1:2 and 1:4) after 120 hours of reaction time. The Baicalein-treated full-length Tau was found to be non-toxic to neuronal cells (Fig. 4.9B).

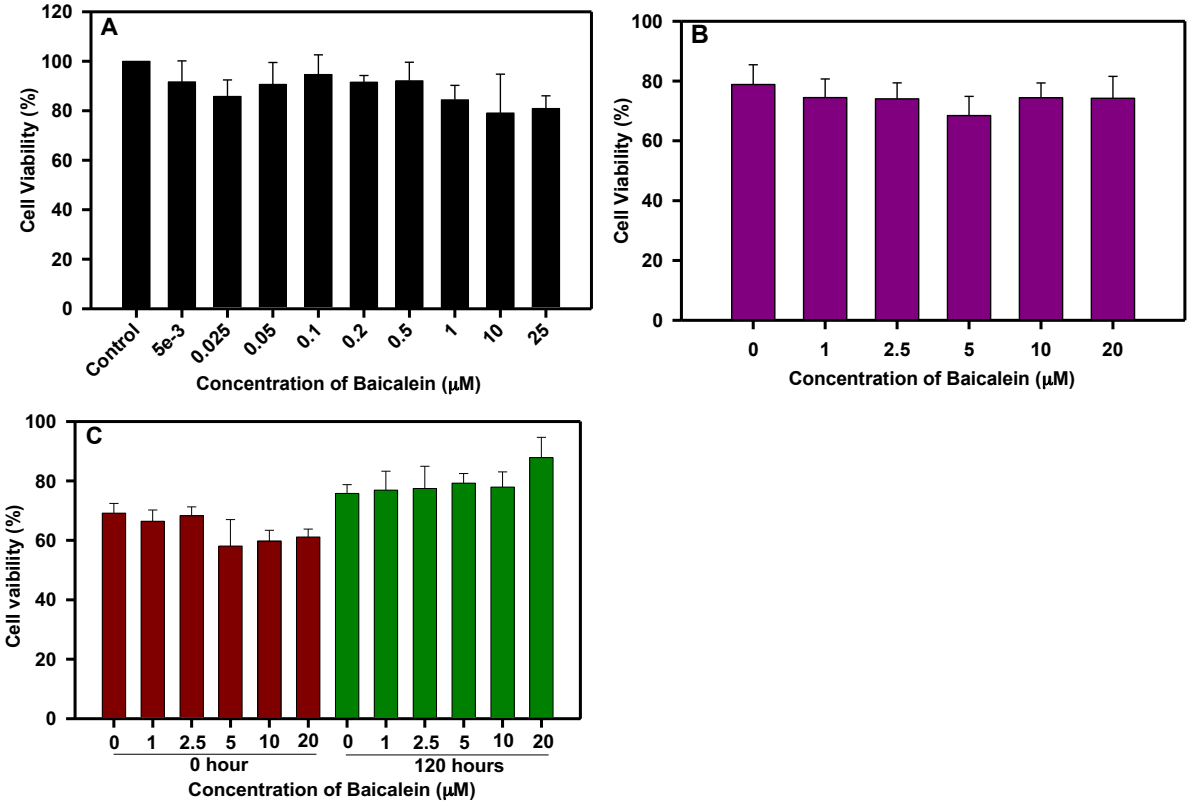

Figure 4.9. Cell toxicity of Baicalein. A) N2a cells treated with a broad range of Baicalein shows no toxicity till 25 μM. B) Baicalein treated soluble Tau shows no significant effect on cell viability implying Baicalein-induced oligomers are non-toxic. C) Baicalein treated Tau aggregates shows a mild rescue of toxicity at 120 hours with the highest concentration of Baicalein suggesting that disaggregated Tau mature filaments are non-toxic to neuro2a cells. This figure is reproduced from Sonawane *et al*., CCAS, (under revision), 2020.

Filamentous Tau was disintegrated by Baicalein and tested for its toxicity. The 0 hour disaggregation reaction mixtures did not show much effect on viability but the 120 hour reaction mixture with highest concentration of Baicalein showed increased viability as compared to control (Fig. 4.9C). The Baicalein-induced Tau oligomers were found to be non-toxic to cells. Thus, the dual role of Baicalein in inhibiting Tau aggregation and dissolving pre-formed Tau fibrils highlights its role as a potential therapeutic molecule.

4.2 Role of EGCG in Tau interaction and pathology

Epigallocatechin-3-gallate (EGCG) is a green tea polyphenol belonging to class flavonoids and sub-class flavanols. EGCG has neuroprotective roles and acts against the pathologies of AD and PD. In AD, EGCG overcomes Aβ pathology by driving non-amyloidogenic processing of APP preventing Aβ-42 formation and accumulation in neuronal cultures[205]. Additionally, EGCG lower the levels of APP in transgenic models suggesting *in vitro* and *in vivo* effect of EGCG in ameliorating Aβ pathology[206]. EGCG is shown to have inhibitory effects in aggregation of repeat Tau K18ΔK280 and prevented neuronal cells from aggregate toxicity[207]. In our study, we focussed on understanding the binding interaction of EGCG with Tau and its efficacy in preventing aggregation of full-length Tau.

4.2.1 Analysis of Tau-EGCG interaction

The full-length Tau comprises of 441 amino acids divided into 2 major domains; the N-terminal projection domain and the C-terminal microtubule-binding domain (Fig. 4.10A). The 4 imperfect repeats are involved in microtubule-binding function of Tau and form the core of paired helical filaments during pathological aggregation of Tau. Though EGCG is known to have beneficial roles in Tau pathology, the interacting parameters between them are not much explored. Thus, we calculated the binding affinity of full-length Tau and EGCG (Fig. 4.10B) by isothermal titration calorimetry (ITC). Any bimolecular reaction is accompanied by either heat discharge (exothermic) or heat absorption (endothermic). ITC measures this heat and provides the dissociation constant (K_d), stoichiometry, entropy (ΔS), enthalpy (ΔH) *etc*. ITC is a sensitive technique and detects the binding affinities from nM to mM range. ITC has advantages as it can measure the binding affinities of spectroscopically silent molecules and is not affected by solution turbity, opacity or heterogeneity. Moreover, it is not affected by ligand and macromolecule sizes and work over wide range of temperatures, salts and pH. ITC for full-length Tau and EGCG detected a multiple binding event. The titration over 25 injections revealed a binging isotherm with initial decrease in enthalpy followed by subsequent increase which indicated initial rapid binding of EGCG which prohibits further binding with Tau (Fig. 4.10C). The signature plot presented negative values for free energy (ΔG) and subsequent enthalpy (ΔH) and entropy (ΔS) and thus confirmed Tau-EGCG binding to be spontaneous and favourable (Fig. 4.10D). The number of interacting sites of 3.48 was deciphered from the heat plot of reactants (EGCG and Tau) *versus* their molar ratios (Fig. 4.10E). Based on the thermodynamic parameters mentioned in Table 4.1 the dissociation constant for Tau and EGCG was calculated to be 74 nM. The thermodynamic parameters obtained by ITC revealed that Tau and EGCG bind to each other in a multiple binding event with initial rapid and saturable binding. The equilibrium is attained quickly with constant association and dissociation of the ligand and protein. EGCG interacts with human serum albumin in a similar way with tight primary binding followed by weaker secondary binding events[208].

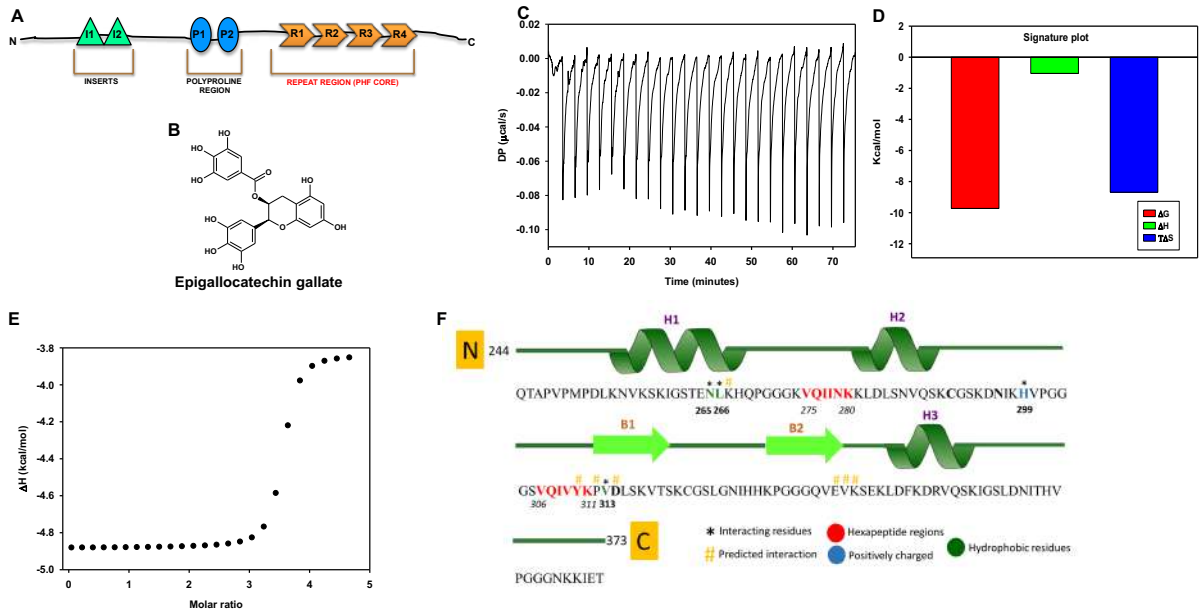

Figure 4.10. The interaction and binding affinity of Tau and EGCG. A) Tau domain organization. B) The structure of polyphenol EGCG. C) Isothermal titration calorimetry carried out for 20 µM full-length Tau and 500 µM EGCG shows multi-site binding between the two. D) Signature plot for Tau EGCG titration showing ΔG, ΔH and TΔS for the interaction. E) The heat plot for Tau-EGCG interaction suggests n = 3.5 binding sites. Thus, there are more than one binding events involved in Tau-EGCG interaction. F) A schematic diagram of the Tau K18 model depicting three predicted alpha helices (H1, H2, and H3) and two predicted beta sheets (B1, B2) with two distinct and characteristic hexa-peptide regions 275VQIINK280 and 306VQIVYK311. The predicted ligand interacting residues, colour coded according to their type of interaction is also shown. This figure is reproduced from Sonawane *et al*., Scientific Reports, 2020.

Titration ratio (Tau : EGCG)	1:25
Temperature (°C)	25.2
Bin	Binding
[Syringe]	500 µM
[Cell]	20 µM
N (sites)	3.48
Kd	74 nM
ΔH (kcal/mol)	-1.04
ΔG (kcal/mol)	-9.73
-TΔS (kcal/mol)	-8.69

Table 4.1. Parameters and calculated values for Tau-EGCG binding constant.

Next, we analysed the binding sites of EGCG on Tau by molecular docking and simulation. As for Baicalein, same model of repeat Tau was utilized for the *in silico* analysis (Fig. 4.10F). The best of Tau EGCG docking gave the glide score and E-models values of -6.388 and -56.130 respectively. The docking of EGCG was carried out in such a way that gallate moiety was placed in a close proximity to predicted β-sheet of Tau and the Epigallocatechin backbone was in proximity to the predicted helices

(Fig. 4.11A). The hydrogen bonds and the hydrophobic interactions contributed extensively to Tau-EGCG interactions. The O4 atom of the hydroxyl group of EGCG interacted with NH of imidazole ring of His 299 with interaction distance of 3.05. The O2 of EGCG interacted with NH_2 of Val 313 with 2.95 interaction distance. The O7 atom of EGCG interacted with NH_2 of Asn 265 and carboxyl group of Val 313 with interaction distances of 3.06 and 3.08 respectively. Further, the O8 and O9 of EGCG showed interaction with carboxyl group of Leu 266 with distances of 2.7 and 3.18 respectively (Fig. 4.11B). The Pi-alkyl interaction was observed with Lys 340 and other residues like Asp 314 and Glu 338 formed Pi-anion electrostatic interaction with benzene rings of EGCG. Additionally, the residues Lys 267, Tyr 310, Pro 312 and Val 339 displayed hydrophobic interactions with EGCG. Among these, Tyr 310 is localized to the hexapeptide motif ^{306}VQIVYK^{311} while others flank both the hexapeptide regions (Fig 4.10F).

Next, the EGCG-Tau docked complex was subjected to molecular dynamic simulation for 50 ns to check the stability of interaction and structural changes which might be involved during the binding. The RMSD of Cα atoms were found to be stable during the first 30 ns of the simulation duration with intermittent fluctuations before stabilizing in the last 5 ns (Fig. 4.11C). These fluctuations can be attributed to local bond destabilization during the Tau-EGCG binding. The EGCG backbone trajectory showed system attained intermittent stability for short durations at various time points, which indicated binding and partial dissociation events of EGCG. Thus, the initial binding pose of EGCG with ^{306}VQIVYK^{311} displayed an initial repositioning during simulation. The Cα RMSD difference of 0.75 between initial and final conformation is an indicative of Tau conformational change upon EGCG binding and converging of system over last few nanoseconds of simulation. The level of compactness of Tau and EGCG complex was obtained by a plotting time (picoseconds) on X- axis and the radius of gyration (Rg) values of Tau and EGCG backbones (nm) on left and right Y-axes respectively (Fig. 4.11D). The calculations of interaction energy between Tau residues and EGCG demonstrated initial dominance of Coulombic interactions followed by Lennard-Jones interactions as the simulation progressed. This suggested the dynamic nature of electrostatic and hydrophobic interactions of Tau-EGCG complex (Fig. 4.11E).

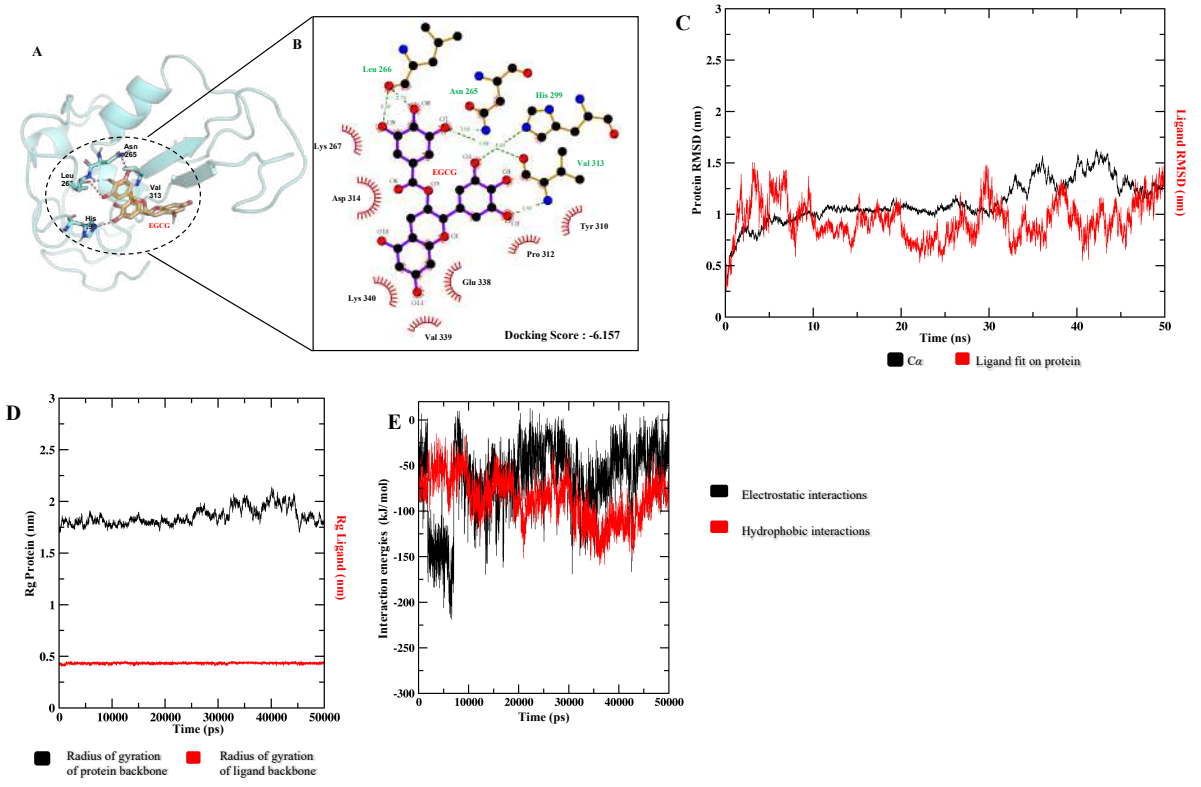

Figure 4.11. Simulation studies of Tau and EGCG. A) The binding pocket of EGCG to the Tau model, shown along with the interacting residues after molecular docking. B) The interaction between EGCG and Tau in the binding pocket is depicted, including the major residues involved and the predicted residues, which might be responsible in further interactions as well as the type of interactions they are involved in are shown. C) The RMSD evolution of the protein (left Y-axis) and that of the ligand (right Y-axis) are shown. While the protein RMSD gives insights into the structural conformation of the protein throughout the simulation, the ligand RMSD indicates how stable the ligand is with respect to the protein and its binding pocket. Both the RMSDs are seen to stabilize as the simulation progresses. The ligand RMSD is notably stable of the two, suggesting that the binding pocket conformation is maintained throughout the simulation. D) The Rg values of protein (left Y-axis) and ligand (right Y-axis) are shown. Both Rg values do not show much variation indicating that the structure of the protein and the binding pose of the ligand are maintained over the course of the simulation. E) The electrostatic and hydrophobic interactions between the ligand and protein over the entire timescale of the simulation are depicted, showing the dominant, yet highly dynamic and transitionary nature of the same. This figure is reproduced from Sonawane *et al*., Scientific Reports, 2020.

The residue-specific interactions during simulation suggested that residues Asn 265, Leu 266 and Val 313 prominently contributed to the hydrogen bond interactions and Lys 267, Tyr 310, Pro 312 and Lys 340 contributed to the hydrophobic interactions important for stabilizing Tau-EGCG complex. The hydrogen bonding dynamics including ion-mediated and water-mediated bonding was maintained during simulation in addition to residue-specific interactions. These interactions are crucial in maintaining Tau-EGCG interaction.

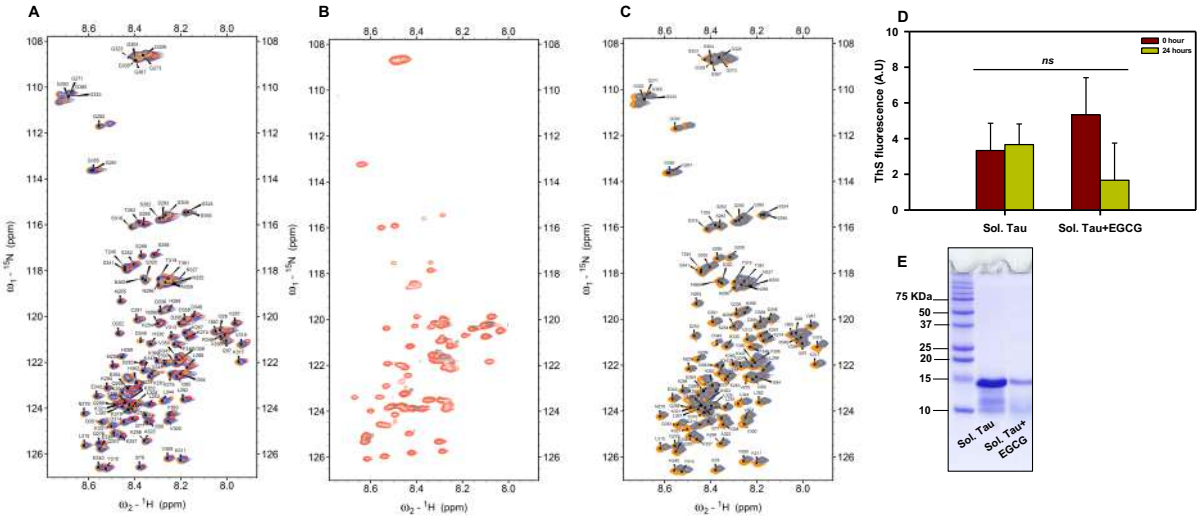

Figure 4.12. NMR spectroscopic studies of repeat Tau with EGCG. 1H-15 N-HSQC plots showing the chemical shift perturbations. For all the NMR experiments a solution of 200 µM of repeat Tau in 500 µL phosphate buffer containing 10% D2O is used. A) Overlay of 1H–15N-HSQC plots (at 278 K) for the titration of 200 µM of repeat Tau against 0 µM (in orange), 100 µM (in blue), 500 µM (in red), 1,000 µM (in olive green) and 2000 µM (in coral, no visible signals) of EGCG. Continuous drop in the intensity of HSQC cross peaks indicates an increasing precipitation of repeat Tau with increasing concentrations of EGCG. B) Overlay of 1H–15N-HSQC plot of repeat Tau at 298 K with that of repeat Tau in presence of 2000 µM of EGCG (sample from titration at 278 K, which was brought back to 298 K). C) Overlay of 1H–15N-HSQC plot of repeat Tau (at 278 K) (without EGCG, golden) along with 1H–15N-HSQC plots measured for the precipitation of 200 µM of repeat Tau in presence of 500 µM of EGCG after t = 0 h (blue) and t = 24 h (grey). Upon addition of 500 µM of EGCG, the HSQC cross peaks are slightly displaced and lost intensity indicating precipitation of repeat Tau. After 24 h standing, no apparent change was observed in the HSQC cross peak intensity. D) ThS fluorescence of NMR samples at 0 and 24 h suggesting no aggregation of repeat Tau in presence of EGCG. E) SDS-PAGE analysis of NMR samples at 24 h showing no aggregation of repeat Tau in presence of EGCG. This figure is reproduced from Sonawane *et al*., Scientific Reports, 2020.

To support the above binding studies, NMR studies were performed by titrating 200 µM ^{15}N labelled repeat Tau with varying concentrations of EGCG with ratios 0, 0.5, 2.5, 5 and 10 (Tau:EGCG) at 278 K. The ^{1}H-^{15}N HSQC NMR spectra did not reveal visible changes in residue-specific interactions or conformational change of Tau (Fig. 4.12A). Interestingly, with the increasing titration of repeat Tau

with EGCG, the signal intensities of HSQC cross peaks declined continuously until no signal was detected at highest concentration of EGCG of 2000 μM. This indicated precipitation of repeat Tau into higher molecular weights forms as the contents of NMR tube also turned turbid. This tube was further allowed to stand for an hour and attain 298K temperature before recording the HSQC spectrum again. This spectrum showed reappearance of very weak signals (Fig. 4.12B, grey), which were superimposed, with HSQC of repeat Tau without EGCG recorded at 298K. This superimposition suggested that a match in two spectra indicating that a small amount of Tau precipitate solubilized back as monomers with native conformation. Next, investigation was carried out to decipher whether at a single concentration of EGCG, Tau precipitate would increase over time. For this, 1H–15N HSQCs for 200 μM of ^{15}N labelled repeat Tau and 500 μM EGCG were acquired at 278K for 24 hours (Fig. 4.12C). The HSQCs for 0 hour (blue) and 24 hours (grey) superimposed perfectly suggesting absence of seeding effect at this ratio. Further to ensure EGCG-mediated Tau precipitation at 2000 μM EGCG at 278K, the contents from the NMR tube were analyzed by ThS fluorescence and SDS-PAGE analysis at 0 and end time point of NMR titrations. ThS recordings did not show increased intensity suggesting that the Tau protein had been actually precipitated and ruled out aggregation (Fig. 4.12D). The SDS-PAGE analysis also confirmed this observation as the end time point sample did not show presence of higher order aggregates (Fig. 12E).

4.2.2 Effect of EGCG on Tau assembly and conformation

The assembly of Tau into PHFs and further into NFTs in the neuronal cells triggers various pathological events leading to neuronal death. One of the methods to induce Tau aggregation is by induction with heparin to form PHFs. This approach enables the study of various Tau aggregation parameters *in vitro* as well as aids in screening Tau aggregation inhibitors. The effect of EGCG on full-length Tau self-assembly was monitored at range of EGCG concentrations (10-500 μM). The progress of aggregation was monitored by ThS fluorescence. The initial fluorescence monitoring was performed every hour till 5 hours to capture the initial stages of Tau aggregation in presence and absence of EGCG. The initial recordings showed increase in ThS fluorescence in all reaction mixtures till 5 hours after which the intensity began to drop proportionate to EGCG concentration. Tau treated with highest concentration of EGCG showed least ThS intensity compared to other reaction mixtures. The gradual drop of intensity suggested decreased aggregation and inhibition of Tau aggregation in presence of EGCG in a concentration-dependent manner (Fig. 4.13A). The plot of ThS intensities at end point of kinetics versus the EGCG concentration gave an IC_{50} value of 64.2 μM (Fig. 4.13B). Tau aggregation proceeds *via* changes in the protein hydrophobicity, which is monitored by fluorescent, dye ANS. The hydrophobicity mapping of Tau in presence and absence of EGCG revealed an initial surge till 5 hours and gradual drop with the increase in concentration of EGCG suggesting inhibition of aggregation (Fig. 4.13C). The status of EGCG-treated Tau was analyzed by SDS-PAGE wherein the reaction mixtures at 0 hour confirmed the presence of soluble Tau protein and absence of any preformed Tau aggregates (Fig. 4.13D). After 6 hours of incubation, a distinct band of Tau tetramers was observed in control as well as treated samples. This band intensified in 500 μM EGCG treatment at 12 hours before diminishing at 24 hours (Fig. 4.13D, 12, 24 hours). This is in accordance with the ThS kinetics, which showed drop in intensity after 24 hours in EGCG treatment. Further increase in incubation showed that EGCG-treated samples showed decrease in Tau aggregation as compared to control (Fig. 4.13D, 120 hours). The densitometric quantification of SDS-PAGE revealed concentration-dependent decrease in Tau aggregation by EGCG (Fig. 4.13E).

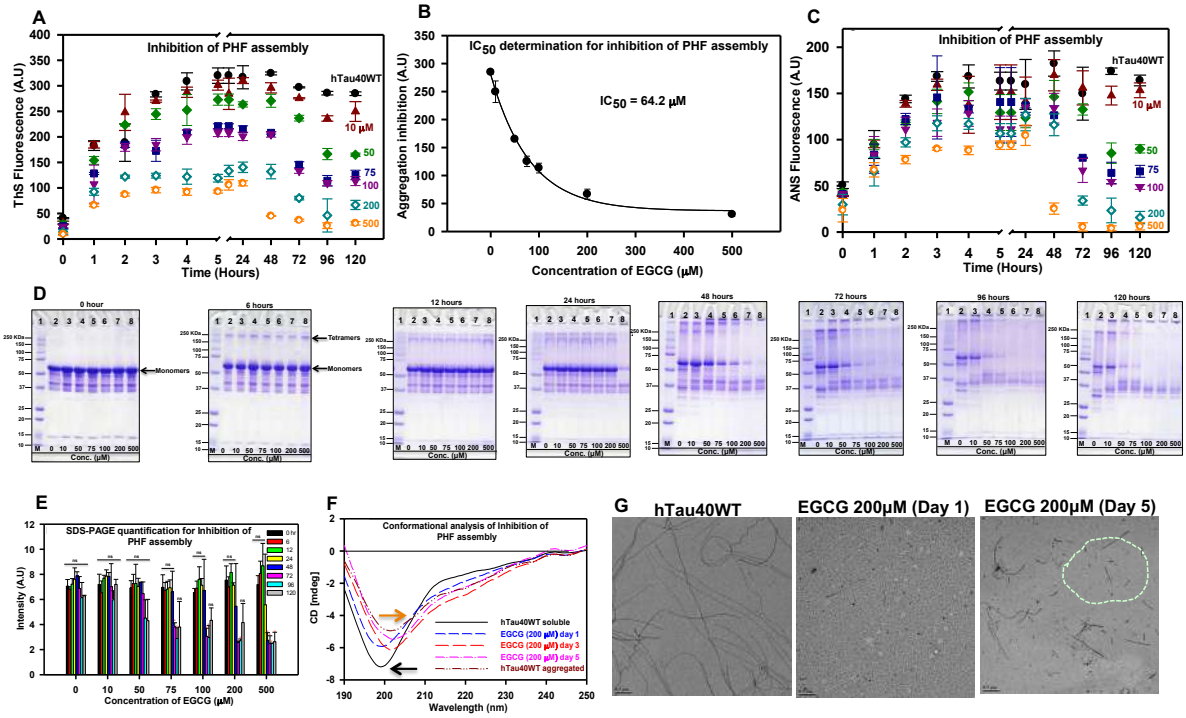

Figure 4.13. EGCG prevents Tau aggregation and changes their conformation *in vitro*. A) The inhibitory effect of EGCG on the polymerization of full-length Tau monitored by ThS fluorescence. B) The IC50 for EGCG for full-length Tau is 64.2 µM. C) The inhibition of Tau PHF assembly assessed by ANS fluorescence shows a time and dose dependent decrease in the hydrophobicity of the Tau protein. D) The analysis of control and EGCG treated samples on the SDS-PAGE shows initial formation of SDS-resistant tetramers at 6 hours of incubation that are slowly abolished in a time and concentration dependent manner. E) The densitometry analysis showing decrease in Tau aggregates $p<0.05$.D). F) The CD analysis of EGCG treatment shows the formation of mixed Tau structures in a time dependent manner. G) The control reaction shows the presence of long mature filaments whereas the EGCG treatment shows increase in the fragility of the Tau filaments at with increasing in time. The 200 µM EGCG treatment shows broken filaments at the day 5 of incubation. This figure is reproduced from Sonawane *et al*., Scientific Reports, 2020.

EGCG is reported to prevent random coil to β-sheet conformation in α-synuclein protein and help maintaining the random coil conformation. Hence, CD spectroscopic analysis was performed to study the effect of EGCG on Tau conformation. The aggregation reaction mixture with Tau and EGCG in 1:10 ratio was analysed by CD at different time intervals with EGCG untreated Tau as a control. The soluble Tau demonstrated a native conformation of random coil whereas EGCG untreated aggregated Tau displayed a partial β-sheet conformation (Fig. 4.13F). The EGCG-treated Tau showed a shift from random coil to β-sheet conformation with increase in incubation period. However, the fluorescence and SDS-PAGE analyses demonstrated absence of aggregation on EGCG treatment. Thus, the partial β-sheet conformation of EGCG-treated Tau might be attributed to aggregates formed in the early phase of kinetics. Next, Tau in presence and absence of EGCG was visualized for morphological characterization by TEM. The aggregated Tau in absence of EGCG formed long filamentous aggregates while EGCG treatment formed only small fragmented filaments with complete absence of long fibrils (Fig. 4.13G). Thus, EGCG curtailed the Tau PHFs formation *in vitro*.

4.2.3 Dissolution of full-length Tau oligomers and fibrils by EGCG

Since EGCG displayed potency in interacting with Tau and inhibiting its aggregation, next studies were aimed to investigate its role in the dissolving Tau oligomers and fibrils, which are crucial for spread of pathology. For the preformed fibrils, EGCG displayed a concentration dependent fall in ThS intensity with time progression. This suggested decrease in fibrillar content in the EGCG treated fibrils as untreated fibrils displayed a stable and stagnant fluorescence (Fig. 4.14A). The calculation of percent

disaggregation based on the end time point fluorescence revealed significant disaggregation of Tau fibrils at all treatment concentrations (Fig. 4.14B). The ANS kinetics for fibril dissociation revealed a similar pattern with decrease in intensity with increasing dose of EGCG suggesting reduced hydrophobicity (Fig. 4.14C). The percent of PHF disassembly calculated based on ANS fluorescence revealed maximum of 85% for 500 µM of EGCG followed by significant disassembly at all EGCG concentrations (Fig 4.14D).

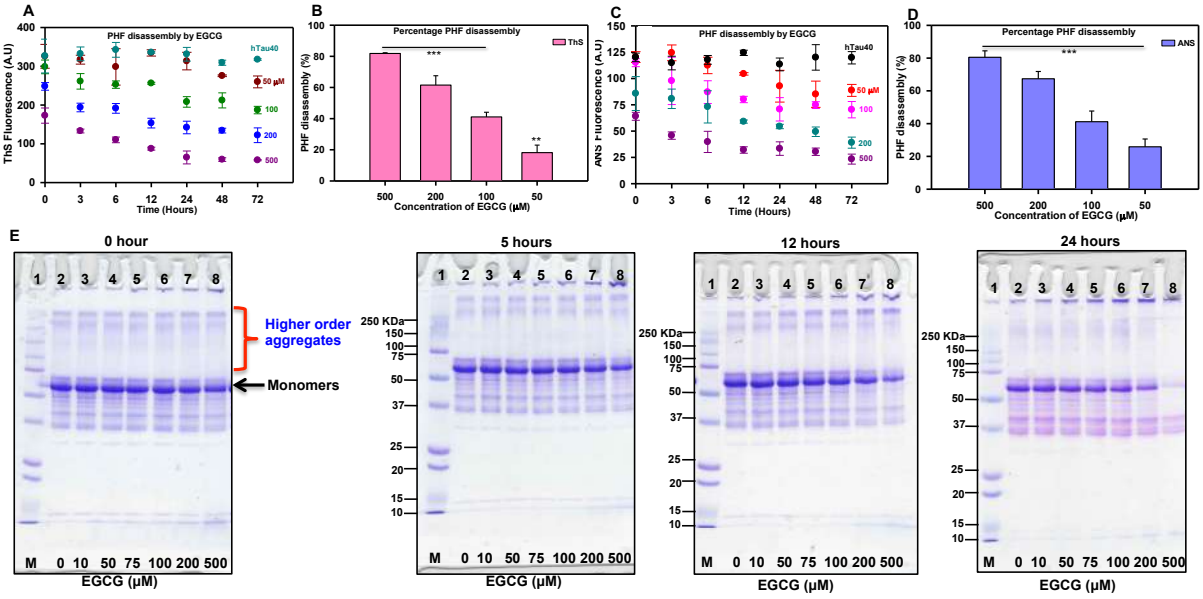

Figure 4.14. The preformed Tau fibrils dissolved by EGCG. A) The EGCG-mediated dissolution of mature Tau fibrils recorded by ThS fluorophore showing the disassembly of PHFs. B) The percent PHF disassembly by EGCG monitored by ThS fluorescence showed 81% disassembly at highest concentration (500 µM) $p<0.001$.C) The ANS fluorescence shows a time-dependent decrease as the fibrils are dissolved. D) The ANS fluorescence shows 80% Tau fibril disassembly $p<0.001$. E) The SDS-PAGE analysis of disassembly of Tau PHFs. This figure is reproduced from Sonawane *et al*., Scientific Reports, 2020.

The SDS-PAGE analysis of fibril dissociation revealed intact higher order Tau aggregation at the initial time point (Fig. 14E, 0 hour). The increase in incubation led to decrease in Tau aggregates on SDS-PAGE conforming dissolution of Tau filaments by EGCG in a concentration dependent manner (Fig. 4.14E).

The effect of EGCG on Tau oligomers was studied by allowing the oligomer formation for 6 hours after which EGCG was added to the reaction mixtures which was considered as a 0 time point. The ThS kinetics remained stable for all the samples till 12 hours after addition of EGCG but slowly started to decline with further incubation in EGCG treated oligomers (Fig. 4.15A). The untreated oligomers maintained a stable saturated ThS fluorescence suggesting intact Tau oligomers. EGCG showed significant oligomer disassembly at all the concentration (Fig. 4.15B). The hydrophobicity of Tau oligomers decreased after 24 hours of EGCG addition, which was monitored by ANS fluorescence (Fig. 4.15C, D). This revealed dissolution of Tau oligomers by EGCG in a concentration- dependent manner. The Tau oligomers prepared were observed as a distinct band on the SDS-PAGE at 0 hour (immediately after EGCG addition) (Fig. 4.15E), which were maintained intact till 12 hours of incubation (Fig. 4.15E). In concordance with kinetics at 24 hours, the Tau oligomers started to diminish on SDS-PAGE indicating dissolution of Tau oligomers by EGCG (Fig. 4.15E).

Thus, in addition to inhibiting Tau assembly, EGCG was found to be potent in dissolving intermediated species of Tau as well as fibrils.

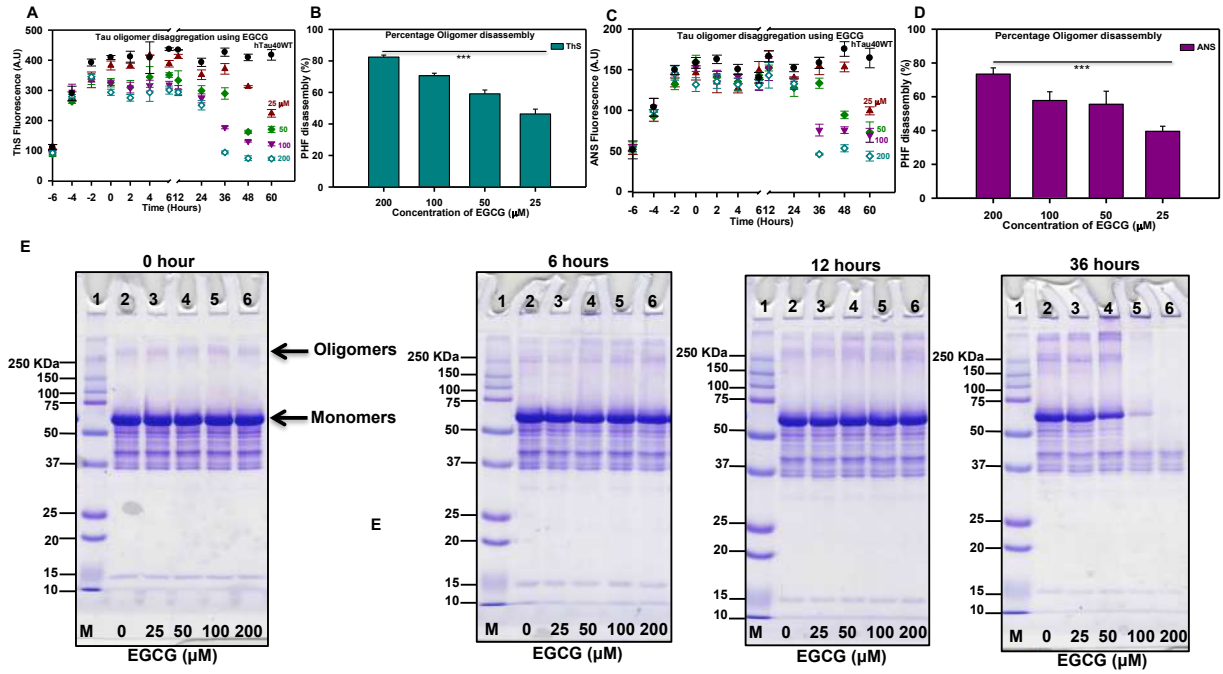

Figure 4.15. The preformed Tau oligomers dissolved by EGCG. A) The ThS fluorescence shows the inhibitory effect of EGCG on the dissolution of Tau oligomers in a concentration-dependent manner. B) Tau oligomer disassembly was 82% by ThS fluorescence at 500 μM ($p<0.001$). C) The ANS fluorescence shows the decrease in intensity with time and concentration suggesting loss of hydrophobicity of Tau oligomers. D) ANS assay showed 75% of Tau oligomer disassembly at 500 μM $p<0.001$. E) The SDS-PAGE analysis shows the presence of oligomers at the time of compound addition (0 h) which are slowly cleared with time. This figure is reproduced from Sonawane *et al*., Scientific Reports, 2020.

4.2.4 Characterization of EGCG-induced higher order Tau aggregates

Aggregation of full-length Tau comprises of a heterogenous mixture of higher order species. Our aim was to characterize these species formed in absence and presence of EGCG for their toxicity. For this we employed size-exclusion chromatography (SEC) to separate the species formed based on their molecular weights. The soluble monomer Tau was run as a negative control. This soluble Tau was eluted at the retention volume of 10.9 ml (Fig. 4.16A, black chromatogram). Next the 0 hour reaction mixtures were run consecutively for EGCG untreated and EGCG treated Tau aggregation reaction mixtures and eluted at the retention volume of monomer (10.9 mL) suggesting absence of preformed higher order species at the commencement of the assay (Fig. 4.16A, blue and pink chromatograms respectively). Next, the SEC was performed after 3 hours of incubation for EGCG untreated and treated Tau. The control as well as EGCG-treated Tau was eluted in two distinct peaks at 8.3 mL and 7.7 mL respectively (Fig. 4.16B). This shift of retention volume toward lower volumes suggested formation of early aggregates (Table 4.2). The SEC for 24 hours incubated samples displayed elution of both samples at 7.6 mL (Fig. 4.16C). Thus, the SEC profile of 3 hours of incubation revealed accelerated initial aggregate species on EGCG treatment as compared to control. Hence, it was necessary to analyze these Tau species for their toxicity in neuroblastoma cultured cells. The 0 hour fractions belonging to monomeric Tau did not affect the viability of the cells. The fractions for higher order species at 3 hours incubation showed reduction in viability of cells in control aggregates but interestingly EGCG-treated Tau showed increased viability as compared to control Tau. Similar observation was made for 24 hours incubated samples (Fig. 4.16D). These viability studies suggested that though EGCG accelerated early aggregates of Tau compared to control, these were less toxic to neuronal cells as compared to control. The binding studies revealed the affinity as well as the probable sites and types of interactions for EGCG and Tau.

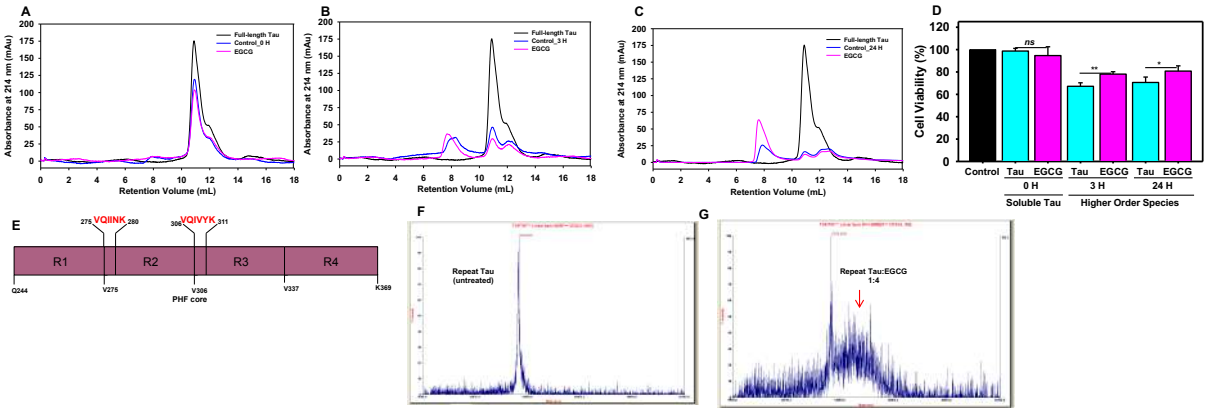

Figure 4.16. SEC for EGCG treated Tau. Tau was subjected to aggregation in presence of heparin as inducer. A) At 0 h Tau was eluted as monomer, both in presence and absence of EGCG. B) Further incubation led to aggregation of Tau, at 3 h of incubation EGCG showed more aggregation in Tau. C) Similarly, at 24 the peak intensity of Tau in presence of EGCG was high when compared to control. This suggests that EGCG is driving Tau towards the formation of higher order aggregates. D) Cell viability studies indicate that these conformers were non-toxic in neuro2A cells. E) Repeat domain of Tau showing two hexapeptide motifs. F) The MALDI-TOF spectra of untreated repeat Tau showing a single peak at desired molecular weight of 13.7 KDa. G) The EGCG treated repeat Tau shows an adjacent peak (red arrow) in addition to the soluble Tau peak suggesting the modification of Tau with EGCG as increase in molecular weight. This figure is reproduced from Sonawane *et al*., Scientific Reports, 2020.

Time (hours)	Tau ±EGCG	Retention Volume (mL)
0	Soluble Tau	10.9
	Control	10.9
	EGCG	10.9
3	Control	8.3
	EGCG	7.7
24	Control	7.9
	EGCG	7.6

Table 4.2. Retention volumes for EGCG treated and control Tau at various time intervals

Moreover, the SEC characterization revealed formation of distinct higher order species with different retention volumes and reduced toxicity as compared to untreated control. Also EGCG is known to covalently modify proteins, thus we analyzed covalent modification of repeat Tau in presence of EGCG by MALDI-TOF analysis (Fig. 4.16E). The untreated soluble repeat Tau displayed a molecular weight of 13.7 KDa as a single peak (Fig. 4.16F). Tau:EGCG at the ratio of 1:4 showed presence of one more peak in addition to the monomer peak (Fig. 4.16G) indicating covalent modification of repeat Tau by EGCG.

Further, in order to check its effect on viability of cells, EGCG was added to the cultured neuroblastoma cells at a range of concentrations (0-200 µM). Interestingly, EGCG was not only found to be non-toxic but also enhanced the neuronal viability as compared to untreated control cells (Fig. 4.17A). The concentration as high as 200 µM did not affect the viability. Further, the cells were exposed to Tau

aggregates in presence or absence of EGCG (0-200 μM) and studied for viability. The exposure of cells to aggregates in absence of EGCG reduced the cell viability significantly as compared to untreated control cells (Fig. 4.17B). The cells exposed together with Tau aggregates and EGCG maintained cell viability and showed enhanced survival at increased concentrations (Fig. 4.17B).

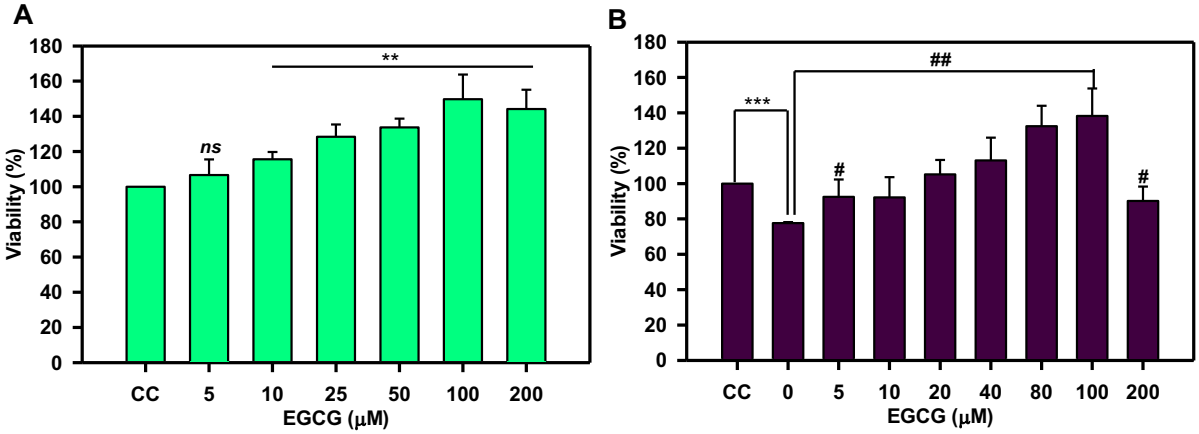

Figure 4.17. Effect of EGCG on cell viability. Toxicity was induced with 5 μM Tau aggregates and rescue in presence of EGCG (0–200 μM) in neuro2a cells. (A) Cell viability assay shows EGCG was non-toxic to neuronal cells at varying concentrations (0–200 μM) $p < 0.001$ and enhance the cell survival. (B) Tau aggregates induce toxicity in neuro2a cells at 0 μM EGCG $p < 0.05$(denoted as *) EGCG significantly rescues toxicity of Tau aggregate mediated toxicity till and enhances viability $p < 0.05$ (denoted as #). This figure is reproduced from Scientific Reports, 2020.

Thus, EGCG was found to impede assembly of full-length Tau as well as dissolved Tau PHFs and oligomers without having toxic effect on neuronal cells.

Chapter 5
Effect of polyamines on Tau aggregation and neuronal cell death pathways

Tau aggregation has been a major target for designing therapeutics in Alzheimer's disease. The aggregation of Tau is induced by various cofactors such as heparin which interacts with the repeat domain of full-length Tau (Fig. 5.1A) and prompts Tau-Tau interaction leading to filament formation. The two hexapeptide motifs ^{275}VQIINK^{280} and ^{306}VQIVYK^{311} in the repeats 2 and 3 respectively are known to play a crucial role in Tau self-assembly. A plethora of molecules have been screened and found potent to be Tau aggregation inhibitors (TAIs) including natural and synthetic molecules. The greatest obstacles for these molecules to be effective in clinical trials is their bioavailability and ability to cross the Blood-brain barrier (BBB). In such a scenario, the molecules naturally produced in the body can be good candidates for the TAIs. Few such molecules have been found to be neuroprotective including neuro hormone melatonin[209]. Polyamines are polyvalent, aliphatic amines with two or more amine groups found in all organisms. Polyamines regulate various cellular functions like cell proliferation, DNA synthesis, cell differentiation, transcription, apoptosis *etc*[210]. Polyamine synthesis takes place in a series of enzymatic conversions of the amino acid arginine (Fig. 5.1B). The first step involves conversion of arginine to ornithine by the enzyme arginase. The conversion of ornithine to putrescine is the rate-limiting step of the pathway and is catalysed by ornithine decarboxylase (ODC). Putrescine is the precursor for the synthesis of two polyamines, spermidine and spermine. Decarboxylated S-adenosylmethionine (SAM) by SAM decarboxylase also serves as a substrate for spermidine synthase in addition to putrescine. The enzymatic action of spermidine synthase yields spermidine which on addition of aminopropyl group by spermine synthase is converted to spermine in the polyamine synthesis cascade. The formation of spermidine and spermine is irreversible and the levels are regulated by the concentration of decarboxylated SAM. Polyamines have a positive effect on memory and learning and increase the longevity in various model systems. The role of polyamines in inducting apoptosis is regulated by the cellular systems as well as their metabolic profiles. The levels of polyamines are altered in neurodegenerative diseases like AD and PD. In our study, we characterized the effect of polyamines spermine and spermidine on Tau aggregation and neuronal death.

5.1 Effect of polyamines on modulation of Tau aggregation

Polyamines are known to regulate various physiological processes and also influence the aggregation of amyloidogenic proteins like Aβ and α-synuclein. We investigated the role of spermine and spermidine on the aggregation of full-length Tau. The classical assay was set up by adding heparin as an inducer of Tau assembly. The progress of aggregation and the associated hydrophobicity changes were monitored by ThS and ANS fluorophores respectively. The polyamines, spermine and spermidine were added to the reaction mixtures at the 50, 100, 200 and 500 μM respectively. The untreated control Tau aggregated progressively as observed by the continuous increase in ThS fluorescence. The saturation of aggregation for the control was attained within 8 hours. Spermine, on the other hand, supressed Tau aggregation till 12 hours, after which the ThS intensity began to increase in 50 μM spermine treated reaction (Fig. 5.1C). Further, in 100 μM spermine, the aggregation was initiated after 24 hours. The higher concentrations of 200 and 500 μM supressed Tau aggregation completely till 72 hours. Thus, spermine increased the lag period of Tau aggregation at least for 12 hours. Spermidine, however supressed Tau aggregation at the higher concentrations of 200 and 500 μM and reached saturation at 48 and 60 hours respectively (Fig. 5.1D). The increasing concentration of polyamines proportionately increased the lag period of Tau aggregation. Table 5.1 presents the lag time (t1) and saturation time (t2) for respective concentrations of polyamines. This summary highlights more potency of spermine in inhibiting the Tau aggregation. Tau aggregation is accompanied by hydrophobicity changes in the protein due to the exposure of the hydrophobic amino acids. As with aggregation, the hydrophobicity changes were minimal in polyamines treated Tau as compared to the untreated control

(Fig. 5.1E, F). The polyamine treated Tau was analysed on SDS-PAGE at 0, 24 and 72 hours. At 0 hour, presence of monomeric soluble Tau was confirmed in polyamines-treated and untreated Tau.

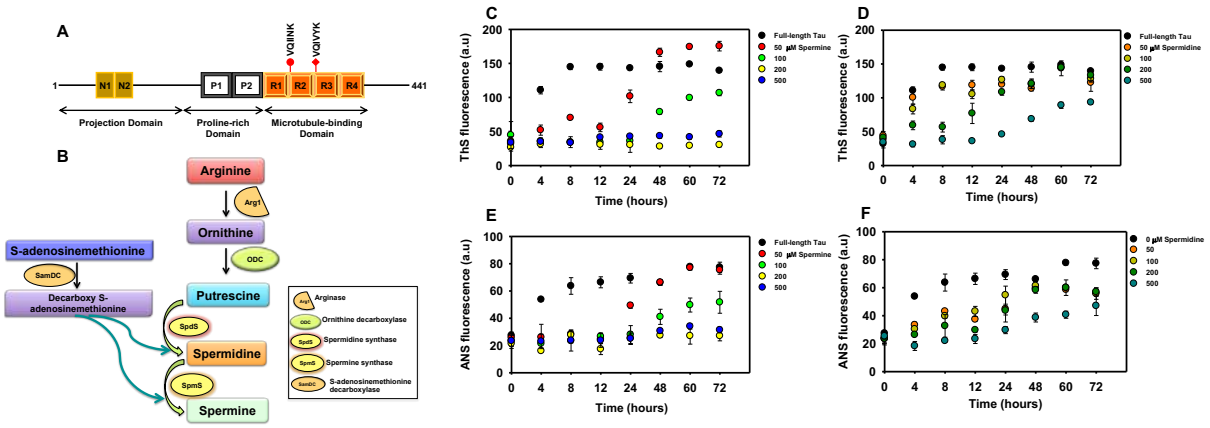

Figure 5.1. Polyamines-mediated Tau aggregation inhibition. A) The N-terminus region of Tau forms the projection domain comprising of two inserts followed by a polyproline stretch. The C-terminus region comprises of microtubule-binding region consisting of four imperfect repeats involved in Tau aggregation. B) Biosynthetic pathway of polyamines. C, D) The fluorescence analysis showed the inhibitory role of spermine on Tau aggregation, which was evidenced by decrease in both ThS and ANS fluorescence. The effect was observed in concentration-dependent manner and was prominent at the highest concentrations of 200 and 500 μM. E, F) Spermidine had poor inhibitory effect when compared to spermine. The higher concentration of 200 μM increased the lag time in Tau aggregation but after 24 hours the increase in fluorescence was observed which indicated Tau aggregation. The error bars represent mean ±SD values.

Polyamines	Concentration	t1	t2
	(μM)	(h)	(h)
Full-length	0	0	8
Spermine	50	12	48
	100	24	60
Spermidine	50	0	4
	100	0	8
	200	8	48
	500	12	60

Table 5.1. The lag time (t1) and the saturation time (t2) for control and polyamine-treated Tau aggregation, highlights the potency of polyamines in delaying Tau aggregation at the respective concentrations.

At 24 hours, higher order aggregates were observed only in control and Tau treated with lower concentrations of polyamines (Fig. 5.2A, B). After 72 hours of incubation higher order aggregates were formed in control and 50 μM of spermine treated Tau. In spermidine treated Tau except 500 μM treatment other groups showed formation of higher order aggregates. The results for SDS-PAGE were confirmed by immunoblotting the reaction mixtures with total Tau antibody (K9JA). The immunoblotting results clearly reflected the findings of SDS-PAGE analysis wherein spermine strongly

inhibited formation of Tau aggregates and spermidine was effective at the higher dose of 500 µM (Fig. 5.2C). Thus, polyamines were found to be effective in preventing *in vitro* Tau aggregation by increasing the lag period of the aggregation kinetics.

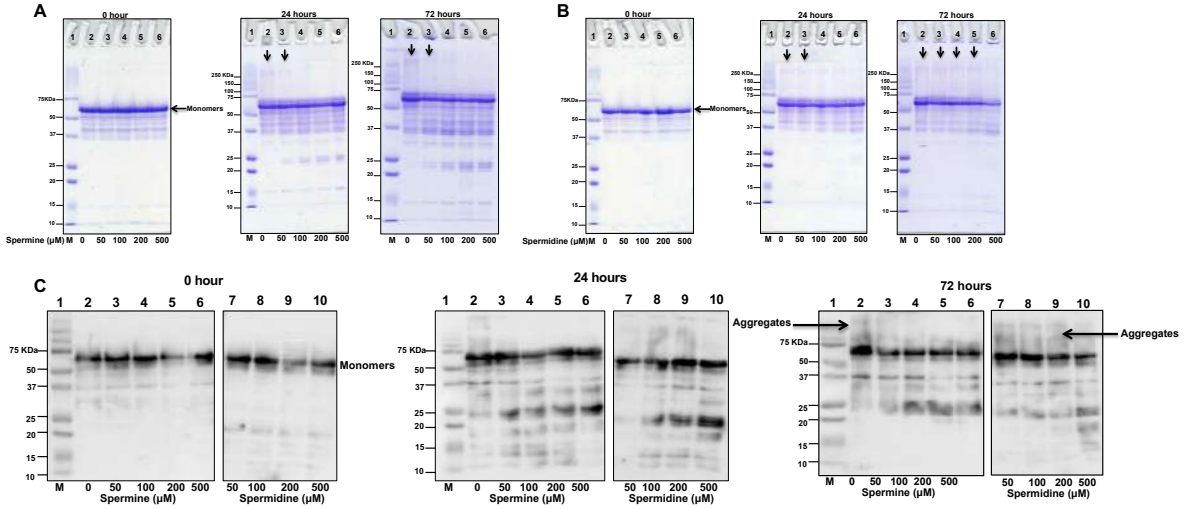

Figure 5.2. SDS-PAGE analysis of Tau aggregation inhibition by polyamines. A) Spermine showed complete inhibition of Tau aggregation as no high molecular weight aggregates (HMW) could be seen. B) Spermidine showed a strong inhibition at higher concentration but the lower concentrations showed presence of HMW aggregates (indicated by black arrows). C) Immunoblot analysis for total Tau suggested that spermine does not allow Tau to polymerize into HMW aggregates till 72 hours, whereas 500 µM of spermidine inhibits Tau aggregation till 24 hours.

5.2 Effect of polyamines on native Tau conformation

Tau aggregation leads to the formation of heterogenous Tau species comprising of soluble monomers and oligomers in addition to insoluble higher molecular weight aggregates. The conformational analysis of this heterogenous population gives a conformation profile of partial β-sheet as opposed to random coil conformation of native soluble protein. The SDS-PAGE analysis and immunoblotting results revealed that the polyamines maintained Tau in the monomeric form. In order to gain further insight into the conformational profile, CD spectroscopy was performed on soluble, untreated aggregated and polyamine-treated Tau. At 0 hour, all the groups showed maximum ellipticity at around 198-200 nm indicating native conformation of soluble Tau (Fig. 5.3 A, C).

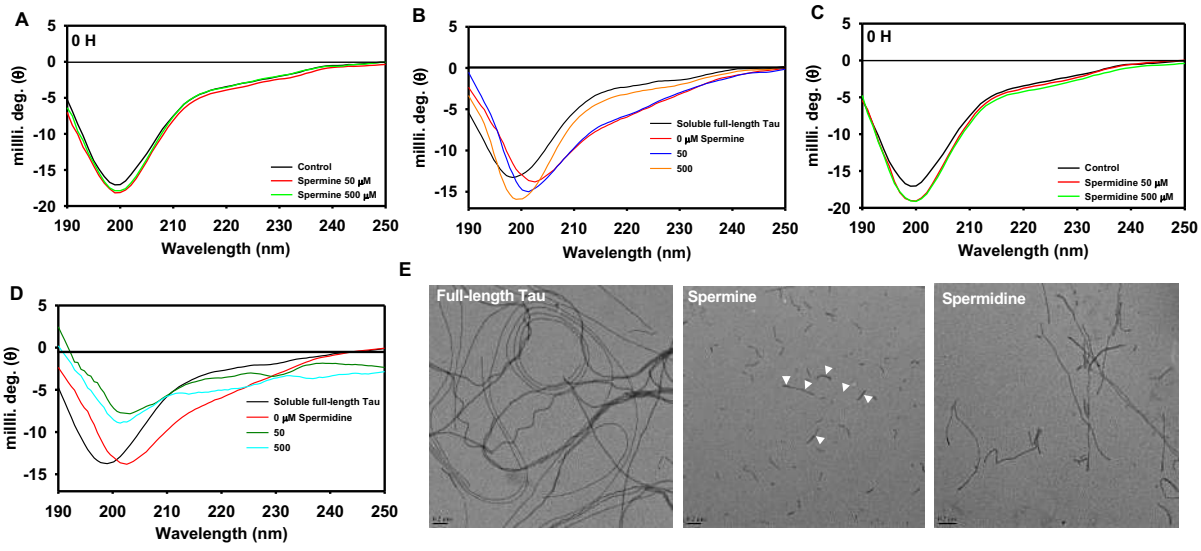

Figure 5.3. Conformational and Morphological changes in Tau aggregates by polyamines. A. The CD spectra of Tau, in presence and absence of spermine showed native conformation of Tau at 0 hour. B. The change in Tau conformation was

observed as a shift towards β-sheet conformation in absence of polyamines (indicated in red). At lower spermine concentration, the shift towards β-sheet was observed. Spermine at 500 μM concentration showed a prominent shift towards its native conformation. C) 0 hour CD spectra of spermidine treated and control Tau show no conformational changes of Tau. D) Spermidine however had no effect as Tau exhibited β-sheet conformation. E) Full-length Tau showed the presence of long Tau fibrils whereas the spermine treated Tau formed smaller fragments of Tau (represented as white arrow) and long fibrils were absent. Spermidine treated Tau exhibited presence of long filaments.

After 72 hours of incubation, the untreated aggregated Tau displayed partial β-sheet conformation as opposed to soluble Tau. Spermine treated Tau maintained the random coil conformation of Tau at both the concentrations of 50 and 500 μM (Fig. 5.3B). But spermidine-treated Tau showed a shift in the spectra toward partial β-sheet conformation (Fig. 5.3D). Thus, spermine prevented Tau form heparin-induced aggregation by maintaining it in its native conformation and monomeric form. Further, transmission electron microscopy imaging revealed long fibrillar aggregates in untreated Tau whereas polyamine treatment led to formation of fragile and broken fragments of Tau (Fig. 5.3E). Thus, polyamines prevented formation of filamentous Tau aggregates and maintained its native conformation.

5.3 Mapping of Tau-polyamines interaction

Since, the polyamines were found to be potent in maintaining Tau in its native form we studied the physical interaction of repeat Tau with polyamines by ^{1}H-^{15}N HSQC NMR experiments. ^{1}H-^{15}N HSQC, a two dimensional NMR experiment represents each amide proton present in proteins as a cross peak (which have to be assigned specific to each sequential residue in the protein by interpretation of a series biomolecular NMR experiments) in the spectrum. It acts as a fingerprint NMR spectrum that represents the conformation of a protein under defined conditions such as temperature and buffer. Any perturbation in the position of the HSQC contour peaks upon addition of a ligand to the protein implies the interaction of the protein with the ligand at the amino acid residues corresponding to the perturbed cross peaks. We titrated 200 μM ^{15}N labelled repeat Tau at 0, 1, 2, 4, 8, 16 stoichiometric ratios of spermine (Fig. 5.4A) and spermidine (Fig. 5.4B) respectively.

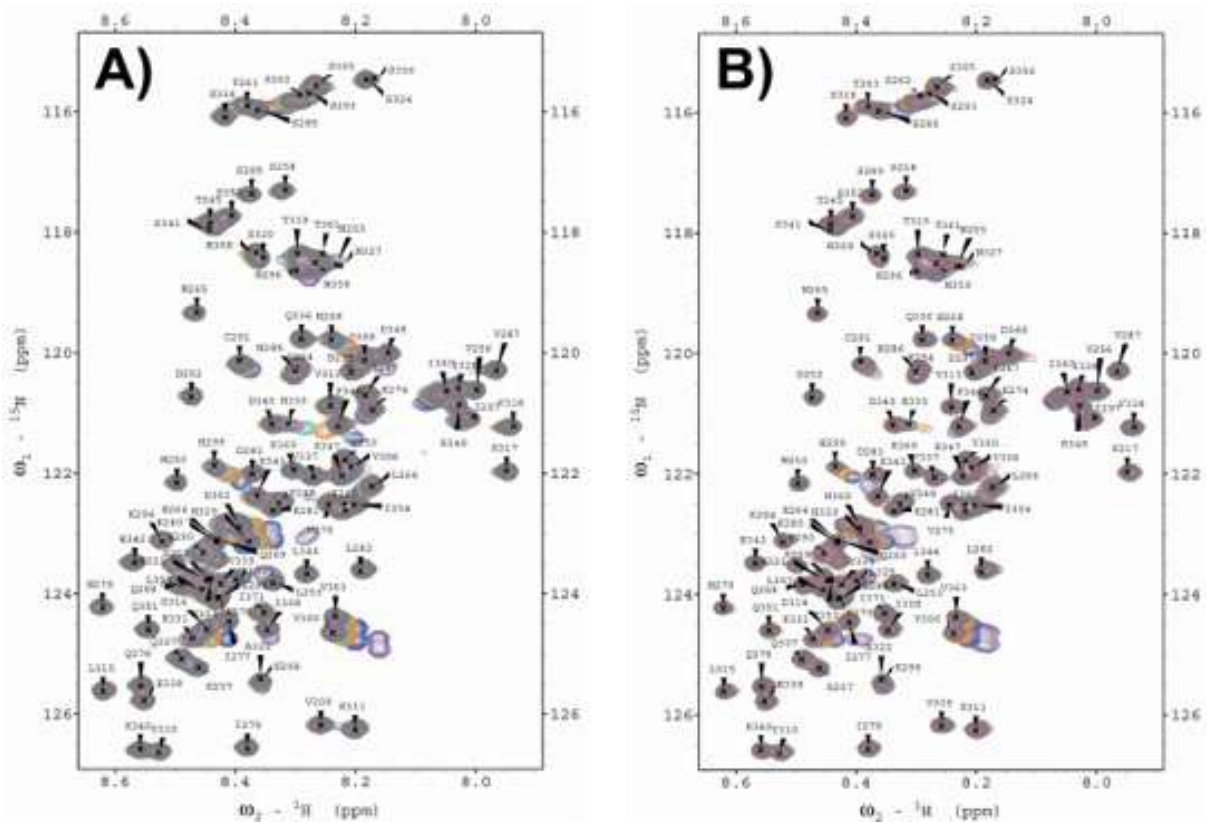

Figure 5.4. ^{1}H-^{15}N HSQC NMR for repeat Tau and polyamines. NMR ^{15}N HSQC chemical shift perturbation plots for the titration of 200 μM solution of repeat Tau with (a) Spermine and (b) Spermidine in various concentration ratios. Color codes for ^{1}H-^{15}N HSQC spectra (with respect to protein : ligand concentration): 1:0 (gray); 1:1 (magenta); 1:2 (turquoise); 1:4 (dark orange); 1:8 (royal blue); 1:16 (medium purple). Each cross peak in the parent ^{1}H-^{15}N HSQC spectrum corresponds to an amide proton (and hence to an amino acid) in the repeat Tau protein sequence. The labels given on each cross peak in the parent ^{1}H-^{15}N HSQC spectrum (gray; repeat Tau in 1:0 ratio with respect spermine/spermidine) indicate the name of the amino acid and its sequential position in the repeat Tau sequence. For clarity, only expanded region of ^{15}N HSQC containing majority of the assigned residues is shown. Residues that are interacting with the polyamines (H268, H299, V300, H329, H330, K331, H362, V363, L266, K267, Q269, K298 and T361 in decreasing order of perturbation) can be identified by the trailing of their corresponding HSQC cross peaks with increasing concentration of polyamines, while the other residues have remained unchanged.

The analysis of the interaction was done by reference ^{1}H-^{15}N HSQC chemical shift assignment for repeat Tau deposited in BMRB with accession number 19253. The analysis revealed identical interaction for both polyamines with repeat Tau. Both the polyamines showed strong chemical shift perturbations of H268, H299, V300, H329, H330, K331, H362, V363 and a moderate perturbation of L266, K267, Q269, I297, K298, I360 and T361 and the interaction at these repeat Tau residues was observed from the initial titrations with 1:1 ratio. The interacting residues of Tau with polyamines was spread across the repeats and could be categorized into 4 regions. L266-K267-H268-Q269 (in repeat 1 domain of Tau), I297-K298-H299-V300 (in repeat 2 domain of Tau), H329-H330-K331 (in repeat 3 domain of Tau) and I360-T361-H362-V363 (in repeat 4 domain of Tau). These results suggests that histidines as the primary interaction sites and the neighbouring residues acting as secondary interacting sites; for example L266, K267, Q269 for interaction with H268; and I297, K298, V300 for interaction with H299.

5.4 Characterization of polyamine-treated Tau

Prior to characterization of polyamine-treated Tau, the polyamines were studied for their toxicity in the neuronal cells. The neuro2a neuroblastoma cells were treated with a wide range of polyamines 100 nM to 200 μM. Both the polyamines were found to be non-toxic to the neuronal cells at all the given doses (Fig. 5.5A, B).

Next aim of the study was to investigate the role of polyamine-treated Tau in neuronal cell viability. For this, the cells were exposed to the reaction mixtures from the end timepoint of the assay. The viability test showed that the untreated aggregated Tau reduced the viability of the neuronal cells compared to control cells (Fig. 5.6A). However, spermine-treated Tau at all concentrations showed increased viability as compared to untreated aggregated Tau. Spermidine-treated Tau showed similar effects at the higher concentration of spermidine (Fig. 5.6B).

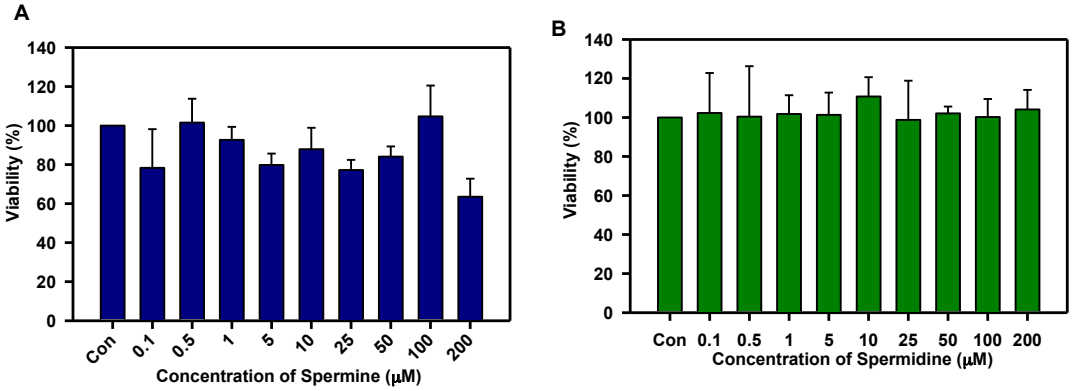

Figure 5.5. Toxicity study of polyamines. A) Spermine did not show visible toxicity in the neuroblastoma cells except for the highest concentrations of 200 μM B) Spermidine maintained the complete viability at a broad range of concentrations from 0.1-200 μM.

This is in conjunction with the aggregation studies wherein spermidine is found to prevent Tau aggregation only at higher concentrations. In addition to MTT, LDH release assay was performed to check for the membrane integrity of neuronal cells on exposure to polyamine-treated Tau. The polyamine-treated Tau did not show changes in LDH release as compared to control cells. However, the Tau treated with highest concentration of spermidine showed reduction in LDH release even compared to control cells. This suggests its potency in protecting neuronal cells from membrane damage (Fig. 5.6C, D). The viability studies show that polyamines drive the Tau to non-toxic species.

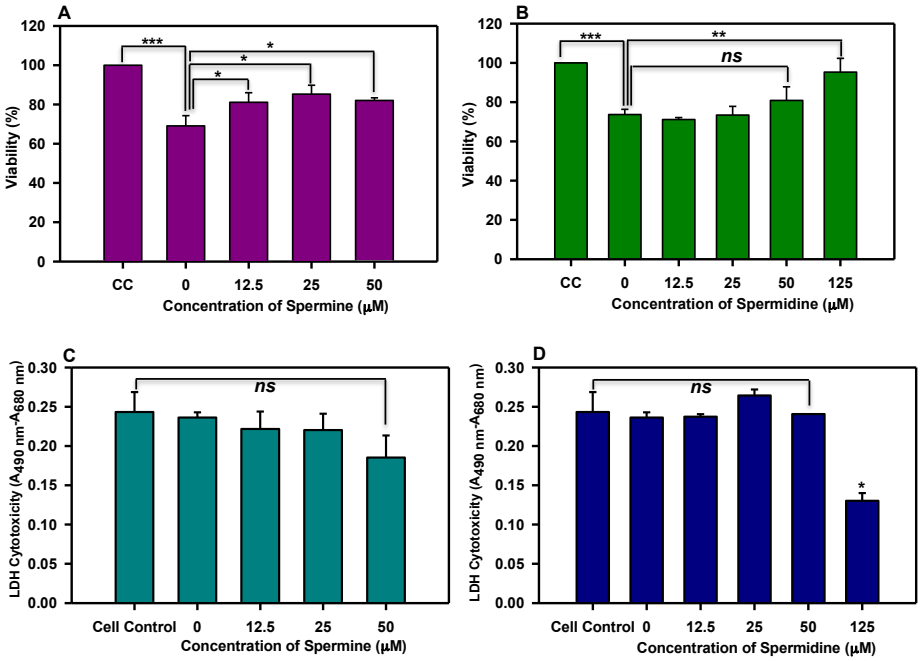

Figure 5.6. Toxicity study of polyamine-treated Tau of neuronal cells. A) The spermine untreated Tau showed a decrease in viability relative to cell control. The polyamine treated Tau rescued the viability of cells as compared to untreated Tau. B) Spermidine treated enhanced the viability of neuro2a cells as compared to untreated Tau. C, D) Membrane leakage assay shows that spermine and spermidine treated Tau does not lead to altered membrane permeability. The error bars represent mean ±SD values. Data is significant at the mean difference between treatment groups where (X − X`) > Tukey's criterion (T).

As mentioned, Tau aggregation forms heterogenous population of species including monomers, oligomers and filamentous aggregates. We separated these species by size-exclusion chromatography from polyamine-treated and untreated reaction mixtures at 0, 24 and 48 hours. At 0 hour, all the groups eluted a single peak of Tau monomer without any higher-order species (Fig. 5.7A). At 24 hours, control as well as the polyamine-treated Tau eluted at lower retention volume in addition to the monomer peak (Fig. 5.7B). The peak with lower retention volume corresponds to the higher molecular weight Tau species. At 48 hours, the peak corresponding to higher molecular weight aggregates increased in intensity in the order control>spermidine while peak for spermine did not change (Fig. 5.7C). Additionally, the eluted fractions were analyzed for their hydrophobicity by ANS assay. This study revealed that the fractions eluted as the higher molecular weight species possessed more hydrophobicity as compared to polyamines treated Tau at all the three time points (Fig. 5.7D). Thus, polyamines inhibited the Tau aggregation by preventing its compaction which is essential for its aggregation to occur.

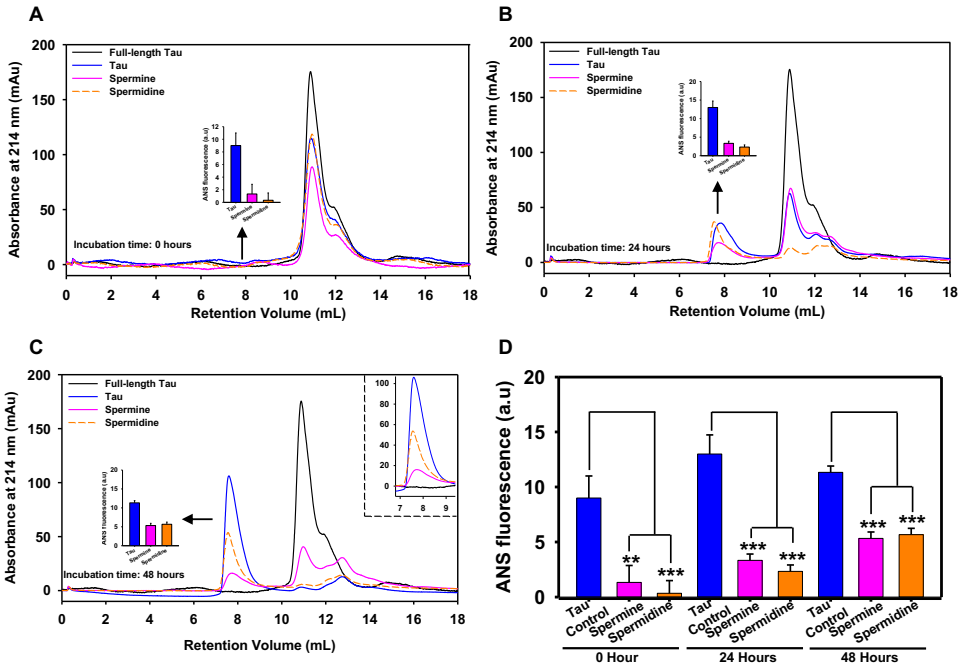

Figure 5.7. Size exclusion chromatography analysis of polyamines treated Tau. A) Initially at 0 H polyamines showed no effect and the retention volume was similar to polyamine-untreated control (Tau) and soluble monomer (Full-length Tau). B) At 24 hours the higher order aggregates were formed. It was evidenced that spermidine had enhanced effect in formation of higher order aggregates when compared to control and spermine. Moreover, the intensity of higher order aggregates in presence of spermine was less, which indicated that it prevented aggregation of Tau. C) At 48 hours, control and spermidine reached saturation where Tau completely aggregated. In presence of spermine only minor proportion of Tau was aggregated as observed by the presence of smaller peak at 8 mL. The comparative hydrophobicity of Tau corresponding the peak are showed as inserts. D) The ANS fluorescence analysis revealed that at 0 hour the hydrophobicity of soluble Tau was less when compared to spermine and spermidine, where spermidine exhibited higher ANS fluorescence. Analyzing the higher order fraction at 24 and 48 hours showed that the hydrophobicity in untreated Tau increased when compared to spermine and spermidine. The error bars represent mean ±SD values. Data is significant at the mean difference between treatment groups where (X − X`) > Tukey's criterion (T).

5.6 Effect of polyamines on neuronal apoptosis

Polyamines are known to regulate various cellular functions and cell apoptosis is one of them, though, the effects vary with cell type. We investigated the role of polyamines in neuronal apoptosis by employing flow cytometry by Annexin V-FITC and propidium iodide labelling. The upper right and lower right quadrants correspond to the cells undergoing late and early apoptosis respectively. The percentages in both these quadrants were summed up to determine the total apoptotic cells. Accordingly, spermine showed decline in apoptosis with increasing concentrations. Spermine exposure of 1, 2, 5 µM lead to apoptosis in 91.9, 86.3 and 80.6% cells respectively (Fig. 5.8A) Similarly, spermidine at 10 and 20 µM caused apoptosis in 93.1 and 80.4% cells respectively. These results suggest that lower concentrations induce apoptosis whereas higher concentrations of polyamines inhibit neuronal apoptosis. Further, polyamines were studied with respect to their caspase-3 activity as it is involved in apoptotic pathway. Both the polyamines did not show significant changes in the capsase-3 activity (Fig. 5.8B), although, spermidine tend to mildly decrease caspase activity at 40 µM concentration (Fig. 5.8C). Thus, polyamines were found to modulate the apoptosis of neuronal cells.

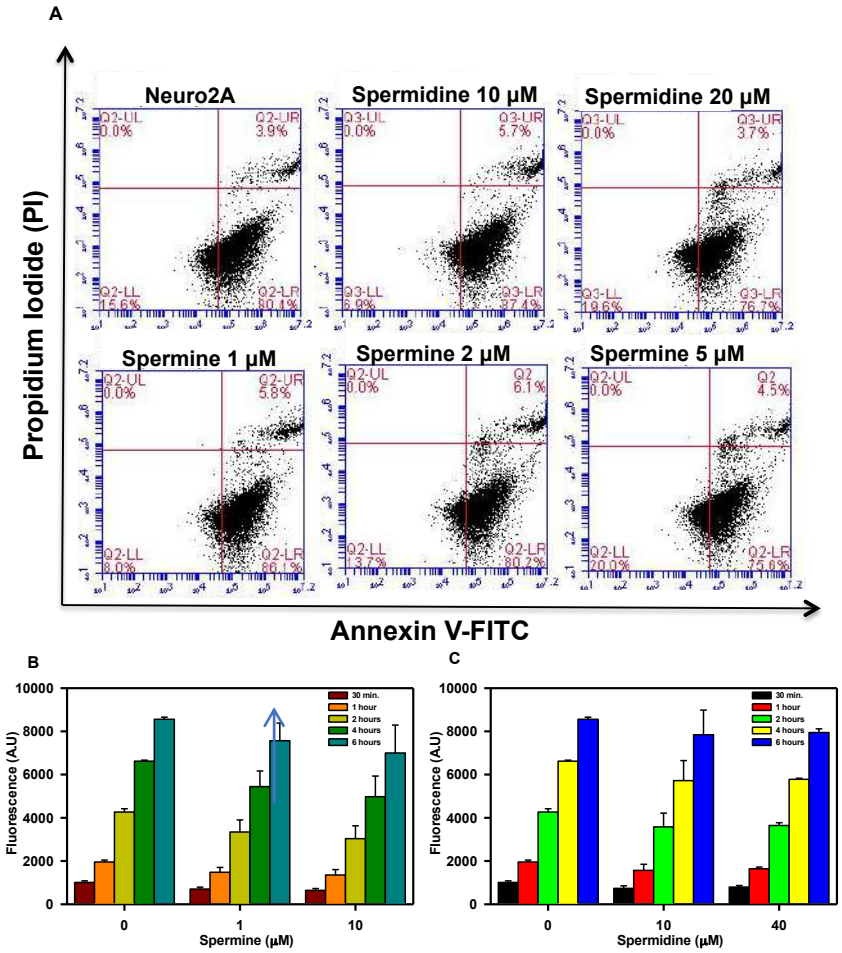

Figure 5.8. Effect of polyamines on apoptosis. A. Polyamines showed decrease in cell death with increase in dose. B. Analysis of caspase activity showed no change in spermine treated cells. C. Spermidine showed a mild decrease in caspase activity with increase in concentration. The error bars represent mean ±SD values. Data is not significant, since the mean difference between treatment groups where (X − X`) < Tukey's criterion (T).

Chapter 6
Discussion

Alzheimer's introduced the clinical features of the senile dementia now known as Alzheimer's disease about 100 years ago, but the supremacy of the in-depth research on the subject commenced in the 1970's. The last few decades have productively propelled the research on AD with varied aspects of the causes, molecular pathophysiology and more importantly the therapeutic interventions. Alzheimer's disease (AD) accounts for 70% of total dementia cases accompanied with insidious memory impairment, the chances of which are elevated with increasing age. While majority of AD cases are known to occur sporadically, mutations in several genes accounts for the less prevalent familial AD. The causal pathologies of AD are famously bifurcated into the Amyloid hypothesis and the Tau hypothesis. For the past 25 years, the amyloid hypothesis (aka the amyloid-β hypothesis) was considered to be the mainstream and nexus of AD pathology[9,211]. This hypothesis suggests accumulation of misfolded peptides Aβ42 and Aβ40, which are the byproducts of the APP metabolism with Aβ42 peptides dominating the plaques composition. The accumulation occurs due to imbalance in the production and clearance of the Aβ peptides. Although, the hypothesis is most prevalent it does not necessarily correlate with the disease progression as well as for therapeutic intervention. Hence, the amyloid hypothesis needed reconsideration due to the following observations;

i. The genetically modified mouse for Aβ pathology, showed accumulation of plaques but there was no evidence of associated cytotoxicity to the neurons as well no Tau NFTs formation[212]
ii. The Aβ deposition is not a mandatory pathology observed in AD brains[213]
iii. The defect APP metabolism is linked to AD rather than the Aβ plaque deposition or accumulation.

On the contrary, Tau hypothesis is found to be the prime cause of AD pathology. The predominant observations, which support this view, are;

i. Presence of hyperphosphorylated Tau inclusions in AD brains [214]
ii. Correlation of extent and localization of Tau NFTs with Braak staging of the disease progression [6]
iii. Observation of Tau lesions prior to Aβ accumulation[215]
iv. Increased neuronal degeneration due to Tau abnormalities and accumulation[31,32]
v. Disruption of neuronal cytoskeleton, signaling and mitochondrial integrity due to Tau dysfunction[216,217]

Thus, Tau plays a major role in AD pathology and is a crucial therapeutic target.

Tau: Central nexus in physiology and AD pathology

Tau was discovered as the prominent microtubule-associated protein (MAP) in the mammalian brain with 6 isoforms in the central nervous system[17]. The 3R isoforms dominate the early developmental stages which are highly phosphorylated and implicated in the synaptic plasticity[15,218]. The adult mammalian brains have equal expression of 4R and 3R isoforms of Tau, which are reported to be concentrated in the axonal region of the neuron. However, in the axon the distribution of Tau differs between the two axonal ends. Tau is concentrated more at the distal ends especially in the growth cones[219]. This concentration gradient of Tau along the axon is maintained by its phosphorylation state wherein phosphorylated Tau is found near the soma region of the axon and dephosphorylated Tau is found at the growing axons[220]. This helps in keeping the dynamicity of the microtubules at the growth cones. However, the impairment in the gradient of phospho-Tau due to aberrant phosphorylation leads to axonal defects such as axonal swellings and varicosities in the early stages of AD[221]. These are correlated with the defective transport of cargo containing vesicles. In addition to predominant axonal localization, Tau is also present in other cellular compartments like nucleus, nucleolus, dendrites and plasma membrane. The ectopic localization of Tau to somatodendritic compartments is partly attributed

to the Tau acetylation that destabilizes the AIS cytoskeleton[60]. The AIS acts as a barrier maintained by interaction of Tau and the microtubules to prevent the diffusion of Tau in the dendrites. The somatodendritic mislocalization of Tau is observed in degenerating neurons in AD and the Tau in this compartment is found to be highly phosphorylated[222]. The somatodendritic Tau also causes impairment in synaptic plasticity by abnormal activation of NMDA receptors in the spines[223]. The role of nuclear Tau has been implicated in the protection of DNA and RNA from damage and maintain the pericentrometric heterochromatin (PCH) framework[224,225]. This physiological function of Tau is hampered in the AD neurons, affecting the PCH integrity. The physiological role of Tau is also implicated in the nucleolar transcription[226] and the abnormal Tau Nuclear Indentations (TNI) have been reported in the early AD patients[227,228]. These TNIs are mapped to only phosphorylated Tau and serve as an early marker. TNIs may contribute to loss of nuclear integrity observed in AD. The association of Tau has also been reported with cellular organelles like ribosomes, Golgi apparatus and endoplasmic reticulum[229]. Tau plays an important at the synapses, which serve as the connections between the neurons. Tau present at both the presynaptic and the post-synaptic compartments in AD is hyperphosphorylated and forms SDS-stable oligomers leading to synaptic dysfunction[230]. Moreover, the synaptic plasticity is mediated by Tau-actin interactions especially in the dendritic spines and presynaptic boutons which helps maintain spine density and release of neurotransmitters[231]. But the pathological Tau mutations in AD and hyperphosphorylation of Tau hampers Tau-actin interactions and curtails these functions[216]. Thus, Tau aggregation due to mutations, hyperphosphorylation and other modifications disrupt its multiple neuronal physiological functions leading to AD. Our studies revolve around the causative agents of Tau pathology as well as solutions to attenuate Tau pathology and related neuronal dysfunction in form of naturally occurring small molecules.

6.1 Tau mutations and post-translational modifications

The FTDP-17 are hereditary Tauopathies accounting for various disorders including Alzheimer's disease, corticobasal degeneration, progressive supranuclear palsy and Pick's disease. The FTDP-mutations in Tau comprise of missense, deletion, transition, and intronic mutations affecting the expression and function of Tau. The splice site or the intronic mutations act to include the exon 10, which codes for R2. This increases the total levels of 4R isoforms disturbing the 3R/4R ratios. The mutations which lie in the exon 10 and affects its alternative splicing are N279K, L284L, ΔK280 and S305N[232]. Other Tau mutations induce aggregation as well as curtail one of the important functions of Tau of microtubule stabilization and these include G272V, ΔK280, P301L, P301S, V337M, R406W[233]. The mutations G272V and V337M are localized to the ends of the microtubule-binding region or the hinge region and may play a in disrupting the secondary structure required for microtubule interaction[234]. These two mutations are also showed to enhance Tau assembly as compared to the wild type Tau[235]. The mutation R406W lies in the carboxy terminal of Tau and mildly affects Tau aggregation as well as microtubule-binding[235]. The mutations P301L and P301S are reported to have greatest propensity of aggregation compared to wild type[35]. Moreover, P301L Tau has a reduced affinity for microtubule interaction. Thus, the mutations have multiple effects on Tau physiology and play a role in AD pathology. The post-translational modifications of Tau are key players in Tau function. Recently, seven types of physiological Tau PTMs have been reported out of which one-third are newly identified[63]. This highlights the higher level of regulation of endogenous Tau than previously suggested. The neurotoxicity of Tau is linked to several PTMs of which phosphorylation is the cardinal modification. Phosphorylation not only controls the self-assembly of Tau but it also plays a decisive role in interaction of Tau with other interacting partners including microtubules. The criteria deciding Tau hyperphosphorylated is subjective to a certain extent as it is based on mole of phosphates per Tau molecule[40]. But this may not be completely true because phosphorylation of certain residues in a

combinatorial manner influences Tau pathogenicity rather than the extent of phosphorylation across the protein. Although, phosphorylation had gained initial attention in Tau pathology, other modifications have also surfaced equally important in Tau pathogenesis like acetylation, methylation, glycation, ubiquitination *etc*. For example acetylation of Tau at the positively charged lysine residues declines its affinity for the microtubules by reducing the overall charge the protein[57]. The reduction in positive charges also sets in self-assembly of Tau triggering its aggregation. In addition to individual PTMs, the cross talk among the various PTMs also affects the fate of Tau modification. For instance, acetylation and ubiquitination modify Tau at the lysine residues but each modification affects Tau in a discreet way. Acetylation precludes Tau ubiquitination, which is required for its degradation[63]. This results in overall increase in endogenous Tau levels elevating the chances of its aggregation. On the other hand phosphorylation of Tau positively regulates its auto acetylation property. Tau phosphorylation at the repeat regions enhances the auto acetylation of Tau[236]. On the contrary, phosphorylation at the KXGS motifs inhibits Tau ubiquitination[237]. Thus, the cross talk among various causal agents inducing Tau pathology like mutations and PTMs might regulate the overall Tau pathogenesis in AD. Hence, we designed our study to decipher the effect of multiple factors on Tau pathology. For example, the first part was designed to study the glycation of the FTDP-17 Tau mutants and the other half dealt with dual (phosphorylation and glycation) modification of Tau.

6.1.1 Glycation of Tau FTDP-17 mutants

Glycation, a non-enzymatic reaction caused by sugars and their reactive intermediates like methylglyoxal (MG) drastically alters protein structure and function. It induces protein aggregation and accumulation due to conferred protease resistance. The presence of glycated Tau in the pathological Tau PHFs from AD brains suggested the role of glycation in stabilization of the PHFs[78]. Glycation was also found to decline Tau's affinity for microtubules[79]. We modified Tau and the 3 FTDP-17 mutants G272V, P301L and R406W by methylglyoxal and determined its role in the various pathological parameters of Tau aggregation. Our studies revealed that the MG-induced aggregation was enhanced in the Tau P301L mutant and suppressed in R406W mutant as compared to the wild-type Tau. Moreover, the advanced glycation end products (AGEs) formation also followed a similar pattern as aggregation. These results are attributed to the local conformational changes caused by specific mutations. The suppressed aggregation and AGEs formation in the R406W mutant as compared to wild type Tau is in agreement with the nature of this mutant to resist modification. The mutant R406W is found to resist phosphorylation by multiple kinases such as GSK-3β, PKA and Rho kinase which might due to mutation-specific local conformational changes[183] However, there are controversial reports regarding the phosphorylation status of this mutant as the post-mortem brains report hyperphosphorylation of R406W Tau[238,239]. These results are also subject to disease stage and progression when compared to *in vitro* data. Thus, the reduced MG-induced aggregation might be due to inaccessibility of preferred glycation sites due to altered conformation. On the contrary, the mutant P301L showed enhanced MG-induced aggregation and AGEs formation as compared to wild type Tau.

The wild type Tau adopts a relatively compact hairpin conformation in solution[23]. In this conformation, the C-terminal of Tau folds upon the repeat region and remains in the vicinity of N-terminal, while N-terminal projects away from the repeats[39] (Fig. 6.1). This might mask the sites responsible for glycation and hence, we observe moderate glycation of wild type Tau as compared to P301L mutant. The P301L mutation is reported to induce extended Tau conformation, which explains enhanced glycation of this mutant with respect to wild-type Tau. The extended conformation allows for more sites to get modified by MG and hence the elevated glycation. Glycation generally induces rigid structural changes in the proteins such as cross β-sheets which favors protein aggregation rather than folding[240,241]. Tau is natively unfolded protein and adopts random coil conformation[242]. The CD spectroscopic analysis of

MG-induced glycated Tau and its mutants did not present significant global conformational change. Thus, the variations in glycation observed could be attributed to local conformational changes. Moreover, glycation is known to have differential effects on 3D-protein conformations, thus explaining the observed CD results[241,243]. Another interesting observation was morphologically distinct glycation-induced Tau aggregates as compared to heparin-induced Tau aggregates. The glycation formed amorphous aggregates of Tau as opposed to fibrillar aggregates. A 2 repeat Tau peptide is reported to form such amorphous aggregates on glycation and does not show formation of filamentous aggregates[244]. Thus, the predisposition to P301L mutation might accelerates Tau pathology in metabolic anomalies like diabetes, as it is more prone to glycation and aggregation by diabetes-related reactive dicarbonyls.

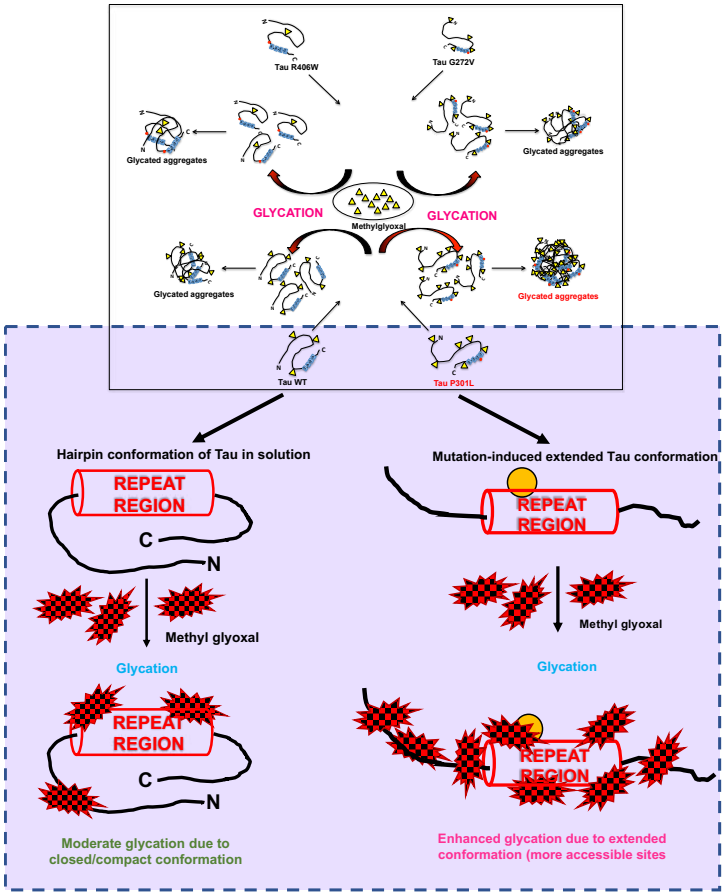

Figure 6.1. Enhanced MG-induced glycation of Tau P301 L. The glycating agent MG shows enhanced glycation for the Tau dementia mutant P301 L with large aggregate formation as compared to wild-type. This might be due to differentially exposed amino acids in WT versus the P301 L mutant that leads to enhanced modification by MG. The other mutant G272V showed basal level of glycation as control whereas R406W mutant showed less glycation as compared to control. Mechanistically, P301L mutation induces extended conformation in Tau, which otherwise adopts a compact hairpin conformation in solution. The extended conformation makes more sites accessible for modification, hence enhanced glycation. This model shows additional pathological feature of a predisposed Tau dementia mutant, which might enhance Tau dysfunction in a combinatorial manner.

6.1.2 Dual modification of Tau

Tau phosphorylation has been studied immensely due to its impact on physiological function and pathological conversion of Tau. Hyperphosphorylation is reported to reduce Tau-microtubule affinity and drive towards aggregation[245]. Similarly, Tau glycation is found predominantly in AD brains with reduced microtubule affinity[78]. Moreover, the PHFs Tau is a product of multiple Tau modifications. Hence, we studied effect of two known aberrant Tau modifications, phosphorylation and glycation on Tau aggregation. It's a well-known fact that in addition to extent of phosphorylation, the site-specific

phosphorylation plays a key role in Tau pathogenesis. The site-directed mutagenesis is employed to make the pseudophosphorylation mutants such that a single site or a combination of sites would be studied for their effect on Tau aggregation and related microtubule assembly[90]. Our study focused on glycation of double pseudophosphorylated mutants (262/404D, 262/396D and 231/262) and their impact on aggregation kinetics. The results suggested no significant differences in MG-induced aggregation propensity of pseudophosphorylation mutants and wild type Tau. These results agree with reported MG-induced aggregation propensities of double pseudophosphorylation mutants, which do not show visible changes. The site-specific pseudophosphorylation might play a role in these results. Moreover, the sites localized in the C-terminal region of Tau like S396 and S404 are known to intensify Tau aggregation on phosphorylation whereas, the sites are located in proline-rich region (T231) and repeat domain (S262) suppress the aggregation[46]. The phosphorylation at S262 residue suppresses the Tau aggregation with overall increase in the phosphorylated sites on Tau. The 3 double mutants employed in our studies have a common pS262, which might be responsible for suppressing MG-induced aggregation. Thus, site-specific pseudophosphorylation affects MG-induced Tau assembly. Further, the mutants 231/262D and 262/396D showed elevated SDS-resistant AGEs formation with respect to wild-type Tau. The study of glycation of pseudophosphorylated Tau by exposure to MG also reports formation of higher order aggregates on SDS-PAGE[96]. The pseudophosphorylation mutants did not reveal any global conformational changes. This has been previously reported for various sites of Tau pseudophosphorylation. Phosphorylation at T231 does not significantly alter Tau conformation. Phosphorylation at this residue leads to some local interactions of salt-bridge formation with surrounding residues but does not change the Tau conformation [246]. Similarly, phosphorylation at S262 induces turn formation and induces local rigidity in conformation but do not affect the global conformation of Tau. Moreover, phosphorylation at the C-terminal has been reported to induce flexibility in Tau[94]. Also, glycation did not alter this native conformation of Tau and its mutants. This might be attributed to the stable random coil conformation of these pseudophosphorylated residues. The morphological analysis revealed presence of amorphous MG-induced aggregates. Similar amorphous aggregates were also observed in Tau pseudophosphorylated mutants glycated by various reactive carbonyls including methyl glyoxal[96]. Glycation of Tau dementia mutants by methyl glyoxal is also being reported to form amorphous aggregates as opposed to heparin-induced fibrillar aggregates[247].
Thus, the study of glycation on with Tau bearing predisposition to pathological transition suggests that glycation can act as an enhancing factor to trigger the self-assembly and impart stabilize the aggregates by imparting resistance to detergents *via* excessive cross-linking.

6.2 Glycation-mediated cytoskeleton abnormalities and rescue by EGCG

One of the important causes of Tau pathology in AD is aberrant post-translational modification. As discussed above, hyperphosphorylation is the most prominent modification implicated in the pathogenesis of Tau. Accordingly, enormous reports are available for Tau hyperphosphorylation and its inhibition as a therapeutic strategy. Accordingly, kinase inhibitors[248] and phosphatase enhancers[249] are being studied, though, not quite successfully. As already discussed above, glycation severely disrupts the protein structure and associated functionality rendering them either prone to aggregation or increases their build up in the cells due to protease resistance. In AD, Tau glycation is present in the purified brain PHFs and dominant sites for glycation of Tau *in vitro* are confined to the repeat region which also serves as the microtubule-binding domain[79,80]. Glycation reduces microtubule-binding affinity of Tau and also induces cellular oxidative stress[81]. In spite of its deleterious impact on Tau, glycation as a therapeutic target is not yet studied. In our studies, we reported EGCG, a polyphenol isolated from green tea as a potent inhibitor of *in vitro* MG-induced Tau glycation. EGCG efficiently inhibited glycation of Tau treated with 5 fold excess of MG. Aminoguanidine, a known glycation inhibitor, inhibited Tau glycation with 2.5 fold excess of MG. EGCG was found to be more potent

which is likely due to its structure that helps trapping of carbonyls with a ratio of 3:1 (EGCG: carbonyls)[250]. Further, the effect of EGCG in inhibiting global glycation in neuroblastoma cells was studied and the results were positive with EGCG visibly inhibiting the MG-induced glycation. Additionally, EGCG also rescued the unique nuclear localization of phospho-Tau AT100, which was disrupted on MG exposure. A study has reported similar results wherein the intracellular AGEs formation induced by MG was inhibited in presence of aminoguanidine. Also, AG was reported to modulate the levels of Tau kinases GSK-3β and p38 MAPK and alter epitope-specific Tau hyperphosphorylation[251]. Effect of EGCG in modulating MG-induced AGEs in neuroblastoma cells can be attributed to its ROS quenching ability *via* Nrf2 pathway in different cell types[252]. As already known, EGCG quenches carbonyls hence this might be the same mechanism by which it might be inhibiting intracellular AGEs formation by MG. This suggested role of EGCG in modulating PTMs of Tau like phosphorylation and glycation as well opens new horizons to explore effect of EGCG on other Tau modifications.

In addition to Tau, glycation modifies the cellular proteins depending on the total concentration, which include abundant cytoskeletal proteins actin and tubulin. Modification of cytoskeletal proteins has a huge impact on neuronal cells, as these are polarized cells with specialized structures, which are maintained by the dynamicity of cytoskeletal proteins. Microtubules composed of tubulin subunits are known for their ability of guided organellar and membrane vesicular trafficking. Microtubules not only provide infrastructure for organellar movements but also acts a basis of fast axonal transport (FAT) in neuronal cells[253]. The organellar movement in neuronal cells can also take place independently of microtubules *via* actin through an ATP-dependent manner. This movement is unidirectional and postulated to be generated by myosin-like motor. This actin-dependent unidirectional organellar mobility also contributes to FAT in neuronal cells[254]. Our study demonstrated severe disruption of both actin and tubulin cytoskeletons in neuronal cells by MG exposure suggesting loss of neuronal functions. Moreover, tubulin glycation affects axonal transport in the rat model of diabetes[255]. Additionally, glycation modifies the lysine residues in the proteins which are required for assembly of tubulin into microtubules[256,257]. Further, assembly of actin into F-actin plays a crucial role in maintaining the spine morphology as well as density in neuronal cells, which is decreased by actin glycation[114,258]. These observations highlight role of glycation in severely affecting cytoskeletal structures and associated functions. We demonstrated role of EGCG in actively inhibiting the MG-induced glycation of actin and tubulin and restoring the neuronal morphology including the neuritic extensions and MTOC, thus, strengthening neuronal structural integrity which is essential in neuronal functioning (Fig. 6.2). EGCG, further stabilized microtubules by maintaining the interactions between end-binding protein (EB1) and microtubules which could be associated *via* Tau[259,260]. Analogous results have been reported for ADP-NAP peptide, which increases the Tau-EB1 interaction and restores Tau-mediated EB1 recruitment to the microtubule ends upon zinc intoxication. Tau has been known to interact with the end-bindings proteins EB1 and 3 and guide their localization to the ends of microtubules in extending neurites in developing neuronal cells. This interaction is postulated to fine tune the microtubule dynamics in neuronal differentiation.

This study highlights the need to focus Tau therapeutics towards modulating aberrant PTMs as well as to maintain the neuronal cytoskeletal structure and integrity.

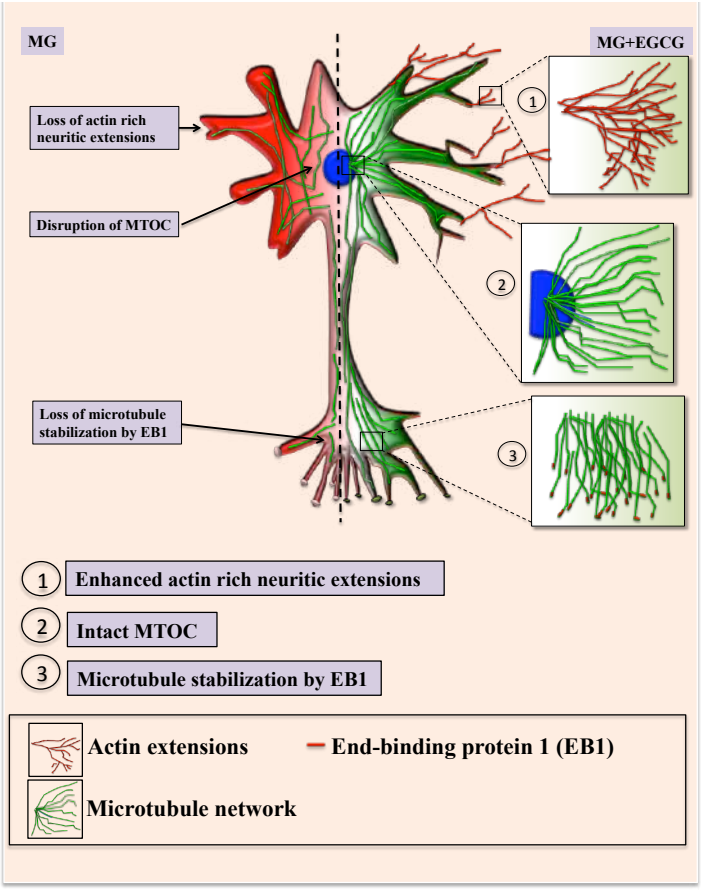

Figure 6.2. EGCG maintains neuronal cell cytoskeleton integrity. Methyl glyoxal treatment leads to glycation of actin and microtubules leading to hampered growth of neuritic extensions and microtubule organization. Microtubule stabilization by +TIP EB1 is also affected resulting in loss of cell morphology. In presence of EGCG, the actin rich neuritic extensions are enhanced which might help in neuronal connections. EGCG also maintains intact MTOC and thus microtubule mediated transport. EGCG also helps in microtubule polymerization *via* EB1 protein thus maintaining and rescuing overall cell integrity.

6.3 Small molecules inhibitors of Tau aggregation

The essence of inhibitors of Tau aggregation lies partly in the process of aggregation itself, as it's a continuous process once initiated. In order to have a potent inhibitor of Tau pathology, a molecule must possess multiple activities. For example, only inhibiting Tau from aggregation would be of little help as the already present aggregate load in the cells would still be hampering neuronal function and leading to the neuronal death. Also the intermediate Tau species like oligomers, which are reported to be extra toxic, also need to be quenched or sequestered and dissolved. Thus, a potent Tau aggregation inhibitor would inhibit Tau aggregation, sequester and degrade oligomers and dissolve preformed Tau fibrils. But in addition to be potent the most important characteristic required is the ability to cross the blood brain barrier. Thus, the charge, size and polarity also play a critical role. Since, Tau pathology is complex, higher dosages may be required which highlights importance of non-toxicity and biocompatibility at generous dosages. Thus, the molecules belonging to the natural origin would be assumed safe as therapeutics though synthetic molecules are also found to be equally potent and non-toxic. We have studied 4 molecules belonging to natural origin, each of which acts at various and multiple steps of Tau aggregation process and modulated Tau pathology.

6.3.1 Baicalein-mediated Tau aggregation inhibition via off-pathway oligomerization

Baicalein is isolated from the root of Chinese herb *Scutellaria baicalensis Georgi* and is reported to overcome AD pathologies like ROS quenching and recovery from cognitive deficiency[203]. Our study

reports the inhibition of Tau aggregation by Baicalein with the IC_{50} of 27.8 μM. A study with similar observation has been reported for α-synuclein, which aggregates in dopaminergic neurons in Parkinson's disease[201]. The IC_{50} for Tau aggregation inhibition has been reported to be 2.7 μM but not with sufficient evidence. This results also prove that Baicalein acts at the initial stages of Tau aggregation like methylene blue, azaphilones, anthraquinones *etc*. In case of α-synuclein, Baicalein was found to enhance oligomer formation. This was evident in our ANS fluorescence studies where Baicalein induced oligomerization of Tau which was observed by increased ANS fluorescence in the initial kinetics. Tau oligomerization exposes hydrophobic patches in the protein, which acts as a binding site for ANS dye and its increased fluorescence[261]. Thus, Baicalein enhanced and sequestered Tau oligomers and inhibited their transition to PHFs. The transition of Tau from monomer to aggregates is accompanied by conformational change for random coil to β-sheet which was also observed in Baicalein stabilized Tau oligomers. Moreover, the Baicalein-induced α-synuclein oligomers also revealed same conformational pattern[262]. The characterization of Baicalein-induced Tau oligomers revealed SDS-resistant nature which is reported for various other polyphenols as well. For example, various polyphenols enhance SDS-resistant Aβ oligomerization which include nordihydroguaiaretic acid (NDGA), resveratrol, and myricetin[263]. A green tea polyphenol EGCG, forms SDS-stable Aβ oligomers through polar and non-polar interactions[264,265]. Concurrent observations were made for α-synuclein with dopamine inducing SDS and heat stable oligomers[266]. The oligomers induced by all these molecules were non-toxic and off-pathway which is in concordance with our study wherein Baicalein induced Tau oligomers were not toxic to neuronal cells. The dissolution of preformed Tau filaments by Baicalein in our study yielded broken and fragile Tau fragments which were similar to the broken Tau filaments observed on treatment with cinnamaldehyde[267]. Also Baicalein is reported to dissolve the similar α-synuclein filaments[201] suggesting a common mechanism of Baicalein in aggregation inhibition and fibril dissolution of amyloidogenic proteins. Baicalein is known to interact with proteins at specific residues. For example, it interacts with human serum albumin at Leu, Arg and Ala residues[268] whereas it modifies lysine residue of Aβ to Schiff's base and binds to tyrosine residue in Aβ[269]. To decipher the interacting sites of Tau with Baicalein, we employed *in silico* studies with repeat Tau (244-373) and Baicalein due to increased disordered nature of full-length Tau, which makes it impossible to model. Our *in silico* study revealed the interaction of both the protein and ligand and MD simulations confirmed the stability of the interaction. The nature of interaction was depicted primarily as hydrophobic which was followed by stabilization *via* water mediated hydrogen bonds. The simulation trajectory also suggested conformational changes in Tau on Baicalein binding which may be attributed to relative flexibility of C7-C4 bond of Baicalein. This agrees with the structure of Baicalein with two adjacent -OH groups with possible ability to modify Tau oligomers. Analogous observations have been made for other flavonoids with adjacent -OH groups[263]. Moreover, we reported covalent modification of repeat Tau by Baicalein suggesting that Baicalein belongs to a class of covalent inhibitors which include oleocanthal, cinnamaldehyde and asperbenzaldehyde[270,271]. The mechanism of these molecules vary though, with oleocanthal modifying ε-amino group of lysines forming imines and cinnamaldehyde and asperbenzaldehyde acting *via* nucleophilic attack of cysteine residues of Tau. On the contrary to both these mechanisms, Baicalein exerts an electrophilic attack *via* oxidation to quinone form[272]. Tau oligomers are reported to be toxic and cause membrane leakage in cells[273]. In contrast, Baicalein mediated Tau oligomers were non-toxic to neuronal cells. Correspondingly, Baicalein showed similar rescue of toxicity of α-synuclein oligomers[274].

Thus, we report Baicalein as a potent molecule since it acts at various stages of Tau aggregation and inhibits it with no toxic effects in the neuronal cells at moderate concentrations (Fig. 6.3.1)

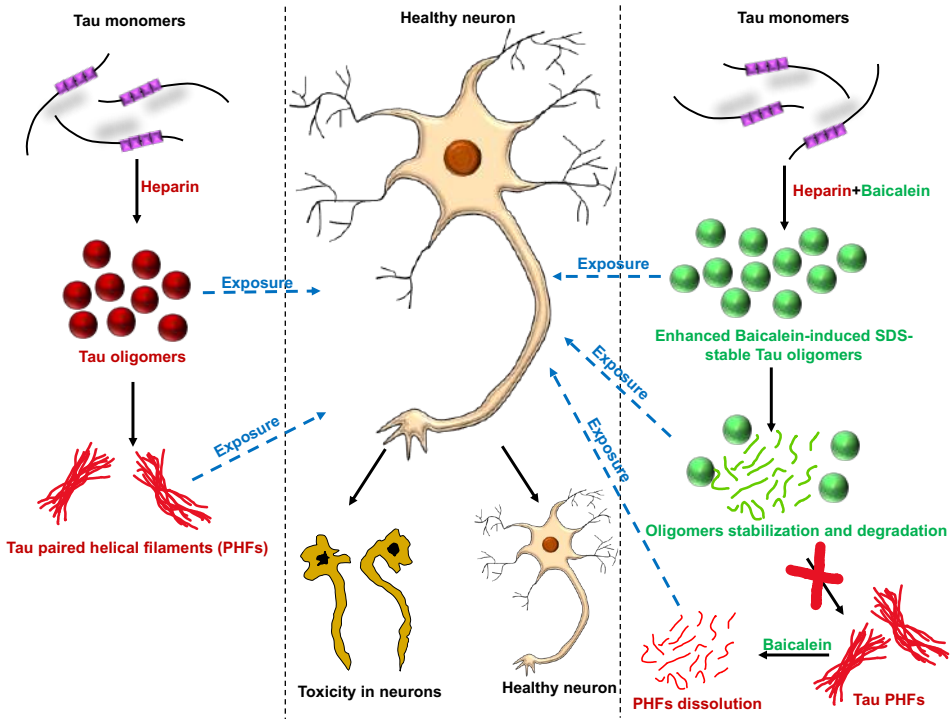

Figure 6.3.1. Dual effect of Baicalein on Tau. Tau in presence of heparin forms mature fibrils via intermediate oligomers formation. On the other hand, Tau in presence of Baicalein and heparin is restricted to form Tau oligomers without further mature fibril formation. These PHFs when exposed with Baicalein are dissolved into smaller fragments. The exposure of heparin-induced Tau oligomers and PHFs to healthy neuronal cells imparts toxicity in neurons and leads to neuronal death. The Baicalein-induced Tau oligomers as well as the dissolved fragments of PHFs do not affect the neuronal health and maintains the morphology. These suggest nontoxic nature of Baicalein-induced Tau oligomers.

6.3.2 Interaction of Epigallocatechin-3-gallate (EGCG) with Tau and its effect on Tau aggregation

EGCG is a famous molecule and has gained huge popularity owing to its multiple effects in plethora of diseases including neurodegenerative diseases. In case of Tau pathology, EGCG is found to inhibit the *in vitro* assembly of aggregation-prone repeat Tau fragment K18ΔK280. Moreover, EGCG was found to be ineffective in preventing heparin-induced assembly of this Tau fragment and aggregation led to the formation of morphologically distinct Tau filaments as compared to control Tau[207]. In our studies, we reported analogous effect of EGCG on the inhibition of heparin-induced assembly of full-length Tau with altered filament morphology. The IC_{50} for Tau aggregation inhibition was found to be 64.2 µM. This value seems to be higher as compared to other TAIs but several inhibitors show varied potency from nM to µM range. For example, molecules such as Thionine and Azure A display inhibitory constants of 98 nM and 108 nM respectively. On the other hand chlorpromazine and tacrine show inhibitory constants of 55.9 µM and more than 100 µM respectively[275]. Moreover the natural aglycone in extra virgin olive oil, oleocanthal, displays IC_{50} value of 2.9 µM and 3 µM for natural and unnatural origin of compound[271]. Thus, the IC_{50} value for EGCG falls on the higher side of the micromolar range which might be attributed to decreased lag phase of Tau aggregation on heparin induction, as the lag phase might be required for efficient interaction of EGCG with monomeric Tau. Due to shortened lag phase, EGCG is forced to bind to the intermediate Tau species, which require greater stoichiometric ratios for efficient inhibition of Tau assembly. The fact that EGCG interacts with monomeric Tau, is also evident from our MALDI-TOF analysis wherein EGCG covalently modifies repeat Tau which might be due to its reported activity in covalently modifying proteins at reduced Cys thiols. Moreover, the observation of higher order band in nitrobluetetrazolium (NBT) staining for Tau and EGCG from the previous studies explains the Tau modifying function of EGCG[207]. In order to gain further insights into the interaction of Tau and EGCG, docking and MD

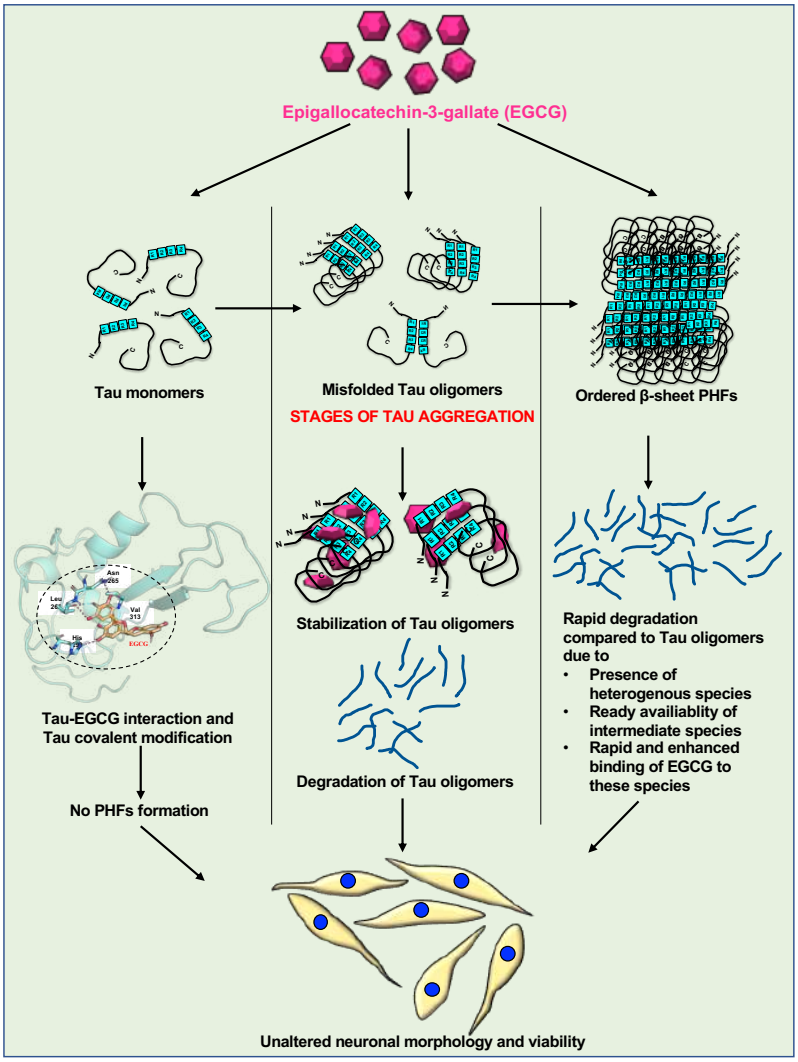

Figure 6.3.2. Effect of EGCG on varied Tau species. Broadly the aggregation process of Tau undergoes initial misfolded oligomer formation before maturing into ordered β-sheet PHFs. EGCG acts at every stage of Tau species and acts respective to the species present. In case of monomer, EGCG interacts at a binging pocket of Tau such that it leads to covalent modification of Tau. Moreover, this Tau is unable to transition into mature filaments and the EGCG-modified Tau does not affect the neuronal cells. With Tau oligomers, EGCG interacts to stabilize these oligomers and prevents them from further aggregation. Further, the stabilized oligomers are gradually degraded by EGCG. These degradation products are non-toxic to cells. EGCG rapidly degrades the mature fibrils as soon as they are treated. The dissolution of PHFs is relatively rapid to oligomers. All the degradation products do not alter the cells on exposure.

simulations were carried out for the complex. Here, repeat Tau was modelled due to difficulties in modelling the full-length Tau due to its increased disordered conformation. The docking of repeat Tau-EGCG complex yielded Leu and Asp as the major interacting residues which were similar to interacting residues of transthyretin complex[276]. Lys 267 was also shown to have major interaction with EGCG. This is in agreement with studies on EGCG and prostatic acid phosphatase (PAP) peptide, wherein lysine was found to be major contributor for interaction with EGCG and important for ligand-binding[277]. This suggests that though the number of interacting residues for EGCG with proteins vary the key interacting residues remain common for most proteins. Since, Tau-EGCG interaction was confirmed by above studies the quantification of the interaction was made by ITC studies. Although, the binding was observed to be strong, the results suggested multi-sites binding event for Tau and EGCG wherein initial binding is rapid and saturable. The equilibrium is attained after the early interaction events after which continuous association and dissociation of Tau-EGCG takes place. This is in agreement with two separate binding events occurring on EGCG-HSA interaction where initial strong binding is followed

by 1000 times weaker secondary binding. As for interaction with proteins[208]. EGCG is also postulated to act *via* a common mechanism to prevent aggregation in the aggregation prone proteins. EGCG is reported to bind with cross-beta structures in the amyloidogenic proteins and prevent its fibrillization[278]. We made similar observations wherein we visualized full-length Tau initial oligomerization in presence of EGCG on SDS-PAGE, which eventually decreased with incubation. On the contrary, the dissolution of preformed PHFs was relatively rapid. This might be due to readily available aggregation intermediated for rapid EGCG binding (Fig. 6.3.2).
Thus, the role of EGCG in inhibiting Tau aggregation and rapid dissolution of Tau PHFs highlights its potential as a strong therapeutic molecule in AD.

6.3.3 Effect of polyamines on Tau aggregation and cell apoptosis

Polyamines are ubiquitous molecules with multitude of functions. They participate in various cellular functions from gene expression to cell proliferation. In neurodegenerative diseases like AD and PD, polyamines levels are altered and this is reported to play a role in disease pathogenesis[279]. The *in vitro* analysis of aggregation prone proteins involved in AD and PD that is Aβ and α-synuclein respectively revealed enhanced aggregation in presence of polyamines[280,281]. In contrast to this, we reported the inhibitory action of polyamines spermine and spermidine on Tau aggregation at 100 - 500 μM concentrations. The mechanistic explanation for this inhibition was obtained from the fluorescence kinetics, which suggested increase in lag period of Tau aggregation in presence of polyamines with spermine showing more potency. These results were contrasting to the previous studies which reported decrease in lag time of aggregation prone proteins Aβ and α-synuclein on polyamine treatment which is attributed to their α helical content. In case of Tau, the same polyamines increased the lag period of aggregation thereby delaying the formation of nucleating species essential for aggregation to proceed. The NMR studies confirmed the physical interaction of polyamines with Tau similar interacting residues. The interaction revolved around the 5-histidine residues of Tau spanning along the 4 repeats. Similar type of interaction were reported for interaction of Aβ with polyamines[280]. Apart from interacting histidine residues the peak pattern did not change throughout the titrations, which suggests only local conformational changes in Tau on interaction with polyamines and intact global conformation. The stereo packing of Tau required for aggregation might be hindered on binding to polyamines which also accounts for the delay in aggregation and altered filament morphology. The NMR studies with α-synuclein suggest contrasting findings with polyamines driving the protein to β-sheet conformation[282]. Our analysis of global conformational changes of Tau in presence of polyamines re-iterated our NMR results wherein polyamines did not alter the protein conformation. Moreover, polyamines maintained the random coil conformation of Tau except for spermidine at lower concentrations. The CD analysis of Aβ and α-synuclein reported transitioning towards β-sheet in time-dependent manner on polyamine exposure. The visualization of filament morphology on polyamine treatment revealed short broken fibres without intact filamentous aggregates. Similar observations were made for Aβ and α-synuclein where they formed amorphous aggregates and lacked filamentous aggregates in presence of polyamines. The size-exclusion chromatography for polyamine treated and untreated Tau resolved into higher order species which had discreet properties. The polyamine treated Tau had reduced hydrophobicity and were less toxic as compared to control untreated Tau. Since polyamines are involved in various cellular pathways including apoptosis, we investigated their role in neuronal apoptosis. Both the polyamines were non-toxic at higher concentrations and reduced apoptosis, indicating a neuroprotective role. The caspase-3 activity analysis suggested spermidine helped decrease caspase-3 activity thus preventing apoptosis. This function of spermidine is reported and further involvement in autophagy *via* inhibition of Beclin-1 cleavage is also studied[283]. In addition to being involved in apoptosis, caspase-3 also acts to enhance Tau cleavage at C-terminal D421 giving

rise to truncated Tau which is prone to aggregation[284]. The D421 truncated Tau is found in AD brain and is known induce conformational changes in Tau, which drives it towards self-assembly[64]. Since, polyamines inhibited caspase-3 activity, they play dual role of preventing apoptosis as well pathological transition of Tau (Fig. 6.3.3).

Thus, polyamines inhibited Tau assembly by maintaining Tau in soluble form such that the nucleation phase and thus the aggregation is delayed. The mechanistic explanation of this was provided by NMR wherein the interacting residues of polyamines match with those of Tau and polyamines might be competing with heparin for binding to Tau thus preventing its aggregation.

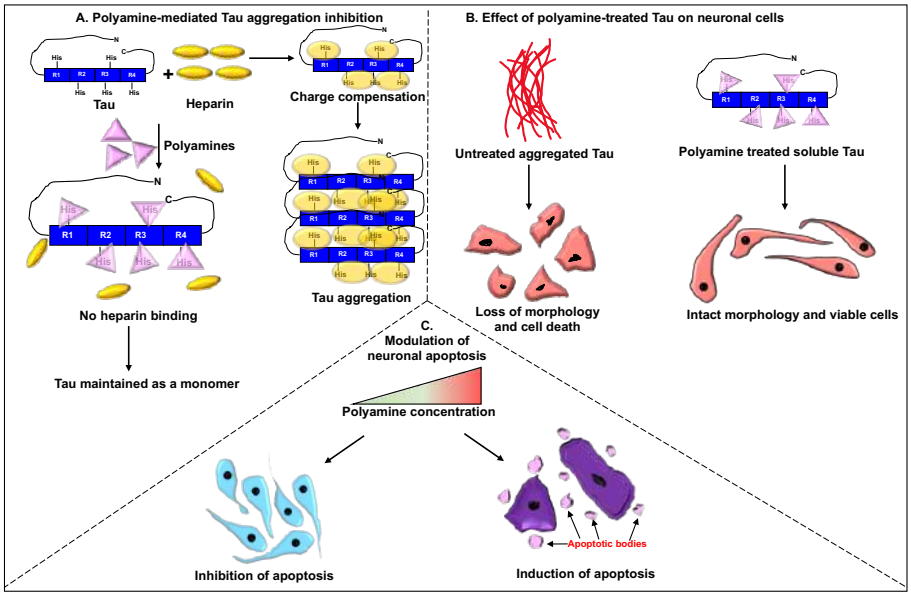

Figure 6.3.3. Multifunctionality of polyamines in AD pathologies. A) Heparin induces Tau aggregation via charge compensation with major interactions with histidine residues. Exposure of Tau together with heparin and polyamines prevents heparin binding due to the common sites of interactions of polyamines and heparin. The polyamine treated Tau maintains in soluble form and does not undergo fibrillization. B) The PHF Tau formed in presence of heparin alone proves to be harmful to cells as it alters the cell morphology and leads to death. On the contrary, polyamine treated soluble Tau does not hamper neuronal integrity and maintains the cell viability. C) Polyamines modulate neuronal apoptosis in a concentration dependent manner. At lower concentrations, polyamines inhibit apoptosis whereas at higher concentrations they induce apoptosis in neuronal cells.

Summary

The aggregation and accumulation of toxic Tau species is one of the paramount factors in the pathology of neurodegenerative diseases like AD, FTDP-17 related Tauopathies, Pick's disease *etc*. This not only increases the load on the cellular clearance machineries but also hampers vital neuronal functions like intracellular transport and synaptic transmission owing to disruption of the cytoskeleton. The neuronal cytoskeleton is of utmost importance as it maintains the specialized the cellular architecture essential for its functioning. The misfolding and aggregation of Tau results due to cellular insults, post-translational modifications and genetic mutations. We hypothesize that the Tau pathology is a result of cross-talk between these discreet factors and aimed our studies on the impact of two factors at a time on the Tau aggregation. The glycation of Tau was studied in presence of other PTMs as well as genetic mutations. Further the impact of small molecules was elucidated on the Tau PTMs, neuronal cytoskeletal architecture and *in vitro* aggregation inhibition. Our findings are summarized as follows:

Glycation modulates the aggregation propensity of mutant Tau proteins:
Glycation is one of the abnormal PTMs which severely disrupts protein rendering it structurally and functionally incompetent. The glycation of genetically predisposed Tau with FTDP-17 mutations by methyl glyoxal, exhibited increased propensity of aggregation as well enhanced formation of advanced glycation end products in the mutant P301L as compared to the wild type Tau. On the other hand, glycation of doubly pseudophosphorylated Tau did not alter the aggregation propensity but enhanced the AGEs formation with the pseudophosphorylation at 231, 262 and 396. Thus, the interplay of causal factors can modulate the Tau pathology exacerbating the disease manifestations.

EGCG rescues Tau glycation and glycation-induced neuronal cytoskeleton disruption:
Glycation modifies the proteins by irreversible cross-linking which enhances the aggregation and accumulation of the proteins in cellular milieu due to protease resistance of the aggregates. Tau glycation in AD is reported to impart stabilization to the paired helical filaments. These stable PHFs persist over the years leading to neuronal degeneration in AD. Thus, we targeted Tau glycation *in vitro* by EGCG which is an active polyphenol of green tea. EGCG prevented Tau glycation *in vitro* as well as inhibited MG-induced AGEs formation in the neuronal cells. EGCG enhanced the neuronal extensions as well as prevented the actin and tubulin glycation by MG thus, maintaining the neuronal cytoskeletal integrity. EGCG also maintained the tubulin-EB1 function aiding in the tubulin polymerization. The role of EGCG in preserving neuronal cytoskeleton is of utmost importance and highlights its potential as a future therapeutic in AD.

Small molecules Baicalein, EGCG and polyamines prevent in vitro Tau aggregation and dissolve the preformed aggregates via varied mechanisms:
The inhibition of Tau aggregation and dissolution of the PHFs is one of the highly explored area in the field of AD therapeutics. Accordingly, numerous molecules have been screened and tested for Tau pathology. We screened two polyphenols (Baicalein and EGCG) and two polyamines (Spermine and Spermidine) against Tau pathology *in vitro.* Baicalein, isolated from the root of herb *Scutellaria Baicalensis* inhibited the aggregation of full-length and repeat Tau by inducing the off-pathway oligomers and preventing filamentous aggregation. Baicalein efficiently dissolved the preformed Tau oligomers and fibrils highlighting dual potency in overcoming Tau pathology in AD. The hydrophobic and the water bridges dominated the Tau-Baicalein interactions which are postulated for its disaggregation activity. On the other hand, EGCG, a green tea polyphenol showed dynamic electrostatic and hydrophobic interactions in the Tau-EGCG complex. The residue-specific interactions in addition to ion-mediated and water-mediated bonding play a crucial role in maintaining the Tau-EGCG complex. EGCG inhibited Tau aggregation in a concentration-dependent manner. The dissolution of PHFs was more prominent as compared to preformed oligomers probably due to readily available intermediate species required for EGCG binding. Both the polyphenols exhibited covalent modification of Tau explaining their role in inhibiting filamentous Tau aggregation. Alternatively, polyamines, Spermine and Spermidine inhibited Tau aggregation by increasing the lag period of Tau aggregation and maintaining Tau in the soluble form. The NMR studies revealed a potent mechanism of interfering heparin binding to Tau thus, preventing its assembly. Polyamine treated Tau did not induce toxicity in the neuronal cells and maintained their morphology. Polyamines modulated neuronal apoptosis in a concentration dependent manner.

Thus, the work conducted comprises the study of effect causal factors of Tau pathology and attempts to modulate these factors in order to prevent Tau and related neuronal pathologies. The study has unraveled multifaceted roles of polyphenols and polyamines making them potent candidates for future therapeutic applications in AD-related pathologies.

Future Directions

Our studies underline the impact of PTMs on Tau pathology and thus the further investigations of modified Tau would help understanding the role of modified in neuronal functions. In accordance with this view the future direction of study would focus on the effect of glycated Tau on the neuronal cells (Fig. I).

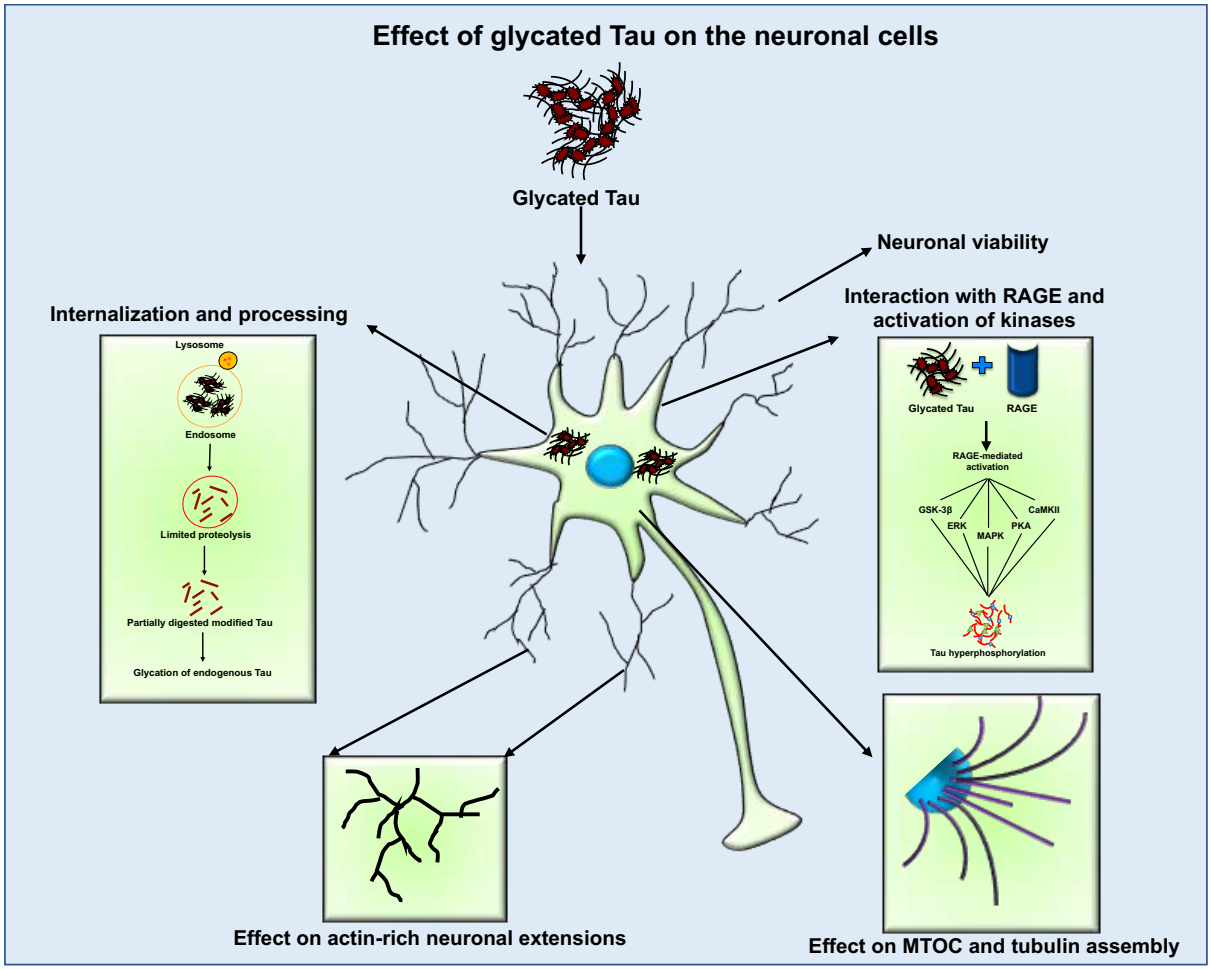

Fig I. The effect of glycated Tau on neuronal cells. The glycated Tau would be assessed for the toxicity to the neurons. The glycated proteins (AGEs) interact with their receptor RAGE, which activates several kinases. These kinases mediate Tau hyperphosphorylation adding to the pathology. The internalization of glycated by bulk endocytosis would initiate its lysosomal degradation. This might be lead to the limited degradation due to nature of glycation and release partially digested peptides which would act as seeds to aggregate endogenous Tau. Glycated Tau could affect the actin and tubulin cytoskeletons affecting the neuronal extensions and MTOC-mediated tubulin assembly.

The glycated Tau would be studied for its effects on various neuronal parameters:

I. Neuronal viability
II. The glycated Tau would be studied for its interaction with RAGE and other scavenger receptors by various interaction techniques
III. The RAGE activation leads to activation of various kinases which are also involved in Tau hyperphosphorylation. Thus, effect of glycated Tau on inducing Tau hyperphosphorylation would be addressed
IV. The internalization of glycated Tau and its endosomal processing would aid in understanding the seeding behavior of glycated Tau.
V. Since, Tau is largely associated with the actin and tubulin cytoskeleton maintenance in neurons, the effect of glycated Tau on these cytoskeletal elements would be deciphered.

References

1 Dugger, B. N. & Dickson, D. W. Pathology of neurodegenerative diseases. *Cold Spring Harbor perspectives in biology* **9**, a028035 (2017).

2 Goedert, M., Masuda-Suzukake, M. & Falcon, B. Like prions: the propagation of aggregated tau and α-synuclein in neurodegeneration. *Brain* **140**, 266-278 (2017).

3 Clavaguera, F., Hench, J., Goedert, M. & Tolnay, M. Invited review: Prion-like transmission and spreading of tau pathology. *Neuropathology and applied neurobiology* **41**, 47-58 (2015).

4 Association, A. s. 2019 Alzheimer's disease facts and figures. *Alzheimer's & Dementia* **15**, 321-387 (2019).

5 Anand, K. S. & Dhikav, V. Hippocampus in health and disease: An overview. *Annals of Indian Academy of Neurology* **15**, 239 (2012).

6 Braak, H. & Braak, E. Neuropathological stageing of Alzheimer-related changes. *Acta neuropathologica* **82**, 239-259 (1991).

7 Tiwari, M. K. & Kepp, K. P. β-Amyloid pathogenesis: Chemical properties versus cellular levels. *Alzheimer's & Dementia* **12**, 184-194 (2016).

8 Selkoe, D. J. Alzheimer's Disease--Genotypes, Phenotype, and Treatments. *Science* **275**, 630-631 (1997).

9 Hardy, J. A. & Higgins, G. A. Alzheimer's disease: the amyloid cascade hypothesis. *Science* **256**, 184-186 (1992).

10 Mandelkow, E.-M. & Mandelkow, E. Tau in Alzheimer's disease. *Trends in cell biology* **8**, 425-427 (1998).

11 Cleveland, D. W., Hwo, S.-Y. & Kirschner, M. W. Purification of tau, a microtubule-associated protein that induces assembly of microtubules from purified tubulin. *Journal of molecular biology* **116**, 207-225 (1977).

12 Weingarten, M. D., Lockwood, A. H., Hwo, S.-Y. & Kirschner, M. W. A protein factor essential for microtubule assembly. *Proceedings of the National Academy of Sciences* **72**, 1858-1862 (1975).

13 Cleveland, D. W., Hwo, S.-Y. & Kirschner, M. W. Physical and chemical properties of purified tau factor and the role of tau in microtubule assembly. *Journal of molecular biology* **116**, 227-247 (1977).

14 Grundke-Iqbal, I. *et al.* Abnormal phosphorylation of the microtubule-associated protein tau (tau) in Alzheimer cytoskeletal pathology. *Proceedings of the National Academy of Sciences* **83**, 4913-4917 (1986).

15 Goedert, M., Spillantini, M., Potier, M., Ulrich, J. & Crowther, R. Cloning and sequencing of the cDNA encoding an isoform of microtubule-associated protein tau containing four tandem repeats: differential expression of tau protein mRNAs in human brain. *The EMBO journal* **8**, 393-399 (1989).

16 McKibben, K. & Rhoades, E. N-terminal Inserts Impact the Global Conformation of Tau and the Tau-Tubulin Complex. *Biophysical Journal* **114**, 508a (2018).

17 Goedert, M., Spillantini, M., Jakes, R., Rutherford, D. & Crowther, R. Multiple isoforms of human microtubule-associated protein tau: sequences and localization in neurofibrillary tangles of Alzheimer's disease. *Neuron* **3**, 519-526 (1989).

18 Kadavath, H. *et al.* Tau stabilizes microtubules by binding at the interface between tubulin heterodimers. *Proceedings of the National Academy of Sciences* **112**, 7501-7506 (2015).

19 Mukrasch, M. D. *et al.* The “jaws” of the tau-microtubule interaction. *Journal of Biological Chemistry* **282**, 12230-12239 (2007).

20 Friedhoff, P., Von Bergen, M., Mandelkow, E.-M., Davies, P. & Mandelkow, E. A nucleated assembly mechanism of Alzheimer paired helical filaments. *Proceedings of the National Academy of Sciences* **95**, 15712-15717 (1998).

21 Eliezer, D. *et al.* Residual structure in the repeat domain of tau: echoes of microtubule binding and paired helical filament formation. *Biochemistry* **44**, 1026-1036 (2005).

22 Sadqi, M. *et al.* α-Helix structure in Alzheimer's disease aggregates of tau-protein. *Biochemistry* **41**, 7150-7155 (2002).

23 Jeganathan, S., von Bergen, M., Brutlach, H., Steinhoff, H.-J. & Mandelkow, E. Global hairpin folding of tau in solution. *Biochemistry* **45**, 2283-2293 (2006).

24 Von Bergen, M., Barghorn, S., Biernat, J., Mandelkow, E.-M. & Mandelkow, E. Tau aggregation is driven by a transition from random coil to beta sheet structure. *Biochimica et Biophysica Acta (BBA)-Molecular Basis of Disease* **1739**, 158-166 (2005).

25 Eschmann, N. A. *et al.* Signature of an aggregation-prone conformation of tau. *Scientific Reports* **7**, 44739 (2017).

26 Alonso, A. d. C., Zaidi, T., Novak, M., Grundke-Iqbal, I. & Iqbal, K. Hyperphosphorylation induces self-assembly of τ into tangles of paired helical filaments/straight filaments. *Proceedings of the National Academy of Sciences* **98**, 6923-6928 (2001).

27 Alonso, A. d. C., Grundke-Iqbal, I. & Iqbal, K. Alzheimer's disease hyperphosphorylated tau sequesters normal tau into tangles of filaments and disassembles microtubules. *Nature medicine* **2**, 783-787 (1996).

28 Gordon-Krajcer, W., Yang, L.-S. & Ksiezak-Reding, H. Conformation of paired helical filaments blocks dephosphorylation of epitopes shared with fetal tau except Ser199/202 and Ser202/Thr205. *Brain research* **856**, 163-175 (2000).

29 Englund, B. *et al.* Clinical and neuropathological criteria for frontotemporal dementia. *J Neurol Neurosurg Psychiatry* **57**, 416-418 (1994).

30 Spillantini, M. G., Bird, T. D. & Ghetti, B. Frontotemporal dementia and Parkinsonism linked to chromosome 17: a new group of tauopathies. *Brain pathology* **8**, 387-402 (1998).

31 Hutton, M. *et al.* Association of missense and 5′-splice-site mutations in tau with the inherited dementia FTDP-17. *Nature* **393**, 702-705 (1998).

32 Spillantini, M. G. *et al.* Familial multiple system tauopathy with presenile dementia: a disease with abundant neuronal and glial tau filaments. *Proceedings of the National Academy of Sciences* **94**, 4113-4118 (1997).

33 Spillantini, M. G. *et al.* Mutation in the tau gene in familial multiple system tauopathy with presenile dementia. *Proceedings of the National Academy of Sciences* **95**, 7737-7741 (1998).

34 LeBoeuf, A. C. *et al.* FTDP-17 Mutations in Tau Alter the Regulation of Microtubule Dynamics AN “ALTERNATIVE CORE” MODEL FOR NORMAL AND PATHOLOGICAL TAU ACTION. *Journal of Biological Chemistry* **283**, 36406-36415 (2008).

35 Nacharaju, P. *et al.* Accelerated filament formation from tau protein with specific FTDP-17 missense mutations. *FEBS letters* **447**, 195-199 (1999).

36 Combs, B. & Gamblin, T. C. FTDP-17 tau mutations induce distinct effects on aggregation and microtubule interactions. *Biochemistry* **51**, 8597-8607 (2012).

37 Bird, T. D. in *GeneReviews®[Internet]* (University of Washington, Seattle, 2018).

38 Mendez, M. F. Early-onset Alzheimer disease. *Neurologic clinics* **35**, 263-281 (2017).

39 Di Primio, C. *et al.* The distance between N and C termini of tau and of FTDP-17 mutants is modulated by microtubule interactions in living cells. *Frontiers in Molecular Neuroscience* **10**, 210 (2017).

40 Köpke, E. *et al.* Microtubule-associated protein tau. Abnormal phosphorylation of a non-paired helical filament pool in Alzheimer disease. *Journal of Biological Chemistry* **268**, 24374-24384 (1993).

41 Biernat, J. *et al.* The switch of tau protein to an Alzheimer-like state includes the phosphorylation of two serine-proline motifs upstream of the microtubule binding region. *The EMBO journal* **11**, 1593-1597 (1992).

42 Goedert, M. *et al.* Epitope mapping of monoclonal antibodies to the paired helical filaments of Alzheimer's disease: identification of phosphorylation sites in tau protein. *Biochemical Journal* **301**, 871-877 (1994).

43 Steinhilb, M. L., Dias-Santagata, D., Fulga, T. A., Felch, D. L. & Feany, M. B. Tau phosphorylation sites work in concert to promote neurotoxicity in vivo. *Molecular biology of the cell* **18**, 5060-5068 (2007).

44 Drewes, G. *et al.* Microtubule-associated protein/microtubule affinity-regulating kinase (p110mark) a novel protein kinase that regulates tau-microtubule interactions and dynamic instability by phosphorylation at the Alzheimer-specific site serine 262. *Journal of Biological Chemistry* **270**, 7679-7688 (1995).

45 Alonso, A. D. *et al.* Phosphorylation of tau at Thr212, Thr231, and Ser262 combined causes neurodegeneration. *Journal of Biological Chemistry* **285**, 30851-30860 (2010).

46 Liu, F. *et al.* Site-specific effects of tau phosphorylation on its microtubule assembly activity and self-aggregation. *European Journal of Neuroscience* **26**, 3429-3436 (2007).

47 Liu, S. J. *et al.* Tau becomes a more favorable substrate for GSK-3 when it is prephosphorylated by PKA in rat brain. *Journal of Biological Chemistry* **279**, 50078-50088 (2004).

48 Lu, P.-J., Wulf, G., Zhou, X. Z., Davies, P. & Lu, K. P. The prolyl isomerase Pin1 restores the function of Alzheimer-associated phosphorylated tau protein. *Nature* **399**, 784-788 (1999).

49 Bulbarelli, A., Lonati, E., Cazzaniga, E., Gregori, M. & Masserini, M. Pin1 affects Tau phosphorylation in response to Aβ oligomers. *Molecular and Cellular Neuroscience* **42**, 75-80 (2009).

50 Xu, L., Zheng, J., Margittai, M., Nussinov, R. & Ma, B. How does hyperphopsphorylation promote tau aggregation and modulate filament structure and stability? *ACS Chemical Neuroscience* **7**, 565-575 (2016).

51 Cripps, D. *et al.* Alzheimer disease-specific conformation of hyperphosphorylated paired helical filament-Tau is polyubiquitinated through Lys-48, Lys-11, and Lys-6 ubiquitin conjugation. *Journal of Biological Chemistry* **281**, 10825-10838 (2006).

52 Petrucelli, L. *et al.* CHIP and Hsp70 regulate tau ubiquitination, degradation and aggregation. *Human molecular genetics* **13**, 703-714 (2004).

53 Zhang, Y.-J. *et al.* Carboxyl terminus of heat-shock cognate 70-interacting protein degrades tau regardless its phosphorylation status without affecting the spatial memory of the rats. *Journal of Neural Transmission* **115**, 483-491 (2008).

54 Shimura, H., Schwartz, D., Gygi, S. P. & Kosik, K. S. CHIP-Hsc70 complex ubiquitinates phosphorylated tau and enhances cell survival. *Journal of Biological Chemistry* **279**, 4869-4876 (2004).

55 Sahara, N. *et al.* In vivo evidence of CHIP up-regulation attenuating tau aggregation. *Journal of neurochemistry* **94**, 1254-1263 (2005).

56 Min, S.-W. *et al.* Acetylation of tau inhibits its degradation and contributes to tauopathy. *Neuron* **67**, 953-966 (2010).

57 Cohen, T. J. *et al.* The acetylation of tau inhibits its function and promotes pathological tau aggregation. *Nature communications* **2**, 1-9 (2011).

58 Irwin, D. J. *et al.* Acetylated tau, a novel pathological signature in Alzheimer's disease and other tauopathies. *Brain* **135**, 807-818 (2012).

59 Gorsky, M. K., Burnouf, S., Dols, J., Mandelkow, E. & Partridge, L. Acetylation mimic of lysine 280 exacerbates human Tau neurotoxicity in vivo. *Scientific reports* **6**, 1-12 (2016).

60 Sohn, P. D. *et al.* Acetylated tau destabilizes the cytoskeleton in the axon initial segment and is mislocalized to the somatodendritic compartment. *Molecular neurodegeneration* **11**, 47 (2016).

61 Min, S.-W. *et al.* Critical role of acetylation in tau-mediated neurodegeneration and cognitive deficits. *Nature medicine* **21**, 1154-1162 (2015).

62 Thomas, S. N. *et al.* Dual modification of Alzheimer's disease PHF-tau protein by lysine methylation and ubiquitylation: a mass spectrometry approach. *Acta neuropathologica* **123**, 105-117 (2012).

63 Morris, M. *et al.* Tau post-translational modifications in wild-type and human amyloid precursor protein transgenic mice. *Nature neuroscience* **18**, 1183-1189 (2015).

64 Gamblin, T. C. *et al.* Caspase cleavage of tau: linking amyloid and neurofibrillary tangles in Alzheimer's disease. *Proceedings of the national academy of sciences* **100**, 10032-10037 (2003).

65 Johnson, G. V., Jope, R. S. & Binder, L. I. Proteolysis of tau by calpain. *Biochemical and biophysical research communications* **163**, 1505-1511 (1989).

66 Arai, T., Guo, J.-P. & McGeer, P. L. Proteolysis of non-phosphorylated and phosphorylated tau by thrombin. *Journal of Biological Chemistry* **280**, 5145-5153 (2005).

67 Chung, C.-W. *et al.* Proapoptotic effects of tau cleavage product generated by caspase-3. *Neurobiology of disease* **8**, 162-172 (2001).

68 Fasulo, L. *et al.* The neuronal microtubule-associated protein tau is a substrate for caspase-3 and an effector of apoptosis. *Journal of neurochemistry* **75**, 624-633 (2000).

69 Rissman, R. A. *et al.* Caspase-cleavage of tau is an early event in Alzheimer disease tangle pathology. *The Journal of clinical investigation* **114**, 121-130 (2004).

70 Garcia-Sierra, F., Mondragon-Rodriguez, S. & Basurto-Islas, G. Truncation of tau protein and its pathological significance in Alzheimer's disease. *Journal of Alzheimer's Disease* **14**, 401-409 (2008).

71 Abraha, A. *et al.* C-terminal inhibition of tau assembly in vitro and in Alzheimer's disease. *Journal of cell science* **113**, 3737-3745 (2000).

72 Amadoro, G., Latina, V., Corsetti, V. & Calissano, P. N-terminal tau truncation in the pathogenesis of Alzheimer's disease (AD): Developing a novel diagnostic and therapeutic approach. *Biochimica et Biophysica Acta (BBA)-Molecular Basis of Disease* **1866**, 165584 (2020).

73 Šoškić, V., Groebe, K. & Schrattenholz, A. Nonenzymatic posttranslational protein modifications in ageing. *Experimental gerontology* **43**, 247-257 (2008).

74 Monnier, V. *et al.* Structure of advanced Maillard reaction products and their pathological role. *Nephrology Dialysis Transplantation* **11**, 20-26 (1996).

75 Singh, V. P., Bali, A., Singh, N. & Jaggi, A. S. Advanced glycation end products and diabetic complications. *The Korean Journal of Physiology & Pharmacology* **18**, 1-14 (2014).

76 Smith, M. A. *et al.* Advanced Maillard reaction end products are associated with Alzheimer disease pathology. *Proceedings of the National Academy of Sciences* **91**, 5710-5714 (1994).

77 Vitek, M. P. *et al.* Advanced glycation end products contribute to amyloidosis in Alzheimer disease. *Proceedings of the National Academy of Sciences* **91**, 4766-4770 (1994).

78 Ledesma, M. D., Bonay, P., Colaco, C. & Avila, J. Analysis of microtubule-associated protein tau glycation in paired helical filaments. *Journal of Biological Chemistry* **269**, 21614-21619 (1994).

79 Ledesma, M. D., Bonay, P. & Avila, J. τ Protein from Alzheimer's disease patients is glycated at its tubulin-binding domain. *Journal of neurochemistry* **65**, 1658-1664 (1995).

80 Nacharaju, P., Ko, L. w. & Yen, S. H. C. Characterization of in vitro glycation sites of tau. *Journal of neurochemistry* **69**, 1709-1719 (1997).

81 Yan, S. *et al.* Glycated tau protein in Alzheimer disease: a mechanism for induction of oxidant stress. *Proceedings of the National Academy of Sciences* **91**, 7787-7791 (1994).

82 Necula, M. & Kuret, J. Pseudophosphorylation and glycation of tau protein enhance but do not trigger fibrillization in vitro. *Journal of Biological Chemistry* **279**, 49694-49703 (2004).

83 Liu, K. *et al.* Glycation alter the process of Tau phosphorylation to change Tau isoforms aggregation property. *Biochimica et Biophysica Acta (BBA)-Molecular Basis of Disease* **1862**, 192-201 (2016).

84 Ko, S.-Y. *et al.* The possible mechanism of advanced glycation end products (AGEs) for Alzheimer's disease. *PLoS One* **10**, e0143345 (2015).

85 Wan, W., Chen, H. & Li, Y. The potential mechanisms of Aβ-receptor for advanced glycation end-products interaction disrupting tight junctions of the blood-brain barrier in Alzheimer's disease. *International Journal of Neuroscience* **124**, 75-81 (2014).

86 Kook, S.-Y., Seok Hong, H., Moon, M. & Mook-Jung, I. Disruption of blood-brain barrier in Alzheimer disease pathogenesis. *Tissue barriers* **1**, 8845-8854 (2013).

87 Cai, Z. *et al.* Role of RAGE in Alzheimer's disease. *Cellular and molecular neurobiology* **36**, 483-495 (2016).

88 Origlia, N., Arancio, O., Domenici, L. & Yan, S. S. MAPK, β-amyloid and synaptic dysfunction: the role of RAGE. *Expert review of neurotherapeutics* **9**, 1635-1645 (2009).

89 Eidenmüller, J. *et al.* Phosphorylation-mimicking glutamate clusters in the proline-rich region are sufficient to simulate the functional deficiencies of hyperphosphorylated tau protein. *Biochemical Journal* **357**, 759-767 (2001).

90 Léger, J., Kempf, M., Lee, G. & Brandt, R. Conversion of serine to aspartate imitates phosphorylation-induced changes in the structure and function of microtubule-associated protein tau. *Journal of Biological Chemistry* **272**, 8441-8446 (1997).

91 Rankin, C. A., Sun, Q. & Gamblin, T. C. Pseudo-phosphorylation of tau at Ser202 and Thr205 affects tau filament formation. *Molecular Brain Research* **138**, 84-93 (2005).

92 Chang, E., Kim, S., Schafer, K. N. & Kuret, J. Pseudophosphorylation of tau protein directly modulates its aggregation kinetics. *Biochimica et Biophysica Acta (BBA)-Proteins and Proteomics* **1814**, 388-395 (2011).

93 Kiris, E. *et al.* Combinatorial Tau Pseudophosphorylation MARKEDLY DIFFERENT REGULATORY EFFECTS ON MICROTUBULE ASSEMBLY AND DYNAMIC INSTABILITY THAN THE SUM OF THE INDIVIDUAL PARTS. *Journal of Biological Chemistry* **286**, 14257-14270 (2011).

94 Fischer, D. *et al.* Conformational changes specific for pseudophosphorylation at serine 262 selectively impair binding of tau to microtubules. *Biochemistry* **48**, 10047-10055 (2009).

95 Haj-Yahya, M. *et al.* Site-Specific Hyperphosphorylation Inhibits, Rather than Promotes, Tau Fibrillization, Seeding Capacity, and Its Microtubule Binding. *Angewandte Chemie* **132**, 4088-4096 (2020).

96 Kuhla, B. *et al.* Effect of pseudophosphorylation and cross-linking by lipid peroxidation and advanced glycation end product precursors on tau aggregation and filament formation. *Journal of Biological Chemistry* **282**, 6984-6991 (2007).

97 Frost, B., Jacks, R. L. & Diamond, M. I. Propagation of tau misfolding from the outside to the inside of a cell. *Journal of Biological Chemistry* **284**, 12845-12852 (2009).

98 Clavaguera, F. *et al.* Transmission and spreading of tauopathy in transgenic mouse brain. *Nature cell biology* **11**, 909-913 (2009).

99 Holmes, B. B. *et al.* Heparan sulfate proteoglycans mediate internalization and propagation of specific proteopathic seeds. *Proceedings of the National Academy of Sciences* **110**, E3138-E3147 (2013).

100 Abounit, S., Wu, J. W., Duff, K., Victoria, G. S. & Zurzolo, C. Tunneling nanotubes: a possible highway in the spreading of tau and other prion-like proteins in neurodegenerative diseases. *Prion* **10**, 344-351 (2016).

101 Wu, J. W. *et al.* Neuronal activity enhances tau propagation and tau pathology in vivo. *Nature neuroscience* **19**, 1085-1092 (2016).

102 Sanders, D. W. *et al.* Distinct tau prion strains propagate in cells and mice and define different tauopathies. *Neuron* **82**, 1271-1288 (2014).

103 Falcon, B. *et al.* Conformation determines the seeding potencies of native and recombinant Tau aggregates. *Journal of biological chemistry* **290**, 1049-1065 (2015).

104 Lasagna-Reeves, C. A. *et al.* Alzheimer brain-derived tau oligomers propagate pathology from endogenous tau. *Scientific reports* **2**, 700 (2012).

105 Calafate, S. *et al.* Synaptic contacts enhance cell-to-cell tau pathology propagation. *Cell reports* **11**, 1176-1183 (2015).

106 Wu, J. W. *et al.* Small misfolded Tau species are internalized via bulk endocytosis and anterogradely and retrogradely transported in neurons. *Journal of Biological Chemistry* **288**, 1856-1870 (2013).

107 Mirbaha, H., Holmes, B. B., Sanders, D. W., Bieschke, J. & Diamond, M. I. Tau trimers are the minimal propagation unit spontaneously internalized to seed intracellular aggregation. *Journal of biological chemistry* **290**, 14893-14903 (2015).

108 Calafate, S., Flavin, W., Verstreken, P. & Moechars, D. Loss of Bin1 promotes the propagation of tau pathology. *Cell reports* **17**, 931-940 (2016).

109 Wegmann, S., Nicholls, S., Takeda, S., Fan, Z. & Hyman, B. T. Formation, release, and internalization of stable tau oligomers in cells. *Journal of neurochemistry* **139**, 1163-1174 (2016).

110 Congdon, E. E., Gu, J., Sait, H. B. & Sigurdsson, E. M. Antibody uptake into neurons occurs primarily via clathrin-dependent Fcγ receptor endocytosis and is a prerequisite for acute tau protein clearance. *Journal of Biological Chemistry* **288**, 35452-35465 (2013).

111 Boluda, S. *et al.* Differential induction and spread of tau pathology in young PS19 tau transgenic mice following intracerebral injections of pathological tau from Alzheimer's disease or corticobasal degeneration brains. *Acta neuropathologica* **129**, 221-237 (2015).

112 Sonawane, S. K. & Chinnathambi, S. Prion-like propagation of post-translationally modified tau in Alzheimer's disease: a hypothesis. *Journal of Molecular Neuroscience* **65**, 480-490 (2018).

113 Costa, A. R., Pinto-Costa, R., Sousa, S. C. & Sousa, M. M. The regulation of axon diameter: from axonal circumferential contractility to activity-dependent axon swelling. *Frontiers in Molecular Neuroscience* **11**, 319 (2018).

114 Basu, S. & Lamprecht, R. The role of actin cytoskeleton in dendritic spines in the maintenance of long-term memory. *Frontiers in molecular neuroscience* **11**, 143 (2018).

115 Elie, A. *et al.* Tau co-organizes dynamic microtubule and actin networks. *Scientific reports* **5**, 9964 (2015).

116 Fontela, Y. C. *et al.* Multivalent cross-linking of actin filaments and microtubules through the microtubule-associated protein Tau. *Nature communications* **8**, 1-12 (2017).

117 Braak, F., Braak, H. & Mandelkow, E.-M. A sequence of cytoskeleton changes related to the formation of neurofibrillary tangles and neuropil threads. *Acta neuropathologica* **87**, 554-567 (1994).

118 Fulga, T. A. *et al.* Abnormal bundling and accumulation of F-actin mediates tau-induced neuronal degeneration in vivo. *Nat Cell Biol* **9**, 139-148, doi:10.1038/ncb1528 (2007).

119 Bamburg, J. R. & Bernstein, B. W. Roles of ADF/cofilin in actin polymerization and beyond. *F1000 biology reports* **2** (2010).

120 Bernstein, B. W., Shaw, A. E., Minamide, L. S., Pak, C. W. & Bamburg, J. R. Incorporation of cofilin into rods depends on disulfide intermolecular bonds: implications for actin regulation and neurodegenerative disease. *Journal of Neuroscience* **32**, 6670-6681 (2012).

121 Bamburg, J. *et al.* ADF/Cofilin-actin rods in neurodegenerative diseases. *Current Alzheimer Research* **7**, 241-250 (2010).

122 Hirano, A. Hirano bodies and related neuronal inclusions. *Neuropathology and applied neurobiology* **20**, 3-11 (1994).

123 Bardai, F. H. *et al.* A conserved cytoskeletal signaling cascade mediates neurotoxicity of FTDP-17 tau mutations in vivo. *Journal of Neuroscience* **38**, 108-119 (2018).

124 Lowery, L. A. & Van Vactor, D. The trip of the tip: understanding the growth cone machinery. *Nature reviews Molecular cell biology* **10**, 332-343 (2009).

125 Schaefer, A. W., Kabir, N. & Forscher, P. Filopodia and actin arcs guide the assembly and transport of two populations of microtubules with unique dynamic parameters in neuronal growth cones. *The Journal of cell biology* **158**, 139-152 (2002).

126 Biswas, S. & Kalil, K. The microtubule-associated protein tau mediates the organization of microtubules and their dynamic exploration of actin-rich lamellipodia and filopodia of cortical growth cones. *Journal of Neuroscience* **38**, 291-307 (2018).

127 Chen, Q. *et al.* Tau protein is involved in morphological plasticity in hippocampal neurons in response to BDNF. *Neurochemistry international* **60**, 233-242 (2012).

128 Leugers, C. J. & Lee, G. Tau potentiates nerve growth factor-induced mitogen-activated protein kinase signaling and neurite initiation without a requirement for microtubule binding. *Journal of Biological Chemistry* **285**, 19125-19134 (2010).

129 Sharma, V. M., Litersky, J. M., Bhaskar, K. & Lee, G. Tau impacts on growth-factor-stimulated actin remodeling. *Journal of cell science* **120**, 748-757 (2007).

130 Utton, M. A., Noble, W. J., Hill, J. E., Anderton, B. H. & Hanger, D. P. Molecular motors implicated in the axonal transport of tau and α-synuclein. *Journal of cell science* **118**, 4645-4654 (2005).

131 Cuchillo-Ibanez, I. *et al.* Phosphorylation of tau regulates its axonal transport by controlling its binding to kinesin. *The FASEB Journal* **22**, 3186-3195 (2008).

132 Stamer, K., Vogel, R., Thies, E., Mandelkow, E. & Mandelkow, E.-M. Tau blocks traffic of organelles, neurofilaments, and APP vesicles in neurons and enhances oxidative stress. *The Journal of cell biology* **156**, 1051-1063 (2002).

133 Gómez-Ramos, A. *et al.* Characteristics and consequences of muscarinic receptor activation by tau protein. *European Neuropsychopharmacology* **19**, 708-717 (2009).

134 Gomez-Ramos, A., Diaz-Hernandez, M., Rubio, A., Miras-Portugal, M. & Avila, J. Extracellular tau promotes intracellular calcium increase through M1 and M3 muscarinic receptors in neuronal cells. *Molecular and Cellular Neuroscience* **37**, 673-681 (2008).

135 Ittner, L. M. *et al.* Dendritic function of tau mediates amyloid-beta toxicity in Alzheimer's disease mouse models. *Cell* **142**, 387-397, doi:10.1016/j.cell.2010.06.036 (2010).

136 Reynolds, C. H. *et al.* Phosphorylation regulates tau interactions with Src homology 3 domains of phosphatidylinositol 3-kinase, phospholipase Cgamma1, Grb2, and Src family kinases. *J Biol Chem* **283**, 18177-18186, doi:10.1074/jbc.M709715200 (2008).

137 Mondragón-Rodríguez, S. *et al.* Interaction of endogenous tau protein with synaptic proteins is regulated by N-methyl-D-aspartate receptor-dependent tau phosphorylation. *J Biol Chem* **287**, 32040-32053, doi:10.1074/jbc.M112.401240 (2012).

138 Pooler, A. M., Noble, W. & Hanger, D. P. A role for tau at the synapse in Alzheimer's disease pathogenesis. *Neuropharmacology* **76 Pt A**, 1-8, doi:10.1016/j.neuropharm.2013.09.018 (2014).

139 Wischik, C. M., Harrington, C. R. & Storey, J. M. Tau-aggregation inhibitor therapy for Alzheimer's disease. *Biochem Pharmacol* **88**, 529-539, doi:10.1016/j.bcp.2013.12.008 (2014).

140 Akoury, E. *et al.* Mechanistic basis of phenothiazine-driven inhibition of Tau aggregation. *Angew Chem Int Ed Engl* **52**, 3511-3515, doi:10.1002/anie.201208290 (2013).

141 O'Leary, J. C., 3rd *et al.* Phenothiazine-mediated rescue of cognition in tau transgenic mice requires neuroprotection and reduced soluble tau burden. *Mol Neurodegener* **5**, 45, doi:10.1186/1750-1326-5-45 (2010).

142 Zhang, B. *et al.* The microtubule-stabilizing agent, epothilone D, reduces axonal dysfunction, neurotoxicity, cognitive deficits, and Alzheimer-like pathology in an interventional study with aged tau transgenic mice. *J Neurosci* **32**, 3601-3611, doi:10.1523/jneurosci.4922-11.2012 (2012).

143 Li, W. *et al.* Inhibition of tau fibrillization by oleocanthal via reaction with the amino groups of tau. *J Neurochem* **110**, 1339-1351, doi:10.1111/j.1471-4159.2009.06224.x (2009).

144 Peterson, D. W. *et al.* Cinnamon extract inhibits tau aggregation associated with Alzheimer's disease in vitro. *J Alzheimers Dis* **17**, 585-597, doi:10.3233/jad-2009-1083 (2009).

145 Rane, J. S., Bhaumik, P. & Panda, D. Curcumin Inhibits Tau Aggregation and Disintegrates Preformed Tau Filaments in vitro. *J Alzheimers Dis* **60**, 999-1014, doi:10.3233/jad-170351 (2017).

146 Paranjape, S. R. *et al.* Azaphilones inhibit tau aggregation and dissolve tau aggregates in vitro. *ACS Chem Neurosci* **6**, 751-760, doi:10.1021/acschemneuro.5b00013 (2015).

147 Gorantla, N. V., Das, R., Mulani, F. A., Thulasiram, H. V. & Chinnathambi, S. Neem Derivatives Inhibits Tau Aggregation. *J Alzheimers Dis Rep* **3**, 169-178, doi:10.3233/adr-190118 (2019).

148 Gorantla, N. V. *et al.* Basic Limonoid modulates Chaperone-mediated Proteostasis and dissolve Tau fibrils. *Sci Rep* **10**, 4023, doi:10.1038/s41598-020-60773-1 (2020).

149 Dubey, T. & Chinnathambi, S. Brahmi (Bacopa monnieri): An ayurvedic herb against the Alzheimer's disease. *Arch Biochem Biophys* **676**, 108153, doi:10.1016/j.abb.2019.108153 (2019).

150 Balmik, A. A. & Chinnathambi, S. Multi-Faceted Role of Melatonin in Neuroprotection and Amelioration of Tau Aggregates in Alzheimer's Disease. *J Alzheimers Dis* **62**, 1481-1493, doi:10.3233/jad-170900 (2018).

151 Balmik, A. A. *et al.* Melatonin interacts with repeat domain of Tau to mediate disaggregation of paired helical filaments. *Biochim Biophys Acta Gen Subj* **1864**, 129467, doi:10.1016/j.bbagen.2019.129467 (2020).

152 Das, R., Balmik, A. A. & Chinnathambi, S. Effect of Melatonin on Tau aggregation and Tau-mediated cell surface morphology. *Int J Biol Macromol* **152**, 30-39, doi:10.1016/j.ijbiomac.2020.01.296 (2020).

153 Vivó, M. *et al.* Polyamines in the basal ganglia of human brain. Influence of aging and degenerative movement disorders. *Neurosci Lett* **304**, 107-111, doi:10.1016/s0304-3940(01)01776-1 (2001).

154 Luo, J. *et al.* Cellular polyamines promote amyloid-beta (Aβ) peptide fibrillation and modulate the aggregation pathways. *ACS Chem Neurosci* **4**, 454-462, doi:10.1021/cn300170x (2013).

155 Antony, T. *et al.* Cellular polyamines promote the aggregation of alpha-synuclein. *J Biol Chem* **278**, 3235-3240, doi:10.1074/jbc.M208249200 (2003).

156 Crowe, A. *et al.* Identification of aminothienopyridazine inhibitors of tau assembly by quantitative high-throughput screening. *Biochemistry* **48**, 7732-7745, doi:10.1021/bi9006435 (2009).

157 Pickhardt, M. *et al.* Anthraquinones inhibit tau aggregation and dissolve Alzheimer's paired helical filaments in vitro and in cells. *J Biol Chem* **280**, 3628-3635, doi:10.1074/jbc.M410984200 (2005).

158 Gorantla, N. V. *et al.* Molecular Cobalt(II) Complexes for Tau Polymerization in Alzheimer's Disease. *ACS Omega* **4**, 16702-16714, doi:10.1021/acsomega.9b00692 (2019).
159 Dubey, T., Gorantla, N. V., Chandrashekara, K. T. & Chinnathambi, S. Photoexcited Toluidine Blue Inhibits Tau Aggregation in Alzheimer's Disease. *ACS Omega* **4**, 18793-18802, doi:10.1021/acsomega.9b02792 (2019).
160 Dubey, T., Gorantla, N. V., Chandrashekara, K. T. & Chinnathambi, S. Photodynamic exposure of Rose-Bengal inhibits Tau aggregation and modulates cytoskeletal network in neuronal cells. *Sci Rep* **10**, 12380, doi:10.1038/s41598-020-69403-2 (2020).
161 Zhu, M. *et al.* The flavonoid baicalein inhibits fibrillation of alpha-synuclein and disaggregates existing fibrils. *J Biol Chem* **279**, 26846-26857, doi:10.1074/jbc.M403129200 (2004).
162 Zhang, S. Q. *et al.* Baicalein reduces β-amyloid and promotes nonamyloidogenic amyloid precursor protein processing in an Alzheimer's disease transgenic mouse model. *J Neurosci Res* **91**, 1239-1246, doi:10.1002/jnr.23244 (2013).
163 Mandel, S., Weinreb, O., Amit, T. & Youdim, M. B. Cell signaling pathways in the neuroprotective actions of the green tea polyphenol (-)-epigallocatechin-3-gallate: implications for neurodegenerative diseases. *J Neurochem* **88**, 1555-1569, doi:10.1046/j.1471-4159.2003.02291.x (2004).
164 Ferreira, N. *et al.* Binding of epigallocatechin-3-gallate to transthyretin modulates its amyloidogenicity. *FEBS Lett* **583**, 3569-3576, doi:10.1016/j.febslet.2009.10.062 (2009).
165 Rambold, A. S. *et al.* Green tea extracts interfere with the stress-protective activity of PrP and the formation of PrP. *J Neurochem* **107**, 218-229, doi:10.1111/j.1471-4159.2008.05611.x (2008).
166 Ehrnhoefer, D. E. *et al.* EGCG redirects amyloidogenic polypeptides into unstructured, off-pathway oligomers. *Nat Struct Mol Biol* **15**, 558-566, doi:10.1038/nsmb.1437 (2008).
167 Esposito, Z. *et al.* Amyloid β, glutamate, excitotoxicity in Alzheimer's disease: are we on the right track? *CNS Neurosci Ther* **19**, 549-555, doi:10.1111/cns.12095 (2013).
168 Lewerenz, J. & Maher, P. Chronic Glutamate Toxicity in Neurodegenerative Diseases-What is the Evidence? *Front Neurosci* **9**, 469, doi:10.3389/fnins.2015.00469 (2015).
169 Lin, T. S. *et al.* An Improved Drugs Screening System Reveals that Baicalein Ameliorates the Aβ/AMPA/NMDA-Induced Depolarization of Neurons. *J Alzheimers Dis* **56**, 959-976, doi:10.3233/jad-160898 (2017).
170 Nanjo, F. *et al.* Scavenging effects of tea catechins and their derivatives on 1,1-diphenyl-2-picrylhydrazyl radical. *Free Radic Biol Med* **21**, 895-902, doi:10.1016/0891-5849(96)00237-7 (1996).
171 Guéroux, M., Fleau, C., Slozeck, M., Laguerre, M. & Pianet, I. Epigallocatechin 3-Gallate as an Inhibitor of Tau Phosphorylation and Aggregation: A Molecular and Structural Insight. *J Prev Alzheimers Dis* **4**, 218-225, doi:10.14283/jpad.2017.35 (2017).
172 Chesser, A. S., Ganeshan, V., Yang, J. & Johnson, G. V. Epigallocatechin-3-gallate enhances clearance of phosphorylated tau in primary neurons. *Nutr Neurosci* **19**, 21-31, doi:10.1179/1476830515y.0000000038 (2016).
173 Desler, C., Lillenes, M. S., Tønjum, T. & Rasmussen, L. J. The Role of Mitochondrial Dysfunction in the Progression of Alzheimer's Disease. *Curr Med Chem* **25**, 5578-5587, doi:10.2174/0929867324666170616110111 (2018).

174 Gibson, G. E., Sheu, K. F. & Blass, J. P. Abnormalities of mitochondrial enzymes in Alzheimer disease. *J Neural Transm (Vienna)* **105**, 855-870, doi:10.1007/s007020050099 (1998).

175 Dragicevic, N. *et al.* Green tea epigallocatechin-3-gallate (EGCG) and other flavonoids reduce Alzheimer's amyloid-induced mitochondrial dysfunction. *J Alzheimers Dis* **26**, 507-521, doi:10.3233/jad-2011-101629 (2011).

176 Heneka, M. T. *et al.* Neuroinflammation in Alzheimer's disease. *Lancet Neurol* **14**, 388-405, doi:10.1016/s1474-4422(15)70016-5 (2015).

177 Chen, Y. C., Shen, S. C., Chen, L. G., Lee, T. J. & Yang, L. L. Wogonin, baicalin, and baicalein inhibition of inducible nitric oxide synthase and cyclooxygenase-2 gene expressions induced by nitric oxide synthase inhibitors and lipopolysaccharide. *Biochem Pharmacol* **61**, 1417-1427, doi:10.1016/s0006-2952(01)00594-9 (2001).

178 Li, F. Q., Wang, T., Pei, Z., Liu, B. & Hong, J. S. Inhibition of microglial activation by the herbal flavonoid baicalein attenuates inflammation-mediated degeneration of dopaminergic neurons. *J Neural Transm (Vienna)* **112**, 331-347, doi:10.1007/s00702-004-0213-0 (2005).

179 Ott, C. *et al.* Role of advanced glycation end products in cellular signaling. *Redox biology* **2**, 411-429 (2014).

180 Angeloni, C., Zambonin, L. & Hrelia, S. Role of methylglyoxal in Alzheimer's disease. *BioMed research international* **2014** (2014).

181 Fokkens, B. T. & Smit, A. J. Skin fluorescence as a clinical tool for non-invasive assessment of advanced glycation and long-term complications of diabetes. *Glycoconjugate journal* **33**, 527-535 (2016).

182 Ke, Y. D., Delerue, F., Gladbach, A., Götz, J. & Ittner, L. M. Experimental diabetes mellitus exacerbates tau pathology in a transgenic mouse model of Alzheimer's disease. *PloS one* **4**, e7917 (2009).

183 Nakamura, M. *et al.* Pathological progression induced by the frontotemporal dementia-associated R406W tau mutation in patient-derived iPSCs. *Stem cell reports* **13**, 684-699 (2019).

184 Goedert, M., Ghetti, B. & Spillantini, M. G. Tau Gene Mutations in Frontotemporal Dementia and Parkinsonism Linked to Chromosome 17 (FTDP-17): Their Relevance for Understanding the Neurogenerative Process. *Annals of the New York Academy of Sciences* **920**, 74-83 (2000).

185 GhoshMoulick, R., Bhattacharya, J., Roy, S., Basak, S. & Dasgupta, A. K. Compensatory secondary structure alterations in protein glycation. *Biochimica et Biophysica Acta (BBA)-Proteins and Proteomics* **1774**, 233-242 (2007).

186 Ahmed, A., Shamsi, A., Khan, M. S., Husain, F. M. & Bano, B. Methylglyoxal induced glycation and aggregation of human serum albumin: biochemical and biophysical approach. *International journal of biological macromolecules* **113**, 269-276 (2018).

187 Tjernberg, L., Hosia, W., Bark, N., Thyberg, J. & Johansson, J. Charge attraction and β propensity are necessary for amyloid fibril formation from tetrapeptides. *Journal of Biological Chemistry* **277**, 43243-43246 (2002).

188 Schmitt, A., Schmitt, J., Münch, G. & Gasic-Milencovic, J. Characterization of advanced glycation end products for biochemical studies: side chain modifications and fluorescence characteristics. *Analytical biochemistry* **338**, 201-215 (2005).

189 Fu, M.-X., Knecht, K. J., Thorpe, S. R. & Baynes, J. W. Role of oxygen in cross-linking and chemical modification of collagen by glucose. *Diabetes* **41**, 42-48 (1992).

190 Zeng, J. & Davies, M. J. Evidence for the formation of adducts and S-(carboxymethyl) cysteine on reaction of α-dicarbonyl compounds with thiol groups on amino acids, peptides, and proteins. *Chemical research in toxicology* **18**, 1232-1241 (2005).
191 Ramasamy, R., Yan, S. F. & Schmidt, A. M. Methylglyoxal comes of AGE. *Cell* **124**, 258-260 (2006).
192 Rahbar, S. *et al.* Evidence that pioglitazone, metformin and pentoxifylline are inhibitors of glycation. *Clinica chimica acta* **301**, 65-77 (2000).
193 Lo, C. Y. *et al.* Trapping reactions of reactive carbonyl species with tea polyphenols in simulated physiological conditions. *Molecular nutrition & food research* **50**, 1118-1128 (2006).
194 Gomez, T. M. & Letourneau, P. C. Actin dynamics in growth cone motility and navigation. *Journal of neurochemistry* **129**, 221-234 (2014).
195 Xu, K., Zhong, G. & Zhuang, X. Actin, spectrin, and associated proteins form a periodic cytoskeletal structure in axons. *Science* **339**, 452-456 (2013).
196 Baas, P. W., Deitch, J. S., Black, M. M. & Banker, G. A. Polarity orientation of microtubules in hippocampal neurons: uniformity in the axon and nonuniformity in the dendrite. *Proceedings of the National Academy of Sciences* **85**, 8335-8339 (1988).
197 Hider, R. C., Liu, Z. D. & Khodr, H. H. in *Methods in enzymology* Vol. 335 190-203 (Elsevier, 2001).
198 Porat, Y., Abramowitz, A. & Gazit, E. Inhibition of amyloid fibril formation by polyphenols: structural similarity and aromatic interactions as a common inhibition mechanism. *Chemical biology & drug design* **67**, 27-37 (2006).
199 Bieschke, J. Natural compounds may open new routes to treatment of amyloid diseases. *Neurotherapeutics* **10**, 429-439 (2013).
200 Ishii, T. *et al.* Human serum albumin as an antioxidant in the oxidation of (−)-epigallocatechin gallate: participation of reversible covalent binding for interaction and stabilization. *Bioscience, biotechnology, and biochemistry* **75**, 100-106 (2011).
201 Zhu, M. *et al.* The flavonoid baicalein inhibits fibrillation of α-synuclein and disaggregates existing fibrils. *Journal of Biological Chemistry* **279**, 26846-26857 (2004).
202 Zhao, W.-Z., Wang, H.-T., Huang, H.-J., Lo, Y.-L. & Lin, A. M.-Y. Neuroprotective effects of baicalein on acrolein-induced neurotoxicity in the nigrostriatal dopaminergic system of rat brain. *Molecular Neurobiology* **55**, 130-137 (2018).
203 Gu, X.-H. *et al.* The flavonoid baicalein rescues synaptic plasticity and memory deficits in a mouse model of Alzheimer's disease. *Behavioural brain research* **311**, 309-321 (2016).
204 Callahan, L. M. & Coleman, P. D. Neurons bearing neurofibrillary tangles are responsible for selected synaptic deficits in Alzheimer's disease. *Neurobiology of aging* **16**, 311-314 (1995).
205 Rezai-Zadeh, K. *et al.* Green tea epigallocatechin-3-gallate (EGCG) modulates amyloid precursor protein cleavage and reduces cerebral amyloidosis in Alzheimer transgenic mice. *Journal of Neuroscience* **25**, 8807-8814 (2005).
206 Ehrnhoefer, D. E. *et al.* EGCG redirects amyloidogenic polypeptides into unstructured, off-pathway oligomers. *Nature structural & molecular biology* **15**, 558 (2008).
207 Wobst, H. J., Sharma, A., Diamond, M. I., Wanker, E. E. & Bieschke, J. The green tea polyphenol (−)-epigallocatechin gallate prevents the aggregation of tau protein into toxic oligomers at substoichiometric ratios. *FEBS letters* **589**, 77-83 (2015).

208 Eaton, J. D. & Williamson, M. P. Multi-site binding of epigallocatechin gallate to human serum albumin measured by NMR and isothermal titration calorimetry. *Bioscience reports* **37** (2017).
209 Balmik, A. A. & Chinnathambi, S. Multi-faceted role of melatonin in neuroprotection and amelioration of Tau aggregates in Alzheimer's disease. *Journal of Alzheimer's Disease* **62**, 1481-1493 (2018).
210 Pegg, A. E. Functions of polyamines in mammals. *Journal of Biological Chemistry* **291**, 14904-14912 (2016).
211 Hardy, J. & Allsop, D. Amyloid deposition as the central event in the aetiology of Alzheimer's disease. *Trends in pharmacological sciences* **12**, 383-388 (1991).
212 Bryan, K. J., Lee, H.-g., Perry, G., Smith, M. A. & Casadesus, G. in *Methods of Behavior Analysis in Neuroscience. 2nd edition* (CRC Press/Taylor & Francis, 2009).
213 Chételat, G. Aβ-independent processes—rethinking preclinical AD. *Nature Reviews Neurology* **9**, 123-124 (2013).
214 Goedert, M. *et al.* in *Cold Spring Harbor symposia on quantitative biology.* 565-573 (Cold Spring Harbor Laboratory Press).
215 Braak, H. & Del Tredici, K. Are cases with tau pathology occurring in the absence of Aβ deposits part of the AD-related pathological process? *Acta neuropathologica* **128**, 767-772 (2014).
216 Fulga, T. A. *et al.* Abnormal bundling and accumulation of F-actin mediates tau-induced neuronal degeneration in vivo. *Nature cell biology* **9**, 139-148 (2007).
217 DuBoff, B., Götz, J. & Feany, M. B. Tau promotes neurodegeneration via DRP1 mislocalization in vivo. *Neuron* **75**, 618-632 (2012).
218 Frandemiche, M. L. *et al.* Activity-dependent tau protein translocation to excitatory synapse is disrupted by exposure to amyloid-beta oligomers. *Journal of Neuroscience* **34**, 6084-6097 (2014).
219 Black, M. M., Slaughter, T., Moshiach, S., Obrocka, M. & Fischer, I. Tau is enriched on dynamic microtubules in the distal region of growing axons. *Journal of Neuroscience* **16**, 3601-3619 (1996).
220 Khatoon, S., Grundke-Iqbal, I. & Iqbal, K. Levels of normal and abnormally phosphorylated tau in different cellular and regional compartments of Alzheimer disease and control brains. *FEBS letters* **351**, 80-84 (1994).
221 Krstic, D. & Knuesel, I. Deciphering the mechanism underlying late-onset Alzheimer disease. *Nature Reviews Neurology* **9**, 25 (2013).
222 Li, X. *et al.* Novel diffusion barrier for axonal retention of Tau in neurons and its failure in neurodegeneration. *The EMBO journal* **30**, 4825-4837 (2011).
223 Ittner, L. M. *et al.* Dendritic function of tau mediates amyloid-β toxicity in Alzheimer's disease mouse models. *Cell* **142**, 387-397 (2010).
224 Violet, M. *et al.* A major role for Tau in neuronal DNA and RNA protection in vivo under physiological and hyperthermic conditions. *Frontiers in cellular neuroscience* **8**, 84 (2014).
225 Mansuroglu, Z. *et al.* Loss of Tau protein affects the structure, transcription and repair of neuronal pericentromeric heterochromatin. *Scientific reports* **6**, 33047 (2016).
226 Bukar Maina, M., Al-Hilaly, Y. K. & Serpell, L. C. Nuclear tau and its potential role in Alzheimer's disease. *Biomolecules* **6**, 9 (2016).
227 Fernández-Nogales, M. *et al.* Huntington's disease is a four-repeat tauopathy with tau nuclear rods. *Nature medicine* **20**, 881-885 (2014).

228 Frost, B., Bardai, F. H. & Feany, M. B. Lamin dysfunction mediates neurodegeneration in tauopathies. *Current Biology* **26**, 129-136 (2016).
229 Tang, Z. *et al.* mTor mediates tau localization and secretion: implication for Alzheimer's disease. *Biochimica et Biophysica Acta (BBA)-Molecular Cell Research* **1853**, 1646-1657 (2015).
230 Tai, H.-C. *et al.* The synaptic accumulation of hyperphosphorylated tau oligomers in Alzheimer disease is associated with dysfunction of the ubiquitin-proteasome system. *The American journal of pathology* **181**, 1426-1435 (2012).
231 Dillon, C. & Goda, Y. The actin cytoskeleton: integrating form and function at the synapse. *Annu. Rev. Neurosci.* **28**, 25-55 (2005).
232 Hutton, M. Missense and splice site mutations in tau associated with FTDP-17: multiple pathogenic mechanisms. *Neurology* **56**, S21-S25 (2001).
233 Hong, M. *et al.* Mutation-specific functional impairments in distinct tau isoforms of hereditary FTDP-17. *Science* **282**, 1914-1917 (1998).
234 Goode, B. L. & Feinstein, S. C. Identification of a novel microtubule binding and assembly domain in the developmentally regulated inter-repeat region of tau. *The Journal of cell biology* **124**, 769-782 (1994).
235 Goedert, M., Jakes, R. & Crowther, R. A. Effects of frontotemporal dementia FTDP-17 mutations on heparin-induced assembly of tau filaments. *FEBS letters* **450**, 306-311 (1999).
236 Cohen, T. J., Friedmann, D., Hwang, A. W., Marmorstein, R. & Lee, V. M. The microtubule-associated tau protein has intrinsic acetyltransferase activity. *Nature structural & molecular biology* **20**, 756 (2013).
237 Dickey, C. A. *et al.* HSP induction mediates selective clearance of tau phosphorylated at proline-directed Ser/Thr sites but not KXGS (MARK) sites. *The FASEB journal* **20**, 753-755 (2006).
238 Miyasaka, T. *et al.* Molecular analysis of mutant and wild-type tau deposited in the brain affected by the FTDP-17 R406W mutation. *The American journal of pathology* **158**, 373-379 (2001).
239 Ikeda, M. *et al.* Accumulation of filamentous tau in the cerebral cortex of human tau R406W transgenic mice. *The American journal of pathology* **166**, 521-531 (2005).
240 Iannuzzi, C., Irace, G. & Sirangelo, I. Differential effects of glycation on protein aggregation and amyloid formation. *Frontiers in molecular biosciences* **1**, 9 (2014).
241 Mendez, D. L., Jensen, R. A., McElroy, L. A., Pena, J. M. & Esquerra, R. M. The effect of non-enzymatic glycation on the unfolding of human serum albumin. *Archives of Biochemistry and Biophysics* **444**, 92-99 (2005).
242 Gorantla, N. V., Shkumatov, A. V. & Chinnathambi, S. in *Tau Protein* 3-20 (Springer, 2017).
243 Luthra, M. & Balasubramanian, D. Nonenzymatic glycation alters protein structure and stability. A study of two eye lens crystallins. *Journal of Biological Chemistry* **268**, 18119-18127 (1993).
244 Ledesma, M., Perez, M., Colaco, C. & Avila, J. Tau glycation is involved in aggregation of the protein but not in the formation of filaments. *Cellular and Molecular Biology (Noisy-le-Grand, France)* **44**, 1111-1116 (1998).
245 Wang, J.-Z., Xia, Y.-Y., Grundke-Iqbal, I. & Iqbal, K. Abnormal hyperphosphorylation of tau: sites, regulation, and molecular mechanism of neurofibrillary degeneration. *Journal of Alzheimer's disease* **33**, S123-S139 (2013).

246 Schwalbe, M. *et al.* Structural impact of tau phosphorylation at threonine 231. *Structure* **23**, 1448-1458 (2015).
247 Sonawane, S. K. & Chinnathambi, S. P301 L, an FTDP-17 Mutant, Exhibits Enhanced Glycation in vitro. *Journal of Alzheimer's Disease*, 1-11 (2020).
248 Lee, V. M., Brunden, K. R., Hutton, M. & Trojanowski, J. Q. Developing therapeutic approaches to tau, selected kinases, and related neuronal protein targets. *Cold Spring Harbor perspectives in medicine* **1**, a006437 (2011).
249 Voronkov, M., Braithwaite, S. P. & Stock, J. B. Phosphoprotein phosphatase 2A: a novel druggable target for Alzheimer's disease. *Future medicinal chemistry* **3**, 821-833 (2011).
250 Sang, S. *et al.* Tea polyphenol (−)-epigallocatechin-3-gallate: a new trapping agent of reactive dicarbonyl species. *Chemical research in toxicology* **20**, 1862-1870 (2007).
251 Li, X.-H. *et al.* Methylglyoxal induces tau hyperphosphorylation via promoting AGEs formation. *Neuromolecular medicine* **14**, 338-348 (2012).
252 Kanlaya, R., Khamchun, S., Kapincharanon, C. & Thongboonkerd, V. Protective effect of epigallocatechin-3-gallate (EGCG) via Nrf2 pathway against oxalate-induced epithelial mesenchymal transition (EMT) of renal tubular cells. *Scientific reports* **6**, 30233 (2016).
253 Schnapp, B. J., Vale, R. D., Sheetz, M. P. & Reese, T. S. Single microtubules from squid axoplasm support bidirectional movement of organelles. *Cell* **40**, 455-462 (1985).
254 Kuznetsov, S. A., Langford, G. M. & Weiss, D. G. Actin-dependent organelle movement in squid axoplasm. *Nature* **356**, 722-725 (1992).
255 Cullum, N., Mahon, J., Stringer, K. & McLean, W. Glycation of rat sciatic nerve tubulin in experimental diabetes mellitus. *Diabetologia* **34**, 387-389 (1991).
256 Mellado, W., Slebe, J. & Maccioni, R. Tubulin carbamoylation. Functional amino groups in microtubule assembly. *Biochemical Journal* **203**, 675-681 (1982).
257 Szasz, J., Burns, R. & Sternlicht, H. Effects of reductive methylation on microtubule assembly. Evidence for an essential amino group in the alpha-chain. *Journal of Biological Chemistry* **257**, 3697-3704 (1982).
258 Terman, J. R. & Kashina, A. Post-translational modification and regulation of actin. *Current opinion in cell biology* **25**, 30-38 (2013).
259 Sayas, C. L. *et al.* Tau regulates the localization and function of End-binding proteins 1 and 3 in developing neuronal cells. *Journal of neurochemistry* **133**, 653-667 (2015).
260 Ramirez-Rios, S. *et al.* Tau antagonizes end-binding protein tracking at microtubule ends through a phosphorylation-dependent mechanism. *Molecular biology of the cell* **27**, 2924-2934 (2016).
261 Kumar, S. *et al.* Stages and conformations of the Tau repeat domain during aggregation and its effect on neuronal toxicity. *Journal of biological chemistry* **289**, 20318-20332 (2014).
262 Hong, D.-P., Fink, A. L. & Uversky, V. N. Structural characteristics of α-synuclein oligomers stabilized by the flavonoid baicalein. *Journal of molecular biology* **383**, 214-223 (2008).
263 Taniguchi, S. *et al.* Inhibition of heparin-induced tau filament formation by phenothiazines, polyphenols, and porphyrins. *Journal of Biological Chemistry* **280**, 7614-7623 (2005).
264 del Amo, J. M. L. *et al.* Structural properties of EGCG-induced, nontoxic Alzheimer's disease Aβ oligomers. *Journal of molecular biology* **421**, 517-524 (2012).

265 Hyung, S.-J. *et al.* Insights into antiamyloidogenic properties of the green tea extract (−)-epigallocatechin-3-gallate toward metal-associated amyloid-β species. *Proceedings of the National Academy of Sciences* **110**, 3743-3748 (2013).

266 Conway, K. A., Rochet, J.-C., Bieganski, R. M. & Lansbury, P. T. Kinetic stabilization of the α-synuclein protofibril by a dopamine-α-synuclein adduct. *Science* **294**, 1346-1349 (2001).

267 Peterson, D. W. *et al.* Cinnamon extract inhibits tau aggregation associated with Alzheimer's disease in vitro. *Journal of Alzheimer's Disease* **17**, 585-597 (2009).

268 Liu, H., Bao, W., Ding, H., Jang, J. & Zou, G. Binding modes of flavones to human serum albumin: insights from experimental and computational studies. *The Journal of Physical Chemistry B* **114**, 12938-12947 (2010).

269 Song, S.-m., Wang, Y.-x., Xiong, L.-m., Qu, L.-b. & Xu, M.-t. Interaction between baicalein and amyloid-β fibrils studied by fluorescence spectroscopy. *Chemical Research in Chinese Universities* **29**, 20-25 (2013).

270 Paranjape, S. R. *et al.* Inhibition of Tau Aggregation by Three Aspergillus nidulans Secondary Metabolites: 2, ω-dihydroxyemodin, asperthecin and asperbenzaldehyde. *Planta medica* **80**, 77 (2014).

271 Li, W. *et al.* Inhibition of tau fibrillization by oleocanthal via reaction with the amino groups of tau. *Journal of neurochemistry* **110**, 1339-1351 (2009).

272 Cisek, K., L Cooper, G., J Huseby, C. & Kuret, J. Structure and mechanism of action of tau aggregation inhibitors. *Current Alzheimer Research* **11**, 918-927 (2014).

273 Flach, K. *et al.* Tau oligomers impair artificial membrane integrity and cellular viability. *Journal of Biological Chemistry* **287**, 43223-43233 (2012).

274 Lu, J. H. *et al.* Baicalein Inhibits Formation of α-Synuclein Oligomers within Living Cells and Prevents Aβ Peptide Fibrillation and Oligomerisation. *Chembiochem* **12**, 615-624 (2011).

275 Wischik, C., Edwards, P., Lai, R., Roth, M. & Harrington, C. Selective inhibition of Alzheimer disease-like tau aggregation by phenothiazines. *Proceedings of the National Academy of Sciences* **93**, 11213-11218 (1996).

276 Miyata, M. *et al.* The crystal structure of the green tea polyphenol (−)-epigallocatechin gallate− transthyretin complex reveals a novel binding site distinct from the thyroxine binding site. *Biochemistry* **49**, 6104-6114 (2010).

277 Popovych, N. *et al.* Site specific interaction of the polyphenol EGCG with the SEVI amyloid precursor peptide PAP (248–286). *The Journal of Physical Chemistry B* **116**, 3650-3658 (2012).

278 Vassallo, N. *Natural compounds as therapeutic agents for amyloidogenic diseases*. Vol. 863 (Springer, 2015).

279 Minois, N., Carmona-Gutierrez, D. & Madeo, F. Polyamines in aging and disease. *Aging (Albany NY)* **3**, 716 (2011).

280 Luo, J. *et al.* Cellular polyamines promote amyloid-beta (Aβ) peptide fibrillation and modulate the aggregation pathways. *ACS chemical neuroscience* **4**, 454-462 (2013).

281 Antony, T. *et al.* Cellular polyamines promote the aggregation of α-synuclein. *Journal of Biological Chemistry* **278**, 3235-3240 (2003).

282 Fernandez, C. O. *et al.* NMR of α-synuclein–polyamine complexes elucidates the mechanism and kinetics of induced aggregation. *The EMBO journal* **23**, 2039-2046 (2004).

283 Yang, Y. *et al.* Induction of autophagy by spermidine is neuroprotective via inhibition of caspase 3-mediated Beclin 1 cleavage. *Cell death & disease* **8**, e2738-e2738 (2017).
284 Means, J. C. *et al.* Caspase-3-dependent proteolytic cleavage of tau causes neurofibrillary tangles and results in cognitive impairment during normal aging. *Neurochemical research* **41**, 2278-2288 (2016).

ABSTRACT

Name of the Student: Shweta Kishor Sonawane **Registration No. :** 10BB14J26024
Faculty of Study: Biological Sciences **Year of Submission:** 2020
AcSIR academic centre/CSIR Lab: CSIR-NCL, Pune **Name of the Supervisor(s):** Dr. Subashchandrabose Chinnathambi

Title of the thesis: Small molecules abet neuronal Cytoskeleton integrity and attenuate pathological Tau aggregation and Glycation

Alzheimer's disease is a type of dementia denoted by progressive neuronal death due to the accumulation of proteinaceous aggregates. This includes Tau neurofibrillary tangles, one of the causes of neuronal degeneration. Post-translational modifications (PTMs) of Tau play a pivotal role in its pathogenesis and acts as a triggering factors in Tau aggregation. While hyperphosphorylation is known to play a pivotal role in tau pathogenesis, evidence suggests that glycation may also play a role. Additionally, genetic predisposition also causes alteration of Tau functions. Thus, Tau has become one of the important therapeutic target in AD. The chemical modulators of Tau PTMs such as kinase inhibitors and antibody based therapeutics have been developed but natural compounds as modulators of Tau PTMs are not explored. Thus, it is important to understand the effect of interplay of two or more causal factors for Tau pathology in order to device the efficient therapeutics.

We studied the crosstalk of glycation and FTDP-17 mutant Tau as well as glycation and pseudophosphorylated Tau. These studies highlighted the enhanced Tau aggregation as a result of combination of two causal factors. This would assist in designing the focussed therapeutic strategies in AD. Further, we report EGCG, a green tea polyphenol, as a modulator of two key Tau PTMs, phosphorylation. EGCG inhibited methyl glyoxal (MG) induced Tau glycation *in vitro* and modulated the phosphorylation in neuroblastoma cells.. EGCG potently inhibited MG induced overall AGEs formation in neuroblastoma cells and modulated the localization of AT100 phosphorylated Tau in the nucleus around the periphery of the nuclear membrane, which was disturbed by MG. It was also observed that MG severely disrupted neuronal cytoskeleton which was rescued by EGCG. EGCG maintained intact Microtubule Organizing Center (MTOC) and polymerization and stabilization of microtubules by Microtubule-associated protein RP/EB family member 1 (EB1). EGCG enhanced actin rich neuritic extensions which might play a role in neuronal connections. Thus, EGCG alleviates the effect of Tau PTMs and maintains neuronal integrity. In addition to PTMs, EGCG also showed residue-specific interaction with Tau and covalently modified Tau. This property has also aided in EGCG-mediated Tau aggregation inhibition and disintegration of PHFs. The investigation of another polyphenol Baicalein against Tau aggregation yielded similar results with a role in inducing and sequestering off-pathway Tau oligomers to prevent filamentous aggregation. Baicalein also exhibited covalent modification of Tau suggesting a common mechanism of polyphenols in Tau aggregation. The screening of polyamines displayed inhibition of Tau aggregation by interfering with the binding of inducer heparin and thus maintain Tau in soluble form. Polyamines also modulated neuronal apoptosis highlighting its potential role in AD-related pathologies.

Details of the publications emanating from the thesis work

List of publication(s) in SCI Journal(s) (published & accepted) emanating from the thesis work

1. **Sonawane SK**, Chinnathambi S*. (2018). Prion-like propagation of post-translationally modified tau in Alzheimer's disease: a hypothesis. **J Mol Neurosci**.;65(4):480-490. **Review**

2. **Sonawane SK***, Chinnathambi S *. (2020). P301 L, an FTDP-17 Mutant, Exhibits Enhanced Glycation *in vitro.* **J Alzheimers Dis**.;75(1):61-71.

3. **Sonawane SK,** Balmik AA, Boral, D, Ramasamy S, & Chinnathambi S**. (**2019). Baicalein suppresses Repeat Tau fibrillization by sequestering oligomers. **Archives of Biochemistry and Biophysics,** 675, 108119.

4. **Sonawane SK**, Chidambaram HK, Boral D, Gorantla NV, Balmik AA , Dangi A, Ramasamy S, Marelli UK, Chinnathambi S*. (2020). EGCG impedes human Tau aggregation and interacts with Tau. **Sci Rep**.;10(1):12579.

List of papers with abstract presented (poster) at national/international conferences or seminars

1. Understanding the Role of Post-Translational Modifications of Axonal Tau in Alzheimer's Disease
Shweta Kishor Sonawane and Subashchandrabose Chinnathambi*

Science Day, CSIR-NCL, 2015
Abstract
Alzheimer's disease is a neurodegenerative disorder characterized by progressive memory loss and dementia. It affects around 4.4 million individuals progressively and the number is rapidly increasing especially in the South Asian and Pacific regions. Two major aggregation prone proteins playing a key role in the pathogenesis of AD are Amyloid βeta (Aβ) and Tau. Tau is a microtubule associated protein having 6 isoforms found in the neuronal axons which plays an important role in microtubule stabilization. It is a highly hydrophilic disordered protein which undergoes aggregation on several post-translational modifications especially phosphorylation. Tau is also known to be glycated, methylated, ubiquitinated but the effect of these modifications on the aggregation kinetics of Tau is not well understood and is still being studied. Glycation is protein modification wherein a sugar moiety reacts irreversibly with a protein and leads to protein crosslinking. Effect of glycation on the aggregation kinetics of Tau is being known but the exact conformational changes occurring due to glycation are not yet well understood. Also the isoform dependent effect of glycation on the tau aggregation is not known. So the focus of our lab is to investigate in depth the effect of glycation on Tau and its isoforms and to study the effect of inhibitors of glycation on Tau aggregation kinetics.

2. Implications of Post- translationally modified Tau isoforms and dementia mutants in Alzheimer's Disease
Shweta Kishor Sonawane , Urvi Goyal and Subashchandrabose Chinnathambi*
Science Day, CSIR-NCL, 2016
Abstract
Alzheimer's disease is a neurodegenerative disorder characterized by progressive memory loss and dementia. It affects around 4.4 million individuals progressively and the number is rapidly increasing especially in the South Asian and Pacific regions. AD is also called as protein misfolding disease as the two major aggregation prone proteins play a key role in the pathogenesis of AD. The Amyloid Beta peptide (1-42) misfolds and forms extracellular plaques whereas Tau protein forms intracellular tangles. Protein misfolding occurs either due to specific mutations (dementia mutants) in the Tau protein or modifications of Tau protein. Tau is a microtubule associated protein having 6 isoforms found in the neuronal axons which plays an important role in microtubule stabilization. Tau protein is composed of two major domains based on their microtubule interactions namely 'assembly domain' which interacts with the microtubules and 'projection domain' which projects away from the microtubules. Tau is an intrinsically discorded protein which undergoes aggregation due to various insults in the cellular environment. Tau is also known to undergo modifications such as phosphorylation glycation, methylation, ubiquitination etc. These modifications alter the native conformation of Tau such that it loses its affinity for microtubules and destabilizes them. Further this modified Tau with altered conformation interacts with itself forming Tau aggregates So the focus of our lab is to investigate in depth the effect of PTMs on Tau isoforms and dementia mutants and to study the effect of inhibitors on the post translationally modified Tau proteins.

3. Glycation does not alter the Tau Conformation in Alzheimer's Disease.
Shweta Kishor Sonawane and Subashchandrabose Chinnathambi*
XXXIV Annual Meeting of Indian Academy of Neurosciences National Brain Research Centre, Manesar, INDIA, October 2016.

Abstract

Alzheimer's Disease (AD) is a neurodegenerative disease characterized by progressive cognitive decline. It accounts for 60%-70% of total dementia cases. The extracellular plaques of amyloid beta and the intracellular neurofibrillary tangles of Tau protein are the hallmarks of AD. Tau is a microtubule-associated protein, which stabilizes the microtubules and maintains neuronal structure as well as trafficking. It is amenable to various post-translational modifications (PTMs), which influences its microtubule binding affinity. The most exclusively studied PTM is hyperphosphorylation, which affects the microtubule binding and leads to Tau aggregation. Other PTMs include glycation, acetylation, methylation, nitration etc. Glycation is an irreversible non-enzymatic addition of sugar to the lysines of protein leading to formation of advanced glycation end-products (AGEs). Glycation modifies protein and alters its structural and functional properties. Pseudophosphorylation of Tau at specific serine and threonine residues impart differential aggregation properties depending on the motifs as well as combination of pseudophosphorylated residues. Apart from the abnormal PTMs, Tau can aggregate due to several mutations in the Tau gene, which are linked to fronto-temporal dementia, and Parkinsonism associated with chromosome 17 (FTDP-17). These FTDP-17 mutations affect the microtubule binding ability of Tau and also alter the Tau 4R:3R isoform ratio. Hence, the overall objective of the study is to elucidate the effect of glycation on the Tau dementia mutants and pseudophosphorylation mutants in the pathology of AD. Since, glycation is an irreversible modification we are also screening the natural herbs for Tau glycation inhibitors.

4. Baicalein Inhibits Tau Aggregation by Inducing and Sequestering Oligomerization in Alzheimer's Disease

Shweta Kishor Sonawane , Abhishek Balmik, and Subashchandrabose Chinnathambi *
Society of Biological Chemists, JNU, 2017

Abstract

Alzheimer's disease is a neurodegenerative disorder caused by protein misfolding, aggregation and accumulation in the brain. Tau is a microtubule-associated protein present in the axons of the neurons, where it helps in the assembly and stabilization of microtubules. A large number of molecules are being screened against these pathogenic proteins but the focus for therapeutics is shifting towards the natural compounds as aggregation inhibitors, mainly due to their minimum adverse effects. Baicalein is a natural compound belonging to the class of flavonoids isolated from the Chinese herb *Scutellaria baicalensis*. Here we applied fluorescence, microscopy, MALDI-TOF, spectrophotometry and other biochemical techniques to investigate the interaction between Tau and Baicalein *in vitro*. We found the aggregation inhibitory properties of Baicalein for full-length as well as the repeat domain of Tau having the two-hexapeptide motifs involved in β-sheet formation. Baicalein has shown its effect on the early aggregates of repeat Tau as well as on the mature fibrils. This potential in dissolving the preformed Tau oligomers as well as mature fibrils can be of utmost importance in therapeutics for Alzheimer`s disease. Our biochemical and biophysical data suggest that the mechanism of aggregation inhibition by Baicalein might be by binding to and sequestering the soluble oligomeric Tau species thus inhibiting the further fibrillization of Tau.

5. Epigallocatechin gallate modulates Tau Post-translational modifications and Cytoskeletal network

Shweta Kishor Sonawane and Subashchandrabose Chinnathambi*
Science Day, CSIR-NCL, 2019
Alzheimer's disease is characterized by intracellular Tau tangles, one of the cause of neuronal degeneration. Post-translational modifications (PTMs) of Tau play a pivotal role in its pathogenesis and acts as a triggering factor in Tau aggregation. Thus, Tau PTMs has become one of the important therapeutic target in AD. The chemical modulators of Tau PTMs such as kinase inhibitors and antibody based therapeutics have been developed but natural compounds as modulators of Tau PTMs are not explored. Here, we report EGCG, a green tea polyphenol, as a modulator of two key Tau PTMs, phosphorylation and glycation. EGCG inhibited methyl glyoxal induced Tau glycation *in vitro.* EGCG potently inhibited overall AGEs formation in neuroblastoma cells as evidenced by immunofluorescence studies. EGCG modulated the localization of AT100 phosphorylated Tau in the nucleus around the periphery of the nuclear membrane, which was disturbed by MG. Further, FA induced Tau phosphorylation was regulated by EGCG along with a key Tau kinase CDK5. MG severely disrupted neuronal cytoskeleton, which was rescued by EGCG. EGCG maintained intact MTOC and polymerization and stabilization of microtubules by EB1. EGCG enhanced actin rich neuritic extensions, which might play a role in neuronal connections. Thus, EGCG alleviates the effect of Tau PTMs and maintains neuronal integrity.

Journal of Molecular Neuroscience
https://doi.org/10.1007/s12031-018-1111-5

Prion-Like Propagation of Post-Translationally Modified Tau in Alzheimer's Disease: A Hypothesis

Shweta Kishor Sonawane [1,2] · Subashchandrabose Chinnathambi [1,2]

Received: 27 March 2018 / Accepted: 20 June 2018

Abstract
The microtubule-associated protein Tau plays a key role in the neuropathology of Alzheimer's disease by forming intracellular neurofibrillary tangles. Tau in the normal physiological condition helps stabilize microtubules and transport. Tau aggregates due to various gene mutations, intracellular insults and abnormal post-translational modifications, phosphorylation being the most important one. Other modifications which alter the function of Tau protein are glycation, nitration, acetylation, methylation, oxidation, etc. In addition to forming intracellular aggregates, Tau pathology might spread in a prion-like manner as revealed by several in vitro and in vivo studies. The possible mechanism of Tau spread can be via bulk endocytosis of misfolded Tau species. The recent studies elucidating this mechanism have mainly focussed on the aggregation and spread of repeat domain of Tau in the cell culture models. Further studies are needed to elucidate the prion-like propagation property of full-length Tau and its aggregates in a more intense manner in vitro as well as in vivo conditions. Varied post-translational modifications can have discrete effects on aggregation propensity of Tau as well as its propagation. Here, we review the prion-like properties of Tau and hypothesize the role of glycation in prion-like properties of Tau. This post-translationally modified Tau might have an enhanced propagation property due to differential properties conferred by the modifications.

Keywords Tau · Post-translational modifications of tau · Propagation of tau · Alzheimer disease · Tauopathies

Abbreviations

AD	Alzheimer's Disease
AMPA	a-amino-3-hydroxy-5-methyl-4-isoxazolepropionic acid
PTMs	Post-translational modifications
AGEs	Advanced Glycation End products
PHFs	Paired helical filaments
CML	Carboxymethyl lysine
LRP	Laminin receptor precursor
LRP1	LDL receptor related protein 1
RAGEs	Receptor for Advanced Glycation End products
CNS	Central nervous system

✉ Subashchandrabose Chinnathambi
s.chinnathambi@ncl.res.in

[1] Neurobiology Group, Division of Biochemical Sciences, CSIR-National Chemical Laboratory, Dr. Homi Bhabha Road, Pune 411008, India

[2] Academy of Scientific and Innovative Research (AcSIR), New Delhi 110025, India

Published online: 07 July 2018

Proteins, in their native conformation are required for normal physiological functioning of all the body cells including cell-to-cell communication, cell metabolism, cell division, etc. In certain diseased conditions the proteins tend to change their native conformation leading to misfolding, aggregation and accumulation in the cells.

Neurodegenerative Diseases

Neurodegenerative diseases are a group of disorders wherein misfolded proteins aggregate and accumulate intracellularly or extracellularly in the brain causing various pathologies, ultimately leading to loss of function of a part or whole of the brain. The area of brain affected, the pathogenic protein involved and the phenotype differ among different neurodegenerative diseases. For example, in Parkinson's disease, α-synuclein protein misfolds and aggregates in the dopaminergic neurons of the brain leading to loss of motor function and typical body gait (Beitz 2014; Eriksen et al. 2005). In Alzheimer's disease (AD), two proteins, Amyloid beta and Tau acquire pathological conformations which accumulate and spread in the hippocampal area of the brain leading to

progressive memory loss and dementia (Selkoe 2001) (Fig. 1). Although the role of prion-like proteins in neurodegenerative diseases has been very well summarized in recent reviews (Clavaguera et al. 2015; Goedert et al. 2017b; Hasegawa et

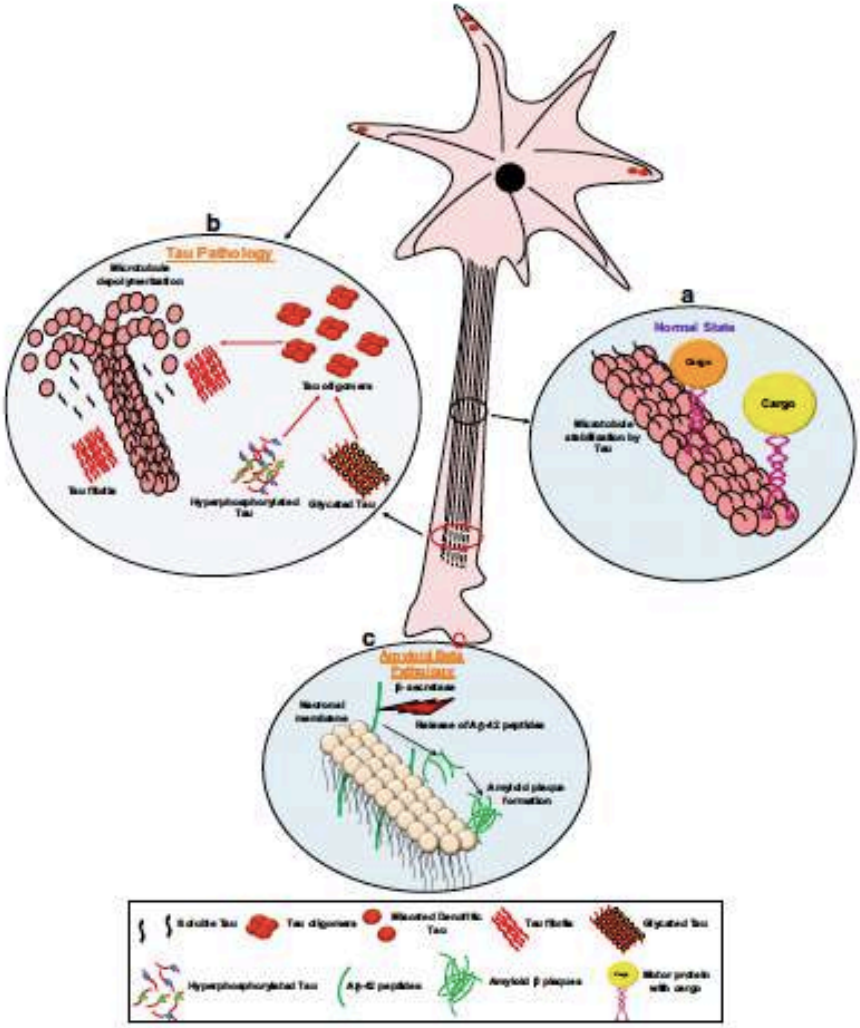

Fig. 1 Neuronal pathophysiology in Alzheimer's Disease. Neuronal structure and function is partly maintained by microtubules and its associated proteins like Tau. In the normal physiological state (A), Tau protein binds to axonal microtubules and stabilizes them, thus leading to normal vesicular transport and neuronal functioning. Whereas in case of AD, Tau protein loses its affinity and dissociates from microtubules (B) owing to various insults and modifications leading to microtubule destabilization thus hampering the vesicular transport. The dissociated Tau protein interact between themselves leading to formation of Tau oligomers which act as seeds for paired helical filament formation. The modified Tau is also missorted to dendrites leading to neuronal dysfunction. Apart from Tau, Amyloid Beta pathology is also found in case of AD (C), wherein membrane bound Amyloid Precursor Protein (APP) is processed by α and β pathways. The processing of APP by α-secretases is non-amyloidogenic. But cleavage of APP by β-secretases followed by γ-secretases releases Aβ-42 peptides. These sticky peptides are amyloidogenic which aggregate and accumulate to form extracellular plaques which disturb the synaptic transmission and lead to neuronal dysfunction finally leading to neuronal death

al. 2017; Walker et al. 2013), the main focus of this review is to summarize the prion-like properties of Tau and present our hypothesis of likely spread of the post-translationally modified Tau prions in the neurons.

Tau and its Role in AD

Tau belongs to the class of microtubule-associated proteins found in axons of the neurons (Binder et al. 1985; Weingarten et al. 1975). The principle physiological function of this protein is stabilization of microtubules, thus helping in axonal transport. Tau is one of the highly soluble proteins and therefore does not adopt a rigid structure. It rather remains natively unfolded or intrinsically disordered (Schweers et al. 1994). Tau protein is composed of two major domains based on their microtubule interactions, namely, 'assembly domain' which interacts with the microtubules and 'projection domain' which projects away from the microtubules. Tau binds to microtubules at the interface of the α and β-tubulin dimer via the residues which are also essential for the aggregation of Tau (Kadavath et al. 2015; Mukrasch et al. 2007). Based on the alternative splicing, Tau consists of six isoforms, of which the four repeat isoforms are distributed in an adult-specific manner while the three repeat isoforms are present since fetal stages (Goedert et al. 1989; Wang and Mandelkow 2016). Tau protein tends to aggregate intracellularly owing to various factors such as mutations (Goedert and Spillantini 2000; LeBoeuf et al. 2008), post-translational modifications, cellular environment, etc. Specific splicing mutations lead to the inclusion of the exon 10 which codes for the repeat 2 in Tau protein and increases the 4R to 3R ratio of Tau protein, and this imbalance might drive the neuropathology of AD (Goedert and Spillantini 2000; Hutton et al. 1998). Missense mutations like P301L, V337 M and R406W decrease the microtubule-binding capacity of Tau and lead to the microtubule destabilization (Hong et al. 1998). Mutations can lead to Tau pathology by either disturbing the isoforms ratio or affecting the microtubule affinity or enhancing the aggregation propensity of Tau (Coppola et al. 2012; D'Souza and Schellenberg 2005; Goedert and Spillantini 2000; Hong et al. 1998; Ingram and Spillantini 2002; LeBoeuf et al. 2008).

Prion-Like Properties of Tau

Prions are known for their pathogenicity and ability to propagate infectivity among various cell types. Various recent research work has focussed on investigating the prion-like properties of aggregated Tau protein and its spread to various brain regions (Goedert et al. 2017a; Goedert 2015).

In early 1990s, Braak and Braak showed that AD pathology spreads in the brain in stages and a region-specific manner (Braak and Braak 1991) suggesting that the protein aggregates formed in one region of the brain spread to the neighboring area leading to spread of the disease. Various researchers have proposed different models of Tau propagation depending on their observations. Misfolded Tau species can be taken up by the cultured neuronal cells as opposed to soluble Tau monomers from an extracellular medium (Frost et al. 2009). Tau release from the neuronal cells is proposed to be a pre-synaptic mechanism stimulated by the neuronal activity (Wu et al. 2016) via calcium dependent AMPA receptor activation (Pooler et al. 2013). Tau fibrils formed intracellularly by the cultured neurons are released from the host cell in the medium and taken up by the neighboring cells in a co-culture. These fibrils taken up, are potent enough to act as seed and influence the aggregation of the native Tau protein in the recipient cells. But the exact mechanism of uptake of Tau fibrils from the cells was not elucidated by these studies (Kfoury et al. 2012). Later, in the same year, Karen Duff and colleagues showed that the extracellular misfolded Tau is internalized at the somatodendritic compartment or axon terminal by the mechanism of bulk endocytosis (Guo and Lee 2011; Wu et al. 2013) with a critical size not less than 3 Tau units of Tau trimers (Mirbaha et al. 2015). The endocytosed Tau aggregates solubilize the vesicular membranes and leak into the cytoplasm thus seeding the native Tau protein of the recipient cell (Calafate et al. 2016; Wegmann et al. 2016). The aggregated Tau is taken up in the cultured brain slices as well as cultured neurons via the clathrin-mediated endocytosis. Several in vivo studies have also demonstrated prion-like propagation of Tau oligomers in the brains of animal models (Clavaguera et al. 2016). AD patient's brain derived Tau oligomers injected in mice showed memory deficits as well as propagation to the neighboring regions like carpous callousum, cortex and hypothalamus suggesting the prion-like spread of the oligomers (Lasagna-Reeves et al. 2012). The transgenic mouse model for human Tau P301S mutation infused unilaterally with brain extracts containing Tau aggregates in the left hemisphere showed the disease development within 2 weeks of inoculation. The spread of infection was observed on the opposite side of both posterior and anterior regions of the brain suggesting that the spread of Tau pathology is based on the synaptic connectivity rather than spatial proximity (Ahmed et al. 2014).

All these studies suggest that aggregated Tau species show prion-like properties of infectivity and spread in cell culture as well as animal models, but the other important property of prions, formation of distinct "conformational strains" has been only recently demonstrated. It was demonstrated that Tau repeat (amino acids 274 to 372) transfected in HEK cell lines leads to the formation of distinct amyloid conformations which can be clonally propagated through different passages. These clonally propagated Tau strains also showed discrete pathologies for the three generations of

transgenic mice (expressing 4R1N P301S) while maintaining their discrete strain properties. The spread of this Tau pathology was to distant synaptically connected regions (Kaufman et al. 2016; Sanders et al. 2014). Apart from being infectious the misfolded Tau seeds can also act as an early biomarker for the detection of AD by a sensitive and specific flow cytometry-based assay at the femtomolar concentration (Holmes et al. 2014).

Post-Translational Modifications of Tau

Post-translational modifications (PTMs) of proteins are essential for their proper folding, function and cellular localization. But PTMs sometimes can confer abnormal properties to proteins. The prion protein PrP is one such example where glycosylation is an important event for its replication of the infectious agent in the periphery and also for its invasion into the CNS (Cancellotti et al. 2010), and the changes to the PrP glycosylation can affect the strain properties of the infectious agent (Cancellotti et al. 2013). Tau protein is also known to undergo multiple PTMs in the physiological conditions which are necessary for its functioning. There are several types of physiological PTMs of Tau protein like phosphorylation, glycosylation, acetylation, glycation, ubiquitination, sumoylation, methylation, nitration, etc. (Gong et al. 2005; Reynolds et al. 2005). These different PTMs regulate the function of Tau at a different level but whether these PTMs can impart the propagation property to Tau is not understood. Though studies by Hyman and group provide evidence on effect of phospho-Tau on propagation, the in-depth knowledge of this aspect is not available (Takeda et al. 2015). Here we will review phosphorylation and glycation as PTMs of Tau and hypothesize whether they can impart any peculiar characteristics to Tau pathology.

Tau Phosphorylation

Phosphorylation is a normal physiological modification of Tau protein which determines its function of maintaining microtubule stability and dynamics. The longest human Tau has around 85 phosphorylation sites including 45 serines, 35 threonines and five tyrosines. The site-specific phosphorylation plays a crucial role in Tau functioning with respect to microtubule-binding, axonal transport, neurite outgrowth and so on (Johnson and Stoothoff 2004). For instance, phosphorylation at Ser 262 in KXGS motif by the MARK kinase leads to reduced microtubule affinity (Drewes et al. 1995; Hanger et al. 2009). The sites distant from the microtubule-binding domain of Tau protein also influence its binding capacity to microtubules. Phosphorylation at Ser 214 or Thr 231 reduces microtubule-binding capability of Tau (Alonso et al. 2010; Cho and Johnson 2003) but it does not lead to or enhance the PHF assembly; rather the phosphorylation at Ser 214 is found to have an inhibitory role on the Tau polymerization (Schneider et al. 1999). The SP/TP motifs also play a crucial role in Tau toxicity as the proline directed kinases such as MAP kinases and GSK-3β phosphorylate these sites and are linked to Tau neurodegeneration (Drewes et al. 1992; Mandelkow et al. 1992). Tau protein contains 14 such SP/TP sites and studies have suggested that these sites work together to cause Tau mediated neurodegeneration in vivo (Steinhilb et al. 2007). Phosphorylation extent of Tau also depends on the interplay of kinases involved. For example, the PKA kinase phosphorylates Tau such that it becomes readily phosphorylated by GSK-3β at the specific epitopes of Tau-1 and PHF-1, thus leading to hyperphosphorylation of Tau and memory loss (Liu et al. 2004). The PKA-kinase phosphorylated Tau also maintains its ability to bind the microtubules and promotes its assembly but requires an osmolyte TMAO for this reaction (Tseng et al. 1999). Hyperphosphorylation of Tau is sufficient to cause the self assembly of Tau into filaments in vivo as well as in vitro conditions and also to inhibit the microtubule assembly (Alonso et al. 2006; Alonso et al. 2001). Tau is most abundant in the axons of the neurons but dendritic missorting of Tau is observed in case of pathological conditions such as hyperphosphorylation and selective phosphorylation by specific kinases such as fyn (Ittner et al. 2010). The hyperphosphorylation of Tau in AD has also been found to be induced by upregulation or downregulation of certain proteins which are indirectly involved in Tau pathology. One such protein is CYF1P2 (Cytoplasmic FMR 1 interacting protein 2), which is known to be downregulated in AD, and represses the local synthesis of APP and αCaMKII kinase at the synapses. αCaMKII kinase is involved in Tau hyperphoshorylation as well as disrupted calcium signaling at the synapses in AD. Thus, downregulation of CYF1P2 indirectly leads to AD by increasing the Aβ-42 levels as well as by αCaMKII kinase mediated Tau hyperphosphorylation (Tiwari et al. 2016). On the other hand, the upregulation of proteolytic calpain activity in the AD brains have shown to enhance the activity of Tau kinases like CDK5 and glycogen kinase synthase-3 leading the Tau hyperphosphorylation (Kurbatskaya et al. 2016). Along with the signaling cascades, the transgenic mouse model rTg4510 overexpressing human Tau bearing a FTDP-17 mutation P310L shows increased levels of post-translationally modified Tau including phospho-Tau (Song et al. 2015). The impact of Tau hyperphosphorylation on aggregation has been explored using molecular dynamic simulations suggesting that hyperphosphorylation might expose the repeat Tau domain for fibrillization by increasing the attraction between the repeat domain and the N-terminal domain and increasing repulsion between the N and C-terminal domains depending on the number and phosphorylated sites (Xu et al. 2016).

Tau Glycation

Glycation is a non-enzymatic post-translational modification wherein excess sugar molecules interact with proteins to form sugar-protein adducts. This reaction is reversible till initial steps of glycation but becomes irreversible after various bond rearrangements, and these irreversible reactions give rise to advanced glycation end-products (AGEs). In AD, glycation as PTM was found to be present only in the diseased brain and not in healthy brains. Early studies have revealed that a fraction of Tau in PHFs from AD brains is glycated whereas; the non-demented brain did not show presence of any glycation (Ledesma et al. 1994). Further, the study by the same group revealed that Tau is preferentially glycated at lysines in the microtubule-binding domain and hence decreases the ability to bind to microtubules (Ledesma et al. 1995), and glycated Tau also induces oxidative stress in the neuronal cell cultures (Yan et al. 1994). The glycation reaction is a set of complex pathways inter-connected with each other which give rise to various types of intermediates. One such highly reactive intermediate is carboxymethyl lysine (CML) which is found to be present in the PHF-Tau from the AD brain (Ko et al. 1999). In vitro glycated Tau can enhance fibrillization by shifting the equilibrium of the kinetics towards fibrillization, but cannot act as a seed for nucleation (Necula and Kuret 2004). Glycation affects polymerization of Tau in an isoform-dependent manner with the 4R2N isoform showing the enhanced aggregation propensity compared to other 4R isoforms, and glycation of 3R2N constitutes to most inclusions among the 3R isoforms (Liu et al. 2016). This suggests the role of inserts in aggregation in addition to the number of repeats. Advanced glycation end products are also found to be accumulated in the brain depending on the age of the individual as well as the stage of AD (Braak stages). As the stage advances, the number of neurons stained for AGEs increases as compared to young and old healthy controls. Glycation also leads to activation of RAGE-mediated pathways which activate several kinases including CaMKII, GSK-3, and MAPK, which are all involved in Tau hyperphosphorylation (Batkulwar et al. 2015; Cai et al. 2016; Fawver et al. 2012; Koriyama et al. 2015; Wei et al. 2015). Thus, there is a possibility that Tau glycation can enhance its phosphorylation and act as an additional factor to enhance the aggregation propensity of Tau in vitro as well as in vivo by stabilizing the aggregates.

Prion-Like Properties of Post-Translationally Modified Tau: Hypothesis

As far as prion diseases are concerned, the major factor playing a role in the conversion of PrP^{C} to PrP^{Sc} is the post-translational modifications like glycosylation and sialic acid addition to the protein (Bolton et al. 1985; Cancellotti et al. 2010; Cancellotti et al. 2013; Caughey et al. 1989). These modifications give rise to different conformational prion strains which propagate the pathology to the various parts of the body. Post-translational modifications such as oxidative and nitrative stress of prion protein have shown to contribute in its aggregation and propagation (Dear et al. 2007). Prion protein is glycated in the N-terminus of humans affected with transmissible spongiform encephalopathies (TSE) but the exact role of glycation in aggregation and propagation of prion protein needs to still be investigated (Choi et al. 2004). As already discussed, Tau protein is known to undergo many post-translational modifications as well as to spread the pathology to different regions of the brain. There might be a possibility that these PTMs may confer some of the prion-like properties to the Tau protein.

Modes of Prion Propagation

Prion protein is known to propagate the disease pathology via various mechanisms. The cell-to-cell transfer is proposed to take place by mechanisms like trogocytosis, exocytosis, limited autophagy, receptor mediated endocytosis and via nanotubes (Klöhn et al. 2013). Trogocytosis is a phenomenon wherein the membrane patches are transferred between the cells. The GPI anchored proteins are known to transfer by this mechanism and since the prion protein is one of the GPI anchored proteins it is postulated to be propagated from cell to cell via trogocytosis (Klöhn et al. 2013). Prions also propagate to homologous as well as heterologous cell types by exosome formation and these prion loaded exosomes act as a potent pool of infectivity spreading the pathology to the distant cells as well (Porto-Carreiro et al. 2005; Vella et al. 2007). Limited autophagy provides more seeds for further aggregation and indirectly propagate the infection. These seeds are more potent templates for prion formation and hence are more toxic (Heiseke et al. 2010). Prions interact with various receptors which help in their internalization as well as propagation. Prions interact with the laminin receptor precursor (LRP) and laminin receptor (LR) on the surface of the neuronal cells and undergo internalization (Gauczynski et al. 2001). Prion protein is also endocytosed by clathrin coated pits via LRP1 (LDL receptor related protein 1) in the neuronal cells. This receptor is also known to bind to Amyloid beta protein which plays a devastating role in AD (Shyng et al. 1994; Taylor and Hooper 2007). Prions avail various modes for their internalization and propagation which can be potential targets for therapeutics. Albeit, Tau protein has shown to be propagated in a prion-like manner but whether PTMs make Tau more efficient in its seeding and propagation is the question. For example, glycation modifies the protein structure, function, decreases protease sensitivity, cross-links proteins and forms protein

aggregates. Phosphorylation and glycation increase the overall negative charge of the protein which might also play a role in its propagation.

AGE modified proteins bind to RAGEs (Receptors for Advanced Glycation Products) as well as scavenger receptors Type I and Type II. The most studied receptor of these types belongs to the immunoglobulin superfamily class of receptors. AGEs bind to RAGE and are internalized via clathrin dependent or independent mechanisms. These internalized endosomes are transported to early endosomes where the AGE-RAGE complex dissociates and AGEs are further processed by lysosomal proteases to small AGE modified peptides. This could be one of the propagation pathways for glycated Tau as prions (Fig. 2). Similar pathways with scavenger receptors might help the uptake and propagation of glycated Tau as the CD36 scavenger receptor binds to AGEs (Gauczynski et al. 2001; Ohgami et al. 2001). As glycated Tau would be resistant to protease degradation in the lysosomal compartment, partial degradation would form small modified peptides which can act as potential seeds for further aggregation of the native Tau protein. The partially digested peptides released in the extracellular space could be taken up by the other cells via receptor mediated endocytosis and hence enhance the propagation. Also, AGE-RAGE interaction elicits immunological response via various signaling pathways including NF-κB which further increase the oxidative stress in the cells (Ott et al. 2014) leading to neuronal death and exposing the dead cell contents to the other neuronal cells. Whether glycation alone or with other modifications such as phosphorylation might give rise to distinct prion-like strains still needs to be studied as these modifications confer different surface charge as well as hydrophobicity to the protein. Apart from these studies, a novel mechanism of propagation of the modified Tau can be via the formation of membrane annular rings which are known to be formed by the amyloid proteins (Lasagna-Reeves et al. 2014) which makes the study of modified Tau in this aspect more intriguing. The potential pathways of prion-like Tau aggregates formation, and their propagation is necessary to understand the mechanism of pathology as well as to target these pathways in order to suppress the disease pathology.

Therapeutic Importance of Studying Prion-Like Propagation of Tau

A plethora of molecules were considered and tested as the potential anti-prion agents, most of which failed in the clinical studies. Few of these include congo red which delays the onset of disease in rodents (Caspi et al. 1998; Corato et al. 2009), heparan sulphate mimetics which eliminate the prion propagation in the Scrapie infected cells (Adjou et al. 2003), polythiophenes (Margalith et al. 2012), etc. All these studies report the efficacy of the molecules in lower model systems and suggest their potential as a future therapeutic against the prion diseases. The current immunotherapy against prions has not demonstrated any encouraging output. One of the obstacles for this is the tolerance of the immune system for the endogenous PrP, while the other reason might be the conformational variant strains of prion protein. Moreover, the monoclonal antibody designed against glycated prion protein serves a good diagnostic marker but whether it can act as a therapeutic is not known (Dvorakova et al. 2011). The review of immunotherapy for prion disease is an elaborate topic in itself and is being reported in these recent studies (Li et al. 2010; Roettger et al. 2013). Immunotherapy has been also reported for clearance Tau aggregates via uptake of antibody through clathrin dependent receptor endocytosis in cultured brain slices and neuronal cells (Congdon et al. 2013). On the other hand, anti-Tau monoclonal antibody 5E2 failed to recover the memory deficit in J20 mouse models for AD. Moreover, treatment with this antibody showed increased mortality in the animals (Mably et al. 2015). Such results demonstrate the practical obstacles for in vivo studies with respect to animal models and demand extensive preclinical investigations for the putative therapeutics before entering the clinical trials. One more barrier in in vivo studies is the seeding and propagation in the animal models. Since Tau is highly soluble, its mere overexpression in animal models does not lead to aggregation in vivo and hampers further seeding and propagation studies. This drawback has been partially overcome by the doxycycline inducible transgenic mouse model which has a regulatable expression of pro-aggregant human Tau repeat

Fig. 2 Hypothetical model for prion-like propagation of post-translationally modified Tau. Three possible modes of prion-like propagation of glycated Tau are hypothesized. Tau is glycated by sugar molecules as well as its reactive intermediates like glyoxal, methylglyoxal (MG) and 3-deoxyglucosan (3-DG). This modifies Tau and leads to Tau cross-linking, finally leading to AGE modified Tau formation. This AGE modified Tau may have several effects in the cell which are yet to be completely elucidated. It might act as a seed for glycation, acting as a glycating agent itself and converting normal Tau into modified Tau. It can also form prion-like variants of Tau protein by template-based conformational conversion. The AGE modified Tau (glycated Tau) might show its propagation by various modes. *1*. Modified Tau might form membrane structures as formed by other amyloid proteins called annular protofibrils (APF) and propagate itself via such membrane pores. *2*. The modified Tau can enter the neighboring cells via receptor mediated endocytosis through RAGEs. The AGE modified Tau can bind to RAGE and taken up by the next cell in the form of endosome. The AGE modified Tau and RAGE dissociate after fusing with the lysosome. RAGE is recycled back to the membrane whereas the modified Tau is partially digested due to limited proteolysis of protease resistant glycated Tau. These partially digested Tau peptides may act as more potent glycation seeds to glycate the normal Tau thus forming a vicious circle. The activation of RAGE signaling would trigger various kinases (involved in Tau hyperphosphorylation) as shown in the figure and lead to Tau aggregation resulting in further enhancement in Tau pathology. *3*. Glycated Tau can also be taken up by bulk endocytosis and propagated in a similar way as shown in the figure

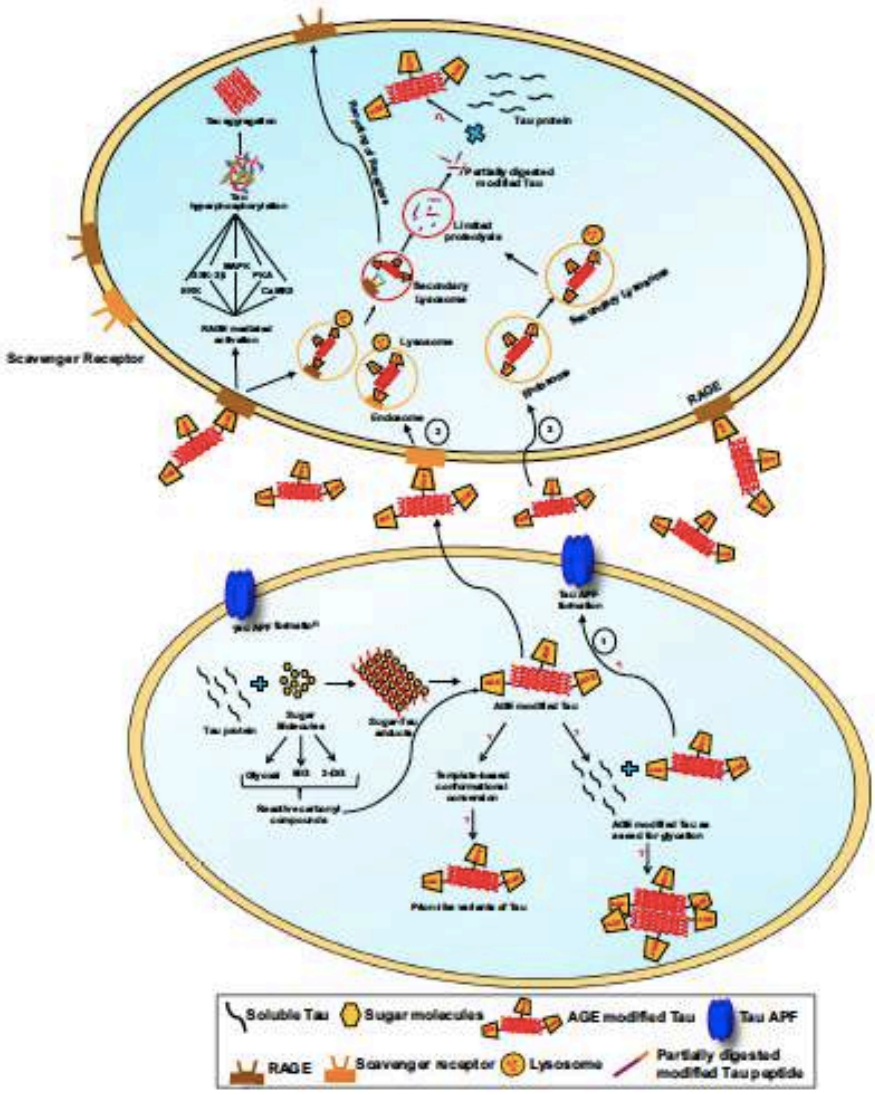

domain. The repeat domain of Tau protein gets overexpressed and acts as a seed to aggregate the endogenous mouse Tau when the expression is induced (Sydow and Mandelkow 2010). Several therapeutics are also being designed and tried to clear the Tau aggregates from the brain in AD including kinase inhibitors, small molecules (Bulic et al. 2009), etc. Most of them show excellent potential in in vitro studies or in animal models but fail in the later clinical trials. For example, tideglusib, a kinase inhibitor, is being reported to ameliorate Tau hyperphosphorylation as well as Aβ deposition in experimental models but has failed to show its efficacy at the phase II trials (Lovestone et al. 2015). Another example is Davunetide, an octapeptide which showed promising neuroprotective effects in varied animal models including amyloid beta toxicity. It has also shown to reduce phosphorylation of Tau at specific Thr 231 which influences the Tau

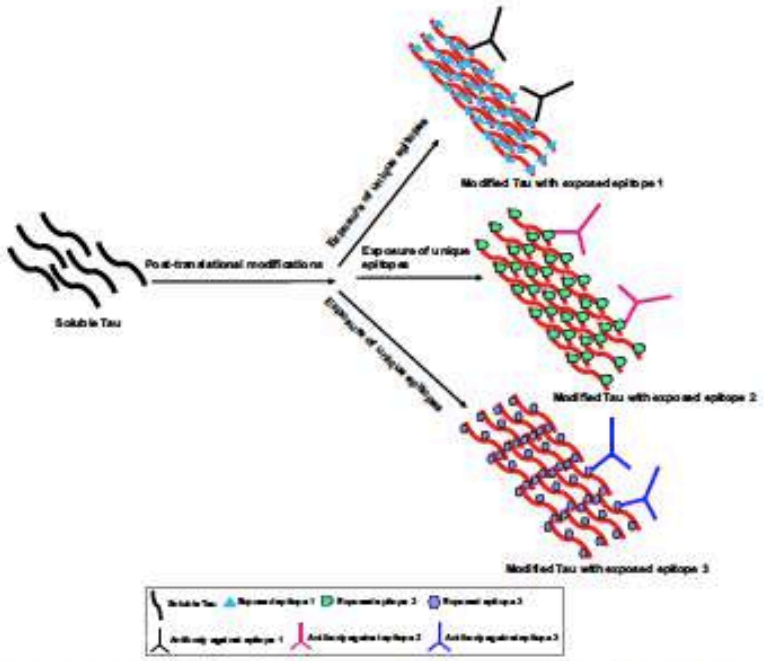

Fig. 3 Therapeutic importance to study prion-like properties of modified Tau: Immunotherapy by far has not been very successful in eliminating the prion pathogenesis. The illustration above tries to hypothesize one of the many reasons for their failure and the therapeutic importance to study modified Tau and its altered properties. Post-translational modifications can modify Tau such that modified Tau can have differently exposed epitopes which might not be recognized by the available antibodies or the targeted drugs. These epitopes can be unique to the modified protein and might not show the antibody cross reactivity, thus escaping the immune system of the body and propagating itself. Insights into the conformational epitopes of Tau can help in understanding the exact nature and characteristics of modified Tau which further can assist in designing the tailor made drugs or antibodies having more target specific effect as shown by different epitope specific antibodies

microtubule-binding (Matsuoka et al. 2007). Such effects necessitated its clinical evaluation but the early clinical analyses carried out in 144 subjects for 12 weeks failed to detect its statistically significant effect on cognitive improvement (Morimoto et al. 2013). There can be varied reasons for this failure. The failure in efficacy at the clinical level might be due to discrete properties of prion-like Tau in different individuals. The prion-like Tau might adopt distinct conformational strains which would be specific for individuals. This has been recently reported for the C-terminal conformational differences for prion protein with differential binding of epitopes to antibody (Saijo et al. 2016). These strains might have different exposed epitopes which might not bind to antibodies designed against some other common epitopes (Furik et al. 2015) (Fig. 3). For example, the Tau C3 antibody specific for the C-terminally truncated Tau can block the propagation of high molecular weight species of Tau (Nicholls et al. 2017). The study of prion-like properties of post-translationally modified Tau would help to design the specific or tailor-made drugs which would be more efficient and specific.

Conclusion

Post-translational modifications can have various implications on the protein characteristics. Here, we have reviewed glycation as a post-translational modification and its putative effects on the prion-like characteristic of Tau protein in AD. As this is an irreversible modification it does permanent damage to the proteins and might enhance its infectivity and propagation throughout the brain, leading to rapid neurodegeneration. In conclusion, it is highly important to study the effect of PTMs on Tau protein behaviour with respect to its propagation and spread in order to design a more targeted drug.

Acknowledgements Shweta Kishor Sonawane acknowledges a fellowship from the Department of Biotechnology (DBT), India. The authors acknowledge Abhishek Balmik and Nalini Vijay Gorantla for proofreading the manuscript and useful comments.

Funding This project was supported in part by grants from the Department of Science and Technology—Science and Engineering Research Board (DST-SERB, Young Investigator grant): SB/YS/LS-355/2013, Department of Biotechnology from Neuroscience Task Force (Medical Biotechnology-Human Development & Disease Biology (DBT-HDDB))-BT/PR/15780/MED/30/1629/2015 and in-house CSIR-National Chemical Laboratory grant MLP029526 and CSIR-network project BSC0115.

Compliance with Ethical Standards

Conflict of Interest Statement The authors have declared no conflict of interest.

References

Adjou KT et al (2003) A novel generation of heparan sulfate mimetics for the treatment of prion diseases. J Gen Virol 84:2595–2603

Ahmed Z et al (2014) A novel in vivo model of tau propagation with rapid and progressive neurofibrillary tangle pathology: the pattern of spread is determined by connectivity, not proximity. Acta Neuropathol 127:667–683

Alonso AC, Zaidi T, Novak M, Grundke-Iqbal I, Iqbal K (2001) Hyperphosphorylation induces self-assembly of τ into tangles of paired helical filaments/straight filaments. Proc Natl Acad Sci 98: 6923–6928

Alonso AC, Li B, Grundke-Iqbal I, Iqbal K (2006) Polymerization of hyperphosphorylated tau into filaments eliminates its inhibitory activity. Proc Natl Acad Sci 103:8864–8869

Alonso AD, Di Clerico J, Li B, Corbo CP, Alaniz ME, Grundke-Iqbal I, Iqbal K (2010) Phosphorylation of tau at Thr212, Thr231, and Ser262 combined causes neurodegeneration. J Biol Chem 285: 30851–30860

Batkulwar KB et al (2015) Investigation of phosphoproteome in RAGE signaling. Proteomics 15:245–259

Beitz J (2014) Parkinson's disease: a review. Front Biosci (Schol Ed) 6: 65–74

Binder LI, Frankfurter A, Rebhun LI (1985) The distribution of tau in the mammalian central nervous system. J Cell Biol 101:1371–1378

Bolton DC, Meyer RK, Prusiner SB (1985) Scrapie PrP 27-30 is a sialoglycoprotein. J Virol 53:596–606

Braak H, Braak E (1991) Neuropathological stageing of Alzheimer-related changes. Acta Neuropathol 82:239–259

Bulic B, Pickhardt M, Schmidt B, Mandelkow EM, Waldmann H, Mandelkow E (2009) Development of tau aggregation inhibitors for Alzheimer's disease. Angew Chem Int Ed 48:1740–1752

Cai Z et al (2016) Role of RAGE in Alzheimer's disease. Cell Mol Neurobiol 36:483–495

Calafate S, Flavin W, Verstreken P, Moechars D (2016) Loss of Bin1 promotes the propagation of tau pathology. Cell Rep 17:931–940

Cancellotti E et al (2010) Glycosylation of PrPC determines timing of neuroinvasion and targeting in the brain following transmissible spongiform encephalopathy infection by a peripheral route. J Virol 84:3464–3475

Cancellotti E et al (2013) Post-translational changes to PrP alter transmissible spongiform encephalopathy strain properties. EMBO J 32: 756–769

Caspi S, Halimi M, Yanai A, Sasson SB, Taraboulos A, Gabizon R (1998) The anti-prion activity of Congo red putative mechanism. J Biol Chem 273:3484–3489

Caughey B, Race RE, Ernst D, Buchmeier MJ, Chesebro B (1989) Prion protein biosynthesis in scrapie-infected and uninfected neuroblastoma cells. J Virol 63:175–181

Cho J-H, Johnson GV (2003) Glycogen synthase kinase 3β phosphorylates tau at both primed and unprimed sites. Differential impact on microtubule binding. J Biol Chem 278:187–193

Choi Y-G et al (2004) Nonenzymatic glycation at the N terminus of pathogenic prion protein in transmissible spongiform encephalopathies. J Biol Chem 279:30402–30409

Clavaguera F, Hench J, Goedert M, Tolnay M (2015) Invited review: prion-like transmission and spreading of tau pathology. Neuropathol Appl Neurobiol 41:47–58

Clavaguera F, Tolnay M, Goedert M (2016) The prion-like behavior of assembled Tau in transgenic mice. Cold Spring Harb Perspect Med 7(10):a024372

Congdon EE, Gu J, Sait HB, Sigurdsson EM (2013) Antibody uptake into neurons occurs primarily via clathrin-dependent Fcγ receptor endocytosis and is a prerequisite for acute tau protein clearance. J Biol Chem 288:35452–35465

Coppola G et al (2012) Evidence for a role of the rare p. A152T variant in MAPT in increasing the risk for FTD-spectrum and Alzheimer's diseases. Hum Mol Genet 21:3500–3512

Couto M et al (2009) Doxorubicin and Congo red effectiveness on prion infectivity in golden Syrian hamster. Anticancer Res 29:2507–2512

Dear D Vet al (2007) Effects of post-translational modifications on prion protein aggregation and the propagation of scrapie-like characteristics in vitro. Biochim Biophys Acta (BBA)-Proteins and Proteomics 1774:792–802

Drewes G et al (1992) Mitogen activated protein (MAP) kinase transforms tau protein into an Alzheimer-like state. EMBO J 11:2131

Drewes G et al (1995) Microtubule-associated protein/microtubule affinity-regulating kinase (p110mark) a novel protein kinase that regulates tau-microtubule interactions and dynamic instability by phosphorylation at the Alzheimer-specific site serine 262. J Biol Chem 270:7679–7688

D'Souza I, Schellenberg GD (2005) Regulation of tau isoform expression and dementia. Biochim Biophys Acta (BBA)-Molecular Basis of Disease 1739:104–115

Dvorakova E, Prouza M, Janovskova O, Panigaj M, Holada K (2011) Development of monoclonal antibodies specific for glycated prion protein. J Toxic Environ Health A 74:1469–1475

Eriksen JL, Wszolek Z, Petrucelli L (2005) Molecular pathogenesis of Parkinson disease. Arch Neurol 62:353–357

Fawver JN, Schall HE, Perrotes Chapa RD, Zhu X, Murray IV (2012) Amyloid-β metabolite sensing: biochemical linking of glycation modification and misfolding. J Alzheimers Dis 30:63–73

Frost B, Jacks RL, Diamond MI (2009) Propagation of tau misfolding from the outside to the inside of a cell. J Biol Chem 284:12845–12852

Funk KE, Mirbaha H, Jiang H, Holtzman DM, Diamond MI (2015) Distinct therapeutic mechanisms of tau antibodies: promoting microglial clearance versus blocking neuronal uptake. J Biol Chem 290:21652–21662

Gauczynski S et al (2001) The 37-kDa/67-kDa laminin receptor acts as the cell-surface receptor for the cellular prion protein. EMBO J 20: 5863–5875

Goedert M (2015) Alzheimer's and Parkinson's diseases: the prion concept in relation to assembled Aβ, tau, and α-synuclein. Science 349: 1255555

Goedert M, Spillantini MG (2000) Tau mutations in frontotemporal dementia FTDP-17 and their relevance for Alzheimer's disease. Biochim Biophys Acta (BBA)-Molecular Basis of Disease 1502: 110–121

Goedert M, Spillantini M, Jakes R, Rutherford D, Crowther R (1989) Multiple isoforms of human microtubule-associated protein tau: sequences and localization in neurofibrillary tangles of Alzheimer's disease. Neuron 3:519–526

Goedert M, Eisenberg DS, Crowther RA (2017a) Propagation of tau aggregates and neurodegeneration Annu Rev Neurosci 40:189–210

Goedert M, Masuda-Suzukake M, Falcon B (2017b) Like prions: the propagation of aggregated tau and α-synuclein in neurodegeneration. Brain J Neurol 140:266

Gong C-X, Liu F, Grundke-Iqbal I, Iqbal K (2005) Post-translational modifications of tau protein in Alzheimer's disease. J Neural Transm 112:813–838

Guo JL, Lee VM-Y (2011) Seeding of normal tau by pathological tau conformers drives pathogenesis of Alzheimer-like tangles. J Biol Chem 286:15317–15331

Hanger DP, Anderton BH, Noble W (2009) Tau phosphorylation: the therapeutic challenge for neurodegenerative disease. Trends Mol Med 15:112–119

Hasegawa M, Nonaka T, Masuda-Suzukake M (2017) Prion-like mechanisms and potential therapeutic targets in neurodegenerative disorders. Pharmacol Ther 172:22–33

Heiseke A, Aguib Y, Schatzl HM (2010) Autophagy, prion infection and their mutual interactions. Curr Issues Mol Biol 12:87

Holmes BB et al (2014) Proteopathic tau seeding predicts tauopathy in vivo. Proc Natl Acad Sci 111:E4376–E4385

Hong M et al (1998) Mutation-specific functional impairments in distinct tau isoforms of hereditary FTDP-17. Science 282:1914–1917

Hutton M et al (1998) Association of missense and 5′-splice-site mutations in tau with the inherited dementia FTDP-17. Nature 393:702–705

Ingram EM, Spillantini MG (2002) Tau gene mutations: dissecting the pathogenesis of FTDP-17. Trends Mol Med 8:555–562

Ittner LM et al (2010) Dendritic function of tau mediates amyloid-β toxicity in Alzheimer's disease mouse models. Cell 142:387–397

Johnson GV, Stoothoff WH (2004) Tau phosphorylation in neuronal cell function and dysfunction. J Cell Sci 117:5721–5729

Kadavath H et al (2015) Tau stabilizes microtubules by binding at the interface between tubulin heterodimers proceedings of the, vol 112. National Academy of Sciences, pp 7501–7506

Kaufman SK et al (2016) Tau prion strains dictate patterns of cell pathology, progression rate, and regional vulnerability in vivo. Neuron 92:796–812

Kfoury N, Holmes BB, Jiang H, Holtzman DM, Diamond MI (2012) Trans-cellular propagation of tau aggregation by fibrillar species. J Biol Chem 287:19440–19451

Kliks P-C, Castro-Seoane R, Collinge J (2013) Exosome release from infected dendritic cells: a clue for a fast spread of prions in the periphery? J Infect 67:359–368

Ko L-w, Ko HC, Nachanju P, Liu W-K, Chang E, Kenessey A, Yen S-HC (1999) An immunochemical study on tau glycation in paired helical filaments. Brain Res 830:301–313

Koriyama Y, Furukawa A, Muramatsu M, Takino J-i, Takeuchi M (2015) Glyceraldehyde caused Alzheimer's disease-like alterations in diagnostic marker levels in SH-SY5Y human neuroblastoma cells. Sci Rep 5:13313

Kurbatskaya K et al (2016) Upregulation of calpain activity precedes tau phosphorylation and loss of synaptic proteins in Alzheimer's disease brain. Acta Neuropathol Commun 4:34

Lasagna-Reeves CA et al (2012) Alzheimer brain-derived tau oligomers propagate pathology from endogenous tau. Scientific Report 2

Lasagna-Reeves CA et al (2014) The formation of tau pore-like structures is prevalent and cell specific: possible implications for the disease phenotypes. Acta Neuropathol Commun 2(1)

LeBoeuf AC et al (2008) FTDP-17 mutations in tau Alter the regulation of microtubule dynamics: an "alternative core" model for normal and pathological Tau action. J Biol Chem 283:36406–36415

Ledesma MD, Bonay P, Colaco C, Avila J (1994) Analysis of microtubule-associated protein tau glycation in paired helical filaments. J Biol Chem 269:21614–21619

Ledesma MD, Bonay P, Avila J (1995) τ protein from Alzheimer's disease patients is glycated at its tubulin-binding domain. J Neurochem 65:1658–1664

Li L, Nagpar S, Cashman NR (2010) Immunotherapy for prion diseases: opportunities and obstacles. Immunotherapy 2:269–282

Liu SJ et al (2004) Tau becomes a more favorable substrate for GSK-3 when it is prephosphorylated by PKA in rat brain. J Biol Chem 279:50078–50088

Liu K, Liu Y, Li L, Qin P, Iqbal J, Deng Y, Qing H (2016) Glycation alter the process of tau phosphorylation to change tau isoforms aggregation property. Biochim Biophys Acta (BBA)-Molecular Basis of Disease 1862:192–201

Lovestone S et al (2015) A phase II trial of tideglusib in Alzheimer's disease. J Alzheimers Dis 45:75–88

Mably AJ et al (2015) Tau immunization: a cautionary tale? Neurobiol Aging 36:1316–1332

Mandelkow E-M, Drewes G, Biernat J, Gustke N, Van Lint J, Jv V, Mandelkow E (1992) Glycogen synthase kinase-3 and the Alzheimer-like state of microtubule-associated protein tau. FEBS Lett 314:315–321

Margalith I et al (2012) Polythiophenes inhibit prion propagation by stabilizing prion protein (PrP) aggregates. J Biol Chem 287:18872–18887

Matsuoka Y et al (2007) Intranasal NAP administration reduces accumulation of amyloid peptide and tau hyperphosphorylation in a transgenic mouse model of Alzheimer's disease at early pathological stage. J Mol Neurosci 31:165–170

Mirbaha H, Holmes BB, Sanders DW, Bieschke J, Diamond MI (2015) Tau trimers are the minimal propagation unit spontaneously internalized to seed intracellular aggregation. J Biol Chem 290:14893–14903

Morimoto BH, Schmechel D, Hirman J, Blackwell A, Keith J, Gold M, Investigators A-S (2013) A double-blind, placebo-controlled, ascending-dose, randomized study to evaluate the safety, tolerability and effects on cognition of AL-108 after 12 weeks of intranasal administration in subjects with mild cognitive impairment. Dement Geriatr Cogn Disord 35:325–339

Mukrasch MD, von Bergen M, Biernat J, Fischer D, Griesinger C, Mandelkow E, Zweckstetter M (2007) The "jaws" of the tau-microtubule interaction. J Biol Chem 282:12230–12239

Necula M, Kuret J (2004) Pseudophosphorylation and glycation of tau protein enhance but do not trigger fibrillization in vitro. J Biol Chem 279:49694–49703

Nicholls SB et al (2017) Characterization of TauC3 antibody and demonstration of its potential to block tau propagation. PLoS One 12:e0177914

Ohgami N, Nagai R, Ikemoto M, Arai H, Kuniyasu A, Horiuchi S, Nakayama H (2001) Cd36, a member of the class b scavenger receptor family, as a receptor for advanced glycation end products. J Biol Chem 276:3195–3202

Ott C, Jacobs K, Haucke E, Santos AN, Grune T, Simm A (2014) Role of advanced glycation end products in cellular signaling. Redox Biol 2:411–429

Pooler AM, Phillips EC, Lau DH, Noble W, Hanger DP (2013) Physiological release of endogenous tau is stimulated by neuronal activity. EMBO Rep 14:389–394

Porto-Carreiro I, Février B, Paquet S, Vilette D, Raposo G (2005) Prions and exosomes: from PrPc trafficking to PrPsc propagation. Blood Cell Mol Dis 35:143–148

Reynolds MR, Berry RW, Binder LI (2005) Site-specific nitration differentially influences τ assembly in vitro. Biochemistry 44:13997–14009

Roettger Y, Du Y, Bacher M, Zerr I, Dodel R, Bach J-P (2013) Immunotherapy in prion disease. Nat Rev Neurol 9:98–105
Saijo E, Hughson AG, Raymond GJ, Suzuki A, Horiuchi M, Caughey B (2016) PrPSc-specific antibody reveals C-terminal conformational differences between prion strains. J Virol 90:4905–4913
Sanders DW et al (2014) Distinct tau prion strains propagate in cells and mice and define different tauopathies. Neuron 82:1271–1288
Schneider A, Biernat J, Von Bergen M, Mandelkow E, Mandelkow E-M (1999) Phosphorylation that detaches tau protein from microtubules (Ser262, Ser214) also protects it against aggregation into Alzheimer paired helical filaments. Biochemistry 38:3549–3558
Schweers O, Schönbrunn-Hanebeck E, Marx A, Mandelkow E (1994) Structural studies of tau protein and Alzheimer paired helical filaments show no evidence for beta-structure. J Biol Chem 269:24290–24297
Selkoe DJ (2001) Alzheimer's disease: genes, proteins, and therapy. Physiol Rev 81:741–766
Shyng S-L, Heuser JE, Harris DA (1994) A glycolipid-anchored prion protein is endocytosed via clathrin-coated pits. J Cell Biol 125:1239–1250
Song L et al (2015) Analysis of tau post-translational modifications in rTg4510 mice, a model of tau pathology. Mol Neurodegener 10:14
Steinhilb ML, Dias-Santagata D, Fulga TA, Felch DL, Feany MB (2007) Tau phosphorylation sites work in concert to promote neurotoxicity in vivo. Mol Biol Cell 18:5060–5068
Sydow A, Mandelkow E-M (2010) Prion-like propagation of mouse and human tau aggregates in an inducible mouse model of tauopathy. Neurodegener Dis 7:28–31
Takeda S et al (2015) Neuronal uptake and propagation of a rare phosphorylated high-molecular-weight tau derived from Alzheimer's disease brain. Nat Commun 6:8490
Taylor DR, Hooper NM (2007) The low-density lipoprotein receptor-related protein 1 (LRP1) mediates the endocytosis of the cellular prion protein. Biochem J 402:17–23
Tiwari SS et al (2016) Alzheimer-related decrease in CYFIP2 links amyloid production to tau hyperphosphorylation and memory loss. Brain 139:2751–2765
Theng H-C, Lu Q, Henderson E, Graves DJ (1999) Phosphorylated tau can promote tubulin assembly. Proc Natl Acad Sci 96:9503–9508
Vella L, Sharples R, Lawson V, Masters C, Cappai R, Hill A (2007) Packaging of prions into exosomes is associated with a novel pathway of PrP processing. J Pathol 211:582–590
Walker LC, Diamond MI, Duff KE, Hyman BT (2013) Mechanisms of protein seeding in neurodegenerative diseases. JAMA Neurol 70:304–310
Wang Y, Mandelkow E (2016) Tau in physiology and pathology. Nat Rev Neurosci 17:22–35
Wegmann S, Nicholls S, Takeda S, Fan Z, Hyman BT (2016) Formation, release, and internalization of stable tau oligomers in cells. J Neurochem 139:1163–1174
Wei Y, Han C, Wang Y, Wu B, Su T, Liu Y, He R (2015) Ribosylation triggering Alzheimer's disease-like tau hyperphosphorylation via activation of CaMKII. Aging Cell 14:754–763
Weingarten MD, Lockwood AH, Hwo S-Y, Kirschner MW (1975) A protein factor essential for microtubule assembly. Proc Natl Acad Sci 72:1858–1862
Wu JW et al (2013) Small misfolded tau species are internalized via bulk endocytosis and anterogradely and retrogradely transported in neurons. J Biol Chem 288:1856–1870
Wu JW et al (2016) Neuronal activity enhances tau propagation and tau pathology in vivo. Nat Neurosci 19:1085–1092
Xu L, Zheng J, Margittai M, Nussinov R, Ma B (2016) How does hyperphosphorylation promote tau aggregation and modulate filament structure and stability? ACS Chem Neurosci 7:565–575
Yan S et al (1994) Glycated tau protein in Alzheimer disease: a mechanism for induction of oxidant stress. Proc Natl Acad Sci 91:7787–7791

Journal of Alzheimer's Disease 75 (2020) 61–71
DOI 10.3233/JAD-191348
IOS Press

P301 L, an FTDP-17 Mutant, Exhibits Enhanced Glycation *in vitro*

Shweta Kishor Sonawane[a,b,*] and Subashchandrabose Chinnathambi[a,b,*]
[a]*Neurobiology Group, Biochemical Sciences Division, CSIR-National Chemical Laboratory, Pune, India*
[b]*Academy of Scientific and Innovative Research (AcSIR), Ghaziabad, India*

Accepted 17 February 2020

Abstract.
Background: Frontotemporal dementia and parkinsonism-linked to chromosome-17 are a group of diseases with tau mutations leading to primary tauopathies which include progressive supranuclear palsy, corticobasal syndrome, and frontotemporal lobar degeneration. Alzheimer's disease is a non-primary tauopathy, which displays tau neuropathology of excess tangle formation and accumulation. FTDP-17 mutations are responsible for early onset of AD, which can be attributed to compromised physiological functions due to the mutations. Tau is a microtubule-binding protein that secures the integrity of polymerized microtubules in neuronal cells. It malfunctions owing to various insults and stress conditions-like mutations and post-translational modifications.
Objective: In this study, we modified the wild type and tau mutants by methyl glyoxal and thus studied whether glycation can enhance the aggregation of predisposed mutant tau.
Methods: Tau glycation was studied by fluorescence assays, SDS-PAGE analysis, conformational evaluation, and transmission electron microscopy.
Results: Our study suggests that FTDP-17 mutant P301 L leads to enhanced glycation-induced aggregation as well as advanced glycation end products formation. Glycation forms amorphous aggregates of tau and its mutants without altering its native conformation.
Conclusion: The metabolic anomalies and genetic predisposition have found to accelerate tau-mediated neurodegeneration and prove detrimental for the early-onset of Alzheimer's disease.

Keywords: Advanced glycation end products, Alzheimer's disease, FTDP-17, tau glycation

INTRODUCTION

Alzheimer's disease (AD) is a progressive neurodegenerative disorder affecting the cognitive functions. Protein misfolding and aggregation in the brain is the major cause for neuronal dysfunction in AD. Amyloid-β (Aβ) and tau proteins aggregate and accumulate causing neuronal death and brain lesions. Aβ pro-aggregant peptide $A\beta_{1-42}$ forms senile plaques extracellularly. Recently, these senile plaques have been implicated in enhancing seeded tau aggregation in mouse brain. Tau aggregation and accumulation hampers neuronal functioning and microtubule stability. Tau is a natively unfolded protein and is involved in microtubule dynamics by association with the labile domain. Tau is a microtubule-associated protein playing a pivotal role in stabilizing the axonal microtubules [1, 2]. Tau protein is broadly divided into two major domains. The N-terminal projection domain consisting of two inserts and a polyproline rich

*Correspondence to: Ms. Shweta Kishor Sonawane and Prof. Subashchandrabose Chinnathambi, Neurobiology group, Division of Biochemical Sciences, CSIR-National Chemical Laboratory (CSIR-NCL), Dr. Homi Bhabha Road, 411008 Pune, India. Tel.: +91 20 25902232; Fax: +91 20 25902648; E-mails: sk.sonawane@ncl.res.in and s.chinnathambi@ncl.res.in

region. The projection domain maintains the flexibility and the hydrophilicity of the protein. The C-terminal region consists of 4 imperfect repeats which function in binding to the microtubules and stabilizing them [3, 4]. Tau has 6 isoforms based on the alternative splicing of exon 2 and 10 [5]. Tau pathology in AD is sporadic as well as genetic. The genetic mutations leading to tau pathology belong to frontotemporal dementia group of mutations. Frontotemporal dementias are the group of disorders characterized by degeneration of cerebral cortex and sub-cortical regions of substantia nigra [6]. The initial reports of familial linkage of disease mutations to the chromosome locus 17q21-22 were published in 1994 for disinhibition-dementia-parkinsonism-amyotrophy complex (DDPAC) [7], which was subsequently grouped under frontotemporal dementia and parkinsonism-linked to chromosome-17 (FTDP-17) in 1996 [8]. FTDP-17 is an autosomal dominant disorder phenotypically characterized by behavioral, motor, and memory impairments [9–11]. Tau mutations are missense, deletion, or silent which either affects the protein coding or the splicing events depending on the locus [12, 13]. The mutations that affect the splicing sites alters the 3 repeat to 4 repeat tau ratios [14]. Moreover, the combination of tau isoforms and the FTDP-17 mutations affect the parameters like aggregation kinetics and aggregate length, thus, having important implication in the disease pathogenesis [15]. Tau missense mutations affect its functions in two ways. Some of these mutations reduce the affinity of tau to microtubules [16] and others render tau to increased aggregation forming neurofibrillary tangles in the brain [17]. The missense FTDP-17 mutations include P301 L, G272 V, V337M, K369I, and R406 W. The mutations G272 V, P301 L, G303 V, S320F, and S352 L, among others, demonstrate increased aggregation propensity compared to the wild type tau [18, 19]. Moreover, the ability to polymerize tau varies with the mutation. The mutations P301 L, G303 V, and S320F induce tubulin polymerization at a slower pace compared to wild type, whereas V337M and E342 V enhanced the rate of tubulin assembly [18]. The slight decrease in the affinity of tau to microtubules can completely hamper the stability of microtubules. Moreover, decreased affinity can render the increased cytoplasmic concentration of tau accelerating its self-assembly and aggregation [20]. Familial AD accounts for 2-5% of the total AD cases and is associated with the early onset of the disease, before 60–65 years of age [21, 22] which includes genetic mutations. In addition, one of the most important aspects of AD is the abnormal post-translational modifications (PTMs) of tau, which hampers its functions and increases the propensity of self-aggregation [2, 23]. Abnormal phosphorylation of tau in AD is studied in its complete depth and is one of the key player of tau pathology in AD [24, 25]. Another important tau PTM is glycation, which reduces tau's affinity for microtubules [26–28]. Glycation affects the proteins by forming cross-links and rendering it protease resistant [29, 30]. It also leads to protein aggregation and accumulation [31, 32]. Few reports suggest that tau glycation might not trigger its fibrillization but may enhance the already initiated fibrillization process [33]. The effect of PTMs on the dementia mutants is still unexplored, whether it can enhance or modulate the tau pathology. Here, we report the effect of glycation on selected tau dementia mutants G272 V, P301 L, and R406 W (Fig. 1A). Glycation enhanced the aggregation of P301 L tau with subsequent increase in advanced glycation end products (AGEs). However, glycation did not alter the global conformation tau.

MATERIALS AND METHODS

Chemicals and reagents

Methyl glyoxal, ThS, ThT, ANS, Glycine, MES, BES, and SDS were obtained from Sigma; Luria-Bertani broth (Himedia); Ampicillin, Heparin, NaCl, Phenylmethylsulfonylfluoride (PMSF), $MgCl_2$, Sodium azide, APS, Ethanol (Mol Bio grade), were purchased from MP biomedicals; IPTG and Dithiothreitol (DTT) were from Calbiochem; EGTA, Tris base, Acrylamide, and TEMED were obtained from Invitrogen. Protease inhibitor cocktail was purchased from Roche. Methyl glyoxal should be handled with care. Any contact with skin and eyes should be avoided. Inhalation of vapors must be avoided. It is advised to wear gloves and safety goggles while handling the chemical.

Tau purification

Protein purification for full-length tau and the FTDP-17 mutants was carried out as previously described. Full-length recombinant tau and mutants were expressed in *E. coli* BL21* strain. The cell pellets were homogenized under high pressure (15,000 psi) in a microfluidics device (Constant Cell

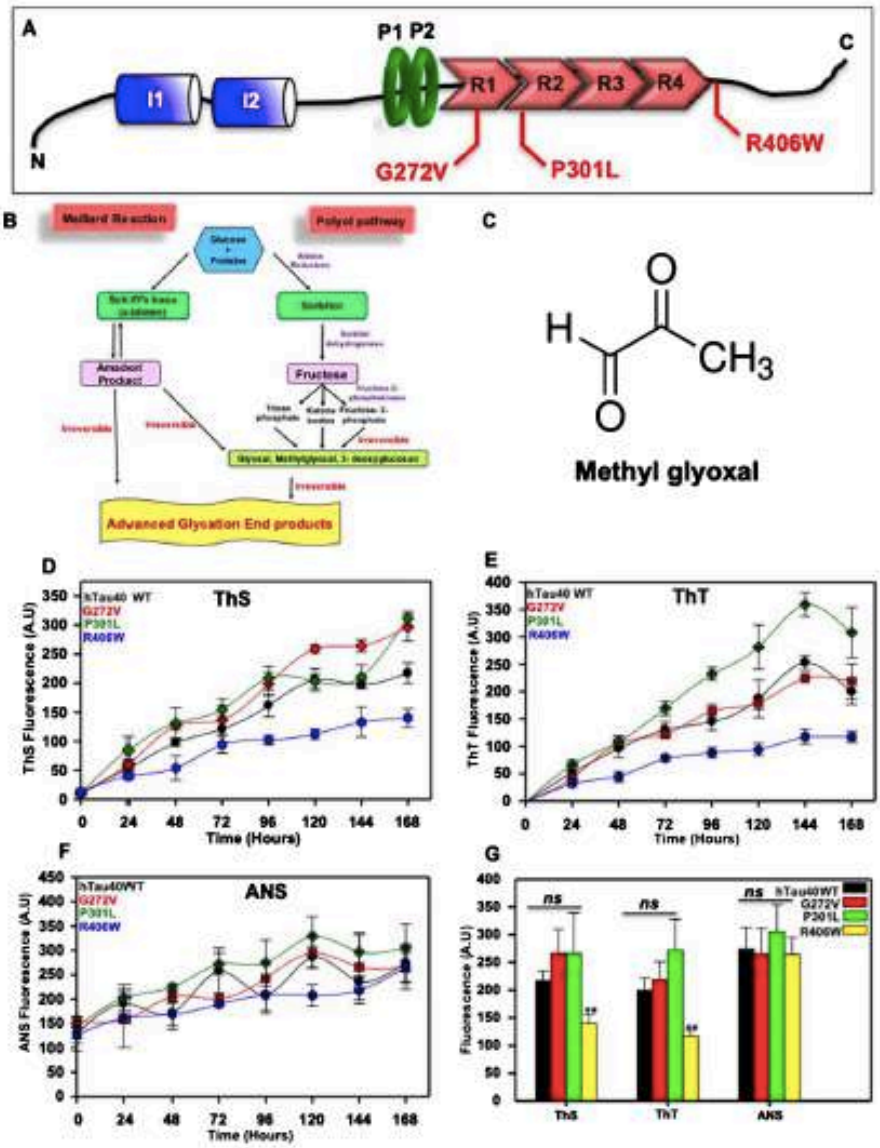

Fig. 1. MG-induced aggregation of tau and FTDP-17 mutants. A) Tau protein showing distinct functional domains with two inserts (blue blocks) at the N-terminal. Polyproline rich region denoted by green rings followed by 4 imperfect repeats (red arrows) involved in microtubule-binding and also involved in tau aggregation. The tau missense mutations are denoted in red, G272 V, P301 L, and R406 W, which are involved in tau dysfunction. B) The polyol pathway showing the formation of reactive metabolites like glyoxal and methyl glyoxal (MG) that are precursors of advanced glycation end products. C) Structure of MG, a reactive aldehyde accumulating in aging brain. D) ThS fluorescence analysis for MG-induced aggregation showing enhanced aggregation of mutants G272 V and P301 L as compared to control. E) ThT fluorescence assay shows similar observation as ThS analysis wherein the mutants show enhanced aggregation propensity as compared to control. F) The hydrophobicity transitions probed by ANS fluorescence reveal no distinct change in wild-type tau versus mutants. G) The comparative analysis of all fluorophores show that R406 W shows suppressed aggregation in presence of MG as compared to wild-type whereas G272 V and P301 L follow the wild-type tau with increased aggregation by MG ($p < 0.01$).

Disruptor). The obtained lysate was heated at 90°C for 15 min after addition of 0.5 M NaCl and 5 mM DTT. The heated lysate was then cooled and centrifuged at 40,000 rpm for 50 min in Optima XPN-100 ultracentrifuge (Beckman coulter). The supernatant was collected and dialyzed in Sepharose A buffer overnight. The obtained dialyzed sample was subjected to a second round of ultracentrifugation and the supernatant was loaded onto the cation exchange column (Sepharose fast flow GE healthcare) for further purification. The bound protein was eluted using an ionic gradient. The eluted fractions were pooled and concentrated for size exclusion chromatography (16/600 Superdex 75pg GE healthcare). The concentration of respective proteins was measured using BCA method.

MG-induced tau aggregation assay

20 μM full-length tau and its FTDP-17 mutants were incubated in BES buffer pH 7.4 with 2.5 mM methyl glyoxal as a glycating agent. The extrinsic fluorophores were added to the reaction mixtures to a concentration of 2.5 μM for thioflavin S and thioflavin T and 400 μM for ANS respectively. The reaction mixture was supplemented with 25 mM NaCl, 0.01% sodium azide, protease inhibitor cocktail, and 1 mM DTT. The mixtures were made in opaque tubes to avoid fluorescence bleaching at 37°C. For measurement of extrinsic fluorophores (ThS, ThT, and ANS), samples were diluted to 5 μM of tau in ammonium acetate (pH 7.0). The excitation/emission for the fluorophores was as follows: ThS 441/521, ThT 435/485, and ANS 375/490. The measurements were acquired in triplicates every 24 h. Background fluorescence was subtracted from the obtained readings. The fluorescence measurements were carried in TECAN Infinite series Pro plate reader.

Measurement of AGEs-specific fluorescence

The reaction mixture was set as mentioned above except the addition of the extrinsic fluorophores. For measurement of AGEs-specific fluorescence, the 50 μL of 20 μM reaction mixture was aliquoted in 384 black-well plate and reading was acquired at excitation/emission 370 nm/430 nm in TECAN Infinite series Pro plate reader. Buffer background was subtracted from the obtained readings.

SDS-PAGE

The glycated tau and mutants were analyzed on 10% SDS-PAGE at the interval of 24 h. 10 μL of the reaction mixtures were analyzed at each time point. Gels were stained with 0.1% Coomassie brilliant blue.

Transmission electron microscopy (TEM)

The glycated proteins were visualized by TEM. 2 μM of glycated proteins were applied to 400 mesh carbon coated copper grids for 1 min. The grids were rinsed with ultra-pure water and stained with 2% uranyl acetate for 2 min. Further the grids were dried and scanned in Tecnai G2 20 S-Twin transmission electron microscope.

CD spectroscopy

Glycation-induced conformational changes were mapped by CD spectroscopy. The modified and unmodified tau proteins were diluted to 3 μM in 50 mM phosphate buffer pH 6.8 in a cuvette with a path length of 1 mm. The scanning was done using Jasco J-815 CD spectrometer under nitrogen atmosphere. The scan was carried out with following parameters; bandwidth 1 nm, scan speed 100 nm/min; scan range 190 to 250 nm, and an average of 5 acquisitions. All the scans were done at 25°C. The buffer baseline was set with phosphate buffer, pH 6.8.

Statistical analysis

The statistical analyses were carried out using unpaired *T*-test by SigmaPlot 10.2. The error bars represent mean ± SD values. 95% confidence intervals were maintained for the analyses.

RESULTS AND DISCUSSION

Tau mutant P301 L shows enhanced MG-induced aggregation

Tau FTDP-17 mutations decrease the microtubule-binding affinity of tau [34] and also enhance the heparin-induced assembly of tau *in vitro* [35]. In our study, we investigated the glycation-induced aggregation of tau and its mutants. Glycation of proteins by sugars and their reactive intermediates, cross-links

and aggregates proteins [36]. Methyl glyoxal (MG) is a highly reactive byproduct of glucose metabolism in glycolysis and polyol pathway (Fig. 1B) and a precursor of AGEs [37] (Fig. 1C). AD brains are reported to show excess accumulation of MG and AGEs [38–40]. In order to study MG-induced protein aggregation, tau and its FTDP-17 mutants G272 V, P301 L, and R406 W were subjected to MG treatment *in vitro* and aggregation kinetics was studied using three fluorescent probes. These extrinsic fluorophores have discreet binding affinities, which give information about varied folding states during the aggregation [41]. We employed three extrinsic fluorophores, Thioflavin S (ThS), Thioflavin T (ThT), and ANS, to study aggregation of tau and its mutants. ThS and ThT are structurally different. ThS has two quaternary nitrogen atoms. Both these dyes have similar binding sites. They bind to β-sheets formed during protein aggregation and fluorescence according to the extent of aggregation. ThS binds to mature fibrils and not to monomers and oligomers. ThS aggregation studies showed that MG enhanced the aggregation of the dementia mutants G272 V and P301 L as compared to wild-type tau (Fig. 1D). R406 W tau had a very low ThS signal intensity suggesting decreased MG-induced aggregation as compared to wild-type control (Fig. 1D). ThT kinetic studies followed the similar trend with P301 L showing highest aggregation propensity and R406 showing the least (Fig. 1E). ThS and ThT followed the similar pattern of kinetics for glycation-induced aggregation. Further, we checked the effect of MG-induced hydrophobicity changes in tau and its mutants by ANS dye. ANS binds to hydrophobic regions of aggregated proteins, which are exposed during the transition of monomers to polymers [42]. These species are transient and might be short lived and hence not captured by ThS and ThT. ANS assay did not show any difference between the tau wild-type and its mutants suggesting that there is no difference of hydrophobicity of proteins while transitioning from monomers to polymers (Fig. 1F).

One of the recent finding suggests that the FTDP-17 mutants enhance oligomer formation under heparin induction especially the P301 L mutant show small and more granular oligomers as compared to wild-type control [43]. But glycation-induced aggregation did not show enhanced oligomerization by ANS fluorescence. Thus, the comparative analyses of tau and its mutants for the extrinsic fluorophores suggest that P301 L and G272 V show more glycation-induced aggregation as compared to control (Fig. 1G). Glycation enhances aggregation propensity of tau mutants (P301 L and G272 V) as compared to wild-type tau.

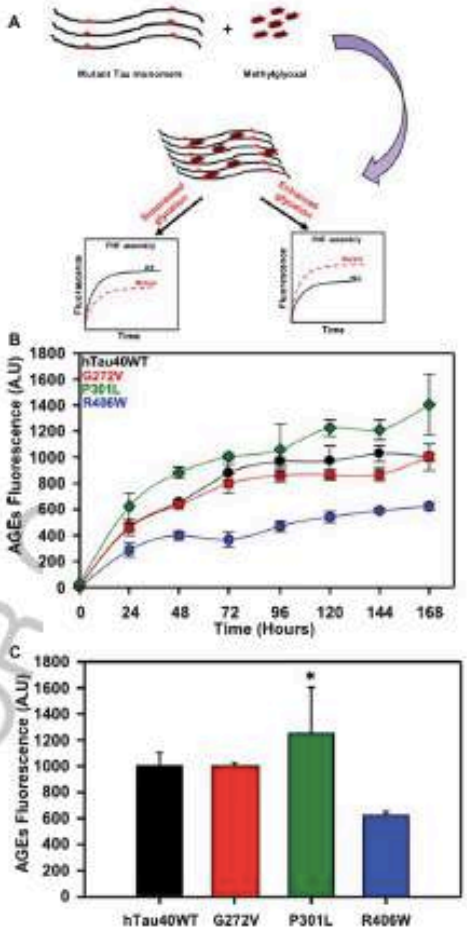

Fig. 2. Advanced glycation end products formation propensity of tau and its mutants. A) Hypothetical model to check the effect of glycation on AGEs formation. The mutants can either demonstrate an increased or decreased propensity for AGEs formation as compared to wild type tau that is quantitated by AGEs-specific fluorescence. B) The AGEs-specific fluorescence reveals increase in intensity with time for tau and its mutants. P301 L mutant shows highest AGEs formation as compared to control. C) The comparison of last time point fluorescence intensity reveals that the mutant P301 L shows more propensity for glycation as compared to wild-type tau ($p < 0.05$).

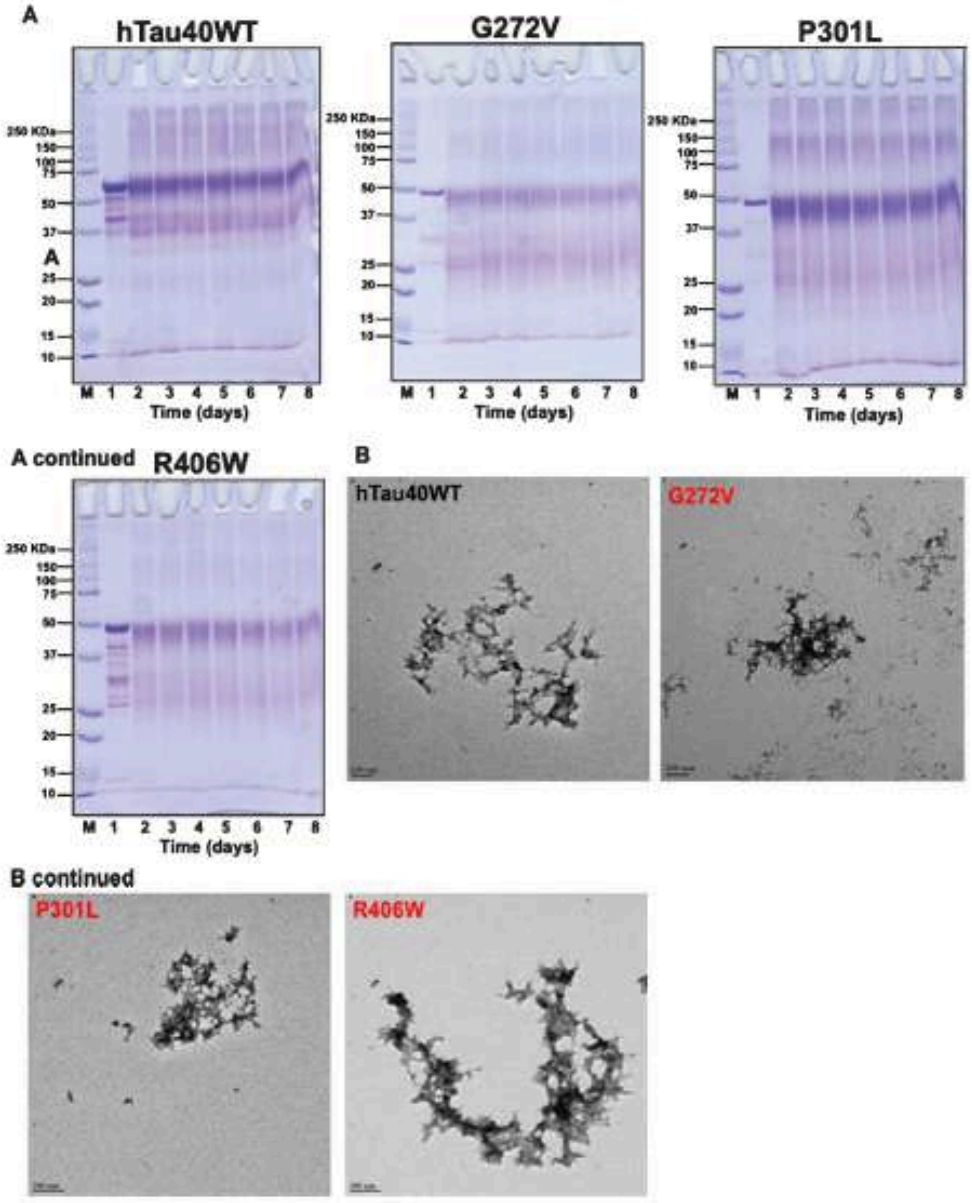

Fig. 3. SDS-PAGE and morphological evaluation of glycated tau proteins. A) SDS-PAGE evaluation of glycated tau shows formation of SDS-resistant glycated proteins, which aggregate and can be visualized as a trail on the separating gel at higher molecular weight than the soluble protein. B) Electron micrographs of the glycated tau and its mutants reveal formation of amorphous aggregates.

P301L tau mutant shows more AGEs formation on MG induction

Glycation of proteins leads to formation of brown and fluorescent protein adducts, which can be quantitated by AGEs-specific fluorescence. AGE-specific fluorescence was initially utilized to study the extent of diabetic complications [44–46]. Further this technique was used as a non-invasive tool to determine the skin fluorescence in diabetic patients [47]. AGE-specific fluorescence is detected at the excitation/emission 300-420/420-600 nm. We hypothesized whether the tau mutations would enhance AGEs formation or suppress it as compared to the wild-type control (Fig. 2A). The glycation induced aggregation studies revealed enhanced aggregation of P301 L mutant over the wild type. Further, the AGEs formation of tau and its mutants was investigated in the presence of MG by the AGEs-specific fluorescence. The tau mutant P301 L showed increased fluorescence as compared to control. G272 V and R406 W mutants showed decreased AGEs-specific fluorescence than wild-type (Fig. 2B). The comparative analysis of AGEs-specific

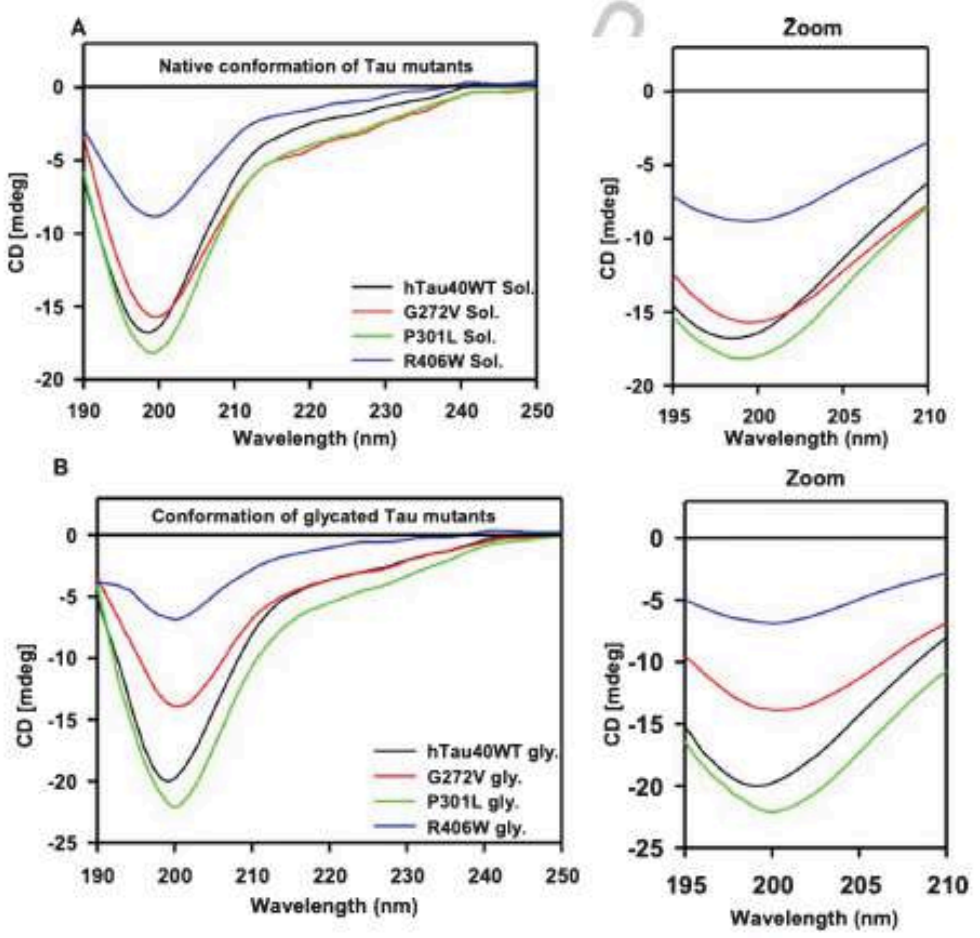

Fig. 4. Effect of glycation on global conformation of tau proteins. A) The native conformation of tau and its FTDP-17 mutants show native random coil conformation and maximum ellipticity at 198 nm. B) Glycation does not alter the global conformation of tau and its mutants. Glycated proteins show native conformation with maximum ellipticity at 198 nm.

fluorescence at 168 h revealed that P301 L showed enhanced AGEs formation as compared to control (Fig. 2C). Although tau glycation for FTDP-17 mutants is unexplored, MG-induced glycation has been found to accelerate tau aggregation in presence of hyperphosphorylation [48]. Thus, dual modification might have an additional impact on the tau pathology. The mutant R406 W showed least AGEs fluorescence as compared to other mutants. This mutant also exhibited least MG-induced aggregation, which might be attributed to the local conformational changes caused by this mutation. Similar reports have been recently published wherein the tau R406 W mutant resists phosphorylation by various kinase [49]. A transgenic experimental model of diabetes mellitus expressing P301 L tau showed increased tau hyperphosphorylation and tangle deposition [50]. Our *in vitro* glycation data suggests P301 L mutant showed enhanced AGEs formation, which supports the *in vivo* findings. Thus, this mutation might play an important role in accelerating brain pathology in early onset of AD.

Protein glycation forms protein cross-linking and aggregation [51] which accumulates steadily over time due to slow clearance of these proteins as they are resistant to most proteases. Moreover, glycation renders more stability [52] to the proteins leading to bulk deposition over the years [53, 54]. In order to study the nature of these aggregates SDS-PAGE analysis was performed at 24-h time intervals. At 0 time point, we observed a single soluble protein band for tau and its FTDP-17 mutants. As the time progressed, the soluble protein was no longer intact and had formed higher order aggregates (Fig. 3A). The aggregates were SDS-resistant and migrated on the separating gel in a continuous trail of cross-linked proteins. The extent of glycation differed between the mutants and the wild type. Mutant P301 L had enhanced glycated

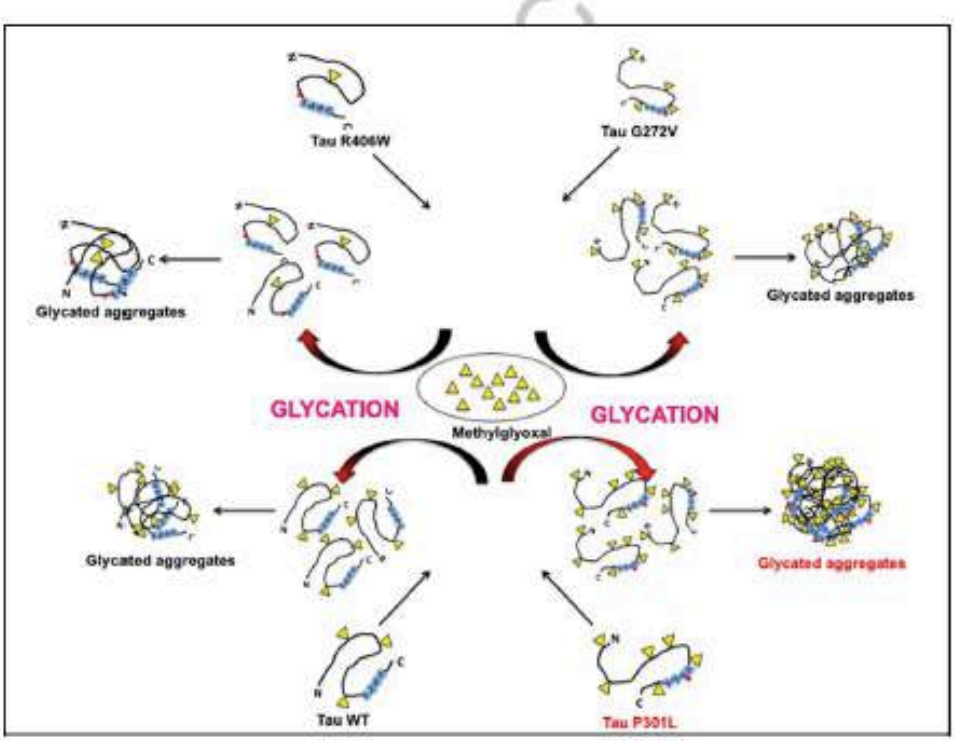

Fig. 5. Enhanced MG-induced glycation of tau P301 L. The glycating agent MG show enhanced glycation for the tau dementia mutant P301 L with large aggregate formation as compared to wild-type. This might be due to differentially exposed amino acids in WT versus the P301 L mutant that leads to enhanced modification by MG. The other mutant G272 V showed basal level of glycation as control whereas R406 W mutant showed less glycation as compared to control. This model shows additional pathological feature of a predisposed tau dementia mutant, which might enhance tau dysfunction in a combinatorial manner.

products on the SDS-PAGE as compared to control. G272 V and R406 W mutants showed decreased glycated proteins on SDS-PAGE as compared to control. Thus, the FTDP-17 mutant P301 L showed enhanced glycation as compared to control. The heparin induced aggregation of tau protein leads to formation of the fibrillar aggregates as visualized by TEM [55]. We visualized the glycation-induced tau aggregates by TEM for tau and its mutants. Glycation led to the formation of amorphous aggregates completely discreet from the heparin-induced fibrillar aggregates (Fig. 3B). The morphology did not alter for tau and its mutants. Similar observation has been previously made for a 2 repeat tau peptide which forms dimers on glycation but does form filamentous aggregates [56].

Glycation does not alter the conformation of tau and its mutants

The modification of proteins in AGEs alters the structure and function of the proteins rendering it prone to aggregation and protease resistant. [31, 57]. Tau is natively random coil lacking a rigid structure. On aggregation, it adopts a partial β-sheet structure [58, 59]. In order to study the effect of glycation on tau and its mutants, we studied the global conformation of glycated and non-glycated soluble tau and its mutants by CD spectroscopy. The conformational analysis of soluble proteins revealed a typical random coil structure (Fig. 4A). The maximum ellipticity was observed at around 198 nm for all the proteins suggesting a complete random coil structure (Fig. 4A zoom). The glycated proteins also showed CD spectra of random coil conformation (Fig. 4B). The maximum ellipticity was unaltered at 198 nm, same as that of soluble protein. Thus, glycation does not alter tau native conformation. This is in conjunction with previous studies wherein glycation can induce the 3D structural changes differently for different proteins [52, 60].

The connection between AD and glycation have been suggested in the earlier reports [61]. Moreover, tau pathology is enhanced due to insulin-mediated hyperphosphorylation suggesting a link between diabetes and tauopathy [62–64]. Hyperphosphorylated tau is known to undergo enhanced glycation [48]. Thus, metabolic anomalies and genetic predisposition have found to accelerate tau-mediated neurodegeneration and prove detrimental for the early-onset of AD (Fig. 5).

ACKNOWLEDGMENTS

This project is supported in part by grants from the Department of Biotechnology from Neuroscience Task Force (Medical Biotechnology-Human Development & Disease Biology (DBT-HDDB))-BT/PR/19562/MED/122/13/2016 and in-house CSIR-National Chemical Laboratory grant MLP029526. SS acknowledges DBT for the fellowship.

Authors' disclosures available online (https://www.j-alz.com/manuscript-disclosures/19-1348r2).

REFERENCES

[1] Lewis SA, Ivanov IE, Lee G-H, Cowan NJ (1989) Organization of microtubules in dendrites and axons is determined by a short hydrophobic zipper in microtubule-associated proteins MAP2 and tau. *Nature* **342**, 498-505.

[2] Sonawane SK, Chinnathambi S (2018) Prion-like propagation of post-translationally modified tau in Alzheimer's disease: A hypothesis. *J Mol Neurosci* **65**, 480-490.

[3] Brandt R, Lee G (1993) Functional organization of microtubule-associated protein tau. Identification of regions which affect microtubule growth, nucleation, and bundle formation in vitro. *J Biol Chem* **268**, 3414-3419.

[4] Gorantla NV, Chinnathambi S (2018) Tau protein squired by molecular chaperones during Alzheimer's disease. *J Mol Neurosci* **66**, 356-368.

[5] Goedert M, Spillantini M, Jakes R, Rutherford D, Crowther R (1989) Multiple isoforms of human microtubule-associated protein tau: Sequences and localization in neurofibrillary tangles of Alzheimer's disease. *Neuron* **3**, 519-526.

[6] Englund B, Brun A, Gustafson L, Passant U, Mann D, Neary D, Snowden J (1994) Clinical and neuropathological criteria for frontotemporal dementia. *J Neurol Neurosurg Psychiatry* **57**, 416-418.

[7] Wilhelmsen K, Lynch T, Pavlou E, Higgins M, Nygaard T (1994) Localization of disinhibition-dementia-parkinsonism-amyotrophy complex to 17q21-22. *Am J Hum Genet* **55**, 1159-1165.

[8] Foster NL, Wilhelmsen K, Sima AA, Jones MZ, D'Amato CJ, Gilman S, Participants C (1997) Frontotemporal dementia and parkinsonism linked to chromosome 17: A consensus conference. *Ann Neurol* **41**, 706-715.

[9] Pijnenburg YA, Mulder JL, Van Swieten JC, Uitdehaag BM, Stevens M, Scheltens P, Jonker C (2008) Diagnostic accuracy of consensus diagnostic criteria for frontotemporal dementia in a memory clinic population. *Dement Geriatr Cogn Disord* **25**, 157-164.

[10] Hulette C, Pericak-Vance MA, Roses A, Schmechel D, Yamaoka L, Gaskell P, Welsh-Bohmer K, Crowther R, Spillantini M (1999) Neuropathological features of frontotemporal dementia and parkinsonism linked to chromosome 17q21-22 (FTDP-17): Duke family 1684. *J Neuropathol Exp Neurol* **58**, 859-866.

[11] Wszolek ZK, Tsuboi Y, Ghetti B, Pickering-Brown S, Baba Y, Cheshire WP (2006) Frontotemporal dementia and parkinsonism linked to chromosome 17 (FTDP-17). *Orphanet J Rare Dis* **1**, 30.

[12] Grover A, Houlden H, Baker M, Adamson J, Lewis J, Prihar G, Pickering-Brown S, Duff K, Hutton M (1999) 5' splice site mutations in tau associated with the inherited dementia FTDP-17 affect a stem-loop structure that regulates alternative splicing of exon 10. *J Biol Chem* **274**, 15134-15143.

[13] Hutton M, Lendon CL, Rizzu P, Baker M, Froelich S, Houlden H, Pickering-Brown S, Chakraverty S, Isaacs A, Grover A, Hackett J, Adamson J, Lincoln S, Dickson D, Davies P, Petersen RC, Stevens M, de Graaff E, Wauters E, van Baren J, Hillebrand M, Joosse M, Kwon JM, Nowotny P, Che LK, Norton J, Morris JC, Reed LA, Trojanowski J, Basun H, Lannfelt L, Neystat M, Fahn S, Dark F, Tannenberg T, Dodd PR, Hayward N, Kwok JB, Schofield PR, Andreadis A, Snowden J, Craufurd D, Neary D, Owen F, Oostra BA, Hardy J, Goate A, van Swieten J, Mann D, Lynch T, Heutink P (1998) Association of missense and 5'-splice-site mutations in tau with the inherited dementia FTDP-17. *Nature* **393**, 702-705.

[14] Hong M, Zhukareva V, Vogelsberg-Ragaglia V, Wszolek Z, Reed L, Miller BI, Geschwind DH, Bird TD, McKeel D, Goate A (1998) Mutation-specific functional impairments in distinct tau isoforms of hereditary FTDP-17. *Science* **282**, 1914-1917.

[15] Mutreja Y, Combs B, Gamblin TC (2018) FTDP-17 mutations alter the aggregation and microtubule stabilization propensity of tau in an isoform-specific fashion. *Biochemistry* **58**, 742-754.

[16] LeBoeuf AC, Levy SF, Gaylord M, Bhattacharya A, Singh AK, Jordan MA, Wilson L, Feinstein SC (2008) FTDP-17 mutations in Tau alter the regulation of microtubule dynamics: An "alternative core" model for normal and pathological Tau action. *J Biol Chem* **283**, 36406-36415.

[17] Nacharaju P, Lewis J, Easson C, Yen S, Hackett J, Hutton M, Yen S-H (1999) Accelerated filament formation from tau protein with specific FTDP-17 missense mutations. *FEBS Lett* **447**, 195-199.

[18] Combs B, Gamblin TC (2012) FTDP-17 tau mutations induce distinct effects on aggregation and microtubule interactions. *Biochemistry* **51**, 8597-8607.

[19] von Bergen M, Barghorn S, Li L, Marx A, Biernat J, Mandelkow E-M, Mandelkow E (2001) Mutations of tau protein in frontotemporal dementia promote aggregation of paired helical filaments by enhancing local β-structure. *J Biol Chem* **276**, 48165-48174.

[20] Santacruz K, Lewis J, Spires T, Paulson J, Kotilinek L, Ingelsson M, Guimaraes A, DeTure M, Ramsden M, McGowan E (2005) Tau suppression in a neurodegenerative mouse model improves memory function. *Science* **309**, 476-481.

[21] Bird TD (2015) Alzheimer disease overview. In *GeneReviews®*[Internet], Adam MP, Ardinger HH, Pagon RA, et al., eds. University of Washington, Seattle.

[22] Mendez MF (2017) Early-onset Alzheimer disease. *Neurol Clin* **35**, 263-281.

[23] Martin L, Latypova X, Terro F (2011) Post-translational modifications of tau protein: Implications for Alzheimer's disease. *Neurochem Int* **58**, 458-471.

[24] Noble W, Hanger DP, Miller CC, Lovestone S (2013) The importance of tau phosphorylation for neurodegenerative diseases. *Front Neurol* **4**, 83.

[25] Johnson GV, Stoothoff WH (2004) Tau phosphorylation in neuronal cell function and dysfunction. *J Cell Sci* **117**, 5721-5729.

[26] Ledesma MD, Bonay P, Colaco C, Avila J (1994) Analysis of microtubule-associated protein tau glycation in paired helical filaments. *J Biol Chem* **269**, 21614-21619.

[27] Ledesma MD, Bonay P, Avila J (1995) Tau protein from Alzheimer's disease patients is glycated at its tubulin-binding domain. *J Neurochem* **65**, 1658-1664.

[28] Nacharaju P, Ko Lw, Yen SHC (1997) Characterization of *in vitro* glycation sites of tau. *J Neurochem* **69**, 1709-1719.

[29] Monnier VM, Kohn RR, Cerami A (1984) Accelerated age-related browning of human collagen in diabetes mellitus. *Proc Natl Acad Sci U S A* **81**, 583-587.

[30] Schnider SL, Kohn R (1981) Effects of age and diabetes mellitus on the solubility and nonenzymatic glucosylation of human skin collagen. *J Clin Invest* **67**, 1630-1635.

[31] Bansode SB, Chougale AD, Joshi RS, Giri AP, Bodhankar SL, Harsulkar AM, Kulkarni MJ (2013) Proteomic analysis of protease resistant proteins in the diabetic rat kidney. *Mol Cell Proteomics* **12**, 228-236.

[32] Dei R, Takeda A, Niwa H, Li M, Nakagomi Y, Watanabe M, Inagaki T, Washimi Y, Yasuda Y, Horie K (2002) Lipid peroxidation and advanced glycation end products in the brain in normal aging and in Alzheimer's disease. *Acta Neuropathol* **104**, 113-122.

[33] Necula M, Kuret J (2004) Pseudophosphorylation and glycation of tau protein enhance but do not trigger fibrillization in vitro. *J Biol Chem* **279**, 49694-49703.

[34] Hasegawa M, Smith MJ, Goedert M (1998) Tau proteins with FTDP-17 mutations have a reduced ability to promote microtubule assembly. *FEBS Lett* **437**, 207-210.

[35] Goedert M, Jakes R, Crowther RA (1999) Effects of frontotemporal dementia FTDP-17 mutations on heparin-induced assembly of tau filaments. *FEBS Lett* **450**, 306-311.

[36] Miranda HV, Outeiro TF (2010) The sour side of neurodegenerative disorders: The effects of protein glycation. *J Pathol* **221**, 13-25.

[37] Allaman I, Bélanger M, Magistretti PJ (2015) Methylglyoxal, the dark side of glycolysis. *Front Neurosci* **9**, 23.

[38] Münch G, Thome J, Foley P, Schinzel R, Riederer P (1997) Advanced glycation endproducts in ageing and Alzheimer's disease. *Brain Res Rev* **23**, 134-143.

[39] Angeloni C, Zambonin L, Hrelia S (2014) Role of methylglyoxal in Alzheimer's disease. *Biomed Res Int* **2014**, 238485.

[40] Richter T, Münch G, Lüth H-J, Arendt T, Kientsch-Engel R, Stahl P, Fengler D, Kuhla B (2005) Immunochemical cross-reactivity of antibodies specific for "advanced glycation endproducts" with "advanced lipoxidation endproducts". *Neurobiol Aging* **26**, 465-474.

[41] Hawe A, Sutter M, Jiskoot W (2008) Extrinsic fluorescent dyes as tools for protein characterization. *Pharm Res* **25**, 1487-1499.

[42] Gasymov OK, Glasgow BJ (2007) ANS fluorescence: Potential to augment the identification of the external binding sites of proteins. *Biochim Biophys Acta* **1774**, 403-411.

[43] Maeda S, Sato Y, Takashima A (2018) Frontotemporal dementia with parkinsonism linked to chromosome-17 mutations enhance tau oligomer formation. *Neurobiol Aging* **69**, 26-32.

[44] Yanagisawa K, Makita Z, Shiroshita K, Ueda T, Fusegawa T, Kuwajima S, Takeuchi M, Koike T (1998) Specific fluorescence assay for advanced glycation end products in blood and urine of diabetic patients. *Metabolism* **47**, 1348-1353.

[45] Jagadeeshaprasad MG, Venkatasubramani V, Unnikrishnan AG, Kulkarni MJ (2018) Albumin abundance and its

glycation status determine hemoglobin glycation. *ACS Omega* **3**, 12999-13008.

[46] Vanniruswamy G, Korwar AM, Jagadeeshaprasad MG, Kulkarni MJ (2017) Targeted quantification of the glycated peptides of human serum albumin. *Methods Mol Biol* **1619**, 403-416.

[47] Fokkens BT, Smit AJ (2016) Skin fluorescence as a clinical tool for non-invasive assessment of advanced glycation and long-term complications of diabetes. *Glycoconj J* **33**, 527-535.

[48] Kuhla B, Hause C, Flach K, Lüth H-J, Arendt T, Münch G (2007) Effect of pseudophosphorylation and cross-linking by lipid peroxidation and advanced glycation end product precursors on tau aggregation and filament formation. *J Biol Chem* **282**, 6984-6991.

[49] Nakamura M, Shiozawa S, Tsuboi D, Amano M, Watanabe H, Maeda S, Kimura T, Yoshimatsu S, Kisa F, Karch CM (2019) Pathological progression induced by the frontotemporal dementia-associated R406W tau mutation in patient-derived iPSCs. *Stem Cell Rep* **13**, 684-699.

[50] Ke YD, Delerue F, Gladbach A, Götz J, Ittner LM (2009) Experimental diabetes mellitus exacerbates tau pathology in a transgenic mouse model of Alzheimer's disease. *PloS One* **4**, e7917.

[51] Iannuzzi C, Irace G, Sirangelo I (2014) Differential effects of glycation on protein aggregation and amyloid formation. *Front Mol Biosci* **1**, 9.

[52] Mendez DL, Jensen RA, McElroy LA, Pena JM, Esquerra RM (2005) The effect of non-enzymatic glycation on the unfolding of human serum albumin. *Arch Biochem Biophys* **444**, 92-99.

[53] Vicente Miranda H, Szegö EM, Oliveira LM, Breda C, Darendelioglu E, de Oliveira RM, Ferreira DG, Gomes MA, Rott R, Oliveira M (2017) Glycation potentiates α-synuclein-associated neurodegeneration in synucleinopathies. *Brain* **140**, 1399-1419.

[54] Münch G, Lüth H, Wong A, Arendt T, Hirsch E, Ravid Ra, Riederer P (2000) Crosslinking of α-synuclein by advanced glycation endproducts—an early pathophysiological step in Lewy body formation? *J Chem Neuroanat* **20**, 253-257.

[55] Huseby CJ, Kuret J (2016) Analyzing tau aggregation with electron microscopy. *Methods Mol Biol* **1345**, 101-112.

[56] Ledesma M, Perez M, Colaco C, Avila J (1998) Tau glycation is involved in aggregation of the protein but not in the formation of filaments. *Cell Mol Biol (Noisy-le-grand)* **44**, 1111-1116.

[57] Aronson D (2003) Cross-linking of glycated collagen in the pathogenesis of arterial and myocardial stiffening of aging and diabetes. *J Hypertens* **21**, 3-12.

[58] Gorantla NV, Shkumatov AV, Chinnathambi S (2017) Conformational dynamics of intracellular tau protein revealed by CD and SAXS. *Methods Mol Biol* **1523**, 3-20.

[59] Gorantla NV, Khandelwal P, Poddar P, Chinnathambi S (2017) Global conformation of tau protein mapped by Raman spectroscopy. *Methods Mol Biol* **1523**, 21-31.

[60] Luthra M, Balasubramanian D (1993) Nonenzymatic glycation alters protein structure and stability. A study of two eye lens crystallins. *J Biol Chem* **268**, 18119-18127.

[61] Colaco C, Harrington CR (1994) Glycation: A pathological modification in neuropathies?: A hypothesis. *Neuroreport* **5**, 859-861.

[62] Chatterjee S, Ambegaokar S, Jackson GR, Mudher A (2019) Insulin-mediated changes in tau hyperphosphorylation and autophagy in a Drosophila model of tauopathy and neuroblastoma cells. *Front Neurosci* **13**, 801.

[63] Gonçalves RA, Wijesekara N, Fraser PE, De Felice FG (2019) The link between tau and insulin signaling: Implications for Alzheimer's disease and other tauopathies. *Front Cell Neurosci* **13**, 17.

[64] Batkulwar K, Godbole R, Banarjee R, Kassaar O, Williams RJ, Kulkarni MJ (2018) Advanced glycation end products modulate amyloidogenic APP processing and Tau phosphorylation: A mechanistic link between glycation and the development of Alzheimer's disease. *ACS Chem Neurosci* **9**, 988-1000.

Archives of Biochemistry and Biophysics 675 (2019) 108119

Contents lists available at ScienceDirect

Archives of Biochemistry and Biophysics

journal homepage: www.elsevier.com/locate/yabbi

Baicalein suppresses Repeat Tau fibrillization by sequestering oligomers

Shweta Kishor Sonawane[a,c,1], Abhishek Ankur Balmik[a,c,1], Debjyoti Boral[b,c], Sureshkumar Ramasamy[b,c], Subashchandrabose Chinnathambi[a,c,*]

[a] Neurobiology Group, Division of Biochemical Sciences, CSIR-National Chemical Laboratory, Dr. Homi Bhabha Road, 411008, Pune, India
[b] Structural Biology Group, Division of Biochemical Sciences, CSIR-National Chemical Laboratory, Dr. Homi Bhabha Road, 411008, Pune, India
[c] Academy of Scientific and Innovative Research (AcSIR), 411008, Pune, India

ARTICLE INFO

Keywords:
Alzheimer disease
Tau protein
Protein aggregation
Paired helical filaments
Microtubule assembly
Baicalein

ABSTRACT

Alzheimer's disease (AD) is a neurodegenerative disorder caused by protein misfolding, aggregation and accumulation in the brain. A large number of molecules are being screened against these pathogenic proteins but the focus for therapeutics is shifting towards the natural compounds as aggregation inhibitors, mainly due to their minimum adverse effects. Baicalein is a natural compound belonging to the class of flavonoids isolated from the Chinese herb *Scutellaria baicalensis*. Here we applied fluorescence, absorbance, microscopy, MALDI-TOF spectrophotometry and other biochemical techniques to investigate the interaction between Tau and Baicalein *in vitro*. We found the aggregation inhibitory properties of Baicalein for the repeat Tau. Overall, the potential of Baicalein in dissolving the preformed Tau oligomers as well as mature fibrils can be of utmost importance in therapeutics for Alzheimer's disease.

1. Introduction

Alzheimer's Disease is a neurodegenerative disorder characterized by memory loss and progressive dementia. The cytosolic Tau aggregates and the extracellular amyloid beta plaques are the typical traits of AD [1–3]. The therapeutics for AD is being designed to act on both the targets in a discreet as well as integrated manner. The efficacy of the drugs designed seems to reduce as the level of trial increases [4,5]. The accumulation of cytosolic neurofibrillary tangles mainly composed of Tau PHFs (paired helical filaments) [6] leads to neuronal degeneration. Along with microtubule stabilization Tau has varied roles such as neurite outgrowth, intracellular trafficking etc. that are hampered in AD due to elevated Tau levels [7,8]. All these neuronal abnormalities and degeneration due to Tau dysfunction and aggregation necessitates screening for molecules to inhibit Tau aggregation as well as to dissolve the preformed aggregates.

Tau aggregation in AD succeeds via several intermediates like oligomers, proto-fibrils, paired helical filaments formation, which when untreated forms neurofibrillary tangles [9–11]. Hence, these intermediates are being targeted for therapeutics in AD. The oligomer species are found to be more toxic than the filamentous aggregates [12] and hence Tau oligomers are gaining much attention as a therapeutic target in AD. Several molecules belonging to different classes like synthetic molecules, natural compounds, peptide inhibitors etc. have found to be potent against Tau aggregation [13–17]. In recent time, methylene blue was found to be a potent molecule in AD [18–20] but failed to show effects on cognitive abilities in a transgenic mouse model of AD [21]. On the other hand, the methylene blue derivatives MTC methylthioninium chloride (MTC); and its reduced form leucomethylthioninium salts (LMTX) has shown positive effects on Tau aggregation inhibition [22] by modifying the cysteine residues to the oxidized forms [23]. Other approaches to inhibit Tau aggregation include targeting PTMs (post-translational modifications) of Tau. Accordingly, kinase inhibitors or phosphatase activators have been screened for these molecules but failed to show potency due to low specificity and less efficiency. Since the ultimate effect of Tau aggregation is microtubule destabilization, an alternative strategy for designing of therapeutics in AD is to screen or synthesize the microtubule stabilizing compounds [24–26]. The natural compounds having varied targets in AD have also shown to have a potential as therapeutics in AD like curcumin, paclitaxel, geldanamycin etc. [27]. Azaphilones, a class of fungal metabolites have shown the aggregation inhibition as well as disaggregation activity for Tau aggregates [28]. The secondary metabolites of *Aspergillus nidulans* like 2,ω-Dihydroxyemodin,

* Corresponding author. Neurobiology group, Division of Biochemical Sciences, CSIR-National Chemical Laboratory (CSIR-NCL), Dr. Homi Bhabha Road, 411008, Pune, India.
E-mail address: s.chinnathambi@ncl.res.in (S. Chinnathambi).
[1] Equal contribution.

https://doi.org/10.1016/j.abb.2019.108119
Received 1 August 2019; Received in revised form 5 September 2019; Accepted 24 September 2019
Available online 27 September 2019
0003-9861/

Asperthecin, and Asperbenzaldehyde having aromatic rings are potent Tau aggregation inhibitors [29]. Oleocanthal, derived from extra virgin olive oil have shown inhibition of Tau aggregation by covalently modifying the protein at its lysine residues [30]. EGCG is an active component of green tea and has been shown to interfere with the aggregation of amyloid beta, α-synuclein as well as Tau in *in vitro* studies [31,32]. Baicalein is a polyphenol compound belonging to the class of flavonoids isolated from the Chinese herb *Scutellaria baicalensis*. Flavonoids are a rich source of anti-oxidants and are known to play a neuroprotective role [33]. Baicalein has been known to exert anti-allergic, anti-carcinogenic anti-inflammatory as well as cardio protective properties. It has also shown a potential for inhibiting aggregation of proteins involved in neurodegenerative diseases. Baicalein not only prevents fibrillization of α-synuclein but also disaggregates the pre-formed fibrils involved in Parkinson's disease [34]. In AD transgenic mouse model, Baicalein has shown to reduce the amyloid-β accumulation and enhance the processing of amyloid precursor protein via α-secretases thus leading to non-amyloidogenic processing of APP [35]. In this study, we report that Baicalein shows a dual property of inhibiting aggregation as well as dissolving the pre-formed fibrils of repeat domain of Tau in *in vitro* conditions at sub micro-molar concentrations. To explore the putative binding site and mode of Baicalein binding with Tau, the molecular docking and simulations were studied with the hexapeptide repeat region. Only this region is amenable to predict the reliable model from the presently available structure information. The dynamics simulation on Tau filament reported previously showed the aggregation mechanism due to hyperphosphorylation [36]. This study would reveal nature of interaction and mechanism of Baicalein in inhibition of Tau aggregates formation.

2. Experimental procedures

2.1. Chemicals and reagents

Baicalein, ThS, ANS, BES, sinapinic acid, BCA reagent and MTT were purchased from Sigma. Heparin, NaCl and sodium azide were purchased from MP Biomedicals. DTT and protease inhibitor cocktail were purchased from Calbiochem and Roche respectively. ECL reagent (32132) and antibodies anti-oligomer A11 rabbit polyclonal (AHB0052) and goat anti-rabbit HRP conjugated (A16110) were purchased from Thermo Fisher Scientific. The cell culture reagents DMEM F12, Fetal Bovine Serum (FBS), Penicillin-Streptomycin (Penstrep), L-glutamine, trypsin-EDTA, 1X phosphate buffered saline (PBS) were purchased from Invitrogen. 10 mM and 1 mM stock of Baicalein was prepared in ethanol. 12.5 mM mother stock of ThS was prepared in 1:1 ethanol: miliQ water, which was further, diluted to 200 μM stock in filtered miliQ water. ANS was prepared as 10 mM stock in filtered miliQ.

2.2. Tau purification

The protein purification was carried out as previously described [37]. In brief, the cell pellets obtained after induction of protein expression were homogenized under high pressure (15,000 psi) in a microfluidics device for 15 min. The obtained lysate was heated at 90 °C for 15 min after addition of 0.5 M NaCl and 5 mM DTT. The heated lysate was then cooled and centrifuged at 40,000 rpm for 50 min. The supernatant was collected and dialyzed in Sepharose A buffer overnight. The obtained dialyzed sample was then subjected to a second round of ultracentrifugation and the supernatant was loaded onto the cation exchange column (Sepharose fast flow GE healthcare) for further purification. The bound protein was eluted using an ionic gradient. The eluted proteins were pooled and concentrated for size exclusion chromatography (16/600 Superdex 75 pg GE healthcare). The Tau concentration was measured using BCA method.

2.3. Molecular modeling

To identify templates for homology model building, a similarity search using Basic Local Alignment Search Tool (BLAST) [38] algorithm was performed against the Protein Data Bank (PDB), to identify high-resolution crystal structures of homologous proteins 63, 64. The sequence identity cut off was set to ≥30% (E-value cut off = 1). Homology modeling of Tau K18 was then carried out using Modeller 9.16 [39] by taking structures homologous to the target proteins as templates, in order to study their structural features, binding mode and affinity with the substrates.

2.4. Model validation and refinement

The initial models obtained, were evaluated for the stereochemical quality of the protein backbone and side chains using PROCHECK and RAMPAGE [40,41]. ERRAT server checked the environments of the atoms in the protein model [42]. Errors in the model structures were also checked with ProSA server [43]. After model validation, initial models were refined using impref minimization of protein preparation wizard and Impact 5.8 minimization [44]. These energy minimized final models were further used for the binding studies with Baicalein.

2.5. Ligand-protein preparation and docking studies

The ligand molecules considered in the present study were downloaded from ZINC compound database in the mol2 format. The protein and ligands were prepared first before proceeding with the docking studies. The water molecules and other hetero atom groups were removed from the protein structures using protein preparation utility of Maestro. Hydrogens were added subsequently to carry out restrained minimization of the models. The minimization was done using impref utility of Maestro in which the heavy atoms were restrained such that the strains generated upon protonation could be relieved. The root mean square deviation (RMSD) of the atomic displacement for terminating the minimization was set as 0.3 A°. Similarly, ligands were refined with the help of LigPrep 2.5 to define their charged state and enumerate their stereoisomers. The processed receptors and ligands were further used for the docking studies using Glide 5.8 [45]. Results from fluorescence microscopy and MALDI-TOF spectrophotometry, indicated that certain flavonoids interact with the Tau protein, influencing their aggregation and disaggregation propensities. Thereby one such flavonoid originally isolated from the roots of *Scutellaria baicalensis* and *Scutellaria lateriflora*, believed to enhance liver health, Baicalein was docked in the binding site cavity of the prepared receptor molecule, aka the protein. A Sitemap analysis [46] was performed on the prepared receptor molecule, to identify the probable binding sites for our ligands of interest, since no prior information was available regarding the same. Next, grids were generated by selecting any of the Sitemap points obtained above. Flexible ligand docking was carried out using the standard precision option.

A total of 6 poses with the respective ligand and different sites were generated and scored on the basis of their docking score, glide score and E-model values. The hydrogen bond interactions between the protein and ligands were visualized using PyMOL.

2.6. Molecular dynamics simulations

The docked complexes were prepared first using protein preparation wizard and then subjected to molecular dynamics simulations for a time scale of 15 ns (ns) using Desmond 3.1 of Maestro [47]. OPLS2005 force field was applied on docked complexes placed in the center of the orthorhombic box solvated in water. Protein was immersed in orthorhombic water box of SPC water model. Total negative charges on the docked structures were balanced by suitable number of counter-ions to make the whole system neutral (10 Cl-ions). The system was initially

energy minimized for maximum 2000 iterations of the steepest descent (500 steps) and the limited memory Broyden–Fletcher–Goldfarb-Shanno (BFGS) algorithm with a convergence threshold of 1.0 kcal/mol/Å. The short and long-range Coulombic interactions were handled by Cutoff and Smooth particle mesh Ewald method with a cut off radius of 9.0 Å and Ewald tolerance of 1e_09. Periodic boundary conditions were applied in all three directions. The relaxed system was simulated for 10ns with a time step of 2.0 fs (fs), NPT ensemble using a Berendsen thermostat at 300K temperature and atmospheric pressure of 1 bar. The energies and trajectories were recorded after every 2.0 ps (ps). The energies and RMSD of the complex in each trajectory were monitored with respect to simulation time. The Galpha atom root mean square fluctuation (RMSF) of each residue was analyzed. The intermolecular interactions between the target and substrate were assessed to check the stability of the complexes.

2.7. Tau aggregation inhibition assay

Tau aggregation inhibition assay was performed with a few modifications in the already described protocol [73]. In brief, the soluble Tau protein was centrifuged at 60,000 rpm for 1 h (Optima Max XP Beckman Coulter) to remove aggregates present if any and 20 μM of soluble Tau protein was incubated in 20 mM BES buffer pH 7.4 with 5 μM of Heparin 17,500 Da in presence of 25 mM NaCl, 1 mM DTT, protease inhibitor cocktail, 0.01% sodium azide, and different concentrations of Baicalein ranging from 0 to 500 μM. The reaction mixtures were incubated at 37 °C.

2.8. Soluble protein assay

The soluble protein of repeat Tau was centrifuged as mentioned above prior setting up the reaction. 20 μM of each protein was incubated with 25 and 100 μM of Baicalein in absence of heparin. The other reaction mixture composition was maintained as mentioned above. A positive and negative control was kept with and without addition of heparin respectively. The reaction mixtures were incubated at 37 °C.

2.9. UV–visible spectroscopy

50 μM Baicalein in 20 mM BES buffer was placed in a cuvette and an absorption spectrum was recorded in 230–450 nm range using Jasco V-530 spectrophotometer. Aliquots of repeat Tau were added to the cuvette in 3.5, 7, 14, 28, 42, 56, 70, 84, 98 μM concentration and respective spectra were recorded for each addition. The total volume of repeat Tau added was less than 100 μl to avoid the dilution effect.

2.10. Repeat Tau disaggregation assay (oligomers and fibrils)

The effect of Baicalein on the dissolution of Tau aggregates was studied by incubating the preformed PHFs with different concentrations of Baicalein at 37 °C. Aggregation of 20 μM repeat Tau was carried out and induced by 5 μM heparin in 20 mM BES, pH 7.4. Repeat Tau oligomers and mature fibrils were prepared prior to the addition of Baicalein by incubating Tau in aggregation conditions for 4 h and 60 h respectively. Baicalein was added in 50–500 μM concentration after 4 h for repeat Tau oligomer disaggregation and after 60 h for fibril disaggregation. ThS and ANS fluorescence assays were employed for monitoring the disaggregation kinetics. 20μl samples from different time points during the course of assay were loaded onto 17% SDS-PAGE and analyzed using Bio-Rad Image Lab software.

2.11. ThS fluorescence assay

ThS fluorescence assay monitored Tau aggregates formation as described. The 5 μl of 20 μM reaction mixtures were diluted in 50 mM ammonium acetate pH 7.0 containing 8 μM of ThS to a final volume of 50 μl. The ratio of protein to ThS was maintained as 1:4 for the fluorescence measurement. Fluorescence measurements were carried out using Tecan Infinite 200 Pro series plate reader. The excitation and emission wavelengths were set at 440 nm and 521 nm respectively. The plate was given a quick shaking for 10 s before the measurement. The readings were carried out in triplicates for each sample at 25 °C. Initial readings were taken within an interval of 1 h till 6 h and later readings were continued at an interval of 12 h each. The fluorescence was normalized for background by subtracting the buffer blank fluorescence.

2.12. ANS fluorescence assay

The level of protein hydrophobicity was measured by ANS fluorescence. The 5 μl of 20 μM reaction mixtures were diluted in 50 mM ammonium acetate pH 7.0 containing 40 μM of ANS to a final volume of 50 μl. The ratio of protein to ANS was maintained as 1:20 for the fluorescence measurement. The excitation was carried out at 390 nm and the emission data was collected at 475 nm. Each sample was read in triplicate and subtracting from respective blanks eliminated the background fluorescence. All measurements were carried out in Tecan Infinite 200 Pro series plate reader at 25 °C. The time points were followed in a similar way as ThS fluorescence.

2.13. SDS-PAGE analysis

Samples left after fluorescence assay were collected and analyzed by SDS-PAGE for visual detection of aggregation inhibition on 17% polyacrylamide gels with different time points. The SDS-PAGE gel quantification was carried out using Image Lab software (Bio-Rad). The quantification for complete individual lanes was carried out using the software and the obtained intensities were plotted in the form of the bar graphs.

2.14. Filter trap assay

The detection of repeat Tau oligomers induced by Baicalein and separated by SEC was carried out by filter trap assay using A11 anti-oligomers rabbit polyclonal antibody. The fractions obtained after SEC were blotted onto Protran 0.45 μm membrane (Amersham Biosciences) using Minifold Dot-Blot System (Amersham Biosciences). The membrane was blocked with 10% milk in PBST (0.01% Tween 20) for 1 h at room temperature. The primary antibody A11 was diluted to 1:2000 and the blot was incubated with it overnight at 4 °C. After washing the unbound antibody thrice with PBST, the blot was incubated with secondary goat anti-rabbit antibody conjugated to HRP for 1 h at room temperature in 1:10000 dilutions. The unbound antibody was washed thrice with PBST. The blot was developed using ECL-Plus reagent and the chemiluminescence was detected on Amersham Imager 600 and quantified using Image Quant TL software.

2.15. Circular dichroism spectroscopy

CD spectroscopy was performed for determination of conformational changes occurring during the aggregation inhibition process using Jasco J-815 CD spectrometer in a cuvette with a path length of 1 mm under nitrogen atmosphere. The scan was carried out with bandwidth 1 nm, scan speed 100 nm/min; scan range 190–250 nm, and an average of 5 acquisitions were taken. In each experiment, measurements were done at 25 °C. The buffer baseline was set with sodium phosphate buffer, pH 6.8. The concentration was maintained 1 μM for repeat Tau for all CD measurements.

2.16. Electron microscopy

Transmission electron microscopy was carried out to qualitatively

determine the Tau filaments formation in presence and absence of Baicalein. 2 μM of the reaction mixtures were applied to 400 mesh carbon coated copper grids for 45 s followed by 2 washes with filtered MilliQ water for 45 s each. The samples were negatively stained for 1 min using 2% uranyl acetate. The dried grids were analyzed using Tecnai G2 20 S-Twin transmission electron microscope.

2.17. Size exclusion chromatography for Tau oligomers

Size-exclusion chromatography was carried out for repeat Tau in presence of Baicalein at different time points in order to characterize the effect of Baicalein on the tendency of oligomerization. Repeat Tau samples were prepared by incubating the protein in 20 μM concentration in 20 mM BES buffer, pH 7.4 with or without Baicalein in 200 μM final concentration. Heparin was added in 1:4 ratios as an inducer of aggregation. Baicalein was added to the reaction mixture after 4h of incubation at 37 °C. The initial incubation was provided for the preparation of lower order oligomers. The time point of Baicalein addition was considered as 0 h. The protein sample was filtered prior to loading on to Superdex 75 10/300 GL column (GE). BSA and Lysozyme were loaded as standards in 3 mg/ml concentration and soluble repeat Tau was loaded as a control. The separation was carried out in PBS buffer. Samples at 0, 6, 12, 24 and 60 h of incubation were subjected to size-exclusion chromatography.

2.18. MALDI-TOF analysis of Baicalein modified Tau

Repeat Tau protein (1 mg/ml) was incubated with different concentrations of Baicalein (5, 10, 25, 50, 100, 200, 500 μM) for 1 h and 12 h at 37 °C respectively. The samples were then diluted 1:20 in Sinapic acid and spotted on the MALDI plate and analyzed using ABSCIEX 4800 MALDI-TOF analyzer.

2.19. Cell culture and toxicity assays

The neuroblastoma N2a cells were seeded in 96 well culture plates at the cell density of 25,000 cells/well. The cells were grown in DMEM F12 media containing 0.5% FBS and antibiotic (Penstrep) for 24 h. For studying the toxicity of Baicalein induced oligomers 10 μl from the SEC fractions was added to cells/well and incubated for 24 h 10 μl of 5 mg/ml MTT (Methylthiazolyldiphenyl-tetrazolium bromide) was added to each well and incubated for 4h at 37 °C. The formazan crystals formed after reduction of MTT by viable cells enzymes were dissolved in 100 μl of 100% DMSO. The purple colour developed was read at 570 nm in Tecan plate reader.

2.20. Statistical analysis

SigmaPlot 10.2 carried all the statistical analyses out using unpaired T-test. The error bars represent mean ± SD values. 95% confidence intervals were maintained for the analyses.

3. Results

3.1. Baicalein binds to Tau in vitro

Tau protein is one of the major microtubule-associated proteins in neuronal axons that mainly functions to stabilize and assemble microtubules. Tau is highly soluble protein and adopts a natively unfolded structure in solution [48]. The repeat domain of Tau plus the proline rich flanking regions confer the property of microtubule binding and assembly (Fig. 1A), where the repeat domain of Tau represents the core of the PHFs. The chemical structure of Baicalein is depicted in (Fig. 1B). Baicalein shows characteristic λ_{max} at two wavelengths 270 nm and 362 nm (Figs. S1B and C). Upon titrating with repeat Tau from 0 to 98 μM, the peak at 362 nm was found to decrease in intensity indicating the binding of Baicalein (Figs. 1D and S1C). The maxima at 362 nm plotted against increasing Tau concentration (0–98 μM) shows a gradual decrease in absorbance intensity (Fig. 1E). The dissociation constant (K_d) for the binding of Tau with Baicalein was found to be 3.5 μM by using the following formula:

$$[C_{Tau}C_{Baicalein}] = \frac{[C_{Tau}] \times [C_{Baicalein}]}{K_d + [C_{Baicalein}]}$$

Where $[C_{Tau}]$ is the initial Tau concentration, $[C_{Baicalein}]$ is the free Baicalein concentration, $[C_{Tau}C_{Baicalein}]$ is the concentration of Tau-Baicalein complex and K_d is the dissociation constant [49–51].

3.2. Molecular models of Tau protein

The molecular structures of repeat Tau were modeled, in order to ascertain the putative binding site of Baicalein and the role of the conserved hexapeptide repeat regions ^{275}VQIINK^{280} and ^{306}VQIVYK^{311} in the interactions with Baicalein (Fig. 1C). It is very challenging to predict the full-length Tau model due to its disordered nature of the regions in both N- and C-terminal. But the hexapeptide repeat region forms the stable secondary structure as reported by many biochemical studies and structural information [52–54]. A BLAST search against PDB identified homologous structures, to be used as templates to build the homology models of this region. Structures of Tau (267–312) bound to microtubules (2MZ7) and shared an identity of 100% and query coverage of 92% with the target sequence, and were thus used for modeling studies.

The initial models were evaluated for their stereochemical parameters. More than 98% of all residues were in the allowed regions of Ramachandran plot. The model refinement phase involved preprocessing the initial models by adding hydrogen's, assigning bond order, and filling missing loops and side chains. Next, the models were subjected to restrained minimization by applying the constraint to converge the non-hydrogen atoms to an RMSD of 0.3 using OPLS 2005 force field. Subsequently, the models were subjected to 500 steps of steepest descent energy minimization followed by 1000 steps of conjugate gradient energy minimization using the same force field. These energy-minimized models were used for docking and molecular dynamics studies.

3.3. Molecular docking of repeat Tau and Baicalein

The docking studies of Baicalein with repeat Tau model generated the best pose with glide score and E-model values of - 5.06 and - 44.365 respectively. The O_1 atom of Baicalein interacts with the NH_2 group of Asn 265 and the NH group of the imidazole ring of His 268. The OH groups involving O_2 and O_4 atoms of Baicalein, interacts with the carboxyl O^- atom of Glu 338, forming hydrogen bonds in the process (Fig. 2A). While the two -OH groups (O_2 and O_4) have an interaction distance of 2.70 Å, 2.0 Å and 1.80 Å respectively, the interactions with the amine group stand at a distance of 2.30 Å for Asn 265. Further hydrophobic interaction was observed with residues Tyr 310 and Val 313, of which one (Tyr 310), interestingly, belongs to the hexapeptide repeat ^{306}VQIVYK^{311} and the other (Val 313) is a flanking residue to the same repeat, a prime area of interest in our study. Another crucial residue His 299 is predicted to have an important interaction with Baicalein via water bridges, which may be involved in the probable mechanism of Tau disaggregation in presence of Baicalein.

3.4. Molecular dynamics simulation of repeat Tau and Baicalein

The Baicalein docked complex was subjected to a simulation of 15 ns time duration to analyze the stability of the interaction and other structural changes. The RMSD graph was plotted by assigning time in ns on the X-axis and RMSD values of the Cα atoms of the protein and ligand in/Å on the left and right Y-axes respectively (Fig. S2). The graph and the snapshots at different time intervals of simulation indicated

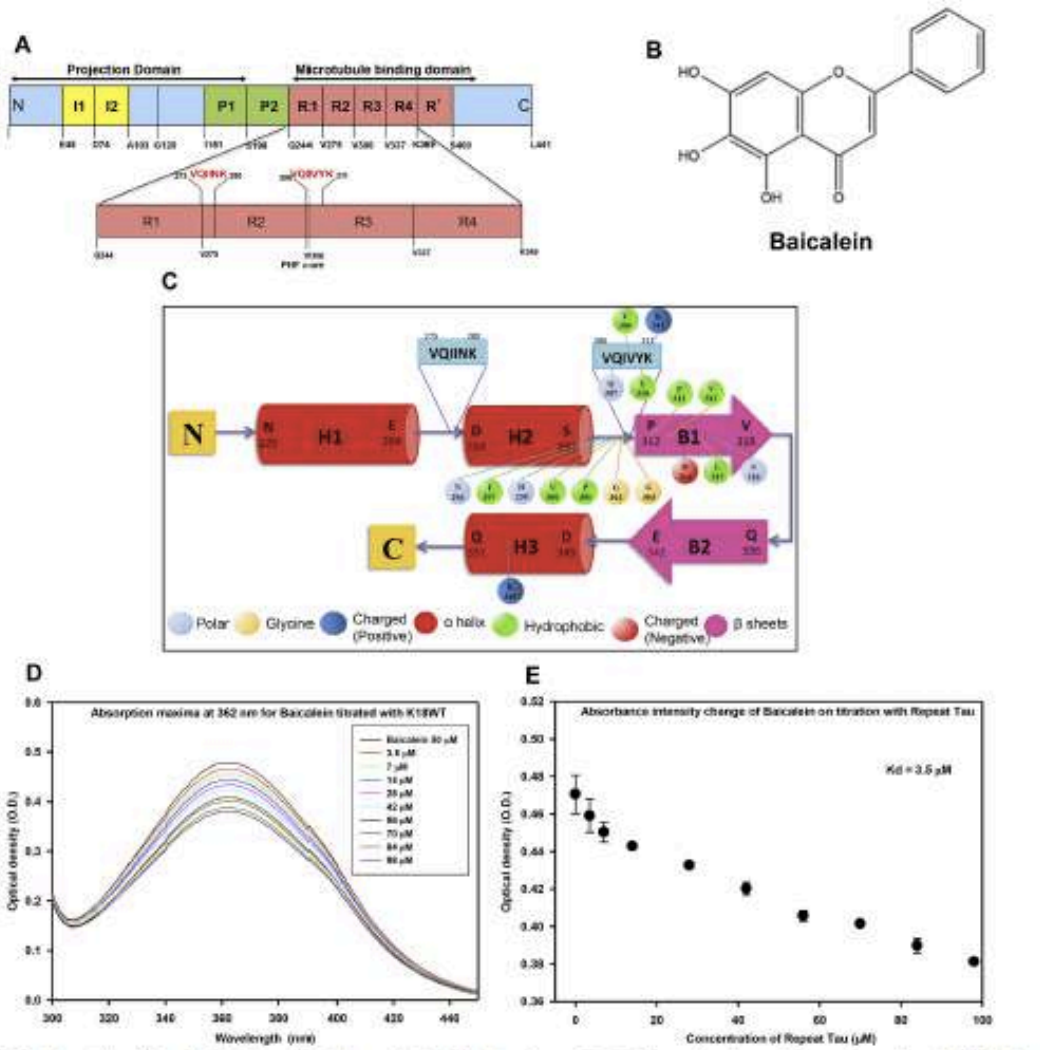

Fig. 1. The interaction of Tau with Baicalein. A) Bar diagram showing full-length and repeat Tau. The figure shows longest isoform of human Tau with 441 amino acids. The yellow blocks represent two inserts of 29 amino acids each at the N- terminal region followed by the polyproline rich region, which gives a transient helix structure. The 4 red boxes represent the four repeats of 30 amino acids each. The K18 construct comprises of only the repeat domain of Tau, which forms the core of Paired Helical Filaments. B) Chemical structure of the flavonoid Baicalein. C) A schematic diagram of the repeat Tau model secondary structure depicting three predicted α helices (H1, H2, and H3) and two predicted β sheets (B1, B2) with two distinct and characteristic hexa-peptide regions ^{275}VQIINK^{280} and ^{306}VQIVYK^{311}. The predicted ligand interacting residues, color coded according to their type of interaction is also shown. D) Figure shows decrease in the absorbance intensity at 362 nm upon increasing the protein concentration against Baicalein. E) The absorbance intensity at 362 nm obtained for different titrations when plotted against respective concentrations gives a plot representing the binding affinity of Tau with Baicalein. (For interpretation of the references to colour in this figure legend, the reader is referred to the Web version of this article.)

that the RMSD of Cα atoms of the generated structures over the complete trajectory is quite stable with minor repositioning of Baicalein with respect to the hexapeptide repeat region ^{306}VQIVYK^{311}. The Cα RMSD between the initial and final conformation after the simulation of docked complex was ~10 Å indicated the considerable conformational change upon binding. During the course of the simulation, a few residues namely Asn 296, Ile 297, His 299, Gln 307, Tyr 310, Lys 311, Val 313 and Leu 315 out of which three residues belong to the hexapeptide region mentioned above, were found to form an increasingly high number of interactions with Baicalein, indicating that these may be crucial residues to stabilize the complex (Figs. 2B and S3).

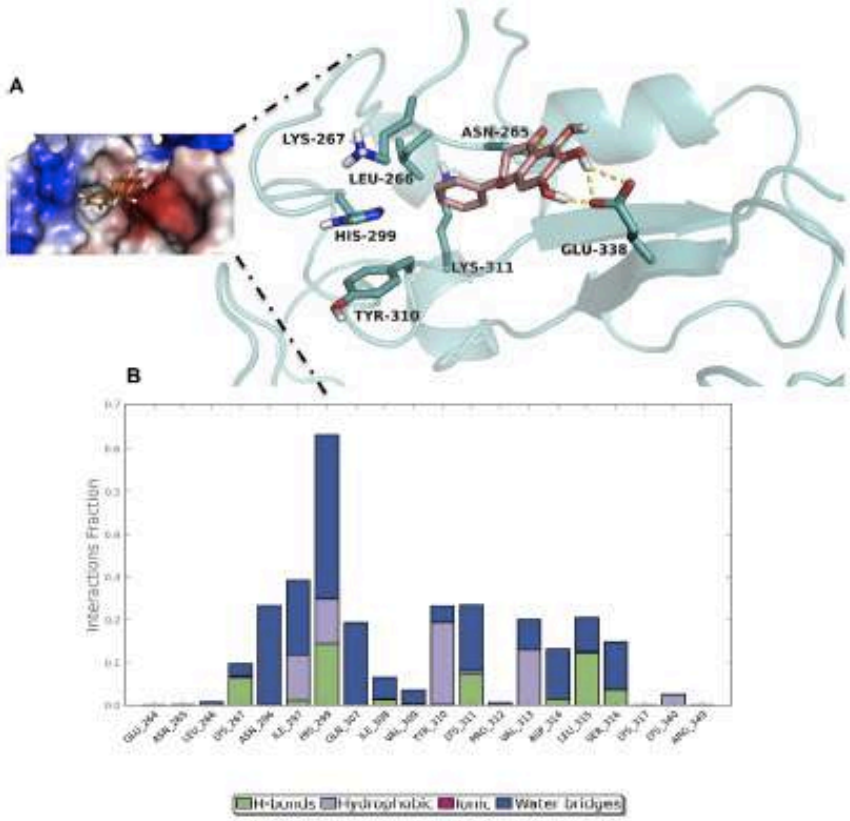

Fig. 2. Docking and Simulation of Tau with Baicalein. A) A detailed snapshot of the ligand-binding pocket of Baicalein in our proposed model of repeat Tau including the interacting residues as indicated and the corresponding surface represented in terms of electrostatic potential. B) A bar diagram depicting the extent of interaction over the course of 15 ns simulation using the same docked structure which indicates that the residues mentioned are majorly involved in the binding and probable biochemistry of the ligand binding to Tau. The protein-ligand interactions or contacts are categorized into four types: Hydrogen Bonds, Hydrophobic, Ionic and Water Bridges.

3.5. Baicalein inhibits Tau aggregation in vitro

Tau is a natively unfolded protein with an overall positive charge. This property makes it possible to aggregate Tau *in vitro* by using polyanionic co-factors like heparin. Heparin is a polymer of glycosaminoglycan monomers, which has a negative charge and induces aggregation of Tau *in vitro* [55,56]. This approach has been widely used to screen for the Tau aggregation inhibitors [18,30,57]. The aggregation inhibition of the repeat Tau by Baicalein was determined using 0, 5, 25, 50, 100, 200, and 500 μM concentrations. The rate of Tau fibril formation was monitored by ThS fluorescence. The ThS fluorescence intensity decreased with increasing concentrations of Baicalein in the treated samples. The ThS fluorescence showed an initial increase in control as well as treated samples till 4h of incubation (Fig. 3A). As the time progressed, the treated samples showed decrease in fluorescence intensity but the control showed stagnant saturated fluorescence suggesting a concentration dependent inhibition of aggregation. The inhibition was observed to occur at an early time point and the IC_{50} value for repeat Tau aggregation inhibition was found to be 35.8 μM of Baicalein (Fig. 3). The pattern of rise and fall in fluorescence intensity for the treated samples suggest that Baicalein might be inducing initial oligomerization of Tau protein and inhibiting the further fibrillization by sequestering these oligomers.

3.6. Baicalein enhances Tau oligomerization in presence of heparin

The *in vitro* formation of PHFs in presence of heparin undergoes various intermittent stages [58], which results in changes in hydrophobicity of the Tau protein [59]. One of the intermittent stages in PHFs formation is the formation of oligomeric species, which acts as a nucleation step to further enhance fibrillization. The primary studies with ThS indicated that Baicalein prevents Tau fibril formation. We further investigated the role of Baicalein in Tau oligomerization. As an intermediate in Tau fibrillization, Tau oligomers show enhanced hydrophobicity due to their partially folded characteristics. ANS is a dye, which emits enhanced fluorescence on interaction with partially, folded or exposed hydrophobic micro domains of the proteins.

Thus, to study the effect of Baicalein on Tau oligomerization and accompanied hydrophobicity changes, we monitored ANS fluorescence for the control as well as treated samples. ANS showed an initial decrease in fluorescence and then the rapid increase before becoming stagnant (Fig. S4). This effect was evident at the earlier time points in

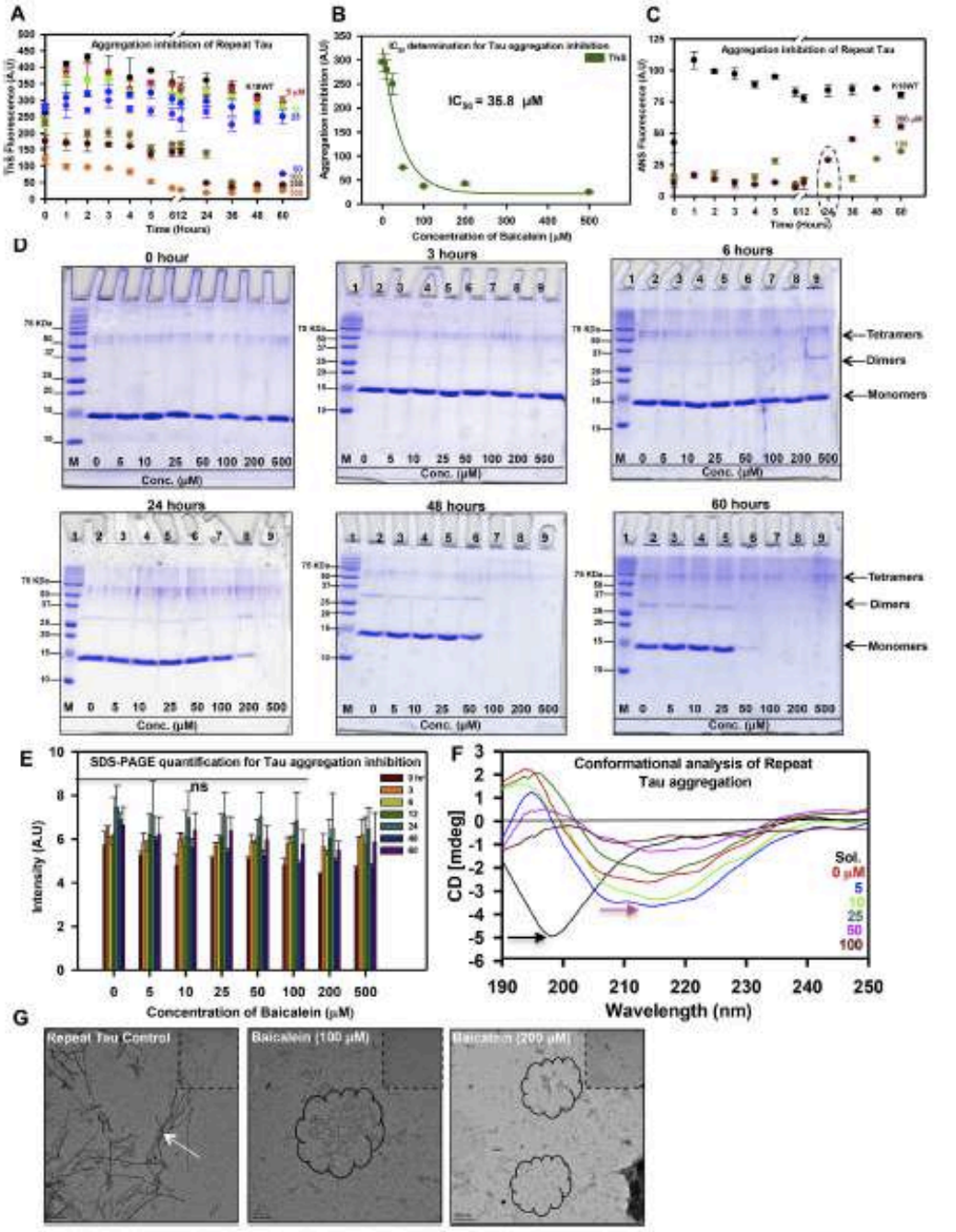

(caption on next page)

Fig. 3. Tau aggregation inhibition by Baicalein. A) The ThS fluorescence show a concentration dependent decrease in intensity suggesting inhibition of repeat Tau aggregation by increasing dose of Baicalein. B) The IC_{50} value for repeat Tau aggregation inhibition was found to be 35.8 μM of Baicalein. C) The ANS fluorescence for the higher concentrations of Baicalein showing initial decrease and further rapid increase in fluorescence at 24 h (dotted circle). D) The SDS-PAGE analysis at zero time point control as well as treated samples does not show presence of any higher order aggregates. With an increase in time there is an increase in higher order oligomers observed especially after 6 h of incubation. At 24 h, the 500 μM of Baicalein (lane 9) shows the presence of dimer as well as tetramer. With increase in incubation time (48 and 60 h), the oligomers are seen in all treated samples with differential intensity. The further incubation reveals the disappearance of these oligomers in concentration dependent manner. E) Quantification for the SDS-PAGE at different time points and different Baicalein concentrations shows decrease in the aggregates at higher concentrations of Baicalein. F) The CD analysis of the repeat Tau aggregation shows a shift in the spectra (pink arrow) in control as well as treated samples as compared to soluble protein (black arrow) indicating a shift towards β-sheet structure. The Sol. represents for soluble protein. G) The electron micrographs show the presence of filamentous aggregates (white arrow) in control as opposed to amorphous aggregates (encircled black) in the Baicalein treated samples. (For interpretation of the references to colour in this figure legend, the reader is referred to the Web version of this article.)

the higher concentrations of Baicalein (Fig. 3C). This behavior of ANS suggests that Baicalein might be involved in initial Tau oligomer formation and sequestration.

3.7. SDS-PAGE analysis reveals the enhanced Tau oligomerization and sequestration by Baicalein

In order to confirm our hypothesis, we carried out SDS-PAGE analysis of the control as well as Baicalein treated samples at different time intervals. We examined 10 μl of all the reaction mixtures at zero time point to rule out the presence of any preformed higher order aggregates (Fig. 3D). At 6 h of incubation, we observed the dimers and tetramers in the highest concentration of Baicalein (Fig. 3D and E) and these oligomers appear in all the concentrations of Baicalein treated samples in a time dependent manner. We observed a complete clearance of dimer and monomers in 500 μM Baicalein treatment after 12 h of incubation but the band for tetramers still remains. At 24 h, 200 μM of Baicalein treated Tau show complete conversion from soluble to higher order oligomers. It is to be noted that this is the exact time point when we see stable decrease in ThS fluorescence and an increase in ANS fluorescence (Fig. 3A, C). This seems to be the point where Baicalein sequesters the oligomers formed and inhibits further fibril formation. These results indicate that Baicalein enhances the oligomerization of Tau and blocks them at an oligomeric stage without further leading to fibril formation.

3.8. Baicalein binds and stabilizes partially folded Tau oligomers

Since Baicalein demonstrated the enhancement of Tau oligomerization and their sequestration, we proceeded further to elucidate the conformation of these oligomers by Circular dichroism spectroscopy. The soluble Tau protein is natively unfolded and showed CD spectra of typical random coil at 198 nm (Fig. 3F). Tau on aggregation shows the structural transition from typical random coil to the β-sheet structure [54]. Tau protein treated with Baicalein showed shift in the wavelength towards a partial β-structure (Fig. 3F) suggesting that Baicalein is able to bind and stabilize the partially folded Tau oligomers.

3.9. Electron microscopy visualization of Baicalein induced Tau aggregation inhibition

The time dependent effect of Baicalein on Tau oligomerization and aggregation inhibition was observed by electron micrographs. The untreated sample showed the presence of long fibrillar structures, which are characteristics of Tau filamentous aggregates (Fig. 3G). On the contrary, the 100 μM Baicalein treated Tau showed presence of only pieces of Tau filaments (Fig. 3G). The electron micrograph observation supports our previous observations that Baicalein prevents Tau fibrillization.

3.10. Baicalein does not cause Tau conformational change

As our results suggested that Baicalein could stabilize Tau oligomers having partial β-sheet structure, it was necessary to understand whether, Baicalein alone can cause the random coil to β-sheet transition of Tau protein. For this, we incubated repeat Tau with Baicalein in absence of heparin. We maintained a positive control (with heparin) and negative control (without heparin) for standard aggregation kinetics. The kinetics for both ThS and ANS did not show any increase in fluorescence for negative control as well as Baicalein treated samples (Figs. S6A and B). The positive control showed an increase in ThS and ANS fluorescence as expected. The SDS-PAGE analysis showed the presence of higher order structures in the positive control from 24 h onwards (Fig. S6C). The sample treated with higher concentration of Baicalein (100 μM) showed presence of very faint higher order bands at a later time point for both the proteins (Fig. S6D). The fluorescence kinetics and the SDS-PAGE analysis clearly suggest that Baicalein might be able to induce Tau oligomerization but at a much slower pace. The structural analysis of these oligomers revealed that they do not show transition to β-sheet structure (Fig. S6E) and do not form Tau fibrils (Fig. S6F). These results clearly suggest that Baicalein might be able to induce soluble Tau oligomers at a slower rate without causing any structural changes.

3.11. Disaggregation and sequestration of repeat Tau oligomers by Baicalein

Oligomers of repeat Tau were prepared by incubating Tau in aggregation conditions for 4 h and then subjected to various concentrations of Baicalein to study the disaggregation of repeat Tau oligomers. ThS fluorescence assay suggested that Baicalein is able to disaggregate preformed oligomers in a concentration dependent manner (Fig. 4A). Baicalein was found to enhance and moderately induce oligomerization as well as sequester oligomers into an aggregation incompetent form. The underlying mechanism of disaggregation may involve the breaking of aggregates into smaller fragments and then inhibiting the reformation of higher order aggregates. It was observed that both ThS and ANS fluorescence was decreased upon addition of Baicalein in 4 h (Fig. 4A and B) incubated samples suggesting disaggregation and decreased hydrophobicity respectively. However, the ANS fluorescence increased after 12 h in all the incubated samples. The SDS-PAGE analysis showed that Baicalein could bind to the preformed oligomers and sequester them at this stage. The presence of a tetramer band in all the concentrations of Baicalein can be observed but the dimer as well as the monomer completely disappears (Fig. 4C). We observed the formation of oligomers on the SDS-PAGE and increase in ANS fluorescence but a complete decrease in ThS fluorescence for the Baicalein treated oligomers. This strongly suggests the role of Baicalein in sequestering the Tau oligomers. The SDS-PAGE quantification for repeat Tau oligomer disaggregation (Fig. 4D) shows a gradual decrease in soluble repeat Tau in a concentration dependent manner. Further, CD spectra analysis for repeat Tau samples treated with a varying range of Baicalein concentrations shows a shift towards the β-sheet structure in all concentrations (Fig. 4E and F). Electron micrographs for disaggregation assay samples shows fragility of Tau aggregates and absence of mature Tau filaments (Fig. 4G). Formation of Baicalein induced oligomers was also evident in size exclusion chromatography (SEC). Repeat Tau incubated with Baicalein leads to formation of oligomers as seen in the SEC profiles for samples at 0, 6, 12, 24, 48 and 60 h (Fig. 5A) as compared to soluble repeat Tau. Further, the repeat Tau was incubated

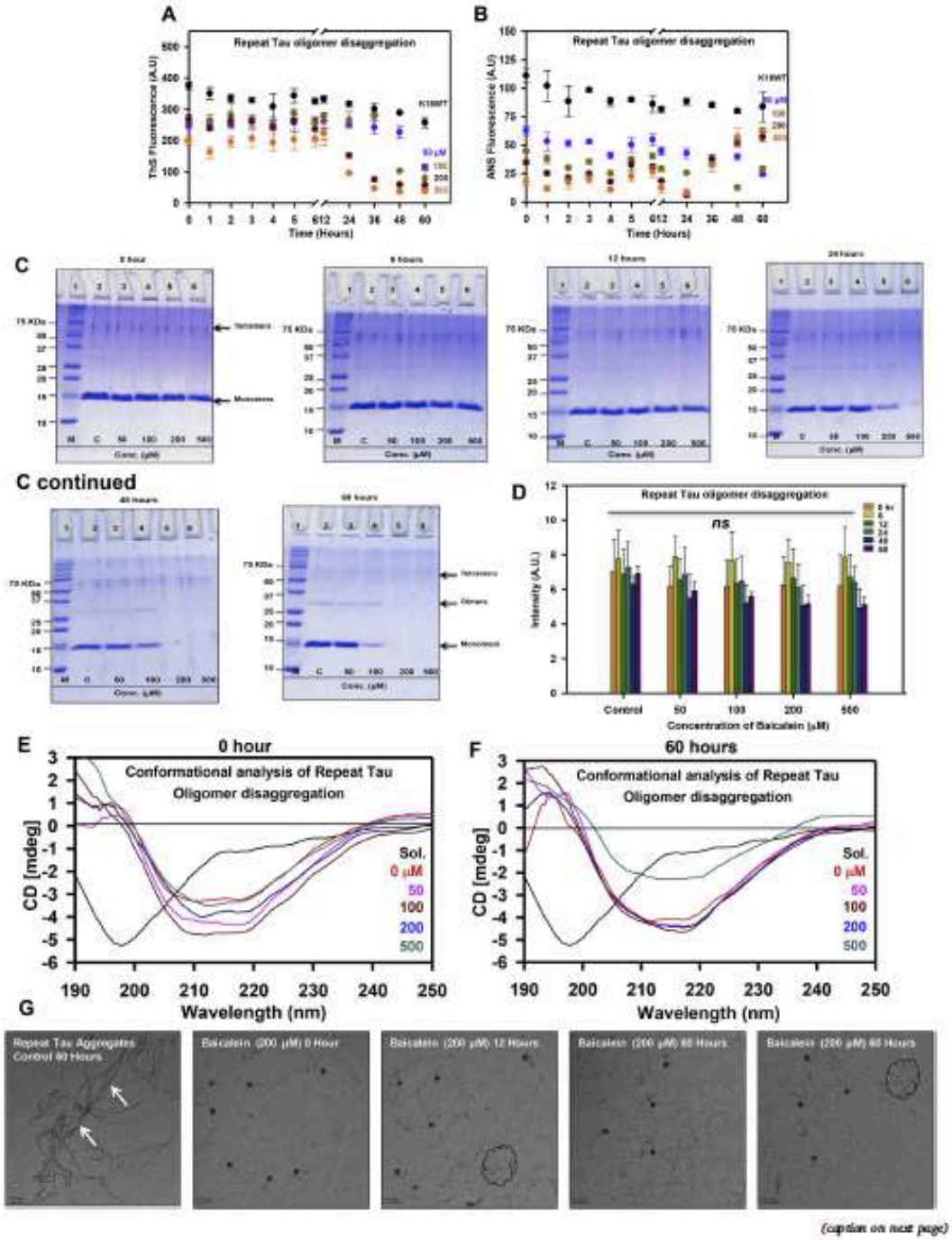

(caption on next page)

Fig. 4. Disaggregation of repeat Tau oligomers by Baicalein. A) Formation of repeat Tau aggregates was monitored by ThS fluorescence after addition of Baicalein at different concentrations after 4 h of incubation. ThS fluorescence shows a marked decrease in a concentration dependent manner. B) ANS fluorescence assay for repeat Tau oligomers disaggregation on addition of different concentrations of Baicalein at 4 h of incubation shows a prominent decrease in fluorescence after Baicalein addition in all the concentrations. There is an increase in fluorescence from 24 h onwards indicating that at higher concentrations Baicalein can increase the hydrophobicity of protein aggregates. C) SDS-PAGE analysis shows a marked decrease in the monomeric form of repeat Tau, which are mostly entrapped as dimeric and tetrameric forms in presence of all different concentrations of Baicalein. D) Quantification of SDS-PAGE showing concentration dependent decrease in intensity for repeat Tau oligomers. E, F) The CD spectra for repeat Tau oligomer disaggregation samples at 0, and 60 h of incubation with different Baicalein concentrations. In all the treated samples, the shift in the spectrum towards β-sheet structure can be observed (shown by pink arrow) as compared to soluble repeat Tau. The Sol. represents for soluble protein. G) Electron micrographs for repeat Tau at 0, 12 and 60 h of incubation with 200 μM Baicalein show smaller broken filaments (black asterisks and encircled area) as compared to untreated control (white arrow). (For interpretation of the references to colour in this figure legend, the reader is referred to the Web version of this article.)

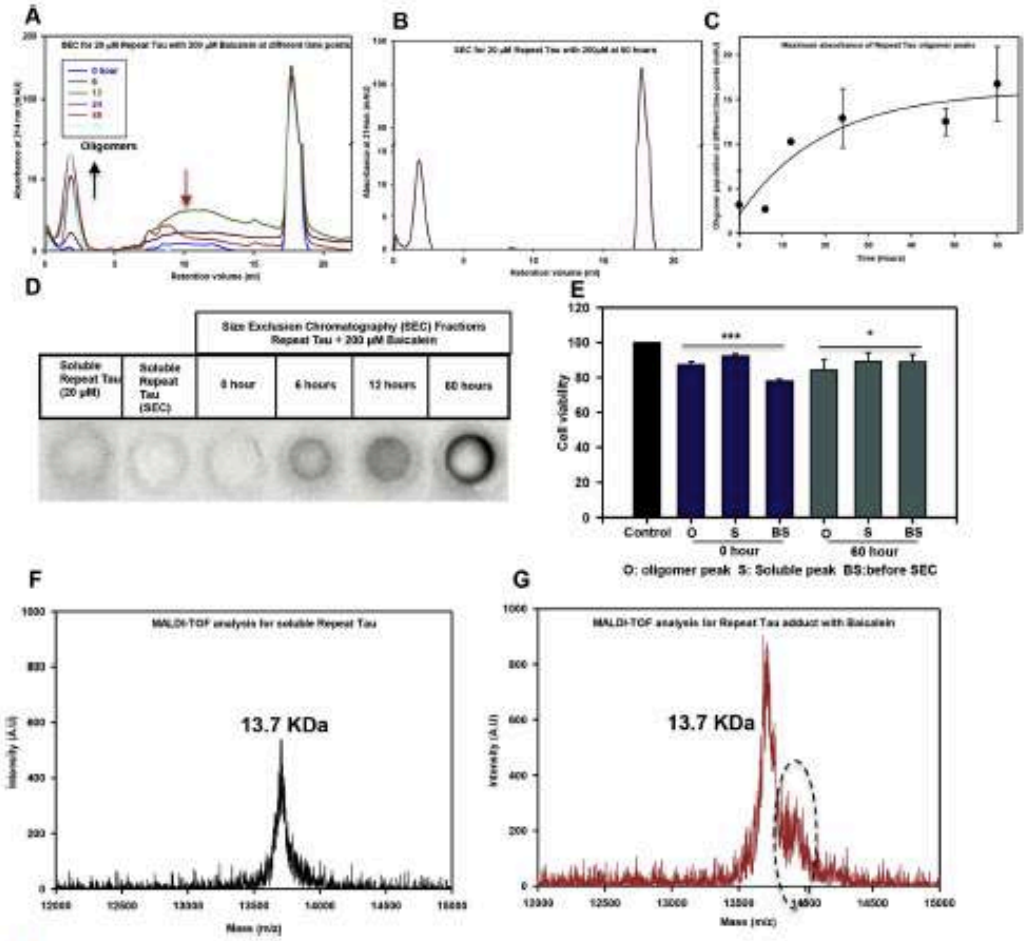

Fig. 5. Size-exclusion chromatography for repeat Tau aggregates. A) Comparison of the chromatograms for repeat Tau incubated with Baicalein at different time points. Figure shows a decrease in dimeric population of repeat Tau (pink arrow) with subsequent increase in the Baicalein stabilized oligomers (black arrow). B) Chromatogram for repeat Tau incubated with Baicalein for 60 h shows increase in oligomer population. C) Maximum absorbance obtained for the peaks for oligomers at different time points shows a gradual increase in Baicalein stabilized oligomers with time. D) The Baicalein induced repeat Tau oligomerization observed by SEC was confirmed by filter trap assay using A11 (anti-oligomers antibody). No significant signal was observed for the soluble repeat Tau before and after SEC confirming absence of oligomers in untreated sample. E) The oligomer as well as the soluble fractions obtained after the SEC of Baicalein treated repeat Tau did not show toxicity on N2a cells. F) The MALDI-TOF analysis of soluble repeat Tau showing 13.7 KDa molecular weight. G) The Baicalein modified Tau showing an adjacent peak of 13.9 KDa in addition to 13.7 KDa peak suggesting covalent modification of repeat Tau by Baicalein. (For interpretation of the references to colour in this figure legend, the reader is referred to the Web version of this article.)

with Baicalein at 1:10 ratio showed presence oligomers while it was absent in the control aggregation sample at 60 h (Fig. 5B), suggesting enhancement of oligomerization in presence of Baicalein. There is an increase in the intensity of peak corresponding to repeat Tau oligomers with respect to time (Fig. 5C). This increase in the population of oligomers as confirmed by probing the obtained fractions with A11 anti-oligomer antibody by filter trap assay (Fig. 5D). An increase in oligomeric population was observed with increase in incubation time, which is in conjunction with the prior results reiterating the role of Baicalein in inducing Tau oligomerization. To further elucidate the nature of these oligomers, we treated the neuro2a cells with the oligomer as well as soluble fractions obtained after SEC. The preformed oligomers treated with Baicalein at 0 h were found to be more toxic as compared to 60 h treated oligomers. The toxicity was reduced in presence of Baicalein though not 100% rescuing the viability of the cells (Fig. 5E).

3.12. Baicalein covalently modifies Tau protein as observed by MALDI-TOF

Baicalein showed oligomer inducing property for Tau in presence of heparin and sequestering these oligomers from further fibrillization. To understand the mechanism by which this occurs, MALDI-TOF analysis was carried out to study whether Baicalein can lead to covalent modification of Tau. The repeat Tau having a theoretical molecular weight of 13.7 KDa was incubated with a range of concentrations of Baicalein for 1 h and 12 h respectively. The samples incubated for 1 h showed an additional peak of 13.9kDa at higher concentration of Baicalein (Figs. 5F and S5D), which was not observed in untreated samples (Figs. 5G and S5A) as well as in lower concentrations of Baicalein (Figs. S5B and C). But after 12h of incubation, all Baicalein treated samples showed a peak adjacent to the peak given by soluble Tau (13.7 KDa) of 13.9 KDa suggesting the covalent modification of repeat Tau by Baicalein (270 Da) (Figs. S5F, G, H) as opposed to untreated (Fig. S5E). Thus, Baicalein could be involved in covalently modifying Tau protein, thus, preventing it from aggregation.

3.13. Baicalein disaggregate mature fibrils of repeat Tau

Disaggregation of repeat Tau fibrils was carried out using different concentrations of Baicalein and monitored by ThS and ANS fluorescence assay. Repeat Tau fibrils were prepared by subjecting the protein to aggregation conditions for 60 h. Initially, after addition of Baicalein, there was decrease in the ThS fluorescence within 12 h in all concentrations of Baicalein suggesting disaggregation of Tau fibrils (Fig. 6A). However, ANS fluorescence decreased initially for 12 h and increased afterwards indicating the formation of oligomers (Fig. 6B). In SDS-PAGE analysis, Baicalein treated samples showed decrease in the population of oligomeric species at different time points (Fig. 6C). The SDS-PAGE quantification for fibril disaggregation (Fig. 6D) shows a gradual decrease in soluble repeat Tau in a concentration dependent manner. This is also supported by the electron micrographs (Fig. 6G), which shows fragility of Tau and absence of mature Tau filaments. Further, CD spectra analysis for repeat Tau samples treated with a varying range of Baicalein concentrations shows a shift towards the β-sheet structure in all concentrations (Fig. 6E and F).

4. Discussion

Aggregation of Tau into insoluble aggregates inside the neuronal cells contributes to the pathogenesis of Alzheimer's disease. The screening of compounds against Tau neurofibrillary tangles has yielded variety of potent molecules [60–62]. Tau pathology undergoes a formation of series of intermittent species and the feasibility of their formation depends on both physiological concentration of free Tau and ability to form aggregation competent conformations [63]. The soluble oligomers of Tau are more toxic than the Tau fibrils [64] and hence the Tau oligomers are gaining more attention as therapeutic targets in AD [65].

The screening for Tau aggregation inhibitors has generally yielded compounds with ring structures, which might have differential interactions with the Tau monomer, Tau aggregates and their intermediates [14,57]. Our current study elucidates that the herbal compound Baicalein binds to specific hydrophobic patches of the repeat domain of Tau and inhibits the Tau aggregation by targeting Tau into soluble oligomers. Similar results have been observed for the structurally similar polyphenol altenusin wherein *in vitro* Tau pathology is inhibited by the polyphenol but the *in vivo* pathology in transgenic mice could not be rescued [66]. The progress of Tau aggregation leads to formation of β-sheet rich structure [54], which provides the stability to these aggregates. Tau aggregation inhibitors either act to weaken the cross beta structures by inserting their rings between the beta sheet stacks or modify the protein or its intermediate aggregates, thus decreasing its aggregation potency [67]. We propose Baicalein belongs to the latter class of inhibitors as it binds and stabilizes the high molecular weight Tau oligomers, which are not capable of fibrillization. The ANS fluorescence clearly suggest the increased hydrophobicity of these sequestered molecules [59,68]. The MALDI analysis reveals the modification of Tau by Baicalein as it forms adduct with repeat Tau as evidenced by an increase in molecular weight of Tau with Baicalein.

In order to shed light on the binding site and the molecular nature of Baicalein interaction with the Tau monomer, we have performed the docking and simulation studies. As the full-length Tau model is impossible to predict due to the disordered nature of the protein, we could get reliable model for the structured regions of Tau only, which is hexapeptide repeat region (244–373). Our results demonstrated that the Baicalein binds to this region. The MD simulation demonstrated that the structure was stable and the nature of interaction is primarily-mediated by hydrophobic interaction and later stabilized by the water-mediated hydrogen bonds. Also, the trajectory of complex simulation suggests the observable conformational change of this aggregation prone region of Tau after Baicalein binding. This conformational dynamicity may be due to the relatively flexible bond between C7-C4 of the Baicalein. This observation is in agreement with the structure of Baicalein as it has two adjacent –OH groups that might have the ability to modify the Tau oligomers and form high molecular weight aggregates, which are visible on SDS-PAGE. Similar mechanism has been postulated for Tau aggregation inhibition with respect to other flavonoids having adjacent –OH groups [69]. Hence, it can be conceived that Baicalein belongs to the class of covalent inhibitor of aggregation. The other potent inhibitors of this class include Oleocanthal, an aldehyde by nature, which reacts with the epsilon amino group of lysine residues to form imines [70]. The mechanism of other covalent inhibitors like cinnamaldehyde and asperbenzaldehyde [29], which are α, β unsaturated aldehydes, involves nucleophilic attack by the cysteine residues of Tau, In contrast, Baicalein a polyalcohol flavonoid can undergo oxidation to quinone form, which is involved in electrophilic attack [71]. The previous studies with aggregation inhibition of α-synuclein have also revealed the similar mechanism of inhibition wherein the oligomers of α-synuclein are prevented to undergo fibril formation in presence of Baicalein [34]. Thus, any inhibitor, which can serve the function of targeting these nucleating species, can be of great therapeutic importance. The effect of Baicalein must be prior to the nucleation as its inhibitory effect on Tau aggregation can be observed early in the course of *in vitro* aggregation. The size-exclusion chromatography results also support this hypothesis, as the Baicalein treated samples showed the disappearance of a peak corresponding to tetramer. Interestingly, there is an appearance of oligomeric species of higher order in the sample incubated with Baicalein. These findings strongly suggest that Baicalein exhibit inhibition activity by sequestration of Tau into oligomers of different nature and taking it off the pathway of aggregation. Although effective against inhibiting fibrillization, Baicalein also worked as a potent molecule for disaggregation of preformed Tau fibrils as well as oligomers (Fig. 7). The ANS fluorescence studies

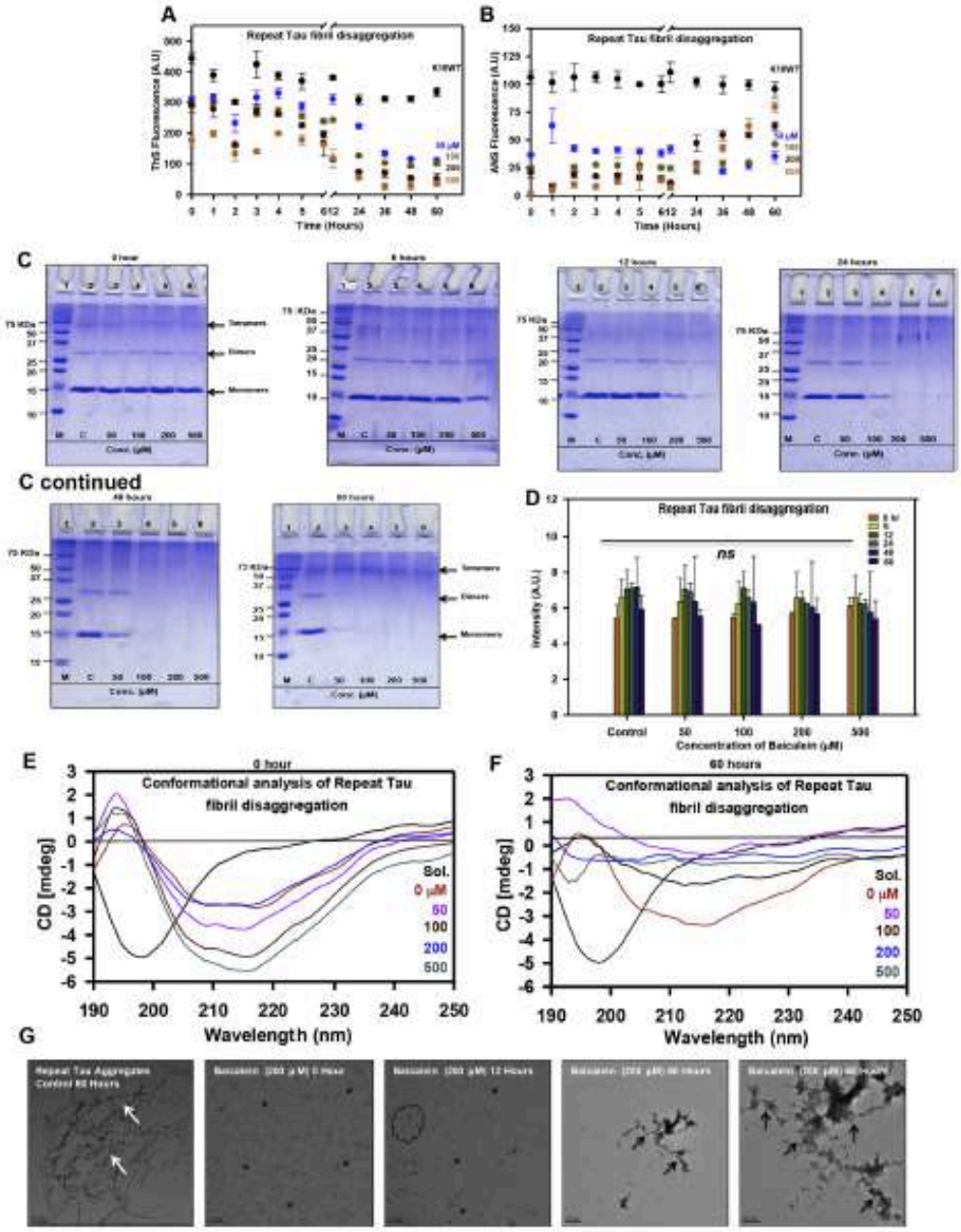

Fig. 6. Disaggregation of repeat Tau fibrils by Baicalein. A) ThS fluorescence for repeat Tau fibril disaggregation shows a decrease with increase in Baicalein concentration and the time of incubation. B) The ANS fluorescence assay for repeat Tau fibrils disaggregation shows more prominent decrease in all concentrations of Baicalein. Furthermore, there is similar increase in ANS fluorescence after 12.

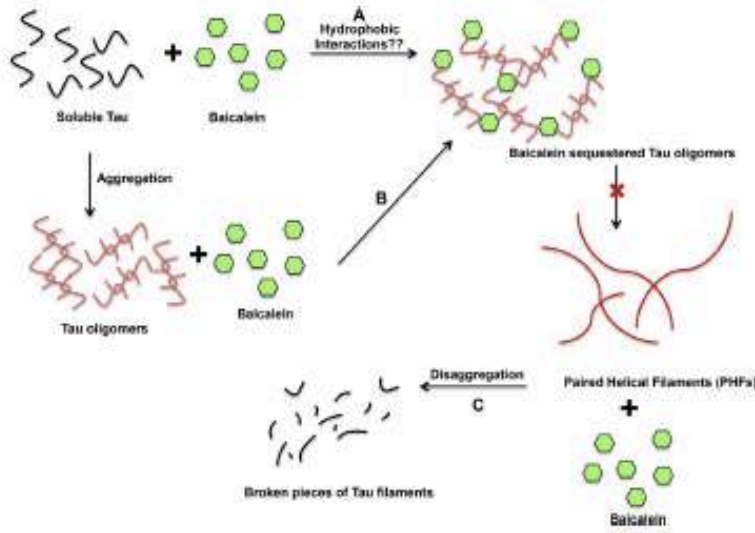

Fig. 7. Model for Baicalein mediated Tau aggregation inhibition and disaggregation. Baicalein may show interaction with various intermittent species of Tau aggregates. A) Baicalein may interact at first step with soluble Tau to induce Tau oligomerization and sequester them based on hydrophobic interactions and prevent their further participation in fibril formation. B) Baicalein might enhance the Tau oligomerization in presence of heparin and further bind these oligomers and inhibit fibril formation. C) Baicalein might also interact with Tau fibrils and lead to their disaggregation leading to formation of small pieces of Tau aggregates.

clearly depict the decrease in fluorescence intensity in the initial stages after Baicalein addition, but are found to increase after 12–24 h at higher concentrations. This behavior of ANS fluorescence can be attributed to the fact that increase in ANS fluorescence depends on binding with hydrophobic residues as well as with cationic amino acids like arginine and lysine [72]. Thus, the Baicalein stabilized oligomer interacts through their cationic residues even though the overall surface hydrophobicity is greatly reduced. The disaggregation potential of Baicalein upon treatment of Tau aggregates signifies that the interaction between these two involves rearrangement of bonds and change in binding energies. If the oligomers formed are stable enough that they do not further interact with other protein species, (either soluble Tau or other oligomers) it can lead to attenuation of further fibrillization of Tau.

Altogether, Baicalein plays a dual role of preventing Tau aggregation as well as dissolving the preformed aggregates and can be further considered for the therapeutic screening.

5. Conclusions

The potency of Baicalein in inhibiting the aggregation of proteins like α-synuclein, amyloid beta and amylin has made this molecule important for screening against the other amyloidogenic proteins. Our current investigation demonstrates the ability of Baicalein to inhibit the Tau aggregation by covalent modification. The simulation and docking studies revealed the interaction of 2 adjacent –OH groups of Baicalein with Leucine 266 of the repeat Tau. These adjacent hydroxyl groups might also be involved in the covalent modification of Tau as observed by MALDI-TOF analysis. Along with hydrogen bonding, the hydrophobic interactions were found to play a role in Tau-Baicalein binding. In summary, Baicalein inhibits the Tau aggregation by inducing the off-pathway oligomer formation and preventing the filamentous aggregate formation thus highlighting its potential to be developed as a future therapeutic agent in AD.

Acknowledgement

This work was supported in part by grants from the Department of Science and Technology-Science and Engineering Research Board DST-SERB/EMR000306 and in-house CSIR-National Chemical Laboratory grant MLP029526. Shweta Kishor Sonawane acknowledges the fellowship from Department of Biotechnology (DBT), India. Abhishek Ankur Balmik acknowledges the Shyama Prasad Mukherjee fellowship (SPMF) from Council of Scientific Industrial Research (CSIR), India. Tau constructs were kindly gifted by Prof. Roland Brandt from University of Osnabruck, Germany and Prof. Jeff Kuret from Ohio State University College of Medicine, USA. We thank Mr. Yugendra R. Patil, Dr. Santhakumari and Dr. Mahesh J Kulkarni for their fruitful discussion on MALDI-TOF.

Appendix A. Supplementary data

Supplementary data to this article can be found online at https://doi.org/10.1016/j.abb.2019.108119.

References

[1] L.M. Ittner, J. Götz, Amyloid-β and tau—a toxic pas de deux in Alzheimer's disease, Nat. Rev. Neurosci. 12 (2011) 67–72.
[2] J. Hardy, Alzheimer's disease: the amyloid cascade hypothesis: an update and reappraisal, J. Alzheimer's Dis. 9 (2006) 151–153.
[3] Y. Wang, E. Mandelkow, Tau in physiology and pathology, Nat. Rev. Neurosci. 17 (1) (2015) 5–21.
[4] S. Lovestone, M. Boada, B. Dubois, M. Hüll, J.O. Rinne, H.-J. Huppertz, M. Calero, M.V. Andrés, B. Gómez-Carrillo, T. León, Aphase II trial of tideglusib in Alzheimer's disease, J. Alzheimer's Dis. 45 (2015) 75–88.
[5] B.H. Mummery, D. Schembri, J. Hinton, A. Blackwell, J. Keith, M. Gold, A.-S. Investigators, A double-blind, placebo-controlled, ascending-dose, randomized study to evaluate the safety, tolerability and effects on cognition of AL-108 after 12 weeks of intranasal administration in subjects with mild cognitive impairment, Dement. Geriatr. Cogn. Disord. 35 (2013) 325–336.
[6] K.S. Kosik, C.L. Joachim, D.J. Selkoe, Microtubule-associated protein tau (tau) is a major antigenic component of paired helical filaments in Alzheimer disease, Proc. Natl. Acad. Sci. 83 (1986) 4044–4048.
[7] K.S. Kosik, L. McGoldrick, Microtubule-associated protein function: lessons from expression in apodopsis fruggipeda cells, Cell Motil. Cytoskelet. 28 (1994) 195–198.
[8] A. Ebneth, R. Godemann, K. Stamer, S. Illenberger, B. Trinczek, E.-M. Mandelkow, E. Mandelkow, Overexpression of tau protein inhibits kinesin-dependent trafficking of vesicles, mitochondria, and endoplasmic reticulum: implications for Alzheimer's disease, The Journal of cell biology 143 (1998) 777–794.
[9] E.-M. Mandelkow, E. Mandelkow, Biochemistry and cell biology of tau protein in neurofibrillary degeneration, Cold Spring Harbor perspectives in medicine 2 (2012) a006247.
[10] K. Iqbal, F. Liu, C.-X. Gong, A.d.C. Alonso, I. Grundke-Iqbal, Mechanisms of tau-

induced neurodegeneration, Acta Neuropathol. 118 (2009) 53–69.
[11] E.-M. Mandelkow, E. Mandelkow, Tau in Alzheimer's disease, Trends Cell Biol. 8 (1998) 425–427.
[12] C.M. Cowan, S. Quraishe, A. Mudher, What is the pathological significance of tau oligomers? Biochem. Soc. Trans. 40 (2012) 693–697.
[13] B. Bulic, M. Pickhardt, B. Schmidt, E.M. Mandelkow, H. Waldmann, E. Mandelkow, Development of tau aggregation inhibitors for Alzheimer's disease, Angew. Chem. Int. Ed. 48 (2009) 1740–1752.
[14] B. Bulic, M. Pickhardt, E.-M. Mandelkow, E. Mandelkow, Tau protein and tau aggregation inhibitors, Neuropharmacology 59 (2010) 276–289.
[15] C. Lawatscheck, M. Pickhardt, S. Wieczorek, A. Grafmüller, E. Mandelkow, H.G. Börner, Generalizing the concept of specific compound formulation additives towards non-fluorescent drugs: a solubilization study on potential anti-alzheimer-active small-molecule compounds, Angew. Chem. Int. Ed. 55 (2016) 8752–8756.
[16] D.M. Holtzman, M.C. Carrillo, J.A. Hendrix, L.J. Bain, A.M. Catafau, L.M. Gault, M. Goedert, E. Mandelkow, E.-M. Mandelkow, D.S. Miller, Tau: from research to clinical development, Alzheimer's Dementia 12 (2016) 1033–1039.
[17] V.M. Lee, K.R. Brunden, M. Hutton, J.Q. Trojanowski, Developing therapeutic approaches to tau, selected kinases, and related neuronal protein targets, Cold Spring Harbor perspectives in medicine 1 (2011) a006437.
[18] A. Crowe, M.J. James, V.M.-Y. Lee, A.B. Smith, J.Q. Trojanowski, C. Ballatore, K.R. Brunden, Aminothienopyridazines and methylene blue affect Tau fibrillization via cysteine oxidation, J. Biol. Chem. 288 (2013) 11024–11037.
[19] C. Wischik, P. Edwards, R. Lai, M. Roth, C. Harrington, Selective inhibition of Alzheimer disease-like tau aggregation by phenothiazines, Proc. Natl. Acad. Sci. 93 (1996) 11213–11218.
[20] R.H. Schirmer, H. Adler, M. Pickhardt, E. Mandelkow, ... , Lest we forget you—methylene blue, Neurobiol. Aging 32 (2011) 2325. e2327-2325. e2316.
[21] J.C. O'Leary, Q. Li, P. Marinec, L.J. Blair, E.E. Congdon, A.G. Johnson, U.K. Jinwal, J. Koren, J.R. Jones, C. Kraft, Phenothiazine-mediated rescue of cognition in tau transgenic mice requires neuroprotection and reduced soluble tau burden, Mol. Neurodegener. 5 (2010) 1.
[22] C.M. Wischik, C.R. Harrington, J.M. Storey, Tau-aggregation inhibitor therapy for Alzheimer's disease, Biochem. Pharmacol. 88 (2014) 529–539.
[23] E. Akoury, M. Pickhardt, M. Gajda, J. Biernat, E. Mandelkow, M. Zweckstetter, Mechanistic basis of phenothiazine-driven inhibition of tau aggregation, Angew. Chem. Int. Ed. 52 (2013) 3511–3515.
[24] C. Ballatore, K.R. Brunden, D.M. Huryn, J.Q. Trojanowski, V.M.-Y. Lee, A.B. Smith III, Microtubule stabilizing agents as potential treatment for Alzheimer's disease and related neurodegenerative tauopathies, J. Med. Chem. 55 (2012) 8979–8996.
[25] B. Zhang, J. Carroll, J.Q. Trojanowski, Y. Yao, M. Iba, J.S. Potuzak, A.-M.L. Hogan, S.X. Xie, C. Ballatore, A.B. Smith, The microtubule-stabilizing agent, epothilone D, reduces axonal dysfunction, neurotoxicity, cognitive deficits, and Alzheimer-like pathology in an interventional study with aged tau transgenic mice, J. Neurosci. 32 (2012) 3601–3611.
[26] K.R. Brunden, B. Zhang, J. Carroll, Y. Yao, J.S. Potuzak, A.-M.L. Hogan, M. Iba, M.J. James, S.X. Xie, C. Ballatore, Epothilone D improves microtubule density, axonal integrity, and cognition in a transgenic mouse model of tauopathy, J. Neurosci. 30 (2010) 13861–13866.
[27] L. Calcul, B. Zhang, U.K. Jinwal, C.A. Dickey, B.J. Baker, Natural products as a rich source of tau-targeting drugs for Alzheimer's disease, Future Med. Chem. 4 (2012) 1751–1761.
[28] S.R. Paranjape, A.P. Riley, A.D. Somoza, C.E. Oakley, C.C. Wang, T.E. Prisinzano, B.R. Oakley, T.C. Gamblin, Azaphilones inhibit tau aggregation and dissolve tau aggregates in vitro, ACS Chem. Neurosci. 6 (2015) 751–760.
[29] S.R. Paranjape, Y.-M. Chiang, J.F. Sanchez, R. Entwistle, C.C. Wang, B.R. Oakley, T.C. Gamblin, Inhibition of Tau aggregation by three Aspergillus nidulans secondary metabolites: 2, ω-dihydroxyemodin, asperthecin, and asperbenzaldehyde, Planta Med. 80 (2014) 77–85.
[30] W. Li, J.B. Sperry, A. Crowe, J.Q. Trojanowski, A.B. Smith III, V.M.Y. Lee, Inhibition of tau fibrillization by oleocanthal via reaction with the amino groups of tau, J. Neurochem. 110 (2009) 1339–1351.
[31] J. Bieschke, J. Russ, R.P. Friedrich, D.E. Ehrnhoefer, H. Wobst, K. Neugebauer, E.E. Wanker, EGCG remodels mature α-synuclein and amyloid-β fibrils and reduces cellular toxicity, Proc. Natl. Acad. Sci. 107 (2010) 7710–7715.
[32] H.J. Wobst, A. Sharma, M.I. Diamond, E.E. Wanker, J. Bieschke, The green tea polyphenol (−)-epigallocatechin gallate prevents the aggregation of tau protein into toxic oligomers at substoichiometric ratios, FEBS Lett. 589 (2015) 77–83.
[33] D. Vauzour, K. Vafeiadou, A. Rodriguez-Mateos, C. Rendeiro, J.P. Spencer, The neuroprotective potential of flavonoids: a multiplicity of effects, Genes & nutrition 3 (2008) 115–126.
[34] M. Zhu, S. Rajamani, J. Kaylor, S. Han, F. Zhou, A.L. Fink, The flavonoid baicalein inhibits fibrillation of α-synuclein and disaggregates existing fibrils, J. Biol. Chem. 279 (2004) 26846–26857.
[35] S.Q. Zhang, D. Obregon, J. Ehrhart, J. Deng, J. Tian, H. Hou, B. Giunta, D. Sawmiller, J. Tan, Baicalein reduces β-amyloid and promotes nonamyloidogenic amyloid precursor protein processing in an Alzheimer's disease transgenic mouse model, J. Neurosci. Res. 91 (2013) 1239–1246.
[36] P.D.Q. Huy, Q.V. Vuong, G. La Penna, P. Faller, M.S. Li, Impact of Cu (II) binding on structures and dynamics of Aβ42 monomer and dimer: molecular dynamics study, ACS Chem. Neurosci. 7 (2016) 1348–1363.
[37] S. Barghorn, J. Biernat, E. Mandelkow, Purification of recombinant tau protein and preparation of Alzheimer-paired helical filaments in vitro, Amyloid Proteins: Methods and Protocols (2005) 35–51.
[38] S.F. Altschul, W. Gish, W. Miller, E.W. Myers, D.J. Lipman, Basic local alignment search tool, J. Mol. Biol. 215 (1990) 403–410.
[39] B. Webb, A. Sali, Protein structure modeling with MODELLER, Protein Structure Prediction, Springer, 2014, pp. 1–15.
[40] R.A. Laskowski, M.W. MacArthur, D.S. Moss, J.M. Thornton, PROCHECK: a program to check the stereochemical quality of protein structures, J. Appl. Crystallogr. 26 (1993) 283–291.
[41] S.C. Lovell, I.W. Davis, W.B. Arendall III, P.I. De Bakker, J.M. Word, M.G. Prisant, J.S. Richardson, D.C. Richardson, Structure validation by Cα geometry: φ, ψ and Cβ deviation, Proteins: Structure, Function, and Bioinformatics 50 (2003) 437–450.
[42] C. Colovos, T.O. Yeates, Verification of protein structures: patterns of nonbonded atomic interactions, Protein Sci. 2 (1993) 1511–1519.
[43] M. Wiederstein, M.J. Sippl, ProSA-web: interactive web service for the recognition of errors in three-dimensional structures of proteins, Nucleic Acids Res. 35 (2007) W407–W410.
[44] G.M. Sastry, M. Adzhigirey, T. Day, R. Annabhimoju, W. Sherman, Protein and ligand preparation: parameters, protocols, and influence on virtual screening enrichments, J. Comput. Aided Mol. Des. 27 (2013) 221–234.
[45] R.A. Friesner, J.L. Banks, R.B. Murphy, T.A. Halgren, J.J. Klicic, D.T. Mainz, M.P. Repasky, E.H. Knoll, M. Shelley, J.K. Perry, Glide: a new approach for rapid, accurate docking and scoring. 1. Method and assessment of docking accuracy, J. Med. Chem. 47 (2004) 1739–1749.
[46] T.A. Halgren, Identifying and characterizing binding sites and assessing druggability, J. Chem. Inf. Model. 49 (2009) 377–389.
[47] K.J. Bowers, D.E. Chow, H. Xu, R.O. Dror, M.P. Eastwood, B.A. Gregersen, J.L. Klepeis, I. Kolossvary, M.A. Moraes, F.D. Sacerdoti, Scalable algorithms for molecular dynamics simulations on commodity clusters, SC'06: Proceedings of the 2006 ACM/IEEE Conference on Supercomputing, IEEE, 2006 43-43.
[48] S. Jeganathan, M. von Bergen, H. Brutlach, H.-J. Steinhoff, E. Mandelkow, Global hairpin folding of tau in solution, Biochemistry 45 (2006) 2283–2293.
[49] P. Chompoonuthon, J. Sucharitakul, B. Panijpan, P. Chaiyen, Measuring binding affinity of Protein – ligand interaction using spectrophotometry: binding of neutral red to riboflavin-binding protein, J. Chem. Educ. 87 (2010) 829–831.
[50] Y.-J. Hu, Y. Liu, J.-B. Wang, X.-H. Xiao, S.-S. Qu, Study of the interaction between monoammonium glycyrrhizinate and bovine serum albumin, J. Pharm. Biomed. Anal. 36 (2004) 915–919.
[51] F. Zsila, Z. Bikádi, M. Simonyi, Probing the binding of the flavonoid, quercetin to human serum albumin by circular dichroism, electronic absorption spectroscopy and molecular modelling methods, Biochem. Pharmacol. 65 (2003) 447–456.
[52] V. Daebel, S. Chinnathambi, J. Biernat, M. Schwalbe, B. Habenstein, A. Loquet, E. Akoury, K. Tepper, H. Müller, M. Baldus, β-Sheet core of tau paired helical filaments revealed by solid-state NMR, J. Am. Chem. Soc. 134 (2012) 13982–13989.
[53] M.D. Mukrasch, J. Biernat, M. von Bergen, C. Griesinger, E. Mandelkow, M. Zweckstetter, Sites of tau important for aggregation populate (beta)-structure and bind to microtubules and polyanions, J. Biol. Chem. 280 (2005) 24978–24986.
[54] M. Von Bergen, S. Barghorn, J. Biernat, E.-M. Mandelkow, E. Mandelkow, Tau aggregation is driven by a transition from random coil to beta sheet structure, Biochim. Biophys. Acta (BBA) - Mol. Basis Dis. 1739 (2005) 158–166.
[55] P. Friedhoff, M. Von Bergen, E.-M. Mandelkow, P. Davies, E. Mandelkow, A nucleated assembly mechanism of Alzheimer paired helical filaments, Proc. Natl. Acad. Sci. 95 (1998) 15712–15717.
[56] M. Goedert, R. Jakes, M. Spillantini, M. Hasegawa, M. Smith, R. Crowther, Assembly of Microtubule-Associated Protein Tau into Alzheimer-like Filaments Induced by Sulphated Glycosaminoglycans, (1996).
[57] M. Pickhardt, Z. Gazova, M. von Bergen, I. Khlistunova, Y. Wang, A. Hascher, E.-M. Mandelkow, J. Biernat, E. Mandelkow, Anthraquinones inhibit tau aggregation and dissolve Alzheimer's paired helical filaments in vitro and in cells, J. Biol. Chem. 280 (2005) 3628–3635.
[58] G. Ramachandran, J.B. Udgaonkar, Understanding the kinetic roles of the inducer heparin and of rod-like protofibrils during amyloid fibril formation by Tau protein, J. Biol. Chem. 286 (2011) 38948–38959.
[59] S. Kumar, K. Tepper, S. Kaniyappan, J. Biernat, S. Wegmann, E.-M. Mandelkow, D.J. Müller, E. Mandelkow, Stages and conformations of the Tau repeat domain during aggregation and its effect on neuronal toxicity, J. Biol. Chem. 289 (2014) 20318–20332.
[60] A. Crowe, C. Ballatore, E. Hyde, J.Q. Trojanowski, V.M.-Y. Lee, High throughput screening for small molecule inhibitors of heparin-induced tau fibril formation, Biochem. Biophys. Res. Commun. 358 (2007) 1–6.
[61] K.R. Brunden, J.Q. Trojanowski, V.M.-Y. Lee, Advances in tau-focused drug discovery for Alzheimer's disease and related tauopathies, Nat. Rev. Drug Discov. 8 (2009) 783–793.
[62] B. Bulic, M. Pickhardt, E. Mandelkow, Progress and developments in tau aggregation inhibitors for Alzheimer disease, J. Med. Chem. 56 (2013) 4135–4155.
[63] E.E. Congdon, S. Kim, J. Bonchak, T. Songrug, A. Matzavinos, J. Kuret, Nucleation-dependent tau filament formation the importance of dimerization and an estimation of elementary rate constants, J. Biol. Chem. 283 (2008) 13806–13816.
[64] K. Flach, I. Hilbrich, A. Schiffmann, U. Gärtner, M. Krüger, M. Leonhardt, H. Waschipky, L. Wick, T. Arendt, M. Holzer, Tau oligomers impair artificial membrane integrity and cellular viability, J. Biol. Chem. 287 (2012) 43223–43233.
[65] L. Gerson-Martínez, G.A. Perry, R.B. Maccioni, Tau oligomers as potential targets for Alzheimer's diagnosis and novel drugs, Tau oligomers 3 (2014) 35.
[66] S.W. Chua, A. Cornejo, J. van Eersel, C.H. Stevens, I. Vaca, M. Cueto, M. Kassiou, A. Gladbach, A. Macmillan, L. Lewis, The polyphenol altenusin inhibits in vitro fibrillization of tau and reduces induced tau pathology in primary neurons, ACS Chem. Neurosci. 8 (2017) 743–751.
[67] M. Margittai, R. Langen, Template-assisted filament growth by parallel stacking of tau, Proc. Natl. Acad. Sci. U.S.A. 101 (2004) 10278–10283.

[68] G. Semisotnov, N. Rodionova, O. Razgulyaev, V. Uversky, A. Gripas, R. Gilmanshin, Study of the "molten globule" intermediate state in protein folding by a hydrophobic fluorescent probe, Biopolymers 31 (1991) 119–128.
[69] S. Taniguchi, N. Suzuki, M. Masuda, S.-i. Hisanaga, T. Iwatsubo, M. Goedert, M. Hasegawa, Inhibition of heparin-induced tau filament formation by phenothiazines, polyphenols, and porphyrins, J. Biol. Chem. 280 (2005) 7614–7623.
[70] M.C. Monti, L. Margarucci, R. Riccio, A. Casapullo, Modulation of tau protein fibrillization by oleuropein, J. Nat. Prod. 75 (2012) 1584–1588.
[71] K. Cook, G.L. Cooper, C.J. Hanby, J. Kent, Structure and mechanism of action of tau aggregation inhibitors, Curr. Alzheimer Res. 11 (2014) 918–927..
[72] O.K. Gasymov, B.J. Glasgow, ANS fluorescence: potential to augment the identification of the external binding sites of proteins, Biochim. Biophys. Acta Protein Proteomomics 1774 (2007) 403–411.
[73] S. Sonawane, et al., Protein-Capped Metal Nanoparticles Inhibit Tau Aggregation in Alzheimer's Disease, ACS Omega (2019) 12833–12840, https://doi.org/10.1021/acsomega.9b01431.

www.nature.com/scientificreports

SCIENTIFIC REPORTS
natureresearch

Check for updates

OPEN

EGCG impedes human Tau aggregation and interacts with Tau

Shweta Kishor Sonawane[1,4], Hariharakrishnan Chidambaram[1,4], Debjyoti Boral[2,4], Nalini Vijay Gorantla[1,4,5], Abhishek Ankur Balmik[1,4,5], Abha Dangi[3,4], Sureshkumar Ramasamy[2,4], Udaya Kiran Marelli[3,4] & Subashchandrabose Chinnathambi[1,4]✉

Tau aggregation and accumulation is a key event in the pathogenesis of Alzheimer's disease. Inhibition of Tau aggregation is therefore a potential therapeutic strategy to ameliorate the disease. Phytochemicals are being highlighted as potential aggregation inhibitors. Epigallocatechin-3-gallate (EGCG) is an active phytochemical of green tea that has shown its potency against various diseases including aggregation inhibition of repeat Tau. The potency of EGCG in altering the PHF assembly of full-length human Tau has not been fully explored. By various biophysical and biochemical analyses like ThS fluorescence assay, MALDI-TOF analysis and Isothermal Titration Calorimetry, we demonstrate dual effect of EGCG on aggregation inhibition and disassembly of full-length Tau and their binding affinity. The IC50 for Tau aggregation by EGCG was found to be 64.2 µM.

Abbreviations

EGCG	Epigallocatechin-3-gallate
AD	Alzheimer's disease
Aβ	Amyloid-β
IAPP	Islet amyloid polypeptide
ITC	Isothermal titration calorimetry
TEM	Transmission electron microscopy
SEC	Size exclusion chromatography
MTT	3-(4,5-Dimethylthiazol-2-yl)-2,5-diphenyltetrazolium bromide
ThS	Thioflavin S
ANS	8-Anilino-1-naphthalenesulfonic acid ammonium salt

The direct causal relationship between neurodegenerative disorders and protein misfolding has been debatable over years[1–3]. The recent advances in studies of misfolded proteins to some extent have shed the light upon the cause-effect interdependence of proteins and diseases[4]. Neurodegenerative diseases are diverse in nature at physiological as well as molecular level. For example, the misfolded proteins involved in Alzheimer's disease (AD) are amyloid-β (Aβ) and Tau (Fig. 1A) whereas[5]; α-Synuclein is a key player in Parkinson's disease. AD is phenotypically characterized by gradual memory loss due to neuronal death[6]. The molecular pathology involves abnormal accumulation of Aβ plaques[7] in the extracellular milieu and cytoplasmic Tau tangles[8,9]. Tau aggregation increases load on clearance machinery of neurons, which finally collapses, and results in neuronal death[10,11]. The physiological function of Tau is to bind microtubules and stabilize them thus aiding in neuronal functioning[12,13]. Tau aggregates abnormally due to multiple factors-like mutations, aberrant post-translational modifications, oxidative stress etc.[14–16]. Abnormal phosphorylation of Tau is one of the key factors implied in its aggregation[17,18]. The factors leading to Tau aggregation have directed the researchers to design and develop the therapeutics against Tau aggregation and AD. Several classes of compounds showing potency in inhibiting Tau aggregation include phenothiazines[19,20], anthraquinones[21], porphyrins, aminothienopyridazines[22], natural compounds (polyphenols [23], secondary metabolites[24], curcumin[25], Oleocanthal[26] etc.). The phenothiazine compounds inhibit Tau-Tau (repeat domain) binding thus preventing Tau aggregation. These compounds have

[1]Neurobiology Group, Division of Biochemical Sciences, CSIR-National Chemical Laboratory, Dr. Homi Bhabha Road, Pune 411008, India. [2]Structural Biology Group, Division of Biochemical Sciences, CSIR-National Chemical Laboratory, Dr. Homi Bhabha Road, Pune 411008, India. [3]Central NMR Facility and Division of Organic Chemistry, CSIR-National Chemical Laboratory, Dr. Homi Bhabha Road, Pune 411008, India. [4]Academy of Scientific and Innovative Research (AcSIR), Pune 411008, India. [5]These authors contributed equally: Nalini Vijay Gorantla and Abhishek Ankur Balmik ✉email: s.chinnathambi@ncl.res.in

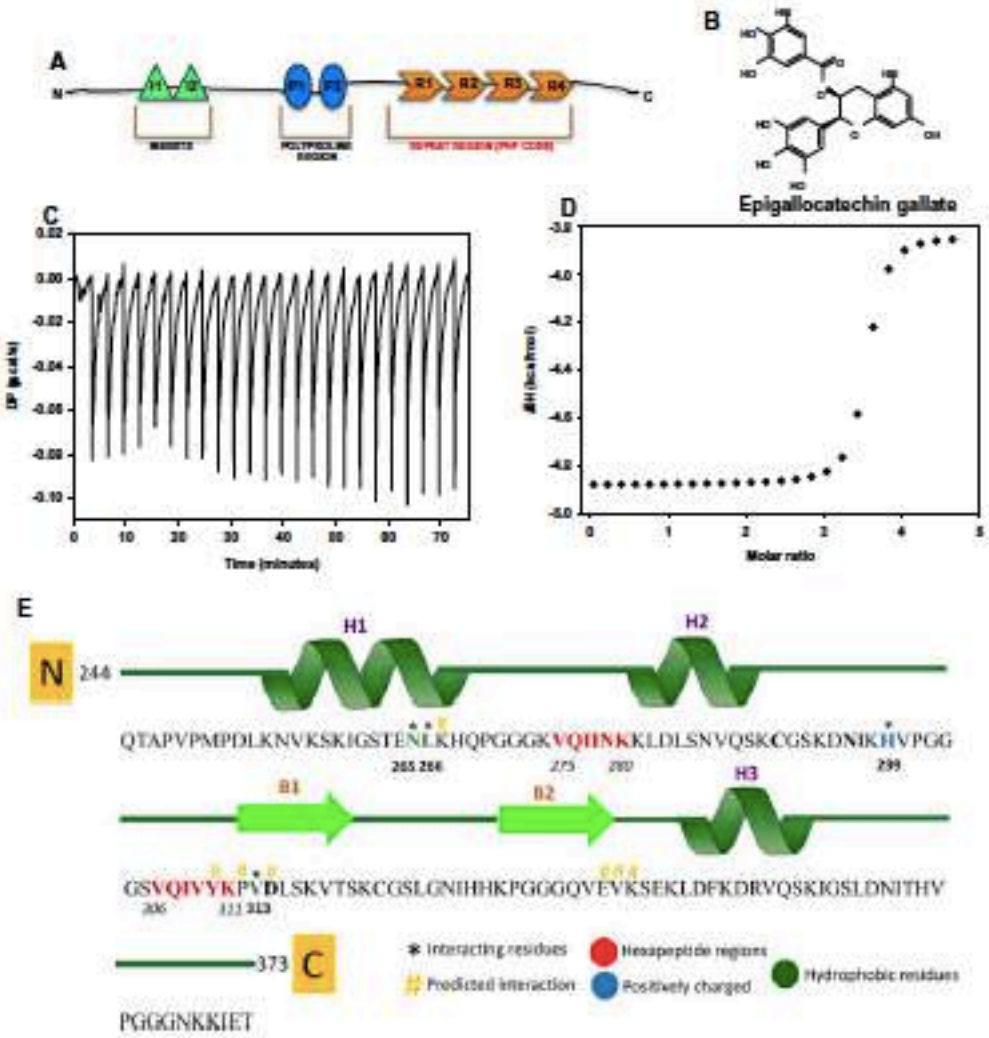

Figure 1. The interaction and binding affinity of Tau and EGCG. (**A**) Tau domain organization. (**B**) The structure of polyphenol EGCG. (**C**) Isothermal titration calorimetry carried out for 20 μM full-length Tau and 500 μM EGCG shows multi-site binding between the two. (**D**) The heat plot for Tau-EGCG interaction suggests n = 3.5 binding sites. Thus, there are more than one binding events involved in Tau-EGCG interaction. (**E**) A schematic diagram of the Tau K18 model depicting three predicted alpha helices (H1, H2, and H3) and two predicted beta sheets (B1, B2) with two distinct and characteristic hexa-peptide regions ^{275}VQIINK^{280} and ^{306}VQIVYK^{311}. The predicted ligand interacting residues, color coded according to their type of interaction is also shown.

a varied potency in inhibiting Tau-Tau binding. For example, Thionine and Azure A have inhibitory constant of 98 nM and 108 nM, respectively whereas chlorpromazine and tacrine have inhibitory constants 55.9 μM and > 100 μM[38]. Oleocanthal, an aglycone in extra virgin olive oil inhibits aggregation of full-length and repeat Tau. The IC50 value for repeat Tau mutant P301L (K18PL) for natural and unnatural oleocanthal was found to be 2.9 μM and 3 μM, respectively[39].

Epigallocatechin-3-gallate (EGCG) is an active component of green tea belonging to class of polyphenols (Fig. 1B). EGCG has been implicated in preventing aggregation of proteins involved in disease conditions[37].

Titration ratio (Tau : EGCG)	1:35
Temperature (°C)	25.2
Bin	Binding
[Syringe]	680 µM
[Cell]	20 µM
N (sites)	3.48
Kd	74 nM
ΔH (kcal/mol)	− 1.04
ΔG (kcal/mol)	− 9.73
− TΔS (kcal/mol)	− 8.68

Table 1. Parameters and calculated values for Tau-EGCG binding constant.

It inhibits aggregation of transthyretin protein involved in peripheral neuropathy[28]. Islet amyloid polypeptide (IAPP) associated with the pathology of type-2 diabetes misfolds and deposits in the β-cells of pancreas. EGCG prevents the amyloid seed formation by IAPP and also disaggregates the preformed amyloid fibrils[29,30]. In scrapie-infected cells EGCG prevented the formation of PrP^{Sc} thus showing its effectiveness against misfolding of prion protein[31]. EGCG has been studied extensively with respect to protein misfolding in AD. EGCG hampers the aggregation of Aβ by inducing off-pathway oligomers that did not stimulate fibrillogenesis. Oxidized EGCG hydrophobically remodels the amyloid fibrils decreasing the competency of oligomers formed[32]. Repeat Tau (K18ΔK280) aggregation is prevented by EGCG at low concentration and rescues the aggregate mediated toxicity of neuronal cells[33]. We show the efficacy of EGCG to prevent the aggregation and disaggregation of full-length Tau in vitro. To further explore the probable binding site, mode of binding and affinity of EGCG with Tau, ITC and molecular docking and simulation studies were done. The binding affinity of full-length Tau with EGCG was determined by ITC whereas the docking and simulation studies were done with the modeled hexapeptide repeat region of Tau.

Results

EGCG interacts with Tau in a multiple binding event. Tau as a therapeutic target in AD has been explored extensively. The protein–ligand binding affinity plays a key role in determining the functional consequences at the molecular level. Full-length Tau and EGCG binding was determined by using isothermal titration calorimetry. ITC result suggests that EGCG binds to Tau at multiple sites. The binding isotherm showing the heat change over the course of titration indicates initial decrease in enthalpy followed by subsequent increase until the end point of titration in a 25 injections program (Fig. 1C). This suggested that the initial binding of EGCG is rapid and constrains the further binding with Tau. However, the negative value of free energy changes (ΔG) of the reaction indicates that EGCG binding to Tau is spontaneous and favourable (Fig. S1). The heat plot between the heat change per mole of the reactants EGCG and Tau and their molar ratio gives the number of interacting sites as 3.48 (Fig. 1D) and the Kd was determined from the thermodynamic parameters as 74 nM (Table 1). These results suggested binding between Tau and EGCG occurs in a multi-sites binding event such that the initial binding events are rapid and saturable. After initial rapid Tau-EGCG interaction, equilibrium is attained where, constant association and dissociation of Tau-EGCG occurs. Similar nature of interaction has been reported for HSA-EGCG interaction where two separate binding events occur. There is initial strong binding between HSA and EGCG followed by 1,000 times weaker secondary binding event[34]. EGCG is thought to act via a common mechanism for various aggregation prone proteins.

Molecular models of Tau protein. In order to determine the putative binding site of EGCG to Tau and check if the hexapeptide repeat regions VQIINK and VQIVYK play any major role in the interactions between EGCG and Tau, a molecular model of Tau was generated. However, since Tau is a highly dynamic and disordered protein, predicting a model for its entire 441 residues is a near impossible task. Yet, the hexapeptide repeat regions are relatively structurally stable as corroborated by other previously reported biochemical and NMR data. So, a stretch of 147 amino acid residues including the hexapeptide regions and a few surrounding residues were used to make the model of Tau (Fig. 1E), which was used for further studies. These residues were finalized based on a BLAST search against PDB, which identified homologous structures, which could be used as templates to build the homology model of this region. NMR based structure of Tau (residue stretch 267–312) bound to microtubules (2MZ7) shared an identity of 100% and query coverage of 92% with the target sequence, and were hence used for modeling studies. The stereochemical parameters of the initial models were verified and it was observed that more than 98% of all residues were placed in the allowed regions of the Ramachandran plot. To further improve the model, refinement strategies involving preprocessing of the initial models (by adding hydrogens, assigning bond order, and filling missing loops and side chains) were performed. Following that, a restrained minimization was performed on the models, by applying constraints, which would serve to converge the non-hydrogen atoms to an RMSD of 0.3 using the OPLS 2005 force field. Finally, the models were subjected to 500 steps of steepest descent energy minimization, followed by 1,000 steps of conjugate gradient energy minimization using the same force field. These energy-minimized models were further used for docking and molecular dynamics studies.

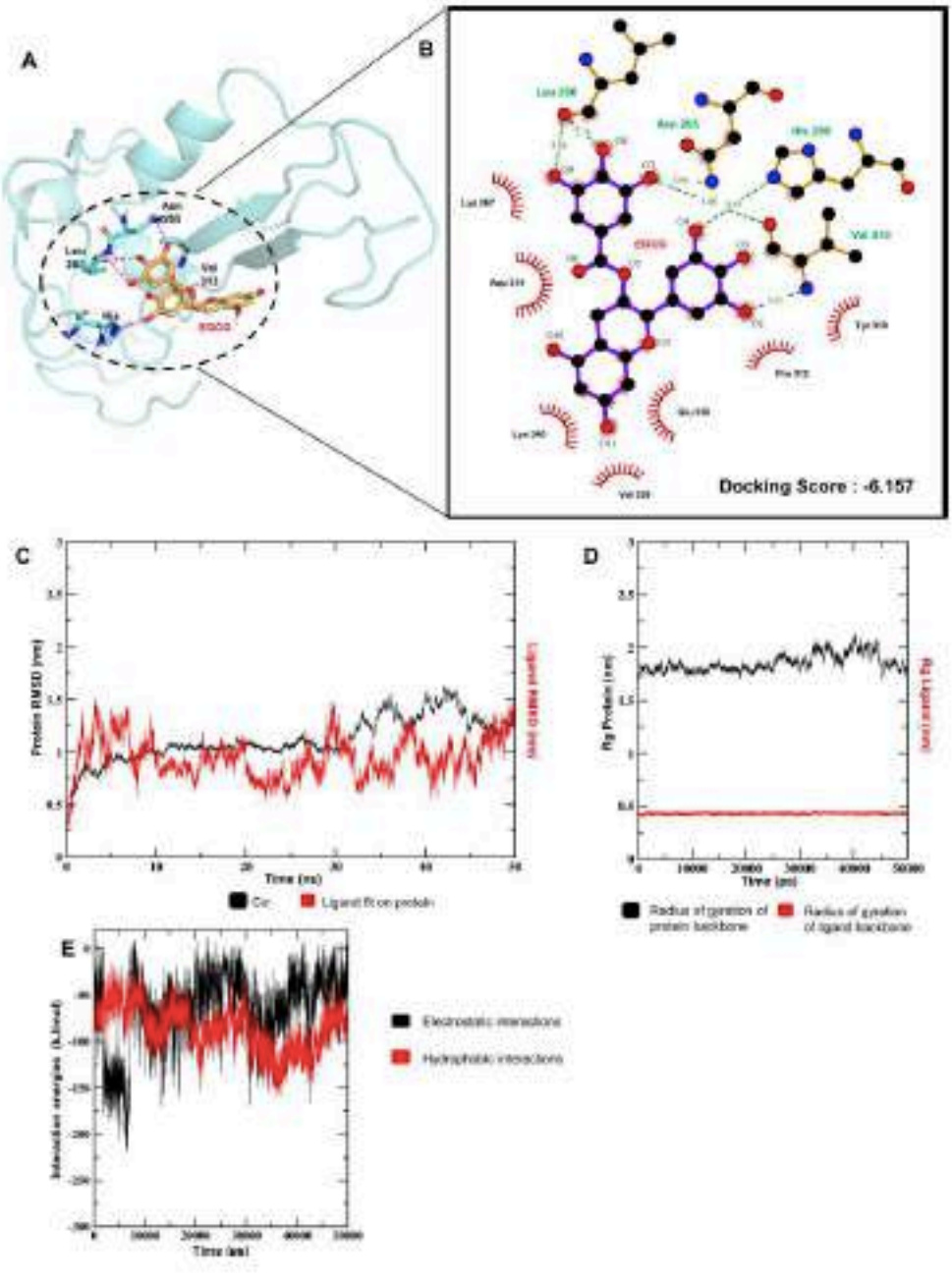
A
B
Docking Score : -6.157
C
Protein RMSD (nm)
Time (ns)
Ligand fit on protein
D
Rg Protein (nm)
Time (ps)
Radius of gyration of protein backbone
Radius of gyration of ligand backbone
E
Time (ps)
Electrostatic interactions
Hydrophobic interactions

◂**Figure 2.** Simulation studies of Tau and EGCG. (**A**) The binding pocket of EGCG to the Tau model, shown along with the interacting residues after molecular docking. (**B**) The interaction between EGCG and Tau in the binding pocket is depicted, including the major residues involved and the predicted residues, which might be responsible in further interactions as well as the type of interactions they are involved in are shown. (**C**) The RMSD evolution of the protein (left Y-axis) and that of the ligand (right Y-axis) are shown. While the protein RMSD gives insights into the structural conformation of the protein throughout the simulation, the ligand RMSD indicates how stable the ligand is with respect to the protein and its binding pocket. Both the RMSDs are seen to stabilize as the simulation progresses. The ligand RMSD is notably stable of the two, suggesting that the binding pocket conformation is maintained throughout the simulation. (**D**) The Rg values of protein (left Y-axis) and ligand (right Y-axis) are shown. Both Rg values do not show much variation indicating that the structure of the protein and the binding pose of the ligand are maintained over the course of the simulation. (**E**) The electrostatic and hydrophobic interactions between the ligand and protein over the entire timescale of the simulation are depicted, showing the dominant, yet highly dynamic and transitionary nature of the same.

Molecular docking of repeat Tau and EGCG. The docking studies of EGCG with repeat Tau model generated the best pose with glide score and E-model values of − 6.388 and − 56.130, respectively. EGCG was docked in a binding pocket in the vicinity of the predicted alpha helices and antiparallel beta sheets with the gallate moiety being in close proximity to the beta sheet and the Epigallocatechin backbone towards the helices (Fig. 2A). The interaction between EGCG and Tau repeats was majorly mediated by hydrogen bonding and hydrophobic interaction. The OH group involving O4 atom of EGCG interacts with the NH group of the imidazole ring of His 299. The OH groups involving the O2 and O7 atoms of EGCG interact with the NH_2 group and carboxyl group of Val 313, respectively. The O7 atom also interacts with the NH_2 group of the carboxamide group of Asn 265, while the OH groups involving the O8 and O9 atoms interact with the carboxyl O atom of Leu 266 forming hydrogen bonds in the process (Fig. 2A). The three OH groups (O7, O8 and O9) have interaction distances of 3.08 Å, 2.7 Å and 3.18 Å, respectively interacting with carbonyl groups. The interactions with the amine groups (by O2, O4 and O7) on the other hand, stand at interaction distances of 2.95 Å, 3.05 Å and 3.06 Å, respectively (Fig. 2B). Further a hydrophobic Pi-alkyl interaction was observed with residue Lys 340 while residues Asp 314 and Glu 338 are found to make a Pi-anion electrostatic interaction with benzene rings of the ligand EGCG. A few other residues Lys 267, Tyr 310, Pro 312 and Val 339 were also involved in hydrophobic interactions with the ligand. Interestingly, one of the interacting residues, Tyr 310 belongs to one of the hexapeptide repeat regions ^{306}VQIVYK^{311} and the others are seen to majorly flank both the hexapeptide repeat regions (^{275}VQEINK^{280} and ^{306}VQIVYK^{311}) (Fig. 1E), both of which are a prime area of interest in our study and thereby may be involved in the probable mechanism of Tau PHF dis-aggregation in presence of EGCG.

Molecular dynamics simulation of repeat Tau and EGCG. The EGCG docked complex was used for a molecular dynamic simulation study of 50 ns time duration to examine the stability of the interaction and other relative structural changes, which could shed some light on the probable molecular events behind the binding of EGCG to Tau. The RMSD graphs plotted by assigning time in nanosecond (ns) on the X-axis and RMSD values of the Cα atoms of the protein and ligand in nanometers (nm), respectively on the left and right Y-axis (Fig. 2C), indicated that the RMSD of Cα atoms of the protein is relatively stable over the first 30 ns of the simulation, then undergoes slight fluctuation, only to re-stabilize in the last 5 ns. The fluctuation may be due to the partial destabilization of local bonds in the binding pocket of the protein due to the EGCG interaction. The ligand backbone over the complete trajectory showed that the system attains stability over short durations at different time points, which might be indicative of the characteristic binding and partial dissociation events showed by EGCG. As a result, we also observed some repositioning of the initial binding pose of EGCG with respect to the hexapeptide repeat region ^{306}VQIVYK^{311} during the course of simulation. The Cα RMSD difference between the initial and final conformation after the simulation of docked complex is therefore ~ 0.75 Å which suggested some overall conformational change in Tau upon binding of EGCG as mentioned above and the system finally converged over the last few nanoseconds. The R_g (Radius of gyration) graph plotted by assigning time in picoseconds (ps) on the X-axis and R_g values of the protein and ligand backbones in (nm) on the left and right Y-axis, respectively (Fig. 2D) also indicated the compactness of the protein and ligand throughout the simulation. The interaction energy calculation between the representative residues and the ligand EGCG showed that both the Coulombic interactions were more prominent in the initial part of the simulation while Lennard-Jones interactions gain prominence as we move towards the end of the simulation, suggesting that the electrostatic and hydrophobic interactions of the Tau-EGCG complex are quite dynamic in nature (Fig. 2E). During the course of the simulation, residues Asn 265, Leu 266 and Val 313 majorly contribute to the hydrogen bond interactions. Other residues like Lys 267, Tyr 310, Pro 312 and Lys 340 contribute extensively to the hydrophobic interactions involving the protein and ligand. The residue specific interactions indicate that these may be the most crucial residues involved in the stabilization of the Tau-EGCG complex. We observed that the overall hydrogen bonding dynamics was maintained over the course of the simulation (Fig. S5). This included other ion-mediated and water mediated hydrogen bonding along with the residue specific interactions, which was maintained in the entire time duration of the simulation. These interactions might be the key to the dynamics between Tau and EGCG interaction.

To predict the binding site of EGCG with a Tau monomer and to gain insight into the molecular nature of the interaction of EGCG with Tau, we performed docking and simulation studies of the same. Tau protein having highly disordered N and C termini is structurally highly dynamic, thereby making it highly improbable to predict a reliable full-length Tau model. However, we have successfully obtained a reliable model for the regions of Tau

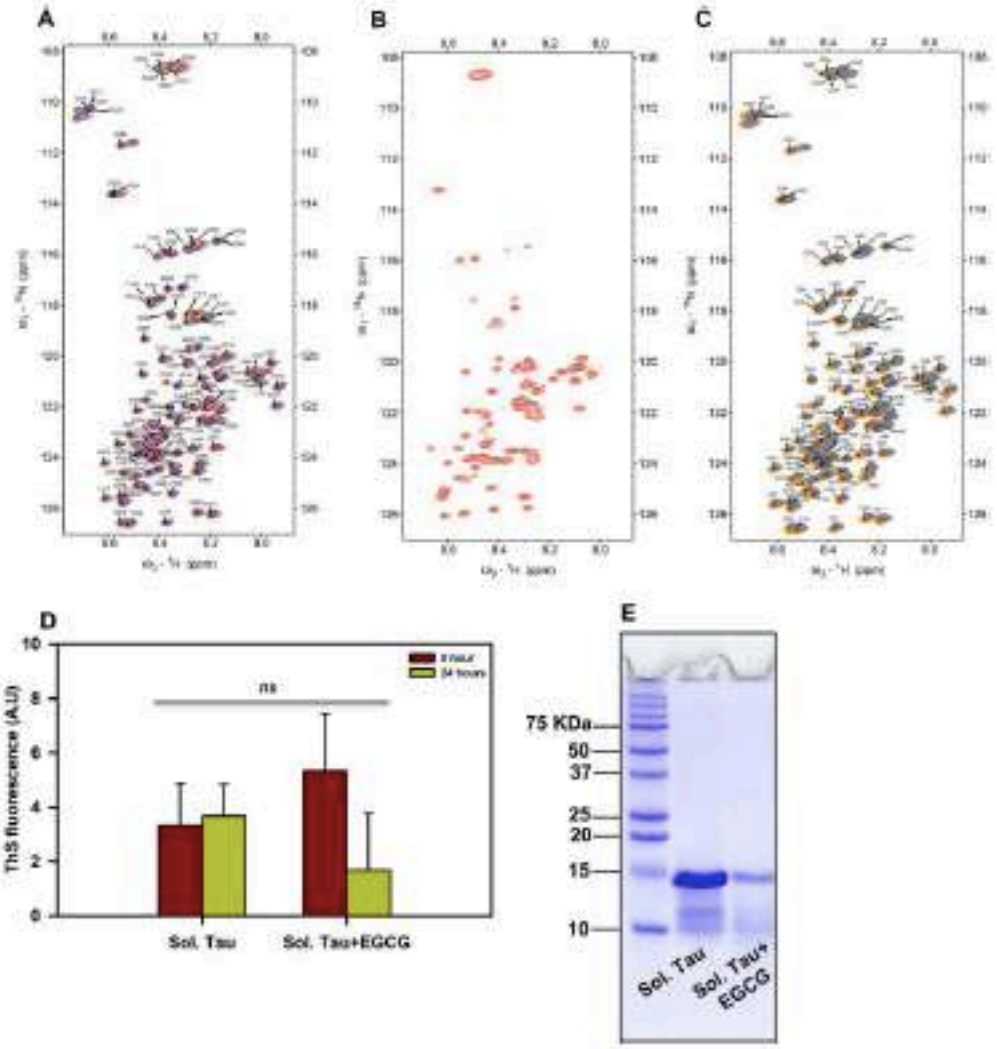

Figure 3. NMR spectroscopic studies of repeat Tau with EGCG. ^{1}H-^{15}N-HSQC plots showing the chemical shift perturbations. For all the NMR experiments a solution of 200 µM of repeat Tau in 500 µL phosphate buffer containing 10% D_2O is used. (A) Overlay of ^{1}H–^{15}N-HSQC plots (at 278 K) for the titration of 200 µM of repeat Tau against 0 µM (in orange), 100 µM (in blue), 500 µM (in red), 1,000 µM (in olive green) and 2000 µM (in coral, no visible signals) of EGCG. Continuous drop in the intensity of HSQC cross peaks indicates an increasing precipitation of repeat Tau with increasing concentrations of EGCG. (B) Overlay of ^{1}H–^{15}N-HSQC plot of repeat Tau at 298 K with that of repeat Tau in presence of 2000 µM of EGCG (sample from titration at 278 K, which was brought back to 298 K). (C) Overlay of ^{1}H–^{15}N-HSQC plot of repeat Tau (at 278 K) (without EGCG, golden) along with ^{1}H–^{15}N-HSQC plots measured for the precipitation of 200 µM of repeat Tau in presence of 500 µM of EGCG after t = 0 h (blue) and t = 24 h (grey). Upon addition of 500 µM of EGCG, the HSQC cross peaks are slightly displaced and lost intensity indicating precipitation of repeat Tau. After 24 h standing, no apparent change was observed in the HSQC cross peak intensity. (D) ThS fluorescence of NMR samples at 0 and 24 h suggesting no aggregation of repeat Tau in presence of EGCG. (E) SDS-PAGE analysis of NMR samples at 24 h showing no aggregation of repeat Tau in presence of EGCG.

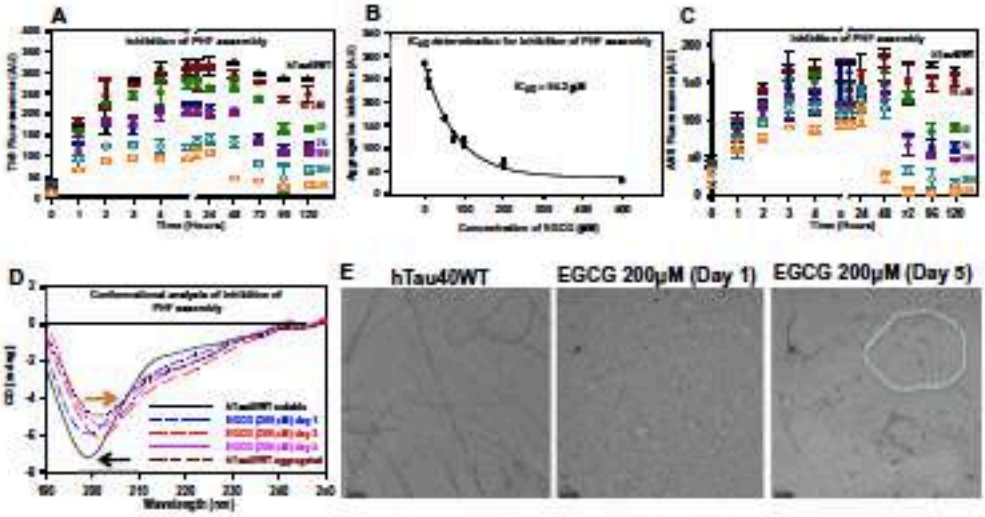

Figure 4. EGCG prevents Tau aggregation and changes their conformation in vitro. (A) The inhibitory effect of EGCG on the polymerization of full-length Tau monitored by ThS fluorescence. (B) The IC_{50} for EGCG for full-length Tau is 64.2 μM. (C) The inhibition of Tau PHF assembly assessed by ANS fluorescence shows a time and dose dependent decrease in the hydrophobicity of the Tau protein. (D) The CD analysis of EGCG treatment shows the formation of mixed Tau structures in a time dependent manner. (E) The control reaction shows the presence of long mature filaments whereas the EGCG treatment shows increase in the fragility of the Tau filaments at with increasing in time. The 200 μM EGCG treatment shows broken filaments at the day 5 of incubation.

surrounding the hexapeptide repeats from available structural data. Our results indicated that EGCG binds to one of these hexapeptide repeats. The nature of interaction is primarily hydrogen bonding, further stabilized by the water-mediated hydrogen bonds and hydrophobic interactions that led to a series of short-term interactions, binding and partial dissociation events throughout the simulation. Towards the end of the simulation timescale, hydrophobic interactions and probably ion or water-mediated hydrogen bonds are found to become more prevalent which suggests notable conformational changes of this aggregation prone region of Tau after EGCG binding.

NMR spectroscopic studies of repeat Tau-EGCG interaction. Interaction between repeat Tau and EGCG was monitored by ^{1}H–^{15}N HSQC NMR spectroscopic studies using 200 μM of ^{15}N labeled repeat Tau dissolved in phosphate buffer. First, repeat Tau was titrated with variable concentrations of EGCG at ratios 0, 0.5, 2.5, 5 and 10 with respect to 200 μM of repeat Tau at 278 K (Fig. 3A). The titration did not reveal any residue specific interaction of EGCG with repeat Tau and no significant conformational reorganization of repeat Tau. However, the intensities of HSQC cross peaks diminished with increasing amounts of EGCG until no signal was detected from the protein at 2000 μM of EGCG, which implies the precipitation of repeat Tau into larger molecular weight forms. Consistently, the contents of the NMR tube have turned turbid over the titration in support with the precipitation and loss of signal. After the titration, the final contents (200 μM of repeat Tau at 2000 μM of EGCG) of the NMR tube were brought to 298 K, allowed to stand for an hour and an HSQC spectrum was recorded (Fig. 3B, grey), which showed very weak signals and was superimposed on the HSQC of repeat Tau (without EGCG) at 298 K. These results indicated that a low concentration of precipitate solubilized back into monomeric repeat Tau, probably with native conformation, as the pattern of HSQC cross peaks of solubilized repeat Tau almost match with that of the native repeat Tau cross-peaks in HSQC. In order to investigate if the repeat Tau precipitate steadily increases over time at a given concentration of EGCG, we have carried out an experiment where ^{1}H–^{15}N HSQCs were acquired for 24 h at 278 K on a 200 μM repeat Tau sample in presence of 500 μM of EGCG (Fig. 3C). As seen from Fig. 3C, the HSQC after t = 0 h (blue) and t = 24 h (grey) are exactly superimposable, indicating no seeding effect of the precipitates at these concentrations. Further to confirm protein precipitation by EGCG, we monitored the ThS fluorescence of the sample from NMR tube at 0 time point and at the end of NMR titrations. It was observed that the precipitate did not give any increased fluorescence suggesting that protein actually precipitated and not aggregated (Fig. 3D). The sample at 24 h was also analyzed by SDS-PAGE and the EGCG sample did not show any higher order aggregates confirming our inference that EGCG precipitates repeat Tau protein (Fig. 3E).

EGCG impedes human full-length Tau assembly. Tau Paired Helical Filaments (PHFs) formation is induced in vitro by a positively charged anionic co-factor heparin. The effect of EGCG on this assembly was studied by adding a range of concentrations (10–500 μM) to the Tau (20 μM) assembly mixtures. The classical fluorescence assay with ThS demonstrated an aggregation impeding effect in presence of EGCG in a concentration-dependent manner. The aggregation was observed to progress till 24 h of incubation after which the fluorescence intensity reduced gradually as time advanced (Fig. 4A). This suggests that EGCG interferes with Tau PHFs assembly and shows 89% inhibition at highest concentration (500 μM) (Fig. S2A). The IC_{50} value for Tau assembly inhibition was determined to be 64.2 μM (Fig. 4B). In the course of PHF assembly, the hydrophobicity of aggregates increases. The effect of EGCG on the hydrophobicity changes during the PHF assembly was monitored by ANS fluorescence. ANS maps the hydrophobicity changes by emitting enhanced fluorescence as the hydrophobicity increases. ANS fluorescence was observed to increase as the initial aggregation of Tau proceeded in control and EGCG treated samples but was seen decreasing in the EGCG treated Tau in a concentration dependent manner with time (Fig. 4C). The percent inhibition with respect to ANS fluorescence was found to be 96% (Fig. S2B). Time dependent SDS-PAGE analysis of EGCG treated Tau was carried out to confirm effects of EGCG on Tau assembly. The 0 h SDS-PAGE profile confirmed the monomeric Tau in control and treated samples (Fig. S3A, 0 h) and absence of any preformed aggregates. At 6 and 12 h a tetramer band is observed in all the lanes suggesting progression of Tau assembly. However, at 24 h, the highest concentration of EGCG (500 μM) shows a complete loss of higher order Tau aggregates. This confirms with the fluorescence kinetics data, which drops after 24 h of incubation (Fig. S3A, 24 h). As the incubation advances all the treated samples show a drop in Tau aggregates on SDS-PAGE as well as its densitometric quantification (Fig. S3B). These results together demonstrate the role of EGCG in inhibiting Tau aggregation.

EGCG causes a partial conformation change of Tau and increases the filament fragility. EGCG has been shown to prevent the formation of β-sheet structure by α-synuclein protein and rather help in adopting the random coil structure[39]. To check its effect on Tau conformation, we treated Tau with 1:10 ratio of EGCG and monitored the conformational changes in a time dependent manner. The aggregated Tau shifts its conformation from random coil to partial β-sheet (Fig. 4D). EGCG treated Tau also showed a partial β-sheet conformation in a time dependent manner. On the other hand, the aggregation kinetics showed an inhibition of PHFs assembly but after only after 24 h wherein basal level of intermediates must have formed. The partial β-sheet conformation might be due to these aggregate intermediates formed during early aggregation phase. The visualization of EGCG mediated inhibition of Tau assembly was carried out by TEM (Transmission Electron Microscopy) analysis. The untreated control showed long and abundant Tau PHFs whereas, the time dependent analysis of EGCG treated Tau showed only small pieces of Tau filaments at day 5 (Fig. 4E). The EGCG treated day 1 samples show almost absence of mature filaments (Fig. 4E). Thus, EGCG hampers the formation of mature Tau PHFs.

EGCG is potent in dissolving preformed Tau filaments and oligomers. Aggregate formation is the key target in AD, but dissolution of the preformed aggregates also needs to be addressed as this aggregate load hampers neuronal function and gradually leads to neuronal death. Thus, EGCG was evaluated for its role in dissolving preformed Tau filaments. The ThS fluorescence kinetics demonstrated a drop in intensity in time dependent manner in EGCG treated reactions as opposed to control, which showed steady fluorescence throughout the incubation (Fig. 5A, S4A). The ANS fluorescence also showed a drop in intensity with time suggesting a decrease in hydrophobicity as the Tau aggregates were dissolved upon EGCG treatment (Fig. 5B, S4B). The SDS-PAGE analysis revealed the dissolution of aggregates in time and concentration dependent manner. The highest concentration of 500 μM showed complete clearance of Tau aggregates at 24 h (Fig. 5C, 24 h lane 8). EGCG is thus potent in inhibiting Tau PHF assembly as well as dissolving the preformed fibrils.

The toxicity of Tau oligomers is more pronounced than the mature aggregates. Tau oligomers were allowed to form till six hours after which EGCG was added to reaction mixtures at various concentrations (25–200 μM). This time point was considered as 0 h. Upon addition the kinetics was monitored at timed intervals. The highest concentration of 200 μM did not show increase in fluorescence from 0 h. The intensity remained stagnant till 12 h and dropped from 24 h onwards. This suggests EGCG captures oligomers and dissolves them and does not allow further aggregation (Fig. 5D, E, S4C, S4D). The oligomers before addition of EGCG were observed on SDS-PAGE (Fig. 5F, 0 h). The addition of EGCG gradually dissolved the oligomers in time dependent manner (Fig. 5F).

Since the in vitro and computational data suggested Tau-EGCG interaction and binding, we further performed MALDI-TOF analysis to check for the covalent modification of repeat Tau (Fig. 6A) by EGCG. EGCG treatment showed the adduct formation with repeat Tau at Tau: EGCG, 1:4 ratios, which can be seen as small peak (Fig. 6C, red arrow) in addition to the peak corresponding to soluble repeat Tau. The untreated control showed a single peak corresponding to 13.7 KDa for repeat Tau (Fig. 6B).

Tau forms non-toxic higher order aggregates in presence of EGCG. Tau forms a mixture of higher order species while aggregating which can be separated by SEC (Size Exclusive Chromatography). The full-length Tau was eluted as a monomer at 0 h (Fig. 7A, indicated in black). After 3 h of incubation Tau was eluted as two distinct peaks at retention volumes 8.3 and 7.7 ml. for control and EGCG, respectively (Fig. 7B), indicating the formation of higher order species. Further at 24, control as well as EGCG treated Tau eluted at the retention volume of 7.6 ml. (Fig. 7C as a single peak indicating the higher order aggregates, Table 2). However, the early species formed at 3 h of incubation clearly demonstrates that EGCG accelerates the formation of Tau aggregates when compared to Tau alone. Neuroblastoma cells treated with the fractions obtained from SEC did not show significant toxicity (Fig. 7D).

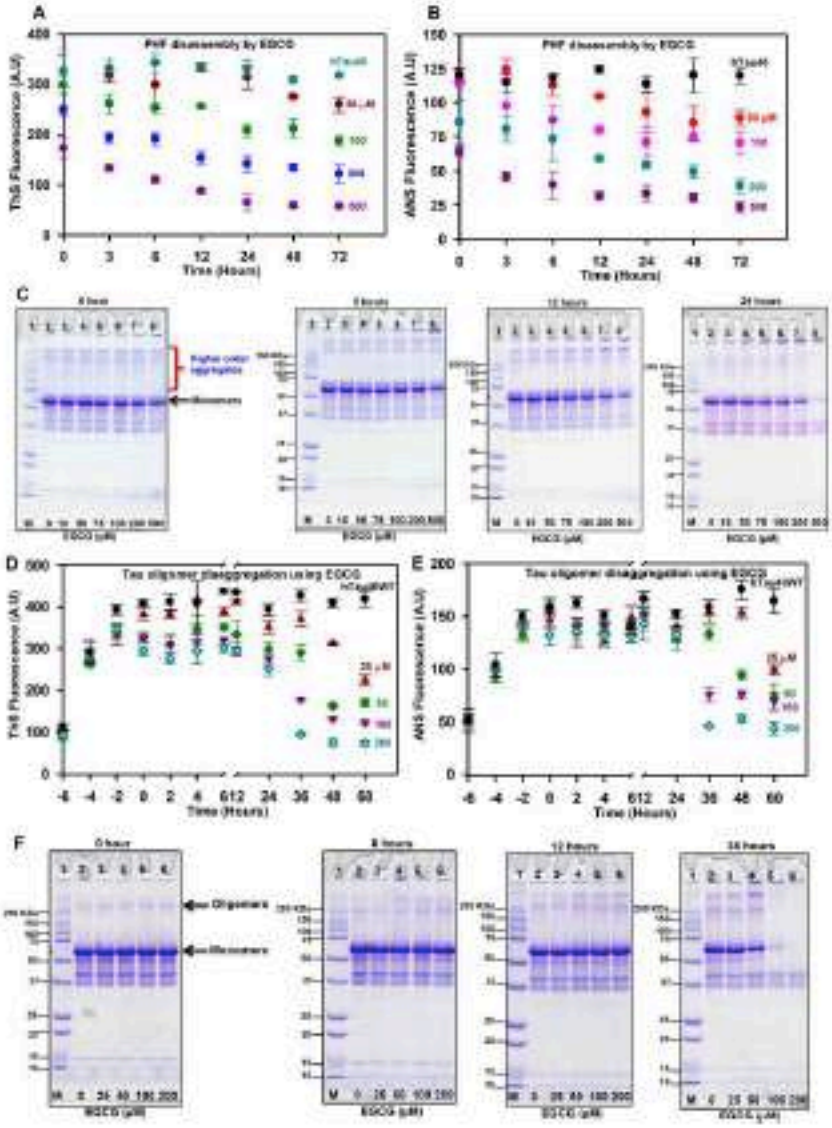

Figure 5. The preformed Tau fibrils and oligomers dissolved by EGCG. (A) The EGCG mediated dissolution of mature Tau fibrils recorded by ThS fluorophore showing the disassembly of PHFs. (B) The ANS fluorescence shows a time dependent decrease as the fibrils are dissolved. (C) The SDS-PAGE analysis of disassembly of Tau PHFs. (D) The ThS fluorescence shows the inhibitory effect of EGCG on the dissolution of Tau oligomers in a concentration dependent manner. (E) The ANS fluorescence shows the decrease in intensity with time and concentration suggesting loss of hydrophobicity of Tau oligomers. (F) The SDS-PAGE analysis shows the presence of oligomers at the time of compound addition (0 h) which are slowly cleared with time.

EGCG enhances neuronal growth. EGCG is a known neuroprotective and antioxidant molecule[27]. Its effect on neurolla cell viability revealed that EGCG is not only non-toxic but it also enhances cell survival with

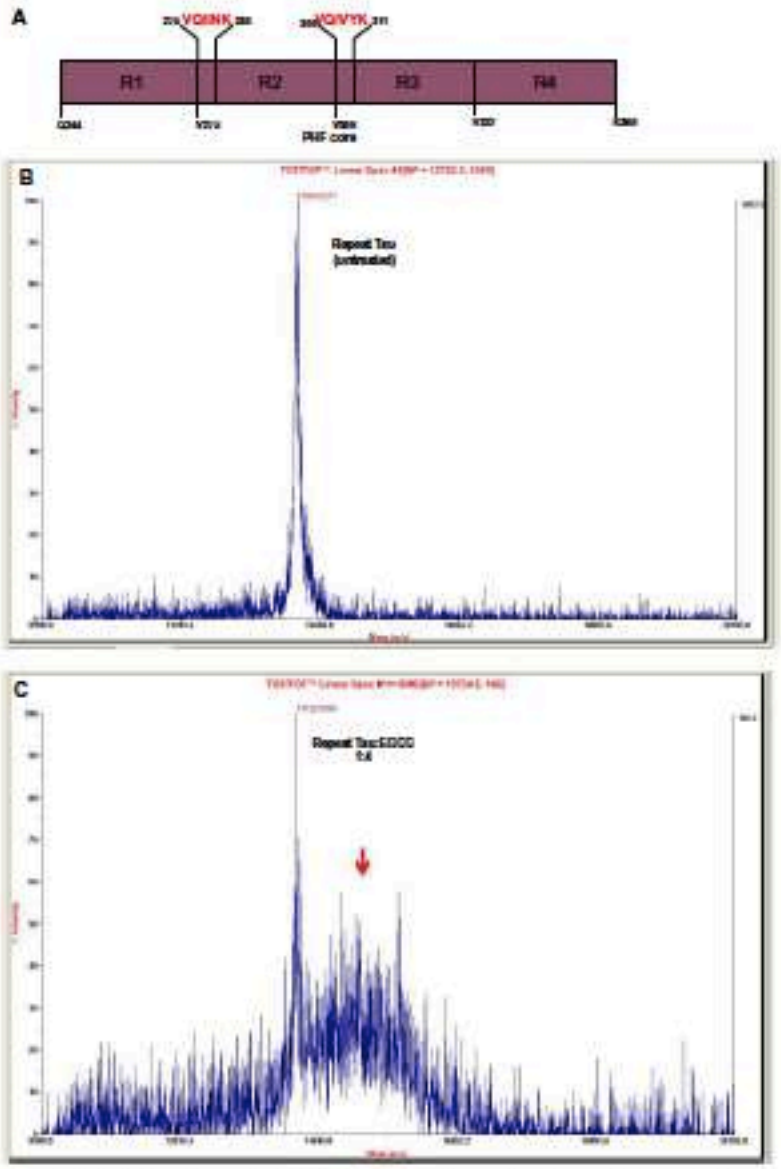

Figure 6. Modification of repeat Tau by EGCG. (A) Repeat domain of Tau showing two hexapeptide motifs. (B) The MALDI-TOF spectra of untreated repeat Tau showing a single peak at desired molecular weight of 13.7 KDa. (C) The EGCG treated repeat Tau shows an adjacent peak (red arrow) in addition to the soluble Tau peak suggesting the modification of Tau with EGCG as increase in molecular weight.

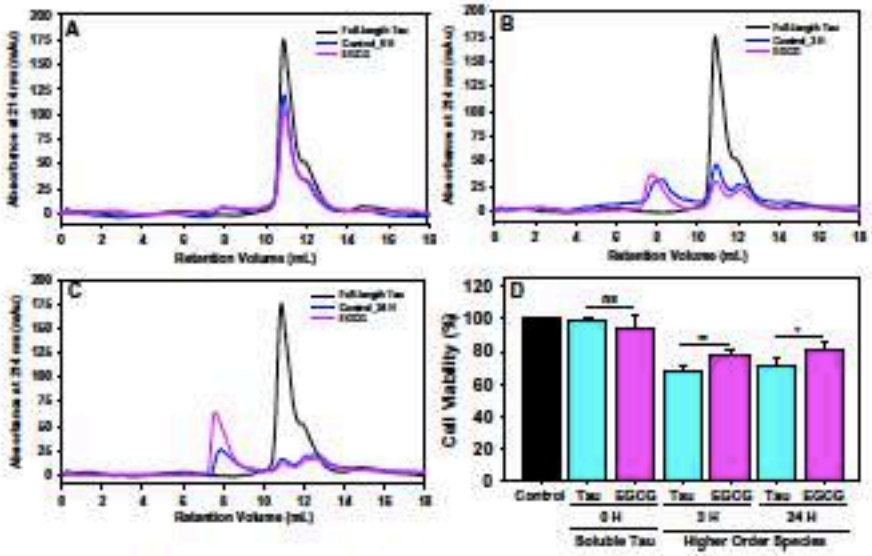

Figure 7. SEC for polyamines treated Tau. Tau was subjected to aggregation in presence of heparin as inducer. (A) At 0 h Tau was eluted as monomer, both in presence and absence of EGCG. (B) Further incubation led to aggregation of Tau, at 3 h of incubation EGCG showed more aggregation in Tau. (C) Similarly, at 24 the peak intensity of Tau in presence of EGCG was high when compared to control. This suggests that EGCG is driving Tau towards the formation of higher order aggregates. (D) Cell viability studies indicates that these conformers were non-toxic in neuro2A cells.

Time (h)	Tau ± EGCG	Retention volume (mL)
0	Soluble Tau	10.9
	Control	10.9
	EGCG	10.9
3	Control	8.3
	EGCG	7.7
24	Control	7.9
	EGCG	7.6

Table 2. Peak retention volumes for EGCG treated and untreated Tau.

varying concentrations (Fig. 8A). Neuro2a cells treated with Tau aggregates (5 μM) and 0 μM of EGCG showed 77% viability as compared to control. When cells were treated with aggregates along with EGCG, a significant rescue of toxicity was observed along with enhanced survival (Fig. 8B).

Discussion

Tau aggregation inhibitors in Alzheimer's disease have yielded numerous hits, which are potent in alleviating the Tau pathology. Several natural compounds are gaining much attention as effective therapeutics against Tau pathology[42,57]. The molecular targets[58,59] of these molecules vary since Tau undergoes a series of intermediate species formation before leading to mature PHFs. We have screened EGCG for its efficacy against full-length human Tau aggregation. EGCG has already been reported to inhibit in vitro aggregation of a mutant repeat Tau (K18ΔK280). However, the heparin induced aggregation of the Tau fragment K18ΔK280 could not be rescued by EGCG[33]. Moreover, this gave rise to Tau filaments that are morphologically different from the untreated filaments. In our study, we demonstrate the inhibition of heparin induced full-length Tau aggregation by EGCG with altered filament morphology and number. The IC_{50} for inhibition is higher as compared to other molecules and this might be due to the fact that heparin induction cuts down on the lag phase, which might be essential for efficient binding of EGCG to monomeric Tau for impeding the Tau assembly. Thus, EGCG might need to bind to the intermediate species to inhibit aggregation in large stoichiometric ratios. EGCG has been implied

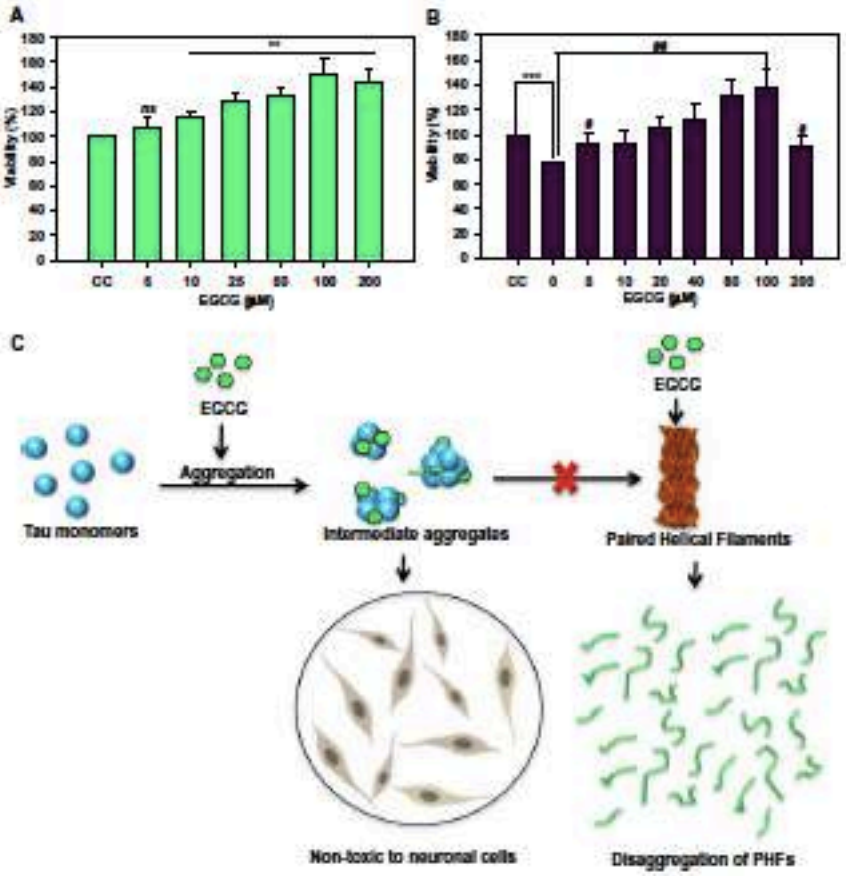

Figure 8. Effect of EGCG on cell viability. Toxicity was induced with 5 μM Tau aggregates and rescue in presence of EGCG (0–200 μM) in neuro2a cells. (A) Cell viability assay shows EGCG was non-toxic to neuronal cells at varying concentrations (0–200 μM) $p < 0.001$ and enhance the cell survival. (B) Tau aggregates induce toxicity in neuro2a cells at 0 μM EGCG $p < 0.05$(denoted as *) EGCG significantly rescues toxicity of Tau aggregate mediated toxicity till and enhances viability $p < 0.05$ (denoted as #). (C) EGCG inhibits Tau aggregation by forming intermediate Tau aggregates and disintegrating them. The intermediate aggregates formed are non-toxic to neuronal cells. On the other hand, when matured Tau fibrils are treated with EGCG, they are disaggregated and cleared.

in covalently modifying proteins at the reduced Cys thiols. Our MALDI-TOF results suggests that EGCG forms adducts with repeat Tau thus explaining the presence of a higher order band in nitrobluetetrazolium (NBT) staining from the previous studies on EGCG and repeat Tau[19]. Along with mechanism of action, the exact interaction of EGCG with the misfolding prone proteins have being studied. Although the number and nature of interacting amino acid residues vary according to proteins, some key interacting residues remain common for such proteins. In EGCG-Tau docking studies we have found Leu and Asp residues showing major interactions, which were also reported to be the interacting residues in transthyretin complex[40]. One of the major contributors in the interactions between Tau and EGCG was found to be Lysine 267 and it has been reported previously, that a lysine residue in prostatic acid phosphatase (PAP) peptide was found to have a strong interaction with EGCG, and was an important residue in ligand binding. ITC results suggested binding between Tau and EGCG occurs in a multi-sites binding event such that the initial binding events are rapid and saturable. After initial rapid Tau-EGCG interaction, equilibrium is attained where, constant association and dissociation of Tau- EGCG occurs. Similar nature of interaction has been reported for HSA-EGCG interaction where two separate binding events occur. There is initial strong binding between HSA and EGCG followed by 1,000 times weaker secondary binding event[16]. EGCG is thought to act via a common mechanism for various aggregation prone proteins. It is

speculated that EGCG binds to the cross-beta short intermediates and prevents further assembly[42]. Our study demonstrated this effect for full-length Tau wherein an initial oligomerization was visualized with SDS-PAGE and later a gradual decrease in the oligomers. On the other hand, the disassembly of Tau PHFs was very rapid. This might be attributed to the already present aggregation intermediates allowing rapid binding and action of EGCG. In titration of repeat Tau with EGCG, NMR spectroscopic studies have shown clear loss of repeat Tau signal intensity with increasing concentrations of EGCG. The repeat Tau signals have all vanished at 1:10 concentration ratio of repeat Tau to EGCG in concurrence with the precipitation observed in the NMR tube. The precipitate from the NMR tube was collected and characterized by ThS. Very poor intensity in ThS fluorescence assay for the precipitate indicates that its morphology is different from regular heparin induced aggregates of Tau or repeat Tau.

The dual role of EGCG in disassembling Tau filaments and quenching the oligomers makes it a potent candidate for future drug designing.

Conclusion

EGCG interacts with full-length Tau at multiple residues with unstable interactions. It inhibits aggregation of full-length Tau and dissolves Tau fibrils and oligomers. We predict that EGCG forms higher order structures and degrades them without allowing the formation of mature aggregates, which was also observed in NMR analysis. The higher order structures formed by EGCG are non-toxic to neuroblastoma cells and EGCG rescues the aggregate mediated toxicity in the neuroblastoma cells (Fig. 8C). Thus, EGCG acts to inhibit Tau aggregation by direct but unstable interactions.

Materials and methods

Chemicals and reagents. Luria–Bertani broth (Himedia); Ampicillin, Heparin, NaCl, Phenylmethylsulfonylfluoride (PMSF), $MgCl_2$, Sodium azide, APS, DMSO, Ethanol (Mol Bio grade), Chloroform, Isopropanol (Mol Bio grade) were purchased from MP biomedicals; IPTG and Dithiothreitol (DTT) from Calbiochem; EGCG, ThS, ANS, Glycine, MES, BES, SDS, MTT from Sigma; EGTA, Tris base, 40% Acrylamide, TEMED from Invitrogen. Protease inhibitor cocktail was purchased from Roche. For cell culture studies, Dulbecco modified eagle's media (DMEM), Fetal bovine Serum (FBS), Phosphate buffer saline (PBS, cell biology grade), Trypsin-EDTA, Penicillin–streptomycin were purchased from Invitrogen.

Tau purification. Protein purification for full-length Tau was carried out as previously described[42]. In brief, full-length recombinant Tau was expressed in *E.coli* BL21* strain. The cell pellets were homogenized under high pressure (15,000 psi) in a microfluidics device for 15 min. The obtained lysate was heated at 90 °C for 15 min after addition of 0.5 M NaCl and 5 mM DTT. The heated lysate was then cooled and centrifuged at 40,000 rpm for 50 min. The supernatant was collected and dialyzed in Sepharose A buffer overnight. The obtained dialyzed sample was then subjected to a second round of ultracentrifugation and the supernatant was loaded onto the cation exchange column (Sepharose fast flow GE healthcare) for further purification. The bound protein was eluted using an ionic gradient. The eluted proteins were pooled and concentrated for size exclusion chromatography (16/600 Superdex 75 pg GE healthcare). The Tau concentration was measured using BCA method[43].

Molecular modelling. To procure templates for homology model building, a similarity search using Basic Local Alignment Search Tool (BLAST) algorithm was performed against the Protein Data Bank (PDB), to identify high-resolution crystal structures of homologous proteins[43,44]. The sequence identity cut off was set to ≥ 30% (E-value cut off = 1). Homology modeling of Tau K18 was then carried out using Modeller 9.16 by taking structures homologous to the target protein as templates, in order to study their structural features, binding mode and affinity with the substrates.

Model validation and refinement. The initial models obtained, were evaluated for the stereochemical quality of the protein backbone and side chains using PROCHECK and RAMPAGE[45]. ERRAT server checked the environments of the atoms in the protein model. Errors in the model structures were also checked with ProSA server[46,47]. After model validation, initial models were refined using impref minimization of protein preparation wizard and Impact 5.8 minimization. These energy minimized final models were further used for the binding studies with their substrates.

Ligand–protein preparation and docking studies. The ligand molecule considered in the present study was downloaded from ZINC compound database in the mol2 format. The protein and ligands were prepared first before proceeding with the docking studies. The water molecules and other heteroatom groups were removed from the protein structures using protein preparation utility of Maestro. Hydrogens were added subsequently to carry out restrained minimization of the models. The minimization was done using impref utility of Maestro in which the heavy atoms were restrained such that the strains generated upon protonation could be relieved. The root mean square deviation (RMSD) of the atomic displacement for terminating the minimization was set as 0.3 Å. Similarly, ligands were refined with the help of LigPrep 2.5 to define their charged state and enumerate their stereoisomers. The processed receptors and ligands were further used for the docking studies using Glide 5.8[48]. Sitemap analysis was performed on the prepared receptor molecule, to identify the probable binding sites for our ligands of interest, since no prior information was available regarding the same[49]. Next, grids were generated by selecting any of the Sitemap points obtained above. Flexible ligand docking was carried out using the standard precision option. A total of 6 poses with the respective ligand and different sites were generated

and scored on the basis of their docking score, glide score and E-model values. The hydrogen bond interactions between the protein and ligands were visualized using PyMOL.

Molecular dynamics simulations. The docked complex with the lowest Glide score and Glide E-model values were used to perform molecular dynamics simulation using the GROningen MAchine for Chemical Simulations V4.5.4 (GROMACS)[30,31] with the CHARMM36 force field. The docked complex was placed in the center of a dodecahedron box solvated in water. The ligand topology files and the other force field parameter files pertaining to the ligand were created using the official CHARMM General Force Field server CGenFF[32,33]. The SPC216 water model was used and the distance between the solute and the box was set to 10 Å. The dimensions of the initial simulation cell were kept at approximately 90 × 90 × 90 Å. for the simulation and the initial energy minimization of the system was carried out by steepest descent minimization for 50,000 steps, till a tolerance of 10 kJ/mol was attained, to make sure that the high energy interactions and steric clashes in the system could be avoided during simulation. A suitable number of Cl^- ions were added to balance the total negative charges on the docked structures to make the whole system neutral using the genion program of GROMACS and the system was again subjected to energy minimization by steepest descent minimization retaining the same parameters. The system was stabilized at 300 K temperature and pressure of 1 bar using the Vrescale, a modified Berendsen thermostat, temperature coupling[34] and Parrinello-Rahman pressure coupling methods[35]. The Partial Mesh Ewald (PME) algorithm[36] was employed for computing electrostatic and van der Waals interactions. A cut off distance of 9 Å and 14 Å was set for Coulomb and van der Waals interactions, respectively. The LINCS algorithm[37] was used to apply rotational constraint to all the bonds. No positional constraints were applied on the system. Periodic boundary conditions were applied in all three directions. The complex in the medium was equilibrated for 100 ps in *NPT* and *NVT* ensembles. Finally, a 50 ns molecular dynamics simulation was carried out for the protein–ligand complex and all trajectories were stored every 2 ps for further analysis. The trajectories were visualized using Visual Molecular Dynamics program (VMD)[38]. The energies and RMSD of the complex in each trajectory were monitored with respect to simulation time. The intermolecular interactions between the target and substrate were assessed to check the stability of the complexes. The R_g (Radius of gyration) was also monitored for the protein and ligand backbones to check their stability in the active site pocket as well as their overall compactness.

NMR spectroscopy. For NMR experiments, a 200 µM solution of ^{15}N labelled repeat Tau protein was prepared in 10:90 D_2O:H_2O aqueous medium of 50 mM phosphate buffer also containing 1 mM DTT. ^1H–^{15}N HSQC experiments have been acquired using 512 increments and 2 k complex points in the indirect and direct dimension, respectively, and 16 scans per increment. The data was processed by Bruker topspin software and analyzed using Sparky. NMR experiments for titration and aggregation of repeat Tau with EGCG were acquired at 278 K on Bruker Avance III HD 700 MHz spectrometer equipped with a TXI probe. Re-dissolving of repeat Tau precipitates (obtained in presence of EGCG) was monitored by acquiring the ^1H–^{15}N HSQC experiments at 298 K.

Isothermal titration calorimetry. Isothermal titration calorimetry was carried out for full-length Tau and EGCG in 1:25 ratio in a PEAQ-ITC micro calorimeter at 25 °C. Full-length Tau (20 µM) was titrated with EGCG (500 µM) EGCG in sodium phosphate buffer, pH 7.4. Titration experiment comprised of a total of 25 injections of 1.5 µl for 3 s at an interval of 180 s between each injection. An initial injection of 0.4 µl was given for stabilization of reaction cell. The data was analyzed and interpreted using PEAQ-ITC software using one set of sites model. The final baseline corrected data and heat plot were plotted using Sigma plot 10.2. The values of ΔG, ΔH and TΔS were used to calculate the binding constant for the interaction.

Tau aggregation assay. The soluble human Tau40wt protein was centrifuged at 60,000 rpm for 1 h (Optima Max XP Beckman Coulter) to ensure presence of monomeric Tau and 20 µM of soluble Tau protein was incubated in 20 mM HES buffer pH 7.4 with 5 µM of Heparin 17,500 Da in presence of 25 mM NaCl 1 mM DTT protease inhibitor cocktail, 0.01% Sodium azide, and different concentrations of EGCG ranging from 0 to 500 µM. EGCG was dissolved in ultrapure water and stored in 4 °C. Aggregation inhibition and disaggregation studies were carried out in presence of 1 mM DTT as a reducing agent. The reaction mixtures were incubated at 37 °C. The aggregation was studied by ThS and ANS fluorescence assay.

ThS fluorescence. The Tau protein in the reaction mixture and ThS were incubated in ammonium acetate pH 7.0 at concentrations of 2 µM and 8 µM, respectively for 10 min. The readings were taken by exciting ThS at 440 nm and collecting the emission data at 521 nm in TECAN Infinite M 200 pro. The buffer measurements were subtracted from the sample readings before plotting the data.

ANS fluorescence. For ANS measurements the Tau and ANS were incubated at 2 µM and 40 µM, respectively in ammonium acetate pH 7.0 for 20 min. The fluorescence measurements were taken at excitation/emission 390 nm/475 nm in TECAN Infinite M 200 pro. The buffer blank were subtracted and the readings were taken in triplicates.

Tau disassembly assay. Tau filaments were prepared to a concentration of 100 µM in the assembly buffer mentioned above for 8 days at 37 °C. After confirmation of the mature filament formation by ThS fluorescence

and SDS-PAGE, these were diluted to 20 μM and with were treated EGCG (0 to 500 μM) at 37 °C. Further, the dissolution of Tau fibrils was monitored by fluorescence assays and SDS- PAGE.

Circular Dichroism Spectroscopy. CD spectroscopy was carried out to check effect of EGCG on Tau aggregation inhibition on Jasco J-815 CD spectrometer. The sample was diluted to 3 μM Tau in sodium phosphate buffer pH 6.8 in a 1 mm cuvette. The bandwidth and scan speed were set as 1 nm and 100 nm/min, respectively. The scan was carried out from 250 to 190 nm with an average of 5 acquisitions. Buffer baseline was subtracted from each reading.

Electron microscopy. The qualitative analysis for Tau aggregation inhibition and disassembly by EGCG was performed by Transmission electron microscopy. The 400 mesh carbon coated copper grids were incubated with 2 μM of the reaction 45 s. The grids were given 2 washes of filtered MilliQ. Further, the grids were incubated with 2% for 1 min and dried. The scanning was performed on Tecnai G2 20 S-Twin transmission electron microscope.

MALDI-TOF analysis. Repeat Tau protein (1 mg/ml) was incubated with EGCG for 12 h at 37 °C. The samples were then diluted 1:20 in Sinapic acid and spotted on the MALDI plate and analyzed using ABSCIEX 4800 MALDI-TOF analyzer.

Size Exclusion Chromatography (SEC). 20 μM of full-length Tau was incubated in assembly buffer in presence and absence of 100 μM EGCG. Tau was subjected to size-exclusion using Superdex 200 increase at 0, 3, 24 h. The change in retention volume was recorded against time of incubation. The intensity of Tau with and without EGCG at each time point in correspondence to retention volume was plotted in terms of bar. The respective fractions obtained after SEC were analysed for their toxicity in neuro2a cells. The SEC experiments were carried out in AKTA Pure M (GE Healthcare).

Cell viability assay. 10,000 neuro2a cells were seeded in 96 well culture plate. The cells were incubated at 37 °C, 5% CO_2. Cells were treated with the fractions for 24 h. Post-treatment cells were treated with 0.5 mg/mL of MTT(3-(4,5-dimethylthiazol-2-yl)-2,5-diphenyltetrazolium bromide) and incubated for 4 h. Thus formed formazone crystals were dissolved in 100 μL of DMSO. This leads to the formation of purple coloured complex whose absorbance was measured at 590 nm in TECAN Infinite Series Pro 200 spectrofluorimeter.

Statistical analysis. All the statistical analyses were carried out using unpaired T-test by SigmaPlot 10. The error bars represent mean ± SD values. 95% confidence intervals were maintained for the analyses.

NMR accession number. Repeat Tau chemical shift assignments deposited in BMRB (accession number: 19253) have been used for the analysis.

Received: 30 November 2019; Accepted: 2 June 2020
Published online: 28 July 2020

References

1. Lansbury, P. T. & Lashuel, H. A. A century-old debate on protein aggregation and neurodegeneration enters the clinic. *Nature* 443, 774 (2006).
2. Selkoe, D. J. Folding proteins in fatal ways. *Nature* 426, 900 (2003).
3. Selkoe, D., Mandelkow, E. & Holtzman, D. Deciphering alzheimer disease. *Cold Spring Harbor Perspect. Med.* 2, a011460 (2012).
4. Chiti, F. & Dobson, C. M. Protein misfolding, functional amyloid, and human disease. *Annu. Rev. Biochem.* 75, 333–366 (2006).
5. Goedert, M. Tau protein and the neurofibrillary pathology of Alzheimer's disease. *Ann. N. Y. Acad. Sci.* 777, 121–131 (1996).
6. Hyman, B. T., Damasio, H., Damasio, A. R. & Hoesen, G. W. V., Alzheimer's Disease. *Annu. Rev. Public Health* 10, 115–140. https://doi.org/10.1146/annurev.pu.10.050189.000555 (1989).
7. Hardy, J. A. & Higgins, G. A. Alzheimer's disease: the amyloid cascade hypothesis. *Science* 256, 184 (1992).
8. Binder, L. I., Guillozet-Bongaarts, A. L., Garcia-Sierra, F. & Berry, R. W. Tau, tangles, and Alzheimer's disease. *Biochim. Biophys. Acta* 1739, 216–223 (2005).
9. Goedert, M. & Spillantini, M. G. A century of Alzheimer's disease. *Science* 314, 777–781 (2006).
10. Keck, S., Nitsch, R., Grune, T. & Ullrich, O. Proteasome inhibition by paired helical filament-tau in brains of patients with Alzheimer's disease. *J. Neurochem.* 85, 115–122 (2003).
11. Keller, J. N., Hanni, K. B. & Markesbery, W. R. Impaired proteasome function in Alzheimer's disease. *J. Neurochem.* 75, 436–439 (2000).
12. Weingarten, M. D., Lockwood, A. H., Hwo, S.-Y. & Kirschner, M. W. A protein factor essential for microtubule assembly. *Proc. Natl. Acad. Sci.* 72, 1858–1862 (1975).
13. Kadavath, H. *et al.* Tau stabilizes microtubules by binding at the interface between tubulin heterodimers. *Proc. Natl. Acad. Sci. USA* 112, 7501–7506 (2015).
14. Wang, Y. & Mandelkow, E. Tau in physiology and pathology. *Nat. Rev. Neurosci.* 17, 22 (2016).
15. Chen, F., David, D., Ferrari, A. & Götz, J. Posttranslational modifications of tau–Role in human tauopathies and modeling in transgenic animals. *Curr. Drug Targets* 5, 503–515 (2004).
16. Mandelkow, E.-M. & Mandelkow, E. Tau in Alzheimer's disease. *Trends Cell Biol.* 8, 425–427 (1998).
17. Grundke-Iqbal, I. *et al.* Abnormal phosphorylation of the microtubule-associated protein tau (tau) in Alzheimer cytoskeletal pathology. *Proc. Natl. Acad. Sci. USA* 83, 4913–4917 (1986).

18. Steinhilb, M. L., Dias-Santagata, D., Fulga, T. A., Felch, D. L. & Feany, M. B. Tau phosphorylation sites work in concert to promote neurotoxicity in vivo. *Mol. Biol. Cell* **18**, 5060–5068 (2007).
19. Wischik, C., Edwards, P., Lai, R., Roth, M. & Harrington, C. Selective inhibition of Alzheimer disease-like tau aggregation by phenothiazines. *Proc. Natl. Acad. Sci. USA* **93**, 11213–11218 (1996).
20. Akoury, E. et al. Mechanistic basis of phenothiazine-driven inhibition of Tau aggregation. *Angew. Chem. Int. Ed.* **52**, 3511–3515 (2013).
21. Pickhardt, M. et al. Anthraquinones inhibit tau aggregation and dissolve Alzheimer's paired helical filaments in vitro and in cells. *J. Biol. Chem.* **280**, 3628–3635 (2005).
22. Taniguchi, S. et al. Inhibition of heparin-induced tau filament formation by phenothiazines, polyphenols, and porphyrins. *J. Biol. Chem.* **280**, 7614–7623 (2005).
23. Ballic, B. et al. Development of tau aggregation inhibitors for Alzheimer's disease. *Angew. Chem. Int. Ed.* **48**, 1740–1752 (2009).
24. Paranjape, S. R. et al. Inhibition of Tau aggregation by three Aspergillus nidulans secondary metabolites: 2, 11-dihydroxyemodin, asperthecin, and asperbenzaldehyde. *Planta Med.* **80**, 77–85 (2014).
25. Ma, Q.-L. et al. Curcumin suppresses soluble tau dimers and corrects molecular chaperone, synaptic, and behavioral deficits in aged human tau transgenic mice. *J. Biol. Chem.* **288**, 4056–4065 (2013).
26. Li, W. et al. Inhibition of tau fibrillization by oleocanthal via reaction with the amino groups of tau. *J. Neurochem.* **110**, 1339–1351 (2009).
27. Mandel, S., Weinreb, O., Amit, T. & Youdim, M. B. Cell signaling pathways in the neuroprotective actions of the green tea polyphenol (-)-epigallocatechin-3-gallate: implications for neurodegenerative diseases. *J. Neurochem.* **88**, 1555–1569 (2004).
28. Ferreira, N. et al. Binding of epigallocatechin-3-gallate to transthyretin modulates its amyloidogenicity. *FEBS Lett.* **583**, 3569–3576 (2009).
29. Meng, G., Aboelnil, A., Plomer, A., Verchere, C. B. & Raleigh, D. P. The flavanol (-)-epigallocatechin 3-gallate inhibits amylin formation by islet amyloid polypeptide, disaggregates amylin fibrils, and protects cultured cells against IAPP-induced toxicity. *Biochemistry* **49**, 8127–8133 (2010).
30. Cao, P. & Raleigh, D. P. Analysis of the inhibition and remodeling of islet amyloid polypeptide amyloid fibers by flavanols. *Biochemistry* **51**, 2670–2683 (2012).
31. Rambold, A. S. et al. Green tea extracts interfere with the stress-protective activity of PrPC and the formation of PrPSc. *J. Neurochem.* **107**, 218–229 (2008).
32. Ehrnhoefer, D. E. et al. EGCG redirects amyloidogenic polypeptides into unstructured, off-pathway oligomers. *Nat. Struct. Mol. Biol.* **15**, 558 (2008).
33. Wobst, H. J., Sharma, A., Diamond, M. I., Wanker, E. E. & Bieschke, J. The green tea polyphenol (-)-epigallocatechin gallate prevents the aggregation of tau protein into toxic oligomers at substoichiometric ratios. *FEBS Lett.* **589**, 77–83 (2015).
34. Faber, J. D. & Williamson, M. P. Multi-site binding of epigallocatechin gallate to human serum albumin measured by NMR and isothermal calorimetry. *Biosci. Rep.* **37**, 228 (2017).
35. Liu, X. et al. Influence of EGCG on α-synuclein (α5) aggregation and identification of their possible binding mode: A computational study using molecular dynamics simulation. *Chem. Biol. Drug Des.* **91**, 162–171 (2018).
36. Calixto, L., Zhang, B., Brisac, U. K., Dickey, C. A. & Baker, B. J. Natural products as a rich source of tau-targeting drugs for Alzheimer's disease. *Future Med. Chem.* **4**, 1751–1761 (2012).
37. Bieschke, J. Natural compounds may open new routes to treatment of amyloid diseases. *Neurotherapeutics* **10**, 429–439 (2013).
38. Lahiri, D. K. et al. A critical analysis of new molecular targets and strategies for drug development in Alzheimer's disease. *Curr. Drug Targets* **4**, 97–112 (2003).
39. Selkoe, D. J. Defining molecular targets to prevent Alzheimer disease. *Arch. Neurol.* **62**, 192–195 (2005).
40. Miyata, M. et al. The crystal structure of the green tea polyphenol (-)-epigallocatechin gallate–transthyretin complex reveals a novel binding site distinct from the thyroxine binding site. *Biochemistry* **49**, 6104–6114 (2010).
41. Andrich, K. & Bieschke, J. *Natural Compounds as Therapeutic Agents for Amyloidogenic Diseases* 139–161 (Springer, Berlin, 2015).
42. Gorantla, N. V., Shkumatov, A. V. & Chinnathambi, S. Conformational Dynamics of Intracellular Tau Protein Revealed by CD and SAXS (2018). *Methods Mol Biol.* **2523**:3–20.
43. Berman, H. M. et al. In *International Tables for Crystallography Volume F: Crystallography of Biological Macromolecules* (eds Rossmann, M. G. & Arnold, E.) 675–684 (Springer, Dordrecht, 2001).
44. Altschul, S. F., Gish, W., Miller, W., Myers, E. W. & Lipman, D. J. Basic local alignment search tool. *J. Mol. Biol.* **215**, 403–410 (1990).
45. Laskowski, R. A., MacArthur, M. W., Moss, D. S. & Thornton, J. M. PROCHECK: a program to check the stereochemical quality of protein structures. *J. Appl. Crystallogr.* **26**, 283–291 (1993).
46. Colovos, C. & Yeates, T. O. Verification of protein structures: patterns of nonbonded atomic interactions. *Protein Sci.* **2**, 1511–1519 (1993).
47. Wiederstein, M. & Sippl, M. J. ProSA-web: interactive web service for the recognition of errors in three-dimensional structures of proteins. *Nucleic Acids Res.* **35**, W407–W410 (2007).
48. Pricner, R. A. et al. Glide: a new approach for rapid, accurate docking and scoring. 1. Method and assessment of docking accuracy. *J. Med. Chem.* **47**, 1739–1749 (2004).
49. Halgren, T. A. Identifying and characterizing binding sites and assessing druggability. *J. Chem. Inf. Model.* **49**, 377–389 (2009).
50. Van Der Spoel, D. et al. GROMACS: fast, flexible, and free. *J. Comput. Chem.* **26**, 1701–1718 (2005).
51. Berendsen, H. J., van der Spoel, D. & van Drunen, R. GROMACS: a message-passing parallel molecular dynamics implementation. *Comput. Phys. Commun.* **91**, 43–56 (1995).
52. Vanommeslaeghe, K. & MacKerell, A. D. Jr. Automation of the CHARMM General Force Field (CGenFF) I: bond perception and atom typing. *J. Chem. Inf. Model.* **52**, 3144–3154 (2012).
53. Vanommeslaeghe, K., Raman, E. P. & MacKerell, A. D. Jr. Automation of the CHARMM General Force Field (CGenFF) II: assignment of bonded parameters and partial atomic charges. *J. Chem. Inf. Model.* **52**, 3155–3168 (2012).
54. Berendsen, H. J., Postma, J. V., van Gunsteren, W. F., DiNola, A. & Haak, J. R. Molecular dynamics with coupling to an external bath. *J. Chem. Phys.* **81**, 3684–3690 (1984).
55. Marinelli, R., Lain, A. & Parrinello, M. Predicting crystal structures: the Parrinello-Rahman method revisited. *Phys. Rev. Lett.* **90**, 075503 (2003).
56. Darden, T., York, D. & Pedersen, L. Particle mesh Ewald: an N· log (N) method for Ewald sums in large systems. *J. Chem. Phys.* **98**, 10089–10092 (1993).
57. Hess, B., Bekker, H., Berendsen, H. J. & Fraaije, J. G. LINCS: a linear constraint solver for molecular simulations. *J. Comput. Chem.* **18**, 1463–1472 (1997).
58. Humphrey, W., Dalke, A. & Schulten, K. VMD: visual molecular dynamics. *J. Mol. Graph.* **14**, 33–38 (1996).

Acknowledgements

This work was supported in part by grant from in-house CSIR-National Chemical Laboratory grants MLP029526. SS and HC acknowledge Department of Biotechnology for fellowship. DB, AD, NV thanks CSIR-UGC for

fellowship. AB acknowledges CSIR-SPMF for fellowship. Author acknowledges Dr. Shailza Singh for valuable inputs on molecular docking and simulation work.

Author contributions

S.K.S., N.V., A.B. and S.C. conducted most of the experiments, analyzed the results, and wrote the paper. H.C., D.B., S.K.R. and S.C. conducted experiments on Tau-ligand docking, molecular simulation and wrote the paper. U.K.M. and A.D. conducted the NMR experiments and analyzed the data. S.C. designed, conceived the idea for the project, provided resources, supervised and wrote the paper.

Competing interests

The authors declare no competing interests.

Additional information

Supplementary information is available for this paper at https://doi.org/10.1038/s41598-020-69429-6.

Correspondence and requests for materials should be addressed to S.C.

Reprints and permissions information is available at www.nature.com/reprints.

Publisher's note Springer Nature remains neutral with regard to jurisdictional claims in published maps and institutional affiliations.